



HAL
open science

Testing Lorentz invariance by binary black holes

Oscar Ramos

► **To cite this version:**

Oscar Ramos. Testing Lorentz invariance by binary black holes. Astrophysics [astro-ph]. Sorbonne Université, 2018. English. NNT : 2018SORUS199 . tel-02447105

HAL Id: tel-02447105

<https://theses.hal.science/tel-02447105>

Submitted on 21 Jan 2020

HAL is a multi-disciplinary open access archive for the deposit and dissemination of scientific research documents, whether they are published or not. The documents may come from teaching and research institutions in France or abroad, or from public or private research centers.

L'archive ouverte pluridisciplinaire **HAL**, est destinée au dépôt et à la diffusion de documents scientifiques de niveau recherche, publiés ou non, émanant des établissements d'enseignement et de recherche français ou étrangers, des laboratoires publics ou privés.



**THÈSE DE DOCTORAT
DE SORBONNE UNIVERSITÉS**

Spécialité : Physique

École doctorale n° 564: Physique en Île-de-France

réalisée

à l'Institut d'Astrophysique de Paris

sous la direction de Enrico BARAUSSE et Luc BLANCHET

présentée par

Oscar RAMOS

pour obtenir le grade de :

DOCTEUR DE SORBONNE UNIVERSITÉS

Sujet de la thèse :

Testing Lorentz invariance within binary black holes

soutenue le 5 octobre 2018

devant le jury composé de :

M ^{me} Danièle STEER	Rapporteuse
M. Eugene LIM	Rapporteur
M ^{me} Marie-Christine ANGONIN	Examinatrice
M. Alexandre LE TIEC	Examinateur
M. Luc BLANCHET	co-Directeur de thèse
M. Enrico BARAUSSE	Directeur de thèse

Table des matières

Introduction	iii
0.1 List of publications	v
0.2 Notations	v
1 Introduction to gravitational wave astronomy	1
1.1 General relativity	1
1.2 Linearized theory	2
1.2.1 The TT-gauge	3
1.3 Interaction of a gravitational wave with a detector	5
1.4 Energy of a gravitational wave	6
1.5 Emission of gravitational waves	9
1.6 Gravitational wave astronomy	12
1.6.1 Binary pulsars	12
1.6.2 Gravitational wave interferometers	14
2 Lorentz Symmetry and its violation	21
2.1 Lorentz symmetry in non-gravitational physics	22
2.2 Lorentz symmetry and the equivalence principle	24
2.2.1 Percolation from the gravitational sector to the matter sector	26
2.2.2 The Einstein equivalence principle as a tool to construct modified theories of gravitation	26
2.3 Khronometric theory	28
2.4 Einstein-æther theory	32
2.5 Experimental constraints	35
2.5.1 Stability and consistency requirements	36
2.5.2 Multi-messenger astronomy	37
2.5.3 Solar system and the weak-field regime	37
2.5.4 Cosmology	38
2.5.5 Binary pulsars and the strong-field regime	38
2.6 Black holes in Lorentz Violating gravity	39
2.6.1 Static, spherically symmetric black holes	40
2.6.2 Black hole 'Charges'	42
2.6.3 Digging further into the black hole	43
2.A Derivation of the field equations	46
2.B Bianchi identity in khronometric theory	47

3	Dipole emission in Lorentz-violating Gravity	49
3.1	Strong equivalence principle and its violations	49
3.2	Point-particle approximation and the sensitivities	53
3.3	Sensitivities and the asymptotic metric	55
3.3.1	Extraction procedure	57
3.4	Dipolar radiation	58
3.4.1	Dissipative PN dynamics	58
3.5	Chapter conclusions	61
4	Slowly moving black holes in Lorentz-violating Gravity	63
4.1	Slowly moving black holes	63
4.1.1	Construction of the Ansatz	64
4.2	Structure of the field equations	69
4.2.1	Boundary conditions	71
4.2.2	Integration to spatial infinity	73
4.2.3	Bisection procedure	74
4.2.4	Consistency relations	78
4.2.5	Extraction of the sensitivities	81
4.2.6	Interior solution and the spin-0 frame	83
4.3	The $\alpha = \beta = 0$ case	90
4.4	Chapter conclusions	97
4.A	Explicit form of the field equations	99
4.B	Regularity of the potentials at the metric horizon	112
5	Open issues and conclusions	115
A	Appendix : academic paper	121
	Bibliographie	139

Introduction

With the advent of gravitational wave astronomy a new chapter in physics has begun. Prior to this new era, gravitational laws were primarily tested in the weakly-gravitating, mildly relativistic regime of the Einstein equations. This early phase has enabled us to establish some firm grounds upon which gravitational theory must be built, culminating with the prediction and detection of gravitational waves. Our modern view of gravity as a dynamical spacetime phenomena started with Einstein's general relativity, which is still today, after more than a century of reign, the leading theory for gravitation. Indeed, general relativity has successfully passed a wild variety of tests contributing to our confidence on it. On the one hand, both of its foundational principles, the Einstein equivalence principle and the principle of special relativity, have strong experimental grounds. On the other hand, general relativity's predictions have been confirmed in the lab and in astrophysics within a broad range of phenomena. Yet, there are hints both coming from theory and observation that suggest that general relativity might not be the last word in gravitational theory.

In the first place, some inconsistencies appear when trying to apply general relativity in regimes where it has not been properly tested. When applying general relativity at cosmological scales (i.e., considering the low energy regime of the Einstein equations) we are forced to admit the existence of new matter fields which have not been found otherwise. Namely, there's the controversial existence of a cosmological constant as well as the more accepted existence of dark matter. In the former case, there is a huge discrepancy between the estimated value coming from our knowledge of particle physics and the measured value (the cosmological constant problem) while for the latter there has been no direct detection ever. On the high energy regime, general relativity cannot avoid the appearance of mathematical singularities through gravitational collapse as stated by the well known singularity theorems.

Secondly, one could expect that a quantum theory of gravity should exist whose classical limit would lead to a metric theory, and particularly to general relativity. But this statement is far from being proved, and the classical limit of quantum gravity might turn to be another metric theory. Furthermore, general relativity is incompatible with quantum mechanics for it is a non-renormalizable theory. Moreover, even if general relativity turned out to be the correct theory of classical gravity there's no best way to understand its strengths and weaknesses than comparing it to other metric theories of gravity.

Thirdly, from a purely logical point of view, what the foundational principles of gravitation can strictly assure us is that gravitational phenomena must be of geometrical character, yet not necessarily general relativity. Indeed, high energy physics suggests the existence of one and only one spin-2 field coupling in a Lorentz invariant way to matter, the metric,

which should therefore extend everywhere in the universe. Experiments show that this tensor field is the only field coupling directly to matter (this property is commonly referred to as the *universal coupling* of the metric). But in order to get from this experimental result to the theory of general relativity, we need to assume that the metric is the only existing gravitational field. Otherwise said, experiments suggest that classical gravitation belongs to a category of theories which we call metric theories of gravitation, and among these, general relativity is its favorite exponent. But this last conclusion is not yet thoroughly proved, and in particular the existence of other gravitational fields has not yet been totally ruled out.

One of the cornerstones of modern physics is Lorentz Invariance (LI), and it's a fundamental part both of general relativity and the Standard Model of particle physics. Among the metric theories that break LI and still survive to experimental tests we find Einstein-æther theory and khronometric theory. One of the landmarks of these theories is the violation of the strong equivalence principle (SEP), which is the extension of the EEP to self-gravitating bodies. The importance of this statement comes from the fact that general relativity does satisfy SEP. Thus, as a theory satisfying the SEP, general relativity verifies the "principle of effacement", allowing us to neglect the internal structure of gravitating objects while describing their orbital dynamics. Once SEP is given up however, the orbital dynamics of a binary system can depend upon internal structure of its components. As an example, the effective gravitational mass can be a function of the state of motion of the body (thus violating Lorentz Invariance), leading to modified dynamics. This change in the orbital dynamics would in turn lead to a modification of the gravitational wave flux. One of the most noticeable changes then is the apparition of dipolar radiation, which is absent in general relativity and detectable in principle by current gravitational wave detectors.

The leading corrections to the orbital dynamics of a self-gravitating object are encoded into the so-called sensitivities. This is precisely what we look for in this work in the particular case of the motion of binary black holes. As a consequence of the arguments previously developed, the sensitivities can be linked to modifications of the flux emitted, and most remarkably to the dipolar emission. Since dipolar emission can be constrained from gravitational wave signals, thus the theory can be constrained as well.

The structure of this thesis will be as follows.

- In chapter 1, we begin by giving a quick introduction to gravitational astronomy and how we use it to test gravitational theory.
- In chapter 2, we will discuss the role of Lorentz symmetry in nature, and in particular in gravity, and we will present the equations and general features of two Lorentz-violating theories : khronometric and Einstein-æther theory. We conclude that chapter by discussing black holes in these Lorentz-violating theories.
- In chapter 3, we show how we can link Lorentz-violations to dipolar emission. In order to do so, we will first show how the sensitivities naturally arise when violating the strong equivalence principle and we will give them a physical definition. Then we will show how the sensitivities can be obtained from a slowly moving solution and how they can be linked to dipolar radiation. The core results of this work are presented in the second part of chapter 4.
- Finally, a discussion on the consequences of this work will be presented as a conclusion in chapter 5.

0.1 List of publications

The work exposed in this manuscript led to the following publication :

O. Ramos and E. Barausse, “Constraints on Hořava gravity from binary black hole observations”, *in preparation*. See Appendix A.

0.2 Notations

Constants and units.

We use units in which the speed of light c is set to 1, although it will sometimes be explicitly written for power-counting purposes. The gravitational constant G is always explicitly written.

Indices and metric signature.

Greek indices $\alpha, \beta, \dots, \mu, \nu, \dots$ take the values 0, 1, 2, 3 while the Latin indices i, j, \dots are used for spatial indices and take the values 1, 2, 3. The metric signature is +, −, −, −, so that the flat metric is $\eta_{\mu\nu} = \text{diag}(1, -1, -1, -1)$.

We adopt the Einstein convention for repeated indices, e.g., $A^{\mu\dots\mu\dots}$ stands for $\sum_{\mu=0,1,2,3} A^{\mu\dots\mu\dots}$, unless the contrary is explicitly stated. In the same way, $B^i{}_i$ and B_{ii} both stand for $\sum_{i=1,2,3} B^i{}_i$, where the sum is carried over spatial indices, unless explicitly stated.

Figures were done using the python library *matplotlib*, unless explicit mention is given in the caption.

1 – Introduction to gravitational wave astronomy

This introductory chapter aims at giving a flavor of gravitational wave astronomy, its foundational principles, status and difficulties. We begin by recalling succinctly the principles and core equations of general relativity in section 1.1, and we then specialize them to the linearized regime in section 1.2. We show how we can find gravitational wave modes within linearized theory, and then describe the interaction between an idealized detector and a gravitational wave passing through in section 1.3. Next, we explain how to describe the energy carried by the gravitational degrees of freedom in section 1.4. Finally, we describe how these principles have been used to study gravitational theory in section 1.6. Of particular interest are gravitational wave interferometers which are described in 1.6.2. Indeed, the applicability of the results of this thesis is based upon the potential of the LIGO-Virgo detectors, as well as to the future LISA mission, to test the fundamental principles of gravitational theory. The following is based on the review articles and books [1, 2, 3, 4].

1.1 General relativity

In brief, general relativity states that the geometry of spacetime itself acquires a dynamical status as it is determined by the matter fields. From the spacetime metric \mathbf{g} one can construct the Riemann tensor \mathbf{R} , given by

$$R^\alpha{}_{\beta\mu\nu} = \partial_\mu \Gamma_{\nu\beta}^\alpha - \partial_\nu \Gamma_{\mu\beta}^\alpha + \Gamma_{\mu\sigma}^\alpha \Gamma_{\nu\beta}^\sigma - \Gamma_{\nu\sigma}^\alpha \Gamma_{\mu\beta}^\sigma, \quad (1.1)$$

where the Christoffel symbols $\Gamma_{\mu\nu}^\alpha$ are defined in terms of the metric and its derivatives as

$$\Gamma_{\mu\nu}^\alpha = \frac{1}{2} g^{\alpha\lambda} (\partial_\mu g_{\lambda\nu} + \partial_\nu g_{\mu\lambda} - \partial_\lambda g_{\mu\nu}). \quad (1.2)$$

From the Riemann tensor we can construct the Ricci tensor as

$$R_{\mu\nu} = R^\lambda{}_{\mu\lambda\nu}, \quad (1.3)$$

and then the scalar curvature as

$$R = g^{\mu\nu} R_{\mu\nu}. \quad (1.4)$$

Then the gravitational dynamics can be deduced from the action

$$S = \frac{1}{16\pi G} \int d^4x \sqrt{-g} R + S_{\text{matter}}[\mathbf{g}, \Psi], \quad (1.5)$$

where S_{matter} is the action of the matter fields, which are collectively denoted by Ψ . Variation with respect to the metric \mathbf{g} leads to the Einstein field equations

$$G_{\mu\nu} = 8\pi G T_{\mu\nu}, \quad (1.6)$$

where \mathbf{G} is the Einstein tensor

$$G_{\mu\nu} = R_{\mu\nu} - \frac{1}{2}R g_{\mu\nu}, \quad (1.7)$$

and the stress energy tensor \mathbf{T} is defined as

$$\delta S_{\text{matter}} = \frac{1}{2} \int d^4x \sqrt{-g} T^{\mu\nu} \delta g_{\mu\nu}. \quad (1.8)$$

From diffeomorphism invariance we deduce the Bianchi identity

$$\nabla_{\mu} G^{\mu\nu} = 0, \quad (1.9)$$

which, together with the Einstein equations implies

$$\nabla_{\mu} T^{\mu\nu} = 0. \quad (1.10)$$

1.2 Linearized theory

In 1916, one year after publishing his field equations, Einstein found that the theory predicted the existence of gravitational waves. Indeed, this can be readily seen by linearizing the Einstein equations; that is, by expanding the field equations around a flat background metric. Let us assume that, for the physical system of interest, it is possible to find a reference frame where we can express the metric as the sum of the Minkowski metric $\eta_{\mu\nu}$ and a perturbation $h_{\mu\nu}$ as

$$g_{\mu\nu} = \eta_{\mu\nu} + h_{\mu\nu}, \quad (1.11)$$

where the components of the perturbation $h_{\mu\nu}$ are such that $|h_{\mu\nu}| \ll 1$. We will assume that this relation holds in a sufficiently large region of spacetime. Since we work only up to linear order in the perturbation $h_{\mu\nu}$ and neglect higher orders, indices are raised or lowered using the flat metric $\eta_{\mu\nu}$. In order to describe the metric by equation (1.11), we are implicitly assuming that our coordinates are approximately Cartesian. Under an infinitesimal gauge transformation (i.e., an infinitesimal coordinate change)

$$x^{\mu} \rightarrow x'^{\mu} = x^{\mu} + \xi^{\mu}(x), \text{ where } |\xi^{\mu}(x)| \ll |x^{\mu}|, \quad (1.12)$$

one has

$$h_{\mu\nu}(x) \rightarrow h'_{\mu\nu}(x') = h_{\mu\nu}(x) - (\partial_{\mu}\xi_{\nu} + \partial_{\nu}\xi_{\mu}). \quad (1.13)$$

Note that, since $|\xi^{\mu}(x)| \ll |x^{\mu}|$ implies $|\partial_{\mu}\xi_{\nu}| \ll 1$, then $|h_{\mu\nu}|$ is still much smaller than 1. Also, under a Lorentz transformation given by $x^{\mu} \rightarrow x'^{\mu} = \Lambda^{\mu}_{\nu} x^{\nu}$ we have, by definition, $\Lambda_{\mu}^{\rho} \Lambda_{\nu}^{\sigma} \eta_{\rho\sigma} = \eta_{\mu\nu}$, so the metric transforms as

$$g_{\mu\nu}(x) \rightarrow g'_{\mu\nu}(x') = \Lambda_{\mu}^{\rho} \Lambda_{\nu}^{\sigma} g_{\rho\sigma}(x) = \eta_{\mu\nu} + \Lambda_{\mu}^{\rho} \Lambda_{\nu}^{\sigma} h_{\rho\sigma}(x), \quad (1.14)$$

from which we deduce that $h_{\mu\nu}$ transforms as a tensor under Lorentz transformations (note that we must restrict boosts to those satisfying $|\Lambda_\mu{}^\rho \Lambda_\nu{}^\sigma h_{\rho\sigma}(x)| \ll 1$). It is clear as well that $h_{\mu\nu}$ is invariant under translations $x^\mu \rightarrow x^\mu + a^\mu$, where \mathbf{a} is a constant vector.

In the linearized regime, the Riemann tensor takes the form

$$R_{\mu\nu\rho\sigma} = \frac{1}{2} \left(\partial_\nu \partial_\rho h_{\mu\sigma} + \partial_\mu \partial_\sigma h_{\nu\rho} - \partial_\mu \partial_\rho h_{\nu\sigma} - \partial_\nu \partial_\sigma h_{\mu\rho} \right). \quad (1.15)$$

This expression is invariant under the gauge transformations (1.12). From the Riemann tensor we can find the Einstein equations in linearized theory in terms of $h_{\mu\nu}$ and its derivatives. To express them, it is convenient to define

$$\bar{h}_{\mu\nu} \equiv h_{\mu\nu} - \frac{1}{2} h \eta_{\mu\nu}, \quad (1.16)$$

where $h \equiv \eta^{\mu\nu} h_{\mu\nu}$. Note that from the definition (1.16) it follows that $\bar{h} \equiv \bar{h}_{\mu\nu} \eta^{\mu\nu} = -h$. Thus, we can invert the relation (1.16) and express $h_{\mu\nu}$ in terms of $\bar{h}_{\mu\nu}$ simply as $h_{\mu\nu} = \bar{h}_{\mu\nu} - \frac{1}{2} \bar{h} \eta_{\mu\nu}$. In terms of $\bar{h}_{\mu\nu}$, the Einstein field equations become

$$\square \bar{h}_{\mu\nu} + \eta_{\mu\nu} \partial^\rho \partial^\sigma \bar{h}_{\rho\sigma} - \partial^\rho \partial_\nu \bar{h}_{\mu\rho} - \partial^\rho \partial_\mu \bar{h}_{\nu\rho} = -\frac{16\pi G}{c^4} T_{\mu\nu}, \quad (1.17)$$

where $\square \equiv \partial_\mu \partial^\mu$ is the d'Alembert operator associated to the Minkowski metric $\eta_{\mu\nu}$. We can further simplify this expression by making use of the gauge freedom (1.12), so as to work in the Lorenz gauge defined by

$$\partial^\nu \bar{h}_{\mu\nu} = 0, \quad (1.18)$$

in which case the Einstein equations take the form

$$\square \bar{h}_{\mu\nu} = -\frac{16\pi G}{c^4} T_{\mu\nu}. \quad (1.19)$$

This equation relates the perturbations of the background flat metric to the stress energy-momentum tensor of the source, and the wave-like character of the equation is visible from the d'Alembertian operator \square .

It is readily seen from equation (1.19) and the Lorenz gauge (1.18) that in the linearized theory we have the energy-momentum conservation law

$$\partial_\mu T^{\mu\nu} = 0. \quad (1.20)$$

1.2.1 The TT-gauge

Outside the source, equations (1.18) and (1.19) reduce to

$$\square \bar{h}_{\mu\nu} = 0; \quad \partial^\nu \bar{h}_{\mu\nu} = 0. \quad (1.21)$$

Solutions to this system can be expressed as a superposition of plane waves :

$$\bar{h}_{\mu\nu}(t, \vec{x}) = \text{Re} \int d^3k A_{\mu\nu}(\vec{k}) e^{i(\vec{k} \cdot \vec{x} - \omega t)}, \quad (1.22)$$

where the complex coefficients $A_{\mu\nu}(\vec{k})$ depend only on the wave-vector \vec{k} and $\omega = |\vec{k}|$. The Lorenz gauge imposes the condition $k^\mu A_{\mu\nu} = 0$, for $k^\mu = (\omega, \vec{k})$. We observe that, outside the source, there still remains a residual gauge freedom given by

$$x^\mu \rightarrow x'^\mu = x^\mu + \xi^\mu \quad \text{with} \quad \square \xi^\mu = 0, \quad (1.23)$$

as the new metric perturbation $\bar{h}'_{\mu\nu}(x') = \bar{h}_{\mu\nu}(x) - (\partial_\mu \xi_\nu + \partial_\nu \xi_\mu - \eta_{\mu\nu} \partial_\rho \xi^\rho)$ still satisfies the Lorenz gauge condition (1.18). We can make use of this residual gauge to impose further conditions on $\bar{h}_{\mu\nu}$. A common choice is the transverse-traceless gauge, or “TT-gauge” for short.

The traceless condition is imposed by choosing ξ^μ such that the new trace \bar{h}' vanishes, that is, such that

$$\bar{h}' = \bar{h} + 2 \partial_\mu \xi^\mu = 0, \quad (1.24)$$

that is,

$$\partial_\mu \xi^\mu = -\frac{1}{2} \bar{h} = \frac{1}{2} h. \quad (1.25)$$

Note that this condition is indeed compatible with $\square \xi^\mu = 0$. In fact, we can set ξ^μ such that it satisfies the initial condition $\partial_\mu \xi^\mu = -\frac{1}{2} \bar{h}$, then ξ^μ will be everywhere determined by the equation $\square \xi^\mu = 0$. Then the evolution equations (1.21) imply that the quantity $\bar{h}' \equiv \bar{h} + 2 \partial_\mu \xi^\mu$ satisfies the equation $\square \bar{h}' = 0$, with null initial conditions. We can therefore conclude that $\bar{h}' = 0$ everywhere else. Thus, choosing some initial data for ξ^μ within a given Cauchy surface, such that (1.24) is satisfied, then the evolution equations ensure that equation (1.23) and (1.24) be satisfied at all points.

Dropping the primes, this condition implies that $\bar{h}_{\mu\nu} = h_{\mu\nu}$, so we can drop the over bar of $\bar{h}_{\mu\nu}$ as well. The transverse condition is achieved by choosing ξ^i such that $h'^{0i} = 0$, that is, satisfying $\partial^0 \xi^i + \partial^i \xi^0 = -h^{0i}$. The general solution to the equation $\square \xi^\mu = 0$ can be written as

$$\xi^\mu(\mathbf{x}) = \text{Re} \int d^3k C^\mu(\vec{k}) e^{i(\vec{k} \cdot \vec{x} - \omega t)}. \quad (1.26)$$

The coefficients $A_{\mu\nu}(\vec{k})$ of equation (1.22) transform as

$$A'_{\mu\nu} = A_{\mu\nu} - 2il_{(\mu} C_{\nu)} + i\eta_{\mu\nu} k^\alpha C_\alpha, \quad (1.27)$$

where $l^\mu = (\omega, -\vec{k})$. Therefore the TT-conditions can be expressed in terms of $C^\mu(\vec{k})$ as

$$0 = \eta^{\mu\nu} A'_{\mu\nu} = \eta^{\mu\nu} A_{\mu\nu} + 2ik^\mu C_\mu, \quad (1.28a)$$

$$0 = A'_{0\nu} = A_{0\nu} - iC_\nu k_0 - iC_0 k_\nu + i\delta_\nu^0 (k^\alpha C_\alpha), \quad (1.28b)$$

for which an explicit solution can be given by

$$C_\mu = \frac{3A_{\rho\sigma} l^\rho l^\sigma}{8i\omega^4} k_\mu + \frac{\eta^{\rho\sigma} A_{\rho\sigma}}{4i\omega^4} l_\mu + \frac{1}{2i\omega^2} A_{\mu\nu} l^\nu, \quad (1.29)$$

In particular, the $\mu = 0$ component of the Lorenz gauge condition reads now

$$\partial^0 h_{00} + \partial^i h_{0i} = \partial^0 h_{00} = 0, \quad (1.30)$$

which implies that h_{00} becomes constant in time. For instance, h_{00} can correspond to the static Newtonian potential of the source. Since we are interested in the variable part of the

gravitational field, which as we will show is the only part carrying energy, we can set h_{00} to zero for simplicity. Together with the transverse gauge condition this means that we can set $h_{\mu 0} = 0$. The spatial components of the Lorenz gauge now read

$$\partial^0 h_{i0} + \partial^j h_{ij} = \partial^j h_{ij} = 0. \quad (1.31)$$

Thus, the transverse-traceless gauge is defined by the conditions

$$h_{\mu 0} = 0; \quad h^i_i = 0; \quad \partial^j h_{ij} = 0. \quad (1.32)$$

A plane-wave solution to the linearized equations can be described in the TT-gauge by $h_{ij}(x) = e_{ij}(k)e^{i\mathbf{k}\cdot\mathbf{x}}$, where $k^\mu = (\omega, \vec{k})$ is the wave four-vector and $e_{ij}(k)$ is the amplitude associated with the mode \mathbf{k} . Choosing the axis of propagation to be the z axis, then we can write

$$h_{ij}(t, z) = \begin{pmatrix} h_+ & h_\times & 0 \\ h_\times & -h_+ & 0 \\ 0 & 0 & 0 \end{pmatrix} \cos[\omega(t - z)], \quad (1.33)$$

or equivalently,

$$ds^2 = dt^2 - dx^2 - dy^2 - dz^2 + (dx^2 - dy^2)h_+ \cos[\omega(t - z)] + 2h_\times \cos[\omega(t - z)]dx dy. \quad (1.34)$$

Any gravitational wave propagating in the direction given by the unitary vector \hat{n} can thus be decomposed into a sum of plane waves in the TT-gauge :

$$h_{ij}(t, \vec{x}) = \sum_{A=+, \times} e_{ij}^A(\hat{n}) \int_{-\infty}^{\infty} df \tilde{h}_A(f) e^{-2\pi i f(t - \hat{n}\cdot\mathbf{x})}, \quad (1.35)$$

where $\tilde{h}_A(f)$ is the Fourier transform of the $A = +$ or \times polarization mode, and e_{ij}^A are polarization tensors defined as

$$e_{ij}^+(\hat{n}) = \hat{u}_i \hat{u}_j - \hat{v}_i \hat{v}_j, \quad e_{ij}^\times(\hat{n}) = \hat{u}_i \hat{v}_j - \hat{v}_i \hat{u}_j, \quad (1.36)$$

where \hat{u} and \hat{v} are unitary vectors such that \hat{n} , \hat{u} and \hat{v} form an orthonormal basis of the Euclidean space.

1.3 Interaction of a gravitational wave with a detector

In general, a gravitational wave passing through a detector will be composed of a superposition of different plane waves as given by equation (1.33). The linearized formalism is ideal to study the propagation of gravitational waves far away from the source and its interaction with a gravitational wave detector, since we can model the latter as an ensemble of test masses. By definition, a test mass is such that its contribution to the gravitational field is negligible. This assumption is reasonable for the mirrors at each end of an interferometer, as their binding gravitational energy is negligible. If we consider a test mass described by the worldline $x^\mu(\lambda)$, where λ is an affine parameter, its motion is determined by the geodesic equation

$$\frac{d^2 x^\mu}{d\lambda^2} + \Gamma_{\alpha\beta}^\mu(x) \frac{dx^\alpha}{d\lambda} \frac{dx^\beta}{d\lambda} = 0. \quad (1.37)$$

The geodesic equation can be derived from an action principle, with the point-particle action

$$S_{\text{pp}} = -m \int d\tau, \quad (1.38)$$

where m and τ are the particle's mass and proper-time, respectively. Then, if we consider a test mass at rest at the time of arrival of the gravitational wave, $\left. \frac{dx^\mu}{d\lambda} \right|_{\lambda=0} = 0$, it follows from equations (1.37) and (1.33) that $\left. \frac{d^2 x^\mu}{d\lambda^2} \right|_{\lambda=0} = 0$ as well, so that position of the test mass does not change as the gravitational wave passes by. However, the proper distance between two test masses (e.g., the two mirrors of a detector) does change due to the gravitational wave's passage, as it can be seen from the metric (1.34). Indeed, if we consider two test masses located at the events $(t, x_1, 0, 0)$ and $(t, x_2, 0, 0)$ respectively, so that their coordinate distance is simply given by $L = x_2 - x_1$, then the proper distance s between them is given by

$$s^2 = \left(1 + h_+ \cos[\omega(t - z/c)]\right) L^2, \quad (1.39)$$

or equivalently, at first order in $h_{\mu\nu}$, by

$$s = \left(1 + \frac{1}{2} h_+ \cos[\omega(t - z/c)]\right) L. \quad (1.40)$$

In general, if the events are separated by the coordinate vector \vec{L} , their proper distance is

$$s = L + h_{ij} \frac{L_i L_j}{2L}. \quad (1.41)$$

so that if we have two test masses placed at each end of a detector, their proper distance evolves as

$$\ddot{s} = \ddot{h}_{ij} \frac{L_i L_j}{2L} + \mathcal{O}(\ddot{h}^2). \quad (1.42)$$

Since it is the proper distance, rather than the coordinate distance, which determines the time of flight of the laser beams traveling between each end of the detector, the presence of a gravitational wave passing by can be determined by measuring the interference pattern (and its changes) of the two laser beams.

1.4 Energy of a gravitational wave

In general, the energy carried by gravitational waves is a subtle subject, since it depends on how we separate the gravitational field between a “background” and a “perturbation” part. In particular, since any form of energy contributes to curvature of spacetime, gravitational waves themselves should also be a source of spacetime curvature. However, the linearized framework excludes the possibility of gravitational waves curving the background flat spacetime, because the background metric is fixed to the Minkowski metric $\eta_{\mu\nu}$. Thus, in order to study the energy carried by gravitational waves it is necessary to adopt a more general point of view where gravitational waves are perturbations over a dynamical curved background :

$$g_{\mu\nu}(x) = \bar{g}_{\mu\nu}(x) + h_{\mu\nu}(x), \quad |h_{\mu\nu}| \ll 1, \quad (1.43)$$

where $\bar{g}_{\mu\nu}$ describes the background metric, and the condition $|h_{\mu\nu}| \ll 1$ assumes that we adopt a coordinate system such that the typical order of the background metric is $|\bar{g}_{\mu\nu}| \sim 1$. From a fundamental point of view, there is no unambiguous way to do this. In particular, one could transfer any x dependence from $\bar{g}_{\mu\nu}$ to $h_{\mu\nu}$ or vice versa. In many situations however, one can uniquely express the total metric as the sum of a background metric $\bar{g}_{\mu\nu}$ and a perturbation $h_{\mu\nu}$ if the physical system allows for a clear separation of scales. For instance, if the typical reduced wavelength λ^1 is much smaller than the characteristic background curvature radius \mathcal{L} , then it is possible to find an intermediate length scale L such that $\lambda \ll L \ll \mathcal{L}$, and define

$$\bar{g}_{\mu\nu} = \langle g_{\mu\nu} \rangle, \quad (1.44a)$$

$$h_{\mu\nu} = g_{\mu\nu} - \bar{g}_{\mu\nu}, \quad (1.44b)$$

where $\langle \cdot \rangle$ represents an average over scales smaller than L . Thus, the small fluctuations corresponding to $h_{\mu\nu}$ have been “smoothed” over in order to produce the background metric $\bar{g}_{\mu\nu}$.

As we will see in section 1.6.2, the LIGO-Virgo interferometers are sensitive to gravitational waves of 10-100 Hz, corresponding to a reduced wavelength $\lambda \sim 50 - 500$ km, while the radius of the Earth is roughly $R_{\oplus} \simeq 6400$ km. Therefore the condition $\lambda \ll R_{\oplus}$ is not accurately fulfilled. Furthermore, the Earth’s Newtonian gravitational potential at the Earth’s surface is $|h_{00}| = 2GM_{\oplus}/R_{\oplus}^2 \sim 10^{-9}$ while the expected gravitational waves amplitudes are of the order $h \sim 10^{-21}$. This implies that any fluctuation up to 10^{-12} of the Earth’s potential is large compared to the gravitational waves. Thus, when considering the interaction between an Earth-based detector and a passing gravitational wave, it is the fact that the Earth’s background gravitational field is slowly varying in time when compared to the gravitational wave that allows us to separate the scales. In other words, the frequencies f_B of the background gravitational field and the perturbation frequencies f are such that $f_B \ll f$. Moreover, we can introduce an intermediate frequency f^* such that $f_B \ll f^* \ll f$, allowing us to take averages over many cycles of the perturbation field, giving us an operational way to separate it from the background gravitational field. Thus, we can compute the background metric as $\bar{g} \equiv \langle g_{\mu\nu} \rangle$, where the $\langle \cdot \rangle$ stands for a spatial or temporal average, i.e., an average over many cycles. For definiteness we will discuss of a spatial average over many wavelengths.

Our goal now is to show how the perturbation propagates on the background metric and how its propagation affects the background metric. Using the decomposition given by equation (1.43), we can expand the Ricci tensor in powers of $h_{\mu\nu}$ as

$$R_{\mu\nu} = \bar{R}_{\mu\nu} + R_{\mu\nu}^{(1)} + R_{\mu\nu}^{(2)} + \mathcal{O}(h^3), \quad (1.45)$$

where $\bar{R}_{\mu\nu}$ depends only on $\bar{g}_{\mu\nu}$, $R_{\mu\nu}^{(1)}$ is linear in $h_{\mu\nu}$ and $R_{\mu\nu}^{(2)}$ is quadratic in $h_{\mu\nu}$. The computation of these quantities in terms of $\bar{g}_{\mu\nu}$ and $h_{\mu\nu}$ is straightforward but tedious, we thus refer to [1, 2] for explicit expressions. Note that, by construction, $\bar{R}_{\mu\nu}$ only contains low modes of the order $\sim 4\bar{k}$, where $\bar{k} = 2\pi/\mathcal{L}$ is the typical wave-vector of the background metric $\bar{g}_{\mu\nu}$. Also, $R_{\mu\nu}^{(1)}$ only contains high-modes because it is linear in $h_{\mu\nu}$. In contrast,

1. That is, $\lambda \equiv \frac{\lambda}{2\pi}$.

$R_{\mu\nu}^{(2)}$ can contain both low and high-modes since it is quadratic $h_{\mu\nu}$, and we will therefore decompose it as $R_{\mu\nu}^{(2)} = \langle R_{\mu\nu}^{(2)} \rangle + (R_{\mu\nu}^{(2)} - \langle R_{\mu\nu}^{(2)} \rangle)$. The low-modes remain essentially unchanged when averaged so that they are included in the part $\langle R_{\mu\nu}^{(2)} \rangle$, and the remainder $(R_{\mu\nu}^{(2)} - \langle R_{\mu\nu}^{(2)} \rangle)$ contains thus the high modes of $R_{\mu\nu}^{(2)}$. Recasting the Einstein equations as

$$R_{\mu\nu} = 8\pi G \left(T_{\mu\nu} - \frac{1}{2} T g_{\mu\nu} \right), \quad (1.46)$$

the above decomposition allow us to split the Einstein equations in a high-mode and a low-mode part. The low-mode part is obtained by taking the average of the field equations

$$\bar{R}_{\mu\nu} = -\langle R_{\mu\nu}^{(2)} \rangle + 8\pi G \left\langle T_{\mu\nu} - \frac{1}{2} T g_{\mu\nu} \right\rangle, \quad (1.47)$$

and the high-mode part can be obtained by taking the difference,

$$R_{\mu\nu}^{(1)} = -(R_{\mu\nu}^{(2)} - \langle R_{\mu\nu}^{(2)} \rangle) + 8\pi G \left(T_{\mu\nu} - \frac{1}{2} T g_{\mu\nu} - \langle T_{\mu\nu} - \frac{1}{2} T g_{\mu\nu} \rangle \right). \quad (1.48)$$

We can define an effective stress-energy tensor for matter $\bar{T}_{\mu\nu}$ such that

$$\bar{T}_{\mu\nu} - \frac{1}{2} \bar{T} \bar{g}_{\mu\nu} = \left\langle T_{\mu\nu} - \frac{1}{2} T g_{\mu\nu} \right\rangle, \quad (1.49)$$

where we introduced the trace $\bar{T} = \bar{g}_{\mu\nu} \bar{T}^{\mu\nu}$. Let us also define

$$t_{\mu\nu} = -\frac{1}{8\pi G} \left\langle R_{\mu\nu}^{(2)} - \frac{1}{2} R^{(2)} g_{\mu\nu} \right\rangle, \quad (1.50)$$

where $R^{(2)} = \bar{g}^{\mu\nu} R_{\mu\nu}^{(2)}$ is the trace of $R_{\mu\nu}^{(2)}$. Finally, introducing the trace $t = \bar{g}^{\mu\nu} t_{\mu\nu} = \frac{1}{8\pi G} \langle R^{(2)} \rangle$, we can express equation (1.47) as

$$\bar{R}_{\mu\nu} - \frac{1}{2} \bar{g}_{\mu\nu} \bar{R} = 8\pi G (\bar{T}_{\mu\nu} + t_{\mu\nu}), \quad (1.51)$$

which shows the contribution of the perturbation to the background curvature. In equations (1.47) and (1.51), the scale of variation of the left-hand side is

$$\bar{R}_{\mu\nu} \sim \partial^2 \bar{g}_{\mu\nu} \sim \frac{1}{\mathcal{L}^2}. \quad (1.52)$$

Using the explicit form of $\langle R_{\mu\nu}^{(2)} \rangle$ one can show [2] that it varies on scales

$$\langle R_{\mu\nu}^{(2)} \rangle \sim (\partial h)^2 \sim \left(\frac{\hbar}{\lambda} \right)^2. \quad (1.53)$$

Thus, in the case absence of matter fields the Einstein equations imply that²

$$\frac{\hbar}{\lambda} \sim \frac{\mathcal{L}}{\hbar G}, \quad (1.54)$$

2. Here \hbar denotes the Planck constant, so that $\hbar G$ has units of lengths squared.

which determines the relative strength of the typical background Riemann tensor $\sim 1/\mathcal{L}^2$ and the gravitational wave curvature $t_{\mu\nu} \sim h^2/\lambda^2$. In the presence of matter fields we will have

$$\frac{h}{\lambda} \ll \frac{\mathcal{L}}{\hbar G}, \quad (1.55)$$

since now the gravitational waves are not the main source contributing to the background curvature.

Far away from the source, the stress-energy tensor of gravitational waves can be expressed in the TT-gauge and is found to be [1, 2]

$$t^{\mu\nu} = \frac{1}{32\pi G} \langle \partial^\mu h_{\alpha\beta}^{\text{TT}} \partial^\nu h_{\text{TT}}^{\alpha\beta} \rangle, \quad (1.56)$$

where h_{ij}^{TT} is assumed to be expressed in the TT-gauge. Thus, in order to compute $t^{\mu\nu}$ we need the Ricci tensor up to $\mathcal{O}(h^2)$, and in the end, the energy carried away from the source by the gravitational wave (and eventually transferred to a gravitational wave detector) can be expressed as

$$t^{00} = \frac{c^2}{32\pi G} \langle \dot{h}_{ij}^{\text{TT}} \dot{h}_{\text{TT}}^{ij} \rangle, \quad (1.57)$$

or equivalently, in terms of the plus and cross amplitudes as

$$t^{00} = \frac{c^2}{16\pi G} \langle \dot{h}_+^2 + \dot{h}_\times^2 \rangle. \quad (1.58)$$

1.5 Emission of gravitational waves

Let us then consider the problem of the generation of gravitational waves by a source, i.e., let us solve equation (1.19) with $T_{\mu\nu} \neq 0$. Far away from the source, the solution with no-incoming radiation conditions in the TT-gauge, is given by

$$h_{ij}(t, \vec{x}) = 4G\Lambda_{ij,kl}(\hat{n}) \int d^3x' \frac{1}{|\vec{x} - \vec{x}'|} T_{kl}(t - |\vec{x} - \vec{x}'|, \vec{x}'), \quad (1.59)$$

where $\hat{n} = \vec{x}/|\vec{x}|$, and $\Lambda_{ij,kl}$ is the projector tensor

$$\Lambda_{ij,kl}(\vec{n}) = P_{ik}P_{jl} - \frac{1}{2}P_{ij}P_{kl}, \quad (1.60)$$

defined in terms of $P_{ij}(\vec{n}) = \delta_{ij} - n_i n_j$. The integral in equation (1.59) corresponds simply to the convolution of the source with the retarded Green function for the wave equation (1.19). The projection into the TT-gauge is used in order to get rid of spurious gauge modes, but one must bear in mind that this is only possible in regions not containing matter fields.

Far away from the source, the field vector \vec{x} is much larger than the vector \vec{x}' parametrizing the source, therefore we can expand $|\vec{x} - \vec{x}'|$ as

$$|\vec{x} - \vec{x}'| \simeq r - \vec{x}' \cdot \hat{n} + \mathcal{O}\left(\frac{d^2}{r}\right), \quad (1.61)$$

where $r = |\vec{x}|$ and d is the typical size of the source. Thus we can expand the source as

$$\begin{aligned} T_{kl}(t - |\vec{x} - \vec{x}'|, \vec{x}') &\simeq T_{kl}(t - r + \vec{x}' \cdot \hat{n}, \vec{x}') \\ &\simeq T_{kl}(t - r, \vec{x}') + x'^i n^i \partial_0 T_{kl}(t - r, \vec{x}') + x'^i x'^j n^i n^j \partial_0^2 T_{kl}(t - r, \vec{x}') + \dots \end{aligned} \quad (1.62)$$

The gravitational field generated by the source is assumed to be sufficiently weak so that the linearized approximation is justified. For a self-gravitating system, this condition also implies that the internal motions be small, and the typical orbital speed of the source v satisfies $v \ll 1$. Since every power x^m contributes with an order $\mathcal{O}(d^m)$ and each time derivative gives a factor $\mathcal{O}(\omega_S)$, where ω_S is the typical frequency of the source satisfying $\omega_S \sim v/d$, then we see that equation (1.62) is an expansion carried in powers of the source speed v . Defining the momenta of the stress tensor T^{ij} as

$$S^{ij}(t) = \int d^3x T^{ij}(t, \vec{x}), \quad (1.63)$$

$$S^{ij,k}(t) = \int d^3x T^{ij}(t, \vec{x}) x^k, \quad (1.64)$$

$$S^{ij,kl}(t) = \int d^3x T^{ij}(t, \vec{x}) x^k x^l, \quad (1.65)$$

and so on and so forth, then we can express (1.59) as

$$h_{ij}(t, \vec{x}) = \frac{4G}{r} \Lambda_{ij,kl}(\hat{n}) \left[S^{kl}(t - r, \vec{x}') + n_m \dot{S}^{kl,m}(t - r, \vec{x}') + \frac{n_m n_p}{2} \ddot{S}^{kl,mp}(t - r, \vec{x}') + \dots \right]. \quad (1.66)$$

We can now express the momenta of T^{ij} in terms of the momenta of T^{00} and T^{0i} using the conservation law $\partial_\mu T^{\mu\nu} = 0$. Indeed, we can define the momenta of the energy density T^{00} as

$$M = \int d^3x T^{00}(t, \vec{x}), \quad (1.67)$$

$$M^i = \int d^3x T^{00}(t, \vec{x}) x^i, \quad (1.68)$$

$$M^{ij} = \int d^3x T^{00}(t, \vec{x}) x^i x^j, \quad (1.69)$$

and so on, as well as the momenta of the linear momentum T^{0i} as

$$P^i = \int d^3x T^{0i}(t, \vec{x}), \quad (1.70)$$

$$P^{i,j} = \int d^3x T^{0i}(t, \vec{x}) x^j, \quad (1.71)$$

$$P^{i,jk} = \int d^3x T^{0i}(t, \vec{x}) x^j x^k, \quad (1.72)$$

and so on and so forth. Then the conservation law (1.20) allow us to find, after straightforward computations, that

$$S^{ij} = \frac{1}{2} \ddot{M}^{ij} \quad (1.73)$$

and similarly for the higher orders in (1.66). For instance, the next to leading order is given by

$$\dot{S}^{ij,k} = \frac{1}{6} \ddot{M}^{ijk} + \frac{1}{3} \left(\ddot{P}^{i,jk} + \ddot{P}^{j,ik} - 2\ddot{P}^{k,ij} \right), \quad (1.74)$$

so that we can express equation (1.66) in terms of the momenta of the energy density and the linear momentum.

In particular, the main contribution to gravitational radiation, in an expansion on v , comes from the source's quadrupole

$$Q^{ij} \equiv \int d^3x \rho(t, \vec{x}) \left(x^i x^j - \frac{1}{3} r^2 \delta^{ij} \right), \quad (1.75)$$

where $\rho(t, \vec{x}) = T^{00}$ is the source's density and $r = |\vec{x}|$. Indeed, the tensor M^{ij} can be decomposed into irreducible representations of the rotation group as

$$\begin{aligned} M^{ij} &= \left(M^{ij} - \frac{1}{3} \delta^{ij} M_{kk} \right) + \frac{1}{3} \delta^{ij} M_{kk} \\ &= Q^{ij} + \frac{1}{3} \delta^{ij} M_{kk}, \end{aligned} \quad (1.76)$$

and clearly the trace $\frac{1}{3} \delta^{ij} M_{kk}$ will vanish as it contracts with the tensor $\Lambda_{ij,kl}$. Thus, it is possible to show that at a distance r far away from the source the emitted gravitational field is, again in the TT-gauge, given by

$$[h_{ij}(t, \vec{x})]_{\text{quad}} = \frac{2G}{r} \Lambda_{ij,kl}(\hat{n}) \ddot{Q}_{kl}(t-r), \quad (1.77)$$

and higher-order multipoles contribute with higher powers of the small parameter v . The power radiated that is associated to this moment is given by

$$\mathcal{P}_{\text{quad}} = \frac{G}{5} \langle \ddot{Q}_{ij} \ddot{Q}^{ij} \rangle. \quad (1.78)$$

This formalism already allows us to understand that, due to the radiation of energy from the source there is some energy carried away by the gravitational modes, and therefore the orbital motion will shrink. To illustrate this point, let us consider a binary system composed of two masses m_1 and m_2 , following a circular orbit of radius r_{12} . Then, the energy of the binary system $E_{\text{binary}} = E_{\text{kinetic}} + E_{\text{potential}}$ is given by

$$E_{\text{binary}} = -\frac{G m_1 m_2}{2r_{12}}. \quad (1.79)$$

Since the radiated energy is being drawn from this energy, we have that $\dot{E}_{\text{binary}} = -\mathcal{P}_{\text{quad}} < 0$, which implies $\dot{r}_{12} < 0$, so that the orbital radius diminishes as well.

Let us stress that the fact that the leading contribution to gravitational radiation comes from a quadrupole moment, instead of a monopole or dipole moment, is due to the conservation of energy and momentum. Indeed, one can easily show that the energy-momentum conservation law (1.20) implies that

$$\dot{M} = 0 \quad \text{and} \quad \dot{P}^i = 0. \quad (1.80)$$

In a more qualitative way, a spherically symmetric system such as a pulsating spherically symmetric star could not radiate since the gravitational potential far away from the source depends only on the star's mass, and as such it will not be affected by the monopole pulsation. Thus, perturbations in the metric can not be propagated from a spherically symmetric source due to mass conservation. The same argument forbids monopole radiation in electromagnetism, since the “monopole” term is the electric charge and is protected by a conservation law. However, while in electromagnetism the leading radiation term is dipolar since there is no conservation law protecting the electric dipole, in our case the “gravitational dipole” is proportional to the linear momentum of the source. Thus, conservation of momentum forbids dipole radiation in general relativity in a similar fashion as to monopole radiation. This means, in particular, that any gravitational system which is symmetric with respect to a given axis will not be able to emit gravitational waves.

1.6 Gravitational wave astronomy

1.6.1 Binary pulsars

The first experimental confirmation of the existence of gravitational waves came with the discovery in 1974 of the first binary pulsar by Hulse and Taylor, PSR J1915+1606 [5], and the subsequent long term study of its properties, leading particularly to the measurement of the binary's orbital decay [6]. This measurement has been found to be in excellent agreement with the prediction for the binary's energy loss due to the emission of gravitational waves as computed by the quadrupole formalism of general relativity [6].

One of the key features of pulsars is that they can be used as extremely precise clocks [7]. In order to achieve this it is necessary to take into account the short-term variability of pulses, called the “weather” of the pulsar, and which can be treated as a noise in the source. Although the profile of each pulse within the same pulsar may wildly differ, the averaged profile of many pulses tends to remain very stable. Thus, using this averaged profile as a reference template so as to eliminate the effects of the weather of the pulsar, the time-of-arrival (TOA) of individual pulses can be computed from timing models. It is then observed that, if we average over several pulses, then the pulsar behaves as an accurate clock (see e.g., [7, 8] for details).

In the case of PSR J1915+1606, the orbital parameters of the binary system are nowadays very well known after more than 30 years of observation [6]. In particular, the pulsar was found to have a (spin) period close to 59 ms, but it has a periodic modulation due to the Doppler effect induced by its orbital motion. From this modulation it is possible to find, with good accuracy, an orbital period $P_b \sim 8$ hours, implying thus an orbital velocity of the order of $v \sim 10^{-3}c$.

At a Newtonian level, the binary's binding energy E_b can be defined as

$$\begin{aligned} E_b &= -\frac{G\mu m}{2a}, \\ &= -\frac{\mu}{2}(Gm)^{2/3} \left(\frac{P_b}{2\pi}\right)^{-2/3}. \end{aligned} \tag{1.81}$$

where a is the semi-major axis, $\mu \equiv m_1 m_2 / m$ is the reduced mass and $m \equiv m_1 + m_2$ is

the total mass. In the second line we used the Kepler's third law, $\left(\frac{P_b}{2\pi}\right)^2 = \frac{a^3}{Gm}$. Then, the energy carried away by gravitational waves can be related to the rate of change of the gravitational binding energy through the balance law

$$\dot{E}_b = -\mathcal{P}_{\text{quad}}, \quad (1.82)$$

where $\mathcal{P}_{\text{quad}}$ is the gravitational wave flux given by (1.78), and can be thus computed from the measured properties of the binary. This energy loss can in turn be easily related to the rate of change of the orbital period P_b , using equation (1.81), as

$$\frac{\dot{P}_b}{P_b} = -\frac{3}{2} \frac{\dot{E}_b}{E_b}. \quad (1.83)$$

The rate of change \dot{P}_b is one of the post-Keplerian parameters of the orbit [9]. These results remain correct when computing the energy loss within a post-Newtonian scheme, without invoking any energy-balance argument [10].

In the case of the Hulse-Taylor binary pulsar, the masses of the pulsar and its companion are found to be [6] $m_p = 1.4414(2)M_\odot$ and $m_c = 1.3867(2)M_\odot$, and thus the Keplerian semi-major axis is $a \simeq 2.2 \times 10^9 \text{m} \simeq 3R_\odot$, where R_\odot is the solar radius. These masses can be computed from the advance rate of the periastron $\langle \dot{\omega} \rangle$, averaged over one orbital period [10]. From the given masses and the relatively short distance by which they are separated, and from the fact that no eclipse is observed, it is believed that the pulsar's companion is also a neutron star. This conclusion thus validates a model where the masses are taken to be point particles.

The evolution of the orbital period is then given by the formula [9, 10, 2]

$$\dot{P}_b = -\frac{192\pi G^{5/3} m_p m_c (m_p + m_c)^{-1/3}}{5c^5} \left(\frac{P_b}{2\pi}\right)^{-5/3} \left(1 + \frac{73}{24}e^2 + \frac{37}{96}e^4\right), \quad (1.84)$$

where $e \simeq 0.61$ is the eccentricity of the orbit. This is a consequence of equation (1.83). The comparison between this prediction and the actual rate of change of the binary's orbital period $(\dot{P}_b)_{\text{measured}}$ is shown in figure 1.1.

More precisely, after taking into account for the relative motion between the Earth and the pulsar due to the Galaxy's rotation, the ratio between the measured orbital period rate and the prediction of general relativity is [11]

$$(\dot{P}_b)_{\text{measured}}/(\dot{P}_b)_{\text{GR}} = 1.0013(21). \quad (1.85)$$

This provides a first test of general relativity, and a proof of the emission of gravitational waves by the system. Let us recall that \dot{P}_b is a function of time, and that this given estimate corresponds to data released in 2004 by Weisberg and Taylor [6].

In general, the remarkable rotational stability of pulsars and the precision of timing models allow one to dig further into the physics of the system [12]. Indeed, even if a given pulsar were a perfectly stable periodic source, the times-of-arrival of its pulses would be modulated by several factors such as the motion of the Earth around the sun, the motion of the solar system in the Galaxy and other peculiar motion effects. Most importantly for us, pulsar timing allows us to measure some general-relativistic effects [12, 13, 14]. More precisely, the

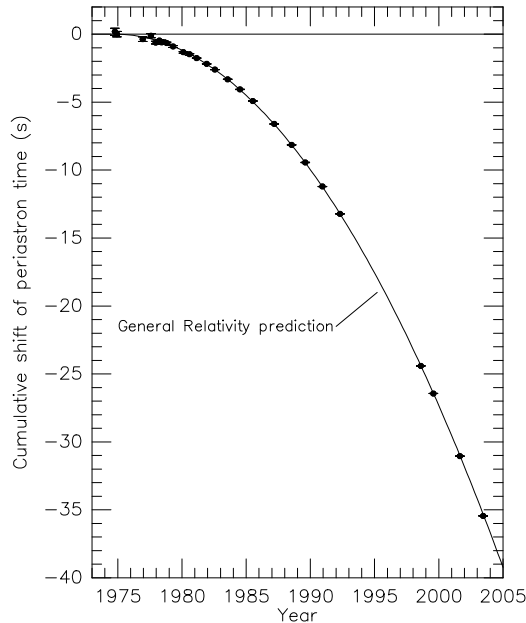


FIGURE 1.1 – Comparison between the orbital decay prediction for PSR B1913+16, using general relativity (in solid line), and the measured orbital decay (in points). The data was taken at the Arecibo radio telescope between 1975 and 2005. Figure taken from [6].

modulations to the time-of-arrival of pulses coming from a pulsar can be decomposed as a sum of effects : the Roemer time delay due to the motion of the Earth in the solar system, the Shapiro time delay due to the effects of the gravitational field on the propagation of light, and the Einstein time delay due to the fact that the measurement concerns proper time instead of coordinate time (see e.g., [2]).

1.6.2 Gravitational wave interferometers

The main idea behind interferometric detectors is to exploit the great accuracy of interferometers at measuring changes of interfering patterns between its arms. Then, as it was pointed out in section 1.3, one can relate the time of flight shift to the amplitude of the gravitational wave h_{ij} through equation (1.42). Although this idea is quite simple, the implementation of it took more than 40 years of preparation and a huge collaboration to realize it in practice.

It can be shown (see [2] for instance), that in order to detect gravitational waves at frequency f_{gw} , the optimal length L of a Michelson interferometer is given by

$$L \simeq 750 \text{ km} \left(\frac{100 \text{ Hz}}{f_{\text{gw}}} \right). \quad (1.86)$$

In the case of Earth-based detectors such as the Laser Interferometer Gravitational-Wave

Observatory (LIGO) and the Virgo interferometer, one is therefore forced to implement resonant Fabry-Perot cavities in each arm so as to reach an effective length of a few hundred km out of the 3-4 km of the actual instrument arms. This means that LIGO is optimized to detect signals around 100 Hz, and among possible sources in this frequency band we find stellar mass black hole binaries [15] and neutron star binaries [16], and more broadly stellar mass objects, for instance pulsars [17] and supernovae [18] at low redshift [19]. See [20] for prediction rates of compact binary coalescences. Among the main complexities of the LIGO-Virgo project, we can mention the mechanical stability of the mirrors reflecting the laser beams at each end, the implementation of the Fabry-Perot cavities, the vacuum pipe required for the cavities, and of course the problem of minimizing the noise coming from of a wild variety of sources. See [21] for more details on these technical issues. The general optical layout of the LIGO interferometers is represented in figure 1.2. Given this setup, the

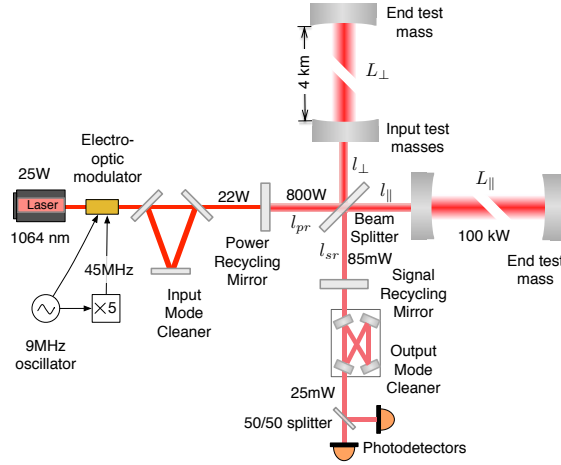


FIGURE 1.2 – Scheme of the optical layout for the LIGO interferometers. Figure extracted from [21].

actual measured signal corresponds to $h(t) = D^{ij}h_{ij}(t)$, where D^{ij} is a tensor characterizing the geometrical features of the detector.

On the 14th of September 2015 at 09 :50 :45 UTC, the LIGO-Virgo collaboration detected the first black hole binary merger in history [22], being thus the first direct detection both of gravitational waves and of the black holes that produced them. While Virgo was not online yet, both of LIGO's observatories captured the signal in their data, and the significance of the detection is estimated to 5.1 sigma. The reconstructed waveform $h(t)$ is shown in figure 1.3, and it corresponds to the coalescence of two black holes of masses $36^{+5}_{-4}M_{\odot}$ and $29^{+4}_{-4}M_{\odot}$, resulting in a final black hole of mass $62^{+4}_{-4}M_{\odot}$, radiating thus an energy equivalent to $3^{+0.5}_{-0.5}M_{\odot}$ [23]. This event being the first detection was remarkable, since at the time it was not widely expected to find black holes with such high masses [23, 24]. Since then, five more events have been found and released within the first two runs O1 and O2 of the LIGO-Virgo collaboration, so that our data for (stellar mass) black hole population as well as for formation models has significantly improved [25, 24]. Furthermore, since 2017 the Virgo interferometer joined LIGO in the search of gravitational wave signals, allowing for the first triple detection of a binary black hole merger (GW170814). The Virgo participation was also essential for the spatial localization of GW170817, leading to the first multi-messenger detection of a

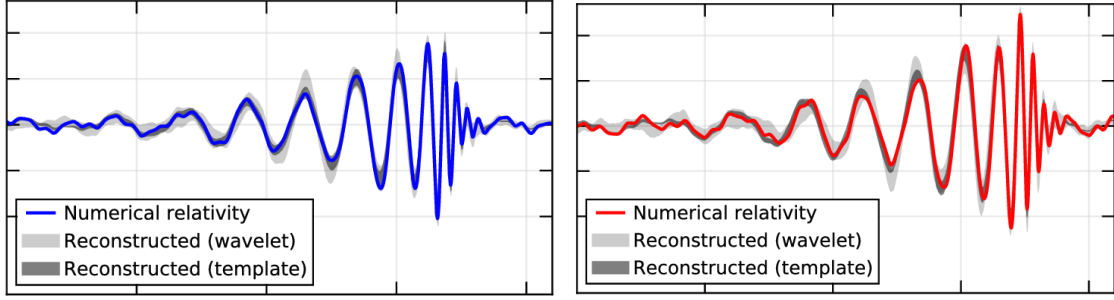


FIGURE 1.3 – Reconstructed waveform $h(t)$ for the detection of GW150914 in Livingston (left) and Hanford (right). Figures taken from [23]

neutron star - neutron star merger [26]. Indeed, an associated Gamma Ray Burst (GRB) was observed by the Fermi Gamma-ray Burst Monitor, just 1.7s after GW170817 [27]. This double detection allowed for further scrutiny in the electromagnetic sector, leading to the discovery of a kilonova and its host galaxy located at 40_{-14}^{+8} Mpc distance from us [28]. The nearly coincident time of arrival of the two signals represents a strong constraint on modified theories of gravity. Indeed, this result implies that the gravitational (tensorial) modes propagate at the same speed as the photons, to within 1 part in 10^{15} .

These detections have been possible thanks to a deep understanding of the nature of the expected signal, as well as of the functioning of the detectors, and more precisely of their noise spectra. If we model the detector signal $s(t)$ as composed by the sum of the gravitational wave signal $h(t)$ and some noise $n(t)$, as

$$s(t) = h(t) + n(t), \quad (1.87)$$

then the problem consists of distinguishing $h(t)$ from $n(t)$. The noise can be characterized by measuring the spectral noise sensitivity $S_n(f)$ as a function of the frequency f , which is shown in figure 1.4. As can be seen from figure 1.4, the detector has a peak of sensitivity around 100 Hz. At lower frequencies, the detector's performance is limited by seismic and Newtonian noise, while at high frequencies the main limitation comes from the quantum shot noise of the lasers. Thus, the observations below 1-10 Hertz would be difficult for Earth-based detectors even if we could further increase the effective arm-length of the interferometers, as seismic and Newtonian noise will still be there.

The difficulty of gravitational wave detection comes from the fact that we expect to have $n(t) \gtrsim h(t)$, so that we must be able to extract an extraordinarily small strain amplitude, typically of the order of $h \sim 10^{-21}$, from a comparatively large noise background. In this context, digging out the gravitational wave signal requires detailed knowledge of the typical scales of variation of the noise $n(t)$ as well as the expected waveform for $h(t)$. More precisely, in order to extract the signal from the noise one can cross-correlate the output of the detector $s(t)$ with a bank of templates that predicts the form the signal according to the equations of general relativity. This match-filtering procedure [29, 30, 31, 32] has the goal of finding a template with the largest correlation with the output of the detector. The methods employed to produce the templates depend on the particular source that one is aiming to detect [33]. Thus, templates banks [34] can be produced via post-Newtonian theory [35], numerical relativity (e.g. [36, 37] or a perturbation theory approach [38] (e.g. the self-force

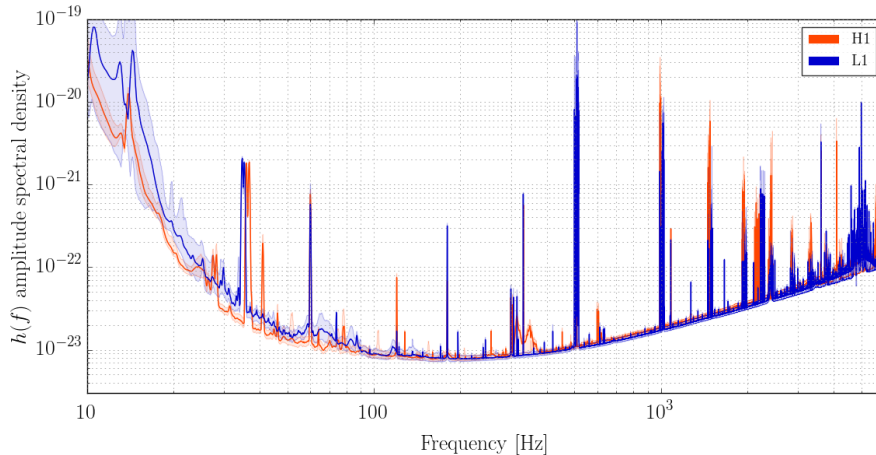


FIGURE 1.4 – The average spectral noise sensitivity of the Advanced LIGO detectors measured in order to determine the significance of GW150914. The curve in red corresponds to Hanford and in blue to Livingston. Figure taken from [23].

formalism [39, 40]).

In the case of a space-based detector such as the Laser Interferometer Space Antenna (LISA), there would be no seismic noise limiting the frequency band from below. Moreover, in space one is allowed to use larger arms, and indeed the project intends to place its satellites at a distance of 2.5 million km, and connecting them by six laser links [41]. The LISA project builds upon the success of the LISA Pathfinder mission [42], and it is expected to be launched around ~ 2030 [41]. This would open a new window in the frequency range from 10^{-4} Hz up to 10^{-1} Hz, corresponding to the heaviest compact objects in the universe. In particular, supermassive black holes ranging from $10^4 - 10^5$ up to $10^7 M_{\odot}$ are expected to be present at the center of almost every massive galaxy in the local universe [43, 44, 45, 46], and therefore when two galaxies merge we expect their black holes to merge as well [47, 48, 49]. This merging would produce signal in the LISA band [41]. According to their masses they could be visible up to $z \sim 20$ [50], or even larger if they exist. The limitation here is due to astrophysics and not to the instrument. Otherwise said, supermassive black holes are not expected to exist above redshift $z \sim 20$ [50, 51], yet LISA has no intrinsic limitation to detect sources of a larger redshift. Another important source for LISA are galactic binaries, and in particular white dwarf binaries, for which around 10000 of them should be detectable in the galaxy alone [52, 53]. These compact binaries emit a continuous and nearly monochromatic gravitational wave signal. A few of them have already been observed in the electromagnetic band, and could be used as verification binaries [54, 55, 56]. We know that these will be detectable by LISA, but we expect many more to be visible. In fact, some $\sim 10^5$ binaries are expected to be individually resolved by LISA [57, 58]. In addition to these resolvable sources, we also expect to observe a background signal due to those of the white dwarf binaries which will not be resolved by LISA [52, 58].

A third type of source for LISA are extreme mass ratio inspirals (EMRIs) [59]. These are black holes binaries where one of the components is a supermassive black hole of mass of $10^5 - 10^6 M_{\odot}$ and the other is a stellar massive black hole of a mass of $\sim 10 - 10^2 M_{\odot}$.

EMRIs evolve very slowly and they spend a large number of orbital cycles in the LISA band before merger [60, 61], allowing for a great accuracy in the measurements. In fact, beside the standard binary parameters such as the mass and spin of its components, EMRIs could be used to measure higher multipoles of the supermassive black hole allowing thus for tests on deviations of the Kerr metric [62]. This provides a test for the no-hair theorem of general relativity, which states that all stationary black hole solutions to the Einstein equations (and the Maxwell equations of electromagnetism) can be completely characterized by their mass and angular momentum (and electric charge, if any) [63, 64, 65]. For more details on EMRIs, see e.g. [40].

Finally, with this new gravitational wave observatory one would be able to study the early phases of inspiraling binaries much before their merger, entering the LISA frequency band months or even years before disappearing for a few weeks and reentering in the LIGO frequency band, so that a follow up could be set up between space-based and ground-based detectors [66]. More precisely, LIGO-Virgo binaries will spend some time in the LISA band before disappearing and entering the LIGO-Virgo band instead. Using the measurements from LISA one could predict the entry to the LIGO-Virgo band within 10 seconds [67]. More interesting for this work though, is the possibility of constraining the dipole emission from LIGO-Virgo binary black holes through LISA [68]. Indeed, most extensions of general relativity, and particularly Lorentz violating gravity, predict the violation of the strong equivalence principle [69, 70, 10]. This effect is measured by a new parameter, called the sensitivity σ , that depends on the structure of each body as well as of the gravitational theory. The physical explanation of the sensitivity will be explored in further detail in chapter 4. This deviation from the universality of free fall leads to a modification of the flux \dot{E}_{GW} emitted by a binary system as compared to the flux predicted by general relativity \dot{E}_{GR} . More precisely, generically there is a new dipole contribution modifying Einstein's quadrupole formula. The gravitational wave flux can be expanded in a post-Newtonian scheme as [71, 72]

$$\dot{E}_{\text{GW}} = \dot{E}_{\text{GR}} \left[1 + B \left(\frac{v}{c} \right)^{-2} + \mathcal{O}(\sigma_1, \sigma_2) + \mathcal{O} \left(\frac{v^2}{c^2} \right) \right], \quad (1.88)$$

where σ_1 and σ_2 are the bodies' sensitivities and $B \propto (\sigma_1 - \sigma_2)^2$ is a parameter whose precise form can be computed for each given theory. Since the flux modification enters as a $\left(\frac{v}{c} \right)^{-2}$ correction, i.e. is a -1PN correction, it can actually dominate the flux emission during the early inspiral, provided that the difference $|\sigma_1 - \sigma_2|$ is sufficiently different from zero. Such an energy loss via a new channel could dramatically reduce the time duration of the inspiral phase, and therefore the arriving time of the binary into the LIGO-Virgo band. Consequently, measuring the gravitational wave flux of binaries allows us to constrain the parameter space of theory under study via the measured bounds on B . Let us remark that, since the sensitivities of stellar objects such as neutron stars and black holes have no reason to be the same, we have that bounds on B obtained from a binary pulsar system are independent from bounds obtained by a binary black hole system. Otherwise said, this is a test of the strong equivalence principle and the universality of free fall. In this way the stellar mass binary black holes in the range of the current LIGO-Virgo detections, if detected prior to their merger by LISA, can give bounds on B of the order of $|B| \lesssim 10^{-8}$ when observed by LISA alone or $|B| \lesssim 10^{-9} - 10^{-8}$ when observed both by space and ground-based detectors

[68]. This is illustrated in figure 1.5, where the aforementioned sources are displayed in the horizontal axis and different points correspond to different observation modes.

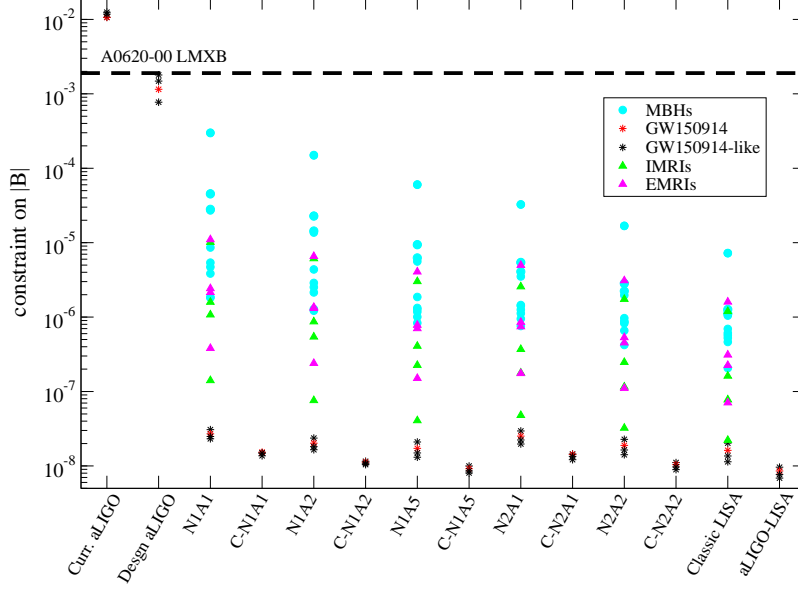


FIGURE 1.5 – 1σ constraints on the parameter B from various black hole binary sources. Among others, stars and plusses stand for GW150914-like BH binaries, filled circles stand for massive BH binaries, and filled triangles stand for EMRIs/IMRIs (i.e., extreme/intermediate mass ratio inspirals). Different points correspond to different instrument configurations : “Curr. aLIGO” stands for LIGO at the time of GW150914, “Design aLIGO” stands for LIGO at design sensitivity, “NxAx” are various six-link LISA configurations, where N1/N2 are respectively pessimistic/target low frequency noise, and A1/A2 are respectively 1Gm/2Gm arms, “Classic LISA” corresponds to a six-link 5-Gm arms and low-frequency noise at the target level design, “C-NxAx” stands for a joint observation LIGO-LISA, and finally “aLIGO-LISA” stands for joint observations between LIGO and Classic LISA [68]. The dashed line stands for the current constraint on vacuum dipole radiation from the low mass x-ray binary A0620-00 [73]. Figure extracted from [68].

The same approach works for either supermassive black hole binaries or extreme (intermediate) mass-ratio inspirals (i.e., systems composed of a stellar (intermediate) mass compact object orbiting a supermassive black hole) as they can enter LISA’s detection frequency band at much earlier stages [66], where dipole emission can become predominant, and this can lead to bounds on B of up to $|B| \lesssim 10^{-7} - 10^{-6}$ for the former, and $|B| \lesssim 10^{-8} - 10^{-7}$ for the latter [68].

Let us remark that, in the case of LIGO-Virgo detectors, this strategy would not prove very efficient, as the black hole binaries enter into the detector’s frequency range at a relatively late stage where $v \sim c$, and thus the bounds on B are only of the order of $|B| \lesssim 10^{-2}$ [74]. This is reflected in figure 1.6, where we can see that binary black hole mergers (in this case GW150914) are more efficient at testing higher v/c orders than pulsars, while for lower PN orders it is the binary pulsars that lead to the most stringent constraint [75].

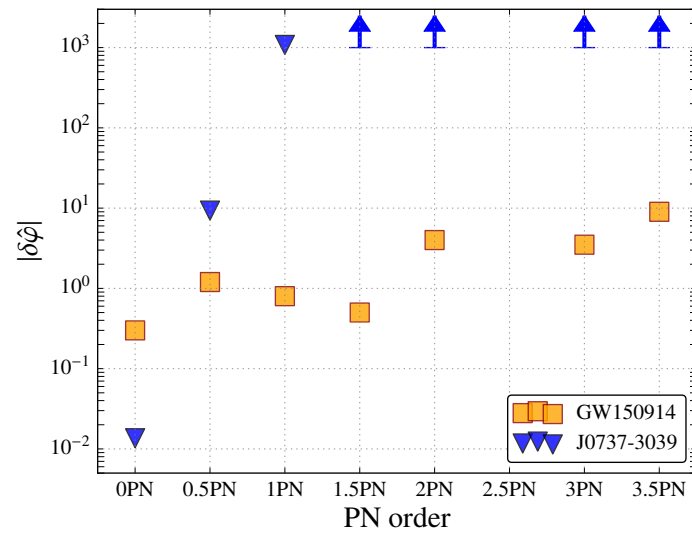


FIGURE 1.6 – (Left panel) Extracted from figure 6 in [75]. 90% upper bounds on the fractional variations of the PN coefficients with respect to their GR values. In orange squares are the bounds obtained from the single-parameter analysis of GW150914. In blue triangles are the bounds extrapolated exclusively from the measured orbital-period derivative \dot{P}_b of the double pulsar J0737-3039 [76].

2 – Lorentz Symmetry and its violation

This thesis aims to test Lorentz symmetry in gravity, particularly by using gravitational waves from black holes. Naturally then, a brief review on this cornerstone principle of Physics is appropriate.

First, in order to motivate the study of Lorentz symmetry in gravity, we will begin by recalling its origin and definition from special relativity in section 2.1. We will also stress in that section the fundamental role of Lorentz invariance in the Standard Model of Particle Physics. In section 2.2 we will argue that there are two empirical principles laying on the foundations of gravitational theory : the Einstein’s principle of equivalence and the principle of special relativity. There we will describe the components that build up the equivalence principle, making clear the role of Lorentz symmetry as one of its ingredients, and therefore its place on the foundations of gravitational theory. After that we will briefly review the diverse class of experiments giving credit to these ideas. We will conclude this section arguing that, based on these well-tested principles, extensions to general relativity should belong to the class of theories called metric theories of gravity.

Next, following a quick discussion on why we should care about testing Lorentz symmetry in gravity, we will show how Lorentz violations can be introduced respecting empirical foundations and mathematical requirements. More specifically, in sections 2.3 and 2.4 we will break Lorentz invariance by introducing a dynamical time-like vector field in two different metric theories of gravity, Einstein-æther and khronometric theory. We will show how the latter is related to the low-energy limit of a proposal for quantum gravity, namely Hořava-Lifshitz gravity [77, 78]. Before engaging into any analytical work, in section 2.5 we will pause to discuss the current state of the art regarding observational constraints on Lorentz violations for these theories.

We will end this chapter by exploring some general features concerning Lorentz-violating gravity in section 2.6, and in particular regarding black holes in these theories. This last section will lay the foundations for the chapters that follow.

2.1 Lorentz symmetry in non-gravitational physics

The principle of independence of the laws of Nature with respect to the observer’s (uniform) motion represented a milestone in the history of Physics.

In order to explicitly see how Lorentz symmetry arises from this principle, we should start from the beginning of it all : let us introduce the notion of inertial frame. By definition, an inertial frame is a reference frame where the motion of bodies that are not subject to any external force is constant, i.e., they move with constant velocity. It follows then that any reference frame moving with constant speed with respect to an inertial frame will also be an inertial frame itself. Now, experience seems to show (see section 2.2) that Nature does satisfy the relativity principle, which states that the laws of Nature are the same in all inertial frames. This means that the equations describing Nature do not change when we transform spatial and time coordinates by passing from one inertial frame to another.

The first appearance of this principle dates back to Galileo [79], who stated it for the laws of classical mechanics. Galileo’s relativity principle can be stated in a mathematical way, requiring that the laws of mechanics be invariant with respect to a set of coordinate transformations called Galilean transformations. Let us consider an inertial frame S describing events by the set of coordinates $\{t, x, y, z\}$, where t is the time and (x, y, z) are Euclidean spatial coordinates. Let us also consider another reference frame S' described by an analogous set of coordinates $\{t', x', y', z'\}$. Let us suppose that their x and x' axes coincide, that S' is moving with respect to S with the speed v along the x axis, and let’s further suppose that both origins coincide at $t = t' = 0$ and that the y' and z' axes are parallel to the y and z axes, respectively. Then, S' is an inertial frame as well and the Galilean transformation between them would be given by the equations

$$t' = t, \tag{2.1a}$$

$$x' = x - vt, \tag{2.1b}$$

$$y' = y, \tag{2.1c}$$

$$z' = z. \tag{2.1d}$$

These very simple transformations laws are at the heart of Newtonian mechanics and they are true to high accuracy in the non-relativistic regimes, defined as such that $v \ll 1$ (let us recall that we use units such that $c = 1$). Unfortunately though, the laws of electromagnetism were found not to be invariant with respect to these transformations, and in particular Galileo’s relativity principle would imply a dependence of the speed of light with respect to the observer’s reference frame. A possible interpretation was given in terms of a putative “aether medium” where the electromagnetic waves would propagate (which has absolutely nothing to do with the “aether field” to be introduced below). The experiments finding no dependence of the speed of light with respect to the observer’s state of motion, such as Michelson-Morley’s interferometer experiment, were a strong clue towards the modern form of the relativity principle.

The laws of electromagnetism were in fact found to be invariant under another set of transformations, found by Lorentz and Poincaré. Based upon this new invariance, Einstein proposed his theory of special relativity in 1905. It enclosed Newtonian mechanics as a low-speed (non-relativistic) limit, and shed a new light on the electromagnetic interaction as well. Taking

the same definitions for the inertial frames S and S' as above, the relation between their respective coordinates is given now by the Lorentz transformations :

$$ct' = \gamma(t - vx), \quad (2.2a)$$

$$x' = \gamma(x - vt), \quad (2.2b)$$

$$y' = y, \quad (2.2c)$$

$$z' = z, \quad (2.2d)$$

where we introduced the Lorentz factor between the two frames,

$$\gamma \equiv \frac{1}{\sqrt{1 - v^2}}. \quad (2.3)$$

This transformation is also called a ‘‘Lorentz boost’’ from the inertial frame S to S' . Thus, non-gravitational physics is, within experimental accuracy, invariant under these transformations, and the symmetry associated to this invariance is what we refer to Lorentz symmetry. We note that time and space coordinates get mixed by these transformations, breaking down the hypothesis of a ‘‘universal time flow’’ that is implicit in the transformations (2.1). Furthermore, it follows that three-dimensional vectors such as the velocity \mathbf{v} are invariant quantities only in the non-relativistic regimes.

Let us remark that, if we consecutively apply two Lorentz boosts \mathcal{L}_1 and \mathcal{L}_2 associated respectively to the velocities \mathbf{v}_1 and \mathbf{v}_2 , one after the other, then the resulting transformation is equivalent to a single Lorentz boost \mathcal{L}_3 associated to the speed \mathbf{v}_3 , given by their composition $\mathcal{L}_3 = \mathcal{L}_2 \circ \mathcal{L}_1$, but for which $\mathbf{v}_3 \neq \mathbf{v}_1 + \mathbf{v}_2$. That is to say, velocities are no longer added linearly as in the non-relativistic case. Furthermore, the inverse of the transformation boosting S' to S would be simply obtained by replacing v into $-v$ in (2.2). And finally, it is clear that by setting v to zero we obtain the identity transformation. Thus, Lorentz transformations behave as a group (having a composition rule, as well as an inverse and identity transformations), and we can use the tools of group theory to further study Lorentz symmetry.

From the point of view of group theory, if we assume that Lorentz invariance is a fundamental symmetry of Nature, then physics must be described in terms of representations of the Lorentz group. In this context, a major role is played by irreducible representations, and in the case of the Lorentz group, the different types of irreducible representations are classified by none other than their spin [80]. Thus at this stage we can readily appreciate that Lorentz invariance is at the core of all particle physics, and in particular of the Standard Model of particle physics, as the construction of all its fields lies heavily on Lorentz invariance.

We could even go further since, from a field theory perspective [81, 82, 83], it would be enough to start from quantum mechanics and Lorentz symmetry to be led to the conclusion that a massless spin-1 particle (the photon) must couple to conserved charges, whereas a massless spin-2 particle (the graviton) must couple to all sources of energy and momentum with the same strength (satisfying thus the equivalence principle). At any rate, it is manifest that Lorentz invariance plays a major role in theoretical physics and the purpose of this section was to expose this for the matter sector.

2.2 Lorentz symmetry and the equivalence principle

We now turn our attention to gravity. The indisputable starting point here is the equivalence principle, for it lies deep at the heart of gravitational theory.

In its original form, it states that the motion of freely falling objects immersed in an external gravitational field is the same for all bodies, regardless of their internal structure and composition. This statement is also referred to as the Universality of free fall.

One can also reformulate this principle in a more similar way to what Galileo and Newton did, stating that the inertial mass of a body m_I , as it enters into Newton's second law, is the same as (or proportional to) its gravitational mass m_G , as it couples to the gravitational field, for instance. Nowadays, this corresponds to what we call the weak equivalence principle (WEP). Thus the ratio m_I/m_G would be a constant independent of the test body's composition and we simply talk of its "mass".

In its modern form [84], the Einstein equivalence principle contains the weak equivalence principle as an ingredient, but goes further by stating that both local position invariance (LPI) and local Lorentz invariance (LLI) are also true. Local Lorentz (position) invariance is the statement that the outcome of any non-gravitational experiment is independent of the velocity (position) of the freely-falling frame in which it is performed. Note that while the universality of free fall is a purely mechanical statement, the principles of LPI and LLI are of a much more universal character since they take into account all observable phenomena, save gravitational experiments. Let us remark that, at least in principle, one could conceive the property of local Lorentz invariance of non-gravitational experiments to be independent to the property of Lorentz invariance in gravitational experiments, and the issue of an underlying interdependence will be discussed in 2.2.1. There is wide experimental evidence in favor of the Einstein equivalence principle, coming from various tests of each its three defining statements (WEP, LLI and LPI). First, deviations from the weak equivalence principle have been tightly constrained through Eötvös-type experiments. The main idea behind this sort of experiment is to look for differences in the ratio of inertial and gravitational masses, m_I/m_G , for laboratory-sized bodies (i.e., whose gravitational binding energy is negligible) of different composition. Indeed, if the motion of two test bodies immersed in a gravitational field g were to differ, then one could state that their inertial and gravitational masses are no longer equal, and their accelerations a are given by $m_I a = m_G g$. Thus, measuring a difference in acceleration corresponds to measuring a difference in gravitational masses. Since the inertial mass m_I of each test body is composed of different forms of mass-energy, such as rest energy, electromagnetic self energy, et cetera, if any of those were to contribute in a different way to the gravitational mass m_G , this would result in a different acceleration a . One could conceive a first order correction in the composing mass-energies to the inertial mass expressed as

$$m_G = m_I + \sum_A \eta^A E^A, \quad (2.4)$$

where E^A is the self energy of the body generated by the interaction A . The dimensionless parameter η^A is called the Eötvös parameter and it measures the strength of the violation of the weak equivalence principle associated to the interaction A . Then, if we measure the difference in the acceleration a_1, a_2 between test bodies of inertial mass m_1 and m_2 , subject

to the same gravitational field, we can get constraints on the Eötvös ratio η defined as

$$\eta \equiv 2 \left| \frac{a_1 - a_2}{a_1 + a_2} \right| = \left| \sum_A \eta^A \left(\frac{E_1^A}{m_{\text{I},1}} - \frac{E_2^A}{m_{\text{I},2}} \right) \right| + \mathcal{O} \left(\left[\frac{\eta^A E^A}{m_{\text{I}}} \right]^2 \right). \quad (2.5)$$

Recently, the first MICROSCOPE [85] data has bound the deviations to no more than 1 part in 10^{15} for bodies whose gravitational binding energy is small, and new proposals have been put forward to test the weak equivalence principle for quantum-entangled systems [86].

Second, local position invariance has been tested by gravitational redshift experiments, which put bounds on a possible spatial dependence of the gravitational redshift of atomic clocks (see for instance [87]), while local time invariance is tested through measurements of the possible evolution of the fundamental constants of non-gravitational physics (see [10] for more details and examples).

Finally, local Lorentz invariance has been tested by a broad class of experiments, e.g., by tests of time-dilation (e.g., [88]), tests of the independence of the speed of light on the source’s velocity (e.g. [89]), tests of the isotropy of the speed of light (e.g. [90]), and of course the classic Michelson-Morley experiment and its successors [91]. Last but not least, from a particle physics perspective, deviations from Lorentz symmetry arising in the matter sector [92, 93, 94, 95] have been tightly constrained by using the standard model extension [96, 97, 98]. This model-independent formalism has proven very efficient on bounding violations of Lorentz symmetry in the matter sector [93] or in the sector coupling matter to gravity [99].

Actually, it is tempting to conclude that any “complete” physical theory should have theoretical connections between the different statements forming the Einstein equivalence principle, so that they would not be all independent. This is known as “Schiff’s” conjecture. While it might be worked out for a given theory, it is hard, if even possible, to find a compelling mathematical “proof” working for every single gravitational theory. Thus we will not develop this idea further and we mention its existence merely for completeness.

Given this firm empirical data we will not try to challenge Lorentz invariance in any of the previously stated forms, namely for the interactions within matter (given by the Standard Model of particle physics) or between matter and the gravitational field (i.e., the universal coupling of matter to the metric). On the contrary we will embrace the conclusions that follow from the Einstein equivalence principle and assume that there is only one gravitational field, the metric, that couples to matter in an universal way.

Yet there still is ample playground for us if we try to check for Lorentz violations in the gravitational sector, i.e., gravity coupling to itself. We could ask what happens, for instance, when we try to generalize the Einstein equivalence principle to bodies whose gravitational binding energy is not negligible. This idea can be stated as the strong equivalence principle (SEP), and since it is a central concept for the rest of this work we will state it more explicitly.

Thus, in an analogous manner to the previous construction of the Einstein equivalence principle, the strong equivalence principle is composed of three parts : the claim that (1) the principle of free fall is also valid for self-gravitating bodies as well as for test bodies (generalization of WEP), (2) the outcome of **any** local test experiment is independent of the position

of the freely-falling frame (generalization of local position invariance), and (3) the outcome of **any** local test experiment is independent of the velocity of the freely-falling frame (generalization of local Lorentz invariance). The mere conception of this principle suggests new paths to explore, for we may want to test whether or not gravity verifies Lorentz invariance as stated in this new stronger way. As we will see later, the strong equivalence principle can prove to be a very useful tool because, on one hand general relativity does satisfy it, while on the other most of modified gravity theories, and particularly Lorentz violating gravity, do not. In the next chapter we will explain how we try to exploit the consequences of this difference.

2.2.1 Percolation from the gravitational sector to the matter sector

While several quantum gravity proposals (string theories with extra-dimensions [100], non-commutative field theory [101] and Hořava gravity [77, 78] for instance) hint towards Lorentz violations appearing in the ultraviolet, i.e., at small scales, it is not completely obvious that we may freely break Lorentz invariance in the gravitational sector without messing things out in the matter sector. Indeed, one could reasonably argue that any gravitational Lorentz violation would percolate into particle physics, and since there are very tight constraints on Lorentz violations in the matter sector, such as those mentioned in sections 2.1 and 2.2, then one would conclude that gravitational Lorentz violations must also be small. There exist counter-examples to this argument, however, and infrared (i.e., at long distances) Lorentz invariance could still be preserved by different mechanisms, even if gravity presents Lorentz violations in the ultraviolet. For instance, it could be protected by supersymmetry [102], or it could be an emergent symmetry appearing at low energies [103, 104] for different reasons, such as a renormalization group flow of the system leading to infrared Lorentz invariance [102, 105], or it could even be an accidental symmetry as suggested by [106]. It has also been proposed that a classically Lorentz invariant matter sector may co-exist with a Lorentz violating gravity sector provided that their interaction is mediated by higher-dimensional operators and is suppressed by a high-energy scale [107]. We therefore conclude that testing Lorentz invariance in the gravitational sector is still a reasonable enterprise since there is an ample spectrum of mechanisms able to control Lorentz violating percolation, despite the stringent constraints from the matter sector.

2.2.2 The Einstein equivalence principle as a tool to construct modified theories of gravitation

Having made the case for the *why* to study Lorentz violating gravity, now we must stop to discuss *how*.

To begin with, let us remark that the empirical support for the Einstein equivalence principle (composed of WEP, LPI and LLI) also helps us characterize the sort of theory we can hope to be viable. Indeed, since the Einstein equivalence principle implies that, locally, it is impossible to distinguish between a gravitational force and an accelerating frame, then we are compelled to conclude that the motion of bodies, in the absence of any external force, is solely determined by the spacetime's structure. This strongly suggests that the only viable (classical) gravitational theories are those satisfying the postulates of metric theories [10], namely :

- spacetime is endowed with a symmetric metric,
- the trajectories of freely falling test bodies are geodesics of that metric, and finally
- in local freely falling reference frames, the non-gravitational laws of physics are those written in the language of special relativity.

Among these metric theories, general relativity occupies a very special place. This can be clearly shown by Lovelock's theorem [108, 109] : the only second-order Euler-Lagrange equation obtainable in a four dimensional space from a scalar density of the form $\mathcal{L} = \mathcal{L}(g_{\mu\nu})$ is

$$\alpha\sqrt{-g}\left(R_{\mu\nu} - \frac{1}{2}Rg_{\mu\nu}\right) + \lambda\sqrt{-g}g_{\mu\nu} = 0, \quad (2.6)$$

where α and λ are constants, while $R_{\mu\nu}$ and R are the Ricci tensor and scalar curvature, respectively. We recognize the Einstein tensor $G_{\mu\nu} = R_{\mu\nu} - \frac{1}{2}Rg_{\mu\nu}$. Note that this gives us the Einstein's field equations in empty space with a cosmological constant $\Lambda = \lambda/\alpha$. The most general scalar density leading to these equations is given by the Lagrangian density

$$\mathcal{L} = \alpha\sqrt{-g}R - 2\lambda\sqrt{-g} + \beta\epsilon^{\mu\nu\rho\sigma}R^{\alpha\beta}{}_{\mu\nu}R_{\alpha\beta\rho\sigma} + \gamma\sqrt{-g}\left(R^2 - 4R^\mu{}_\nu R^\nu{}_\mu + R^{\mu\nu}{}_{\rho\sigma}R^{\rho\sigma}{}_{\mu\nu}\right) \quad (2.7)$$

where β and γ are constants. Here $\epsilon^{\mu\nu\rho\sigma}$ is the four dimensional Levi-Civita symbol, defined such that $\epsilon^{\mu\nu\rho\sigma}$ is totally anti-symmetric and such that $\epsilon^{0123} = 1$. The third term, proportional to β , is called Pontryagin scalar and is a total derivative in any number of dimensions, while the fourth term, proportional to γ , is called the Gauss-Bonnet invariant and is a topological invariant. The Gauss-Bonnet invariant is also a total derivative in the case of a four dimensional spacetime. These terms are called Lovelock's invariants and neither of them contributes to the field equations.

In order to get an insight on the special position of general relativity, let us state explicitly the hypotheses that lead to this theorem. We have assumed that (1) the metric tensor is the only field involved in the gravitational action, (2) we work in a four-dimensional space time, (3) we only accept up to second order derivatives of the metric in the field equations, (4) the dynamics can be derived from an action principle, and (5) locality.

There is another way to approach this result. Because of diffeomorphism invariance, the variation of a scalar Lagrangian with respect to the metric $g_{\mu\nu}$ gives a conserved 2-tensor. However, within a 4-dimensional Riemannian variety, the only conserved symmetric 2-tensor constructed from the metric and its derivatives is the Einstein tensor $G_{\mu\nu}$. Thus, in the absence of matter fields, the gravitational dynamics is uniquely determined if we consider only one gravitational field, the metric, and if we assume diffeomorphism invariance, a four-dimensional spacetime, derivatives of the metric in the field equations no higher than second order (this ensures stability), locality, and finally, if we assume that the dynamics are derived from an action principle.

Lovelock's theorem implies that if we want to step further from general relativity we need to break at least one of these assumptions. For the sake of this thesis we will give up the hypothesis of the metric as unique gravitational field, and consider a new gravitational field mediating the way in which the matter fields create the metric. As we will see further on, this new field breaks local Lorentz invariance as generalized to gravitating objects while still satisfying the Einstein equivalence principle.

2.3 Khronometric theory

In both Einstein-æther [110] and khronometric theory [111], Lorentz symmetry is violated by introducing a dynamical time-like vector field, the “æther”. Since the æther field defines a preferred time direction at each spacetime event, it immediately follows that boost symmetry, and therefore Lorentz symmetry, is broken. The Einstein equivalence principle is protected by coupling the matter fields only to the metric $g_{\mu\nu}$. The dynamics of the new vector field appears only in the gravitational sector, meaning that in the action it interacts only with the metric. Then its effects on matter only appear as a consequence of its effect on the metric, as required by the Einstein equivalence principle.

In this section we will first introduce khronometric theory as a low-energy limit of Hořava gravity. So let us begin by succinctly characterizing the latter as a proposal for quantum gravity.

The main idea behind Hořava’s theory [77, 78] is to introduce an anisotropy between space and time within the framework of quantum field theory. This anisotropy appears at high energies (i.e., small distances), so that spacetime would be isotropic in the low energy regime. While usual relativistic conformal field theories are compatible with scaling symmetry (implying physical processes with no characteristic length scale), Hořava gravity is constructed so that it will be compatible with Lifshitz scaling with dynamical exponent z . Lifshitz scaling is defined as an anisotropic scaling of the time t and space coordinates \mathbf{x} given by

$$t \rightarrow \lambda^z t, \quad \mathbf{x} \rightarrow \lambda \mathbf{x}, \quad (2.8)$$

where $\lambda \in \mathbb{R}$ is a constant and z is the dynamical exponent measuring the anisotropy. Lorentz boosts (2.2) are the transformations

$$(t, x^i) \rightarrow \frac{1}{\sqrt{1-v^2}}(t - v_j x^j, x^i - v^i t), \quad (2.9)$$

which together with (2.8) gives

$$(t, x^i) \rightarrow \frac{1}{\sqrt{1-\lambda^{2-2z}v^2}}(\lambda^z t - \lambda^{2-z}v_j x^j, \lambda x^i - \lambda v^i t), \quad (2.10)$$

since $v \rightarrow \lambda^{1-z}v$. We can see that Lifshitz scaling and Lorentz symmetry are compatible only for $z = 1$. Thus, for $z = 1$ spacetime symmetry can be enhanced to include the Lorentz group, while for any other value of z , boost invariance is explicitly broken. Hořava gravity is designed to have a dynamical exponent $z = 3$ in the UV, so that at short distances it describes the interaction of non-relativistic gravitons [77]. The main interest of this gravitational theory is that it becomes power-counting renormalizable in 3+1 dimensions [112]. At long distances, Hořava gravity naturally flows to the relativistic value $z = 1$ [78, 77, 102] leading to emergent infrared Lorentz-invariance.

In order to encode the special role given to time in (2.8), spacetime is viewed as a differentiable manifold of dimension $d = 4$ carrying a new geometric structure. Technically speaking, the additional structure is that of a codimension-one foliation : this means that spacetime can be decomposed into submanifolds, the leaves of the foliation, which are of

dimension $d-1$ and fit together continuously. See, e.g., [113, 114] for a rigorous definition of foliations in a manifold. The leaves of this preferred foliation play the role of hypersurfaces of constant time, therefore it is easier to introduce the theory using the formalism of ADM 3+1 split.

Let us suppose that the spacetime manifold is foliated by three-dimensional space-like hypersurfaces Σ_T , labeled by some preferred time function T , which we call the “khronon”¹. The metric $g_{\mu\nu}$ will induce a spatial metric $\gamma_{\mu\nu}$ on each of the hypersurfaces, which can be expressed as

$$\gamma_{\mu\nu} = g_{\mu\nu} - u_\mu u_\nu, \quad (2.11)$$

where u^μ is a time-like unit vector field orthogonal to the hypersurface. This means that we can express it as being proportional to ∇T . Thus we will have

$$u_\mu = \frac{\partial_\mu T}{\sqrt{g^{\mu\nu} \partial_\mu T \partial_\nu T}} \equiv N \nabla_\mu T, \quad (2.12)$$

where N is the lapse function. The extrinsic curvature $K_{\mu\nu}$ is defined as half the Lie-derivative of the induced metric $\gamma_{\mu\nu}$, taken orthogonal to the hypersurface, i.e., in the direction of \mathbf{u} :

$$K_{\mu\nu} = \frac{1}{2} \mathcal{L}_{\mathbf{u}} \gamma_{\mu\nu} = \frac{1}{2} u^\rho \nabla_\rho \gamma_{\mu\nu} + \gamma_{\rho(\mu} \nabla_{\nu)} u^\rho. \quad (2.13)$$

Using a coordinate system adapted to the foliation (i.e., using T as time), the gravitational part of the action of Hořava gravity can be expressed as [78, 111]

$$S_{HL} = \frac{1}{16\pi G_{HL}} \int dT d^3x N \sqrt{\gamma} \left(L_2 + \frac{1}{M_\star^2} L_4 + \frac{1}{M_\star^4} L_6 \right) \quad (2.14)$$

where G_{HL} is a bare gravitational constant (its relation to the measured value of Newton’s gravitational constant is given below), γ is the determinant of the spatial metric $\gamma_{\alpha\beta}$, and M_\star is a new mass scale suppressing the Lagrangians L_4 and L_6 , which are of fourth and sixth order in spatial derivatives, respectively, but contain no time derivative [78, 111]. It is the introduction of these higher spatial derivatives in the action that leads to the different scaling of space and time in the UV, leading in turn to a theory that is power-counting renormalizable [112]. The presence of these higher order terms has an important role in the causal structure of the theory, for they allow for higher order dispersion relations. This issue will be discussed further in the section dedicated to black holes in Lorentz violating theories.

The precise form of L_4 and L_6 is not relevant for this work. In fact, for astrophysical applications, and particularly for the study of (stellar or supermassive) black holes, one can neglect these higher order terms. On the one hand, based on dimensional arguments, the error introduced when neglecting the L_4 and L_6 Lagrangians on a black hole solution of mass M is of the order $\mathcal{O}(G_N^{-2} M^{-2} M_\star^{-2}) = \mathcal{O}(M_{\text{Planck}}^4 / (M_\star M)^2)$. On the other hand, the suppressing mass M_\star has a broad viable range, and its lowest conceivable value corresponds to a rather weak bound $M_\star \gtrsim 10^{-2}$ eV [115, 10]. This lower bound comes from taking into account the constraints on Lorentz violation only from the gravity sector [10, 115]; any

1. From Greek $\chi\rho\nu\nu\omicron\varsigma$, time.

other bound would depend on the details of the percolation of Lorentz gravitational violations into the matter sector, which is poorly understood and model dependent. Taking this lowest bound for $M_\star \sim 10^{-2}$ eV would mean an error of the order of $10^{-18}(10M_\odot/M)^2$ or smaller when neglecting the higher order Lagrangians, which is clearly acceptable for black holes in the range of the LIGO/Virgo detectors, as well as for LISA. For completeness, let us also remark that the mass scale M_\star is also bound from above so that $M_\star \leq 10^{16}$ GeV [115]. This bound comes from imposing that the theory remains power-counting normalizable [78, 116, 117, 118] by letting it be perturbative at all scales.

The low-energy Lagrangian L_2 corresponds precisely to the Lagrangian of khronometric theory and can be expressed as

$$L_2 = K_{ij}K^{ij} - \frac{1+\lambda}{1-\beta}K^2 + \frac{1}{1-\beta}\mathcal{R} + \frac{\alpha}{1-\beta}a_i a^i, \quad (2.15)$$

where $K \equiv \gamma^{ij}K_{ij}$, \mathcal{R} is the scalar curvature associated to the spatial metric, $a^\mu \equiv u^\nu \nabla_\nu u^\mu$ is the acceleration of the congruence and finally, α , β and λ are coupling constants of the theory. The total action of khronometric theory is thus

$$S_{\text{kh}} = \frac{1}{16\pi G_{HL}} \int dT d^3x N \sqrt{\gamma} \left(K_{ij}K^{ij} - \frac{1+\lambda}{1-\beta}K^2 + \frac{1}{1-\beta}\mathcal{R} + \frac{\alpha}{1-\beta}a_i a^i \right) + S_{\text{matter}}[\mathbf{g}, \Psi]. \quad (2.16)$$

Here S_{matter} is the matter action, where the matter fields Ψ are minimally coupled to the metric \mathbf{g} (in order to respect the equivalence principle, as a direct coupling would entail test particle motion dependent on gravitational fields other than the metric). This action is invariant under foliation-preserving diffeomorphisms

$$T \rightarrow \tilde{T}(T), \quad x^i \rightarrow \tilde{x}^i(x, T). \quad (2.17)$$

Note that the bare gravitational constant G_{HL} can be related to the measured value of Newton's gravitational constant G_N , as measured locally by Cavendish-like experiments, by [119, 120]

$$G_N = \frac{G_{HL}}{(1-\alpha/2)(1-\beta)}. \quad (2.18)$$

Although the introduction of Hořava gravity relies on an explicit decomposition between time and space coordinates, the theory can still be written covariantly. To illustrate this point we will cast the action of khronometric theory in an explicitly covariant form as

$$S_{\text{kh}} = \frac{-1}{16\pi G_{\text{EA}}} \int d^4x \sqrt{-g} \left(R + c_\sigma \sigma_{\mu\nu} \sigma^{\mu\nu} + \frac{1}{3}c_\theta \theta^2 + c_a a_\mu a^\mu \right) + S_{\text{matter}}[\mathbf{g}, \Psi], \quad (2.19)$$

where g is the metric determinant, the bare gravitational constant is $G_{\text{EA}} = G_{HL}/(1-\beta)$, R is the scalar curvature associated to the four-dimensional metric, $c_\sigma = \beta$, $c_\theta = 3\lambda + \beta$ and $c_a = \alpha$. We have used the standard decomposition for a congruence $\nabla \mathbf{u}$, where ∇ is the covariant derivative associated to the metric \mathbf{g} , given by

$$\nabla_\mu u_\nu = \omega_{\mu\nu} + \sigma_{\mu\nu} + \frac{1}{3}\theta \gamma_{\mu\nu} - a_\mu a_\nu, \quad (2.20)$$

where θ is the expansion of the congruence world lines, $\omega_{\mu\nu}$ is the rotation (vorticity) tensor, and $\sigma_{\mu\nu}$ is the shear tensor. They are given explicitly by

$$\theta \equiv \nabla \cdot \mathbf{u} = \nabla_{\mu} u^{\mu}, \quad (2.21)$$

$$\omega_{\mu\nu} \equiv \frac{1}{2}(\gamma^{\alpha}_{\nu} \nabla_{\alpha} u_{\mu} - \gamma^{\alpha}_{\mu} \nabla_{\alpha} u_{\nu}) = \nabla_{[\mu} u_{\nu]} - a_{[\nu} u_{\mu]}, \quad (2.22)$$

$$\sigma_{\mu\nu} \equiv \frac{1}{2}(\gamma^{\alpha}_{\nu} \nabla_{\alpha} u_{\mu} + \gamma^{\alpha}_{\mu} \nabla_{\alpha} u_{\nu}) + \frac{1}{3}\theta \gamma_{\mu\nu} = \nabla_{(\mu} u_{\nu)} - a_{(\nu} u_{\mu)} + \frac{1}{3}\theta \gamma_{\mu\nu}. \quad (2.23)$$

Note that the æther's vorticity $\omega_{\mu\nu}$ is identically zero since \mathbf{u} is a hypersurface orthogonal field, as can be easily verified from its definition.

As we will soon see, this covariant representation of khronometric theory can be easily linked to Einstein-æther theory (see equation (2.32) below), and we want to exploit this similarity to derive the field equations of both theories in a similar fashion. Therefore we will reserve a detailed derivation of the field equations from the action to section 2.4, and we will simply give the resulting equations for khronometric theory to conclude this section.

The field equations of khronometric theory are obtained by varying the action (2.19) with respect to the metric and the khronon T . After variation of the action S_{kh} , we get a tensor equation generalizing the Einstein field equations, and a vector equation (the “khronon equation”) given by

$$E_{\mu\nu} = 0, \quad (2.24)$$

$$\nabla_{\mu} \left(\frac{\mathbb{E}^{\mu}}{\|\nabla T\|} \right) = 0. \quad (2.25)$$

where $\|\nabla T\| \equiv \sqrt{g^{\rho\sigma} \nabla_{\rho} T \nabla_{\sigma} T}$. We refer to Appendix 2.A for more details on the derivation of the field equations. The tensors $E_{\mu\nu}$ and \mathbb{E}_{μ} are defined as follows :

$$E_{\mu\nu} \equiv G_{\mu\nu} - T_{\mu\nu}^{\text{kh}} - 8\pi G_{\text{EA}} T_{\mu\nu}^{\text{matter}}, \quad (2.26)$$

where

$$T_{\text{matter}}^{\mu\nu} = \frac{-2}{\sqrt{-g}} \frac{\delta S_{\text{matter}}}{\delta g_{\mu\nu}}, \quad (2.27)$$

is the matter stress-energy tensor, and

$$\mathbb{E}_{\mu} \equiv \gamma_{\mu\nu} \left(\nabla_{\rho} J^{\rho\nu} - \alpha a_{\rho} \nabla^{\nu} u^{\rho} \right) = 0, \quad (2.28)$$

where we introduced $J^{\rho}_{\mu} \equiv \lambda \theta \delta_{\mu}^{\rho} + \beta \nabla_{\mu} u^{\rho} + \alpha a_{\nu} u^{\mu}$. In (2.26) the khronon stress-energy tensor is given by

$$\begin{aligned} T_{\mu\nu}^{\text{kh}} \equiv & \nabla_{\rho} \left[J_{(\mu}^{\rho} u_{\nu)} - J^{\rho}_{(\mu} u_{\nu)} - J_{(\mu\nu)} u^{\rho} \right] + \left[u_{\sigma} \nabla_{\rho} J^{\rho\sigma} - \alpha a^2 \right] u_{\mu} u_{\nu} \\ & + \alpha a_{\mu} a_{\nu} + \frac{1}{2} (\lambda \theta^2 + \beta \nabla_{\mu} u^{\nu} \nabla_{\nu} u^{\mu} + \alpha a^2) g_{\mu\nu} + 2\mathbb{E}_{(\mu} u_{\nu)}, \end{aligned} \quad (2.29)$$

Moreover, in the same way in which diffeomorphism invariance implies the Bianchi identities in general relativity, we can derive an equivalent set of identities for khronometric theory. The result is the following generalized Bianchi identity :

$$\nabla_{\mu} E^{\mu\nu} = \kappa u^{\nu}, \quad (2.30)$$

where κ is as

$$\kappa \equiv -\frac{1}{2} \|\nabla T\| \nabla_\mu \left(\frac{\mathbb{E}^\mu}{\|\nabla T\|} \right). \quad (2.31)$$

We refer to Appendix 2.B for a derivation of this new result. It can be shown [120] that the khronon equation is a consequence of the Einstein equation and the Bianchi identity, so that it is not in fact an independent equation in khronometric theory. This is an important result and will be exploited later when solving the field equations.

2.4 Einstein-æther theory

From the previous action (2.19) we are naturally lead to Einstein-æther's action by allowing the æther field to be non-hypersurface orthogonal. This means that we can now introduce a new term proportional to the vorticity $\omega_{\mu\nu}$, so that the action becomes

$$S_{\text{EA}} = \frac{-1}{16\pi G_{\text{EA}}} \int d^4x \sqrt{-g} \left(R + c_\sigma \sigma_{\mu\nu} \sigma^{\mu\nu} + c_\omega \omega_{\mu\nu} \omega^{\mu\nu} + \frac{1}{3} c_\theta \theta^2 + c_a a_\mu a^\mu + \lambda (g^{\mu\nu} u_\mu u_\nu - 1) \right) + S_{\text{matter}}[\mathbf{g}, \Psi]. \quad (2.32)$$

Note that in order to keep the unit norm for the æther vector \mathbf{u} we introduced a Lagrange multiplier λ reinforcing this condition. Actually, the gravitational part is more commonly expressed as [121, 122, 120]

$$S = \frac{-1}{16\pi G_{\text{EA}}} \int \left(R + M^{\alpha\beta}{}_{\mu\nu} \nabla_\alpha u^\mu \nabla_\beta u^\nu + \lambda (g^{\mu\nu} u_\mu u_\nu - 1) \right) \sqrt{-g} d^4x, \quad (2.33)$$

where g is the metric determinant, R is the Ricci scalar and

$$M^{\alpha\beta}{}_{\mu\nu} = c_1 g^{\alpha\beta} g_{\mu\nu} + c_2 \delta_\mu^\alpha \delta_\nu^\beta + c_3 \delta_\mu^\beta \delta_\nu^\alpha + c_4 u^\alpha u^\beta g_{\mu\nu}. \quad (2.34)$$

This is the most generic action that is diffeomorphism-invariant and quadratic in the derivatives of the æther field \mathbf{u} .

The new coupling constants c_1 , c_2 , c_3 and c_4 , which define the parameter space of the theory, are related to the old coefficients of (2.32) by the relations

$$c_\theta = 3c_2 + c_1 + c_3, \quad (2.35)$$

$$c_a = c_1 + c_4, \quad (2.36)$$

$$c_\sigma = c_1 + c_3, \quad (2.37)$$

$$c_\omega = c_1 - c_3. \quad (2.38)$$

Thus the total action of Einstein-æther theory is given by

$$S_{\text{EA}} = \frac{-1}{16\pi G_{\text{EA}}} \int \left(R + L_{\text{EA}} + \lambda (g_{\mu\nu} u^\mu u^\nu - 1) \right) \sqrt{-g} d^4x + S_{\text{matter}}[\mathbf{g}, \Psi], \quad (2.39)$$

where we introduced the notation

$$L_{\text{EA}} = M^{\alpha\beta}{}_{\mu\nu} \nabla_\alpha u^\mu \nabla_\beta u^\nu, \quad (2.40)$$

Variation of the action can now be performed with respect to the metric $g^{\mu\nu}$, the æther field u^μ and the Lagrange multiplier λ , leading to the Euler-Lagrange equations

$$G_{\mu\nu} + \frac{\delta L_{\text{EA}}}{\delta g^{\mu\nu}} - \frac{1}{2}L_{\text{EA}} g_{\mu\nu} - \lambda u_\mu u_\nu - 8\pi G_{\text{EA}} T_{\mu\nu}^{\text{matter}} = 0, \quad (2.41a)$$

$$\frac{\delta L_{\text{EA}}}{\delta u^\mu} + 2\lambda u_\mu = 0, \quad (2.41b)$$

$$g_{\mu\nu} u^\mu u^\nu - 1 = 0, \quad (2.41c)$$

where $G_{\mu\nu} \equiv R_{\mu\nu} - \frac{1}{2}R g_{\mu\nu}$ is the Einstein tensor and

$$T_{\text{matter}}^{\mu\nu} = \frac{-2}{\sqrt{-g}} \frac{\delta S_{\text{matter}}}{\delta g_{\mu\nu}}, \quad (2.42)$$

is the matter stress-energy tensor. Notice that the Lagrange multiplier can be computed from the vector equation after contraction with u^μ , by using the unit norm equation (2.41c). Thus it is manifest that

$$\lambda = -\frac{1}{2}u^\mu \frac{\delta L_{\text{EA}}}{\delta u^\mu}, \quad (2.43)$$

and we can plug this value both in the tensor equation (2.41a) and in the vector equation (2.41b). The former leads to a set of modified Einstein field equations

$$E_{\mu\nu} \equiv G_{\mu\nu} - T_{\mu\nu}^{\text{EA}} - 8\pi G_{\text{EA}} T_{\mu\nu}^{\text{matter}} = 0, \quad (2.44)$$

while the latter yields the æther equations

$$\mathbb{E}_\mu \equiv \left(\nabla_\alpha J^{\alpha\nu} - c_4 a_\alpha \nabla^\nu u^\alpha \right) (g_{\mu\nu} - u_\mu u_\nu) = 0, \quad (2.45)$$

where we introduced $J^\alpha{}_\mu \equiv M^{\alpha\beta}{}_{\mu\nu} \nabla_\beta u^\nu$. In fact, the vector \mathbb{E}_μ is related to the variations in (2.41b) by

$$\mathbb{E}_\mu = -\frac{1}{2} \left[\frac{\delta L_{\text{EA}}}{\delta u^\mu} - \left(u^\rho \frac{\delta L_{\text{EA}}}{\delta u^\rho} \right) u_\mu \right] = -\frac{1}{2} (g_{\mu\nu} - u_\mu u_\nu) \frac{\delta L_{\text{EA}}}{\delta u_\nu}, \quad (2.46)$$

meaning that the term proportional to δu^μ in the variation of the action (2.39) is $-2\mathbb{E}_\mu \delta u^\mu$.

Explicit computation leads to the æther stress-energy tensor as

$$\begin{aligned} T_{\mu\nu}^{\text{EA}} \equiv & \nabla_\alpha \left[J_{(\mu}{}^\alpha u_{\nu)} - J^\alpha{}_{(\mu} u_{\nu)} - J_{(\mu\nu)} u^\alpha \right] + c_1 \left[(\nabla_\alpha u_\mu)(\nabla^\alpha u_\nu) - (\nabla_\mu u_\alpha)(\nabla_\nu u^\alpha) \right] \\ & + \left[u_\beta \nabla_\alpha J^{\alpha\beta} - c_4 a^2 \right] u_\mu u_\nu + c_4 a_\mu a_\nu + \frac{1}{2} M^{\rho\sigma}{}_{\alpha\beta} \nabla_\rho u^\alpha \nabla_\sigma u^\beta g_{\mu\nu}, \end{aligned} \quad (2.47)$$

These are precisely the same quantities that we introduced in section 2.3, equations (2.24), (2.25), (2.26) and (2.28) in order to express the field equations for khronometric theory, expressed in terms of the coupling constants of Einstein-æther theory. In fact, expressing the khronometric action as

$$S_{\text{kh}} = \frac{-1}{16\pi G_{\text{EA}}} \int (R + L_{\text{EA}}) \sqrt{-g} d^4x + S_{\text{matter}}[\mathbf{g}, \Psi], \quad (2.48)$$

we can perform variation with respect to T instead of \mathbf{u} , using the definition (2.12) to express δu^μ as

$$\delta u^\mu = \left(g^{\mu\nu} - u^\mu u^\nu \right) \frac{\partial_\nu \delta T}{\|\nabla T\|} - \frac{1}{2} u^\mu u_\rho u_\sigma \delta g^{\rho\sigma}. \quad (2.49)$$

This allows us to express the variations as

$$\delta S_{\text{kh}} = \frac{-1}{16\pi G_{\text{EA}}} \int \left[\left(E_{\mu\nu} + 2\mathbb{E}_{(\mu} u_{\nu)} \right) \delta g^{\mu\nu} + 2\nabla_\nu \left(\frac{\mathbb{E}^\nu}{\|\nabla T\|} \right) \delta T \right] \sqrt{-g} \, d^4x + S_{\text{matter}}[\mathbf{g}, \Psi], \quad (2.50)$$

which leads to the khronometric equations as stated in (2.24) and (2.25), once we identify $T_{\mu\nu}^{\text{EA}}$ with $T^{\text{kh}} - 2\mathbb{E}_{(\mu} u_{\nu)}$.

Let us remark that not all the terms of L_{EA} are independent in khronometric theory, because the parameter space of khronometric theory is a three dimensional one. Indeed, as long as we restrict our attention to orthogonal solutions, any multiple of the vorticity

$$\omega_{\mu\nu} \omega^{\mu\nu} = \frac{1}{2} \left(\nabla_\mu u_\nu \nabla^\mu u^\nu - \nabla_\mu u_\nu \nabla^\nu u^\mu - a^2 \right), \quad (2.51)$$

can be added to the action (2.39) with impunity. For instance, we could absorb c_1 by adding a term $-2c_1 \omega_{\mu\nu} \omega^{\mu\nu}$, leading to the new coefficients $c'_1 = 0$, $c'_2 = c_2$, $c'_3 = c_1 + c_3$ and $c'_4 = c_1 + c_4$. In general, we can relate the coefficients α , β and λ via the mapping

$$\lambda = c_2, \quad \beta = c_1 + c_3, \quad \alpha = c_1 + c_4. \quad (2.52)$$

Note that any hypersurface-orthogonal solution to the Einstein-æther equations is also a solution to khronometric theory, though the converse does not always hold. That is, if we find a solution to the equations

$$\begin{aligned} E_{\mu\nu} &= 0, \\ \mathbb{E}_\mu &= 0, \end{aligned} \quad (2.53)$$

where \mathbf{u} is an hypersurface-orthogonal field, then it follows that there exists a khronon field T such that $u = \nabla T / \|\nabla T\|$, and such that the equations

$$\begin{aligned} E_{\mu\nu} - 2\mathbb{E}_{(\mu} u_{\nu)} &= 0, \\ \nabla_\mu \left(\frac{\mathbb{E}_\mu}{\|\nabla T\|} \right) &= 0, \end{aligned} \quad (2.54)$$

are satisfied. However, a khronometric solution to the field equations (2.54) does not necessarily satisfy (2.53), since it is not guaranteed that $\mathbb{E}^\mu = 0$.

Since we still have general covariance in these theories, we can make use of infinitesimal gauge transformations in order to show that solutions must also satisfy a modified set of Bianchi identities in the same way as in general relativity. Indeed, if we make an infinitesimal change of coordinates given by a 4-vector ϵ^μ , the action (2.39) will change as

$$\delta_\epsilon S_{\text{EA}} = \frac{-1}{16\pi G_{\text{EA}}} \int \left(E_{\mu\nu} \mathcal{L}_\epsilon g^{\mu\nu} - 2\mathbb{E}_\mu \mathcal{L}_\epsilon u^\mu \right) \sqrt{-g} \, d^4x, \quad (2.55)$$

where \mathcal{L}_ϵ is the Lie derivative with respect to the vector ϵ^μ . After inserting the given Lie derivatives

$$\begin{aligned}\mathcal{L}_\epsilon g^{\mu\nu} &= -2\nabla^{(\mu}\epsilon^{\nu)}, \\ \mathcal{L}_\epsilon u^\mu &= \epsilon^\rho \nabla_\rho u^\mu - u^\rho \nabla_\rho \epsilon^\mu,\end{aligned}\tag{2.56}$$

we can proceed to integration by parts in order to obtain the relation

$$\nabla_\mu (E^{\mu\nu} - u^\mu \mathbb{E}^\nu) = \mathbb{E}_\mu \nabla^\nu u^\mu,\tag{2.57}$$

which is a generalization of the standard Bianchi identity $\nabla_\mu G^{\mu\nu} = 0$ for the case of Einstein-æther theory. It can be easily seen that we do indeed recover the standard GR relation in the limit where the c_i go to zero.

In the case of khronometric theory, the action (2.50) will transform under an infinitesimal change of coordinates as

$$\delta_\epsilon S_{\text{kh}} = \frac{-1}{16\pi G_{\text{EA}}} \int \left[E_{\mu\nu} \mathcal{L}_\epsilon g^{\mu\nu} + 2\nabla_\nu \left(\frac{\mathbb{E}^\nu}{\|\nabla T\|} \right) \mathcal{L}_\epsilon T \right] \sqrt{-g} d^4x,\tag{2.58}$$

where the Lie derivative of T is $\mathcal{L}_\epsilon T = \epsilon^\nu \nabla_\nu T$. After integration by parts, this leads to the Bianchi identity for khronometric theory, equation (2.31).

At this stage, we can argue that the Einstein equations together with the Bianchi identities imply the khronon equation (2.25). Indeed, the change in the action (2.58) can be rewritten as

$$\delta_\epsilon S_{\text{kh}} = \int \left[\left(\frac{\delta S}{\delta \mathbf{g}} \right) \mathcal{L}_\epsilon \mathbf{g} + \left(\frac{\delta S}{\delta \Psi} \right) \mathcal{L}_\epsilon \Psi + \left(\frac{\delta S}{\delta T} \right) \mathcal{L}_\epsilon T \right],\tag{2.59}$$

and let us suppose that the Einstein equation is satisfied, so that $\delta S/\delta \mathbf{g} = 0$, and let us further suppose that the matter field equations are also satisfied, i.e. $\delta S/\delta \Psi = 0$. On the one hand, since the total variation $\delta_\epsilon S_{\text{kh}}$ must vanish, we obtain the following identity

$$\int \left(\frac{\delta S}{\delta T} \right) \mathcal{L}_\epsilon T = 0,\tag{2.60}$$

which must hold for every vector ϵ^μ defining the coordinate transformation. On the other hand, since T defines the time foliation the derivative $\mathcal{L}_\epsilon T$ cannot vanish, and furthermore can be varied at will by choosing different vector fields ϵ^μ . We therefore conclude that $\delta S/\delta T$ must vanish, that is, the khronon equation is satisfied.

2.5 Experimental constraints

In this section we will review the current observational constraints on Lorentz violating gravity, and particularly khronometric and Einstein-æther theory. Let us stress that the weak equivalence principle is verified in both Einstein-æther and khronometric theory due to the universal coupling of the metric to the matter fields. Since the æther field does not couple directly to matter, its effects on it must only come as a residual of its coupling with the gravitational field. Therefore we expect these effects to occur only in curved spacetime, while being small within nearly flat spacetimes. As mentioned in section 2.2.1, however, there still could be some measurable effects due to Lorentz violation in gravity, allowing us to reduced the parameter space for these theories. These constraints are varied, and we will present them in the following.

2.5.1 Stability and consistency requirements

First, from a theoretical point of view we would like to have stable propagating modes with positive energy in flat spacetime. Indeed, it has been shown [123, 124] that, besides the standard spin-2 mode for metric perturbations, gravitational perturbations propagate via spin-0 modes for both Einstein-æther and khronometric theory, and also via spin-1 modes for Einstein-æther. Also, we will require their propagation speed to be greater than the speed of light for otherwise they would decay in a detectable Cherenkov-like emission. That is, in the same way as a charged particle emits radiation while traveling faster than the speed of light in a given medium, high energy cosmic rays should decay into the new propagation channels while traveling faster than the gravitational modes [125, 126]. Since this Cherenkov like emission is not observed within high energy cosmic rays, one can give lower bounds to the speed of gravitational wave modes. Denoting the squared speed of the spin- i propagation mode as s_i^2 we have for Einstein-æther theory that [123]

$$s_0^2 = \frac{(2 - c_{14})c_{123}}{c_{14}[2(1 + c_2)^2 - c_{123}(1 + c_2 + c_{123})]}, \quad (2.61a)$$

$$s_1^2 = \frac{c_1 - \frac{1}{2}c_1^2 + \frac{1}{2}c_3^2}{(1 - c_{13})c_{14}}, \quad (2.61b)$$

$$s_2^2 = \frac{1}{1 - c_{13}}, \quad (2.61c)$$

where c_{ij} and c_{ijk} are shorthands for $c_i + c_j$ and $c_i + c_j + c_k$, respectively, and for khronometric theory we have

$$s_0^2 = \frac{(\alpha - 2)(\beta + \lambda)}{\alpha(\beta - 1)(2 + \beta + \lambda)}, \quad (2.62a)$$

$$s_2^2 = \frac{1}{1 - \beta}, \quad (2.62b)$$

which actually coincides with (2.61a) and (2.61c).

The stability of the propagation modes together with the no-Cherenkov condition impose in khronometric theory [126, 127, 115]

$$\begin{aligned} 0 < \beta < 1/3, \quad \lambda > \frac{\beta(\beta + 1)}{1 - 3\beta}, \\ 0 < \beta < 1/3, \quad \lambda < -\frac{2 + \beta}{3}, \\ 1/3 < \beta < 1, \quad \frac{\beta(\beta + 1)}{1 - 3\beta} < \lambda < -\frac{2 + \beta}{3}. \end{aligned} \quad (2.63)$$

while for Einstein-æther we have the bounds [126, 123]

$$0 \leq c_+ \leq 1, 0 \leq c_- \leq \frac{c_+}{3(1 - c_+)}, \quad (2.64)$$

where $c_{\pm} \equiv c_1 \pm c_3$.

2.5.2 Multi-messenger astronomy

The most stringent constraint comes from the recent simultaneous detection of a binary neutron star merger and the associated gamma ray burst (GRB) [28]. In fact, the propagation speed s_2 of the tensor mode, i.e., gravitational waves, cannot differ from the speed of light c (which we set to 1) by more than one part in 10^{15} . Yet this speed is found to depend on the values of the theories' parameters. For khronometric theory we have [124] $s_2^2 = 1/(1 - \beta)$ (not the Lorentz boost), so this implies a very tight bound on β given by

$$|1/s_2^2 - 1| = |\beta| \lesssim 10^{-15} \quad (2.65)$$

In the case of Einstein-æther, the ratio between the speed of light and the tensor mode's squared speed is given by [123]

$$|c^2/c_t^2 - 1| = |c_1 + c_3| \lesssim 10^{-15}, \quad (2.66)$$

which corresponds precisely to the same constraint from khronometric theory since $\beta = c_1 + c_3$.

2.5.3 Solar system and the weak-field regime

Third, in the weak-regime and small velocity limit, both khronometric and Einstein-æther theory reduce to Newtonian gravity [119], with Newton's gravitational constant G_N being related to the bare gravitational constant by

$$G_N = \frac{G_{\text{EA}}}{1 - \frac{c_{14}}{2}} = \frac{G_{\text{HL}}}{(1 - \alpha/2)(1 - \beta)}, \quad (2.67)$$

where, again, c_{ij} stands for $c_i + c_j$. Corrections to Newtonian gravity are described by the post-Newtonian formalism. Thus, Solar system tests allow one to constrain the parameter space of the theory via its parametrized post-Newtonian parameters. Only two PPN parameters, α_1 and α_2 , are non-zero in Einstein-æther and khronometric theory, in contrast with general relativity. They correspond to preferred frame effects and in GR they are both exactly zero. Current constraints bound them to remain very small, $\alpha_1 \lesssim 10^{-4}$ and $\alpha_2 \lesssim 10^{-7}$ [10]. In both khronometric and Einstein-æther theory these observations can be used to shrink the parameter space to a two-dimensional space. On the one hand, for khronometric theory we have [124]

$$\alpha_1 = 4 \frac{\alpha - 2\beta}{\beta - 1} = -4\alpha, \quad (2.68)$$

$$\alpha_2 = \frac{\alpha_1}{8 + \alpha_1} \left[1 + \frac{\alpha_1(1 + \beta + 2\lambda)}{4(\beta + \lambda)} \right] = \frac{\alpha}{\alpha - 2} \left[1 - \alpha \frac{1 + 2\lambda}{\lambda} \right], \quad (2.69)$$

where we used the multi-messenger constraint (2.65) to simplify each expression. Solar system bounds are thus given by

$$\begin{aligned} 4|\alpha| &\lesssim 10^{-4}, \\ \left| \frac{\alpha}{\alpha - 2} \right| \left| 1 - \alpha \frac{1 + 2\lambda}{\lambda} \right| &\lesssim 10^{-7}. \end{aligned} \quad (2.70)$$

These constraints are satisfied if we set $|\alpha| \lesssim 10^{-7}$, in which case λ must only satisfy the rather curious bound from below $|\lambda| \gtrsim 10^{-7}$, but is left completely unbound from above. Let us remark that, if we were not to use the multi-messenger constraint to set $\beta = 0$, solar system bounds can be satisfied by the simple condition

$$|\alpha_1| = 4 \left| \frac{\alpha - 2\beta}{\beta - 1} \right| \leq 10^{-6} \left[1 + \frac{\alpha_1(1 + \beta + 2\lambda)}{4(\beta + \lambda)} \right]^{-1}, \quad (2.71)$$

which constrains α but leaves unconstrained the other couple parameters β and λ . For this reason, in practice we will choose to work setting $\alpha = 2\beta$ all throughout this work and consider only the space allowed for β and λ , before setting β to zero. Similarly, for Einstein-æther theory we could expand the theory using α_1 and α_2 as dimensionless small numbers. One then finds that [122, 121]

$$c_2 = \frac{c_3^2 - c_1 c_3 - 2c_1^2}{3c_1} = 0, \quad (2.72)$$

$$c_4 = -\frac{c_3^2}{c_1} = -c_1, \quad (2.73)$$

to leading order in α_1 and α_2 , where we used again the results from the previous section. This leaves the parameter space of Einstein-æther depending only on one parameter, c_1 .

2.5.4 Cosmology

For khronometric theory, the Friedmann equation takes the same form as in general relativity but with a gravitational constant G_C related to G_N as [128]

$$\frac{G_N}{G_C} = \frac{2 + \beta + 3\lambda}{2 - \alpha}, \quad (2.74)$$

to leading order in α_1 [129, 130]. This means that the Universe expands with an effectively rescaled Newton's constant, leading to a decrease of the expansion rate of the Universe, independently of the matter content. Consequently, the change in the rate of cosmic expansion leads to a modification of the production of primordial elements during Big Bang Nucleosynthesis (BBN). However, from cosmology, and particularly from the agreement between the metal abundances predicted by BBN and observations, we get a bound on the difference between the cosmological gravitational constant G_C and Newton's gravitational constant G_N given by $|G_C/G_N - 1| \leq 1/8$ [119]. Once combined with the Cherenkov/stability constraints these bounds reduce the viable parameter space to a narrow strip near the λ axis [129] (i.e., for $\alpha = \beta = 0$).

In the case of Einstein-æther theory, once we take into account the solar system constraints it turns out that the ratio $G_N \approx G_C$ up to terms of order $\mathcal{O}(10^{-4})$, which means that cosmological observations (and more particularly the BBN) do not reduce significantly the viable parameter space of the theory. This was worked out in [122, 130].

2.5.5 Binary pulsars and the strong-field regime

Finally, binary pulsars can also be used to put on constraints to the parameter space of Lorentz violating theories. On the one hand, one could try to reduce the parameter space in

an analogous manner to the previous section, using the strong-field counterparts of the PPN parameters α_1 and α_2 . As we mentioned above, deviations from the PPN parameters within the weak-regime allow us to constraint the parameters of the theory. Similarly, their strong-regime counterparts are also constrained through binary and isolated pulsar observations. Denoting them by the use of an overhead hat we have $|\hat{\alpha}_1| \lesssim 10^{-5}$ and $|\hat{\alpha}_2| \lesssim 10^{-9}$ [131, 132].

On the other hand, as it will be further explained in the next chapter, Lorentz violation generically leads to a violation of the universality of free fall, and in turn, with this change in the dynamics there is a generic emission of dipole gravitational radiation which can be measured (cf. section 1.6.2). This effect is encoded in a set of parameters called the sensitivities, which will be properly discussed in the next chapter. However, observations of binary pulsars and their period decay rate is in agreement to GR's prediction within observational uncertainties (cf. section 1.6.1), and one can therefore put constraints into the parameter space [129]. The constraints coming from dipolar radiation in binary pulsars are much stronger than those coming from the strong field PPN parameters, as illustrated in figures 7 and 8 of [129]. One could summarize these bounds by stating that the couplings cannot be much larger than a few percent, that is, $|c_i| \lesssim 10^{-2}$ in general, save for λ that has a weaker bound $\lambda \lesssim 0.1$.

2.6 Black holes in Lorentz Violating gravity

The notion of a black hole relies on the causal structure of special relativity, which in turn relies on Lorentz symmetry. Indeed, the main feature defining a black hole is its event horizon. Moreover, the specificity of the event horizon is that it defines a causal boundary separating the inner region from the exterior of the black hole. Now, this possibility exists in general relativity because signals are confined to propagate within future-directed light cones, and this in turn is due to the Lorentzian causal structure of the theory.

Once we give up Lorentz symmetry however, the very notion of an event horizon becomes subtle. As we will soon discuss, this will result in the appearance of “new horizons” to be taken into account. These horizons will be defined with respect to new degrees of freedom introduced by Lorentz violation in the gravity sector. As discussed in section 2.5.1, besides the standard metric spin-2 mode there are spin-1 and spin-0 gravity modes which propagate at superluminal speeds (in order to avoid Cherenkov radiation, cf. section 2.5.1), meaning that the surface trapping them is inside the metric horizon.

In this section we will discuss these new features as they were known before this thesis and more specifically we will focus on static and spherically symmetric black holes in Einstein-æther theory and khronometric theory. Thus we will revise some previous results, following particularly [133], while at the same time introducing the notation to be used in the next chapter.

Let us first recall that, as it follows from the field equations (2.24), (2.25) and (2.44), (2.45), any hypersurface-orthogonal solution to Einstein-æther equations is also a khronometric solution, though the converse is not necessarily true. In particular, static spherically symmetric solutions, such as a spherically symmetric static black hole [133], are the same in both theories and we can extend the results obtained within one theory to the other. This result is not completely obvious and in fact it will no longer be true neither for a rotating

black hole [134, 135], nor for a moving black hole. Thus, in this section we will formulate the equations describing static spherically symmetric black holes within khronometric theory, bearing in mind that these results are trivially transposed to Einstein-æther theory due to spherical symmetry. Furthermore, we will make use of the fact that in khronometric theory the æther equation is a consequence of the modified Einstein equation and the Bianchi identities in order to get rid of it.

As mentioned before, a first crucial result concerns the existence of new “horizons” besides the standard matter/light horizon. Indeed, as mentioned in section 2.5.1, gravitational perturbations in both Einstein-æther and khronometric theory exhibits a spin-0 modes and in Einstein-æther there also exists a spin-1 mode of propagation besides the standard spin-2 mode for metric perturbations [123, 124]. These new modes have different speeds (larger than the speed of light, so that there is no matter Cherenkov radiation) each defining thus a new notion of “horizon” with respect to them. These horizons correspond to null surfaces for the effective metric

$$g_{\alpha\beta}^{(i)} = g_{\alpha\beta} + (s_i^2 - 1)u_\alpha u_\beta, \quad (2.75)$$

where s_i is the propagation speed of the spin- i mode. Note that the spin-1 horizon should play no physical role in the static spherically symmetric case, since it is not a propagating mode in khronometric theory and this solution coincides with Einstein-æther’s solution (this is in agreement with symmetry considerations as well).

Furthermore, as one gives up Lorentz Invariance there is in principle no reason to restrain dispersion relations only to linear relations. Thus, let us consider higher-order dispersion relations such as

$$\omega^2 = k^2 + a k^4 + b k^6, \quad (2.76)$$

where ω is the angular frequency, k is the wave number and a and b are constants with the appropriate dimensions. The new powers are suggested by the form of the action of Hořava gravity (equation (2.14)), and there could be even higher powers of k involved. This would lead to arbitrarily high speeds of propagation in the UV, which could in principle escape any of the aforementioned horizons. It has been found however, that there exists an innermost surface inside which the æther flow forces all motion to fall to the center, regardless of its propagation speed [127]. Because of this, such inmost surface has been called the “Universal Horizon”. In order to give further details about these surfaces we will need to state and solve the field equations (or rather present the numerical solutions already obtained by [133]).

2.6.1 Static, spherically symmetric black holes

The static, spherically symmetric black hole solution has been already presented in [133]. In solving the field equations we found it useful to work in Eddington-Finkelstein coordinates $\{v, r, \theta, \phi\}$, for they are regular at the metric horizon. In these coordinates, the metric Ansatz can be expressed as

$$ds^2 = f(r)dv^2 - 2B(r)dvdr + r^2d\Omega^2, \quad (2.77)$$

while the æther vector takes the form

$$u_\mu dx^\mu = \frac{1 + f(r)A(r)^2}{2A(r)}dv - A(r)B(r)dr, \quad (2.78)$$

where $A(r)$ corresponds to the time component of the contravariant æther vector, $u^\nu = A(r)$. In order to keep the simplicity in the notation, we will express most of our computations in terms of Einstein-æther coupling coefficients, c_1, c_2, c_3, c_4 , but this is no problem as they can be easily cast back in terms of the khronometric coupling coefficients α, β and λ using the relations (2.52). In particular, the limit $\alpha, \beta, \lambda \rightarrow 0$ corresponds to the limit of vanishing c_i s. Let us anticipate that, since we recover general relativity in the limit of vanishing coupling constants $c_i \rightarrow 0$, we should recover the Schwarzschild solution for $f(r)$ and $B(r)$ in this limit, namely $f(r) = 1 - \frac{2GM}{r}$ and $B(r) = 1$.

Plugging the Ansatz (2.77), (2.78) into the modified field equations give us a system of ordinary differential equations where the non-trivial independent components of the tensor equation $E^\mu{}_\nu = 0$ ² can be denoted as³ $B_i = 0$ for $i = 1, 2, 3$ and $C_0 = 0$. The equations $\mathbf{B} = 0$ are of the second order for f and A and of the first order on B , but we find that $C_0 = 0$ contains fewer derivatives, i.e., at most one derivative in f and A and no derivative in B . The system of equations $\mathbf{B} = 0$ can be diagonalized on f'' , A'' , and B' , so that schematically we have

$$\begin{aligned} f''(r) &= f''(r, f(r), A(r), B(r), f'(r), A'(r)), \\ A''(r) &= A''(r, f(r), A(r), B(r), f'(r), A'(r)), \\ B'(r) &= B'(r, f(r), A(r), B(r), f'(r), A'(r)), \\ 0 &= C_0(r, f(r), A(r), B(r), f'(r), A'(r)), \end{aligned} \tag{2.79}$$

All these expressions are algebraic functions on the coupling coefficients c_i and analytic on r . We can make use of the Bianchi identity (2.30) to prove that C_0 corresponds to a constraint equation, in the same manner as the Bianchi identity of general relativity implies the momentum and Hamiltonian constraints. Indeed, the non-identically zero components of the Bianchi identity are given by

$$\nabla_2 E^2{}_1 = \kappa u_1, \tag{2.80}$$

$$\nabla_2 E^2{}_2 = \kappa u_2, \tag{2.81}$$

where ∇_2 is the covariant derivative with respect to the second variable, i.e., the r variable. From these two equations we find that the quantity

$$C_0 \equiv u_2 E^2{}_1 - u_1 E^2{}_2, \tag{2.82}$$

will satisfy the relation

$$\nabla_r C_0 = E^2{}_1 \nabla_r u_2 - E^2{}_2 \nabla_r u_1. \tag{2.83}$$

Expanding the covariant derivatives we find that C_0 satisfies the evolution equation

$$\frac{d}{dr} C_0 = \alpha(r) C_0 + \beta_i(r) B_i, \tag{2.84}$$

2. Actually, we use the tensor $E^\mu{}_\nu$ instead of $E^{\mu\nu}$, because in this form we can easily make use of the Bianchi identity (2.30) to elucidate the structure of dynamical and constraint equations as it will soon be discussed.

3. B_i stands here for “background”, as opposed to the equations appearing at $\mathcal{O}(v)$. Not to be confused with the function $B(r)$.

where $\alpha(r)$ and $\beta_i(r)$ are analytic functions on the c_i 's and the functions f , A and B . It follows that, if the initial conditions satisfy the constraint $C_0 = 0$ and we solve for the equations of motion $\mathbf{B} = 0$ everywhere, then the constraints will be satisfied everywhere in virtue of its evolution equation.

2.6.2 Black hole 'Charges'

This structure would mean, in principle, that there are 5-1=4 initial conditions required at any given point in order to integrate the system. Indeed, on the one hand, the system $\mathbf{B} = 0$ containing five derivatives in total, one would require 5 initial conditions at each point in order to integrate it. On the other hand, the equation $C_0 = 0$ must also be satisfied at the initial integration point (and thanks to its evolution equation it will be satisfied everywhere else as well), reducing by 1 the total number of independent initial conditions. For numerical reasons we choose to integrate from the metric horizon r_h , where $f(r_h) = 0$, so that then we are left with only three independent initial conditions. Nevertheless, generic solutions (i.e., for random initial conditions) are not asymptotically flat, and imposing this condition leads to a two-dimensional family of solutions. Asymptotically flat solutions are obtained by shooting of the initial parameters, as will be further discussed in chapter 4 for the perturbed solution. This is to be contrasted to general relativity where asymptotic flatness follows from the field equations. This can be understood by solving perturbatively the field equations near spatial infinity. The asymptotic form of f , A and B has been found to be for a suitable gauge [136, 127, 133] :

$$\begin{aligned} f(r) &= 1 + \frac{F_1}{r} + \frac{c_1 + c_4}{48} \frac{F_1^3}{r^3} + \dots \\ A(r) &= 1 - \frac{F_1}{2r} + \frac{A_2}{r^2} + \left(\frac{F_1^3}{16} - \frac{c_1 + c_4}{96} F_1^3 - F_1 A_2 \right) \frac{1}{r^3} + \dots \\ B(r) &= 1 + \frac{c_1 + c_4}{16} \frac{F_1^2}{r^2} - \frac{c_1 + c_4}{12} \frac{F_1^3}{r^3} + \dots, \end{aligned} \quad (2.85)$$

where the constants F_1 and A_2 will specify all the other coefficients of the solution. Notice that the solution does indeed go to the Schwarzschild solution when we take all the c_i equal to zero. It is readily seen that the constant F_1 can be related to the total mass M_{tot} as measured by a distant observer, via the relation $2G_N M_{\text{tot}} = -F_1$, so the question arises as to what is the nature of the parameter A_2 .

At this stage one could be tempted to conclude that for each given mass, there is a one-dimensional family of solutions characterized by a new charge or "hair". However, there is only one solution in this family which is also regular at the spin-0 horizon [137, 136, 133]. Thus, while the constant F_1 can be related to the ADM mass M_{tot} , the value of A_2 must be chosen such that the solution doesn't present any singularity at the spin-0 horizon. This condition is justified by the fact that numerical simulations for spherically symmetric collapse seem to produce regular, stationary black holes, with nothing special about the spin-0 location [138]. Thus, after selecting the correct value for $A_2 = A_2^{\text{reg}}(M_{\text{tot}})$ physical solutions belong to a one-dimensional family of solutions parametrized by the mass M_{tot} .

2.6.3 Digging further into the black hole

Outside the metric horizon and within the allowed parameter space, static Lorentz-violating black holes are very similar to black holes of general relativity [133]. Indeed, let us consider the spacetime outside the metric horizon and associate to it an astrophysically-measurable parameter. For instance, the location of the innermost stable circular orbit (ISCO) determines the inner edge of thin accretion disks and their radiative efficiency [139, 140]. As it can be seen in figure 2.1, the fractional deviation away from general relativity, computed for small coupling coefficients (both in khronometric and Einstein-æther theory). The deviations obtained by [133] were found to be typically no larger than a few

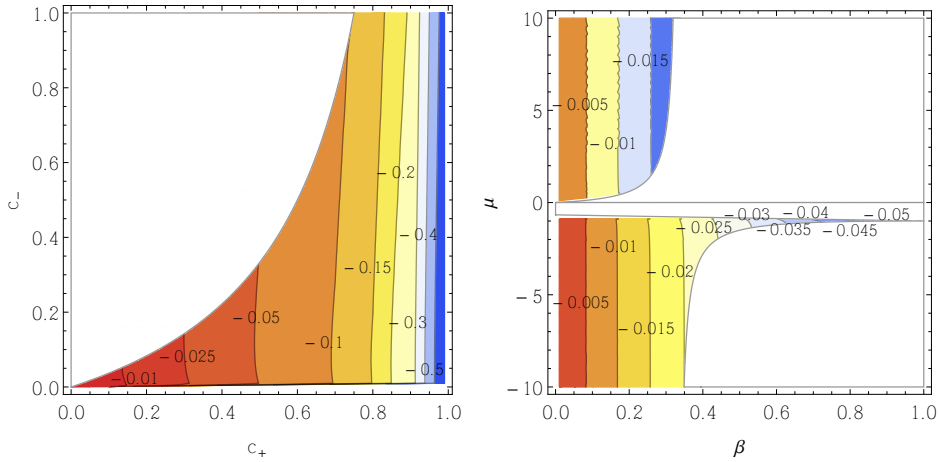


FIGURE 2.1 – *Left panel* : fractional deviation of the location of the ISCO (for Einstein-æther theory), characterized by the dimensionless product $\omega_{\text{ISCO}} r_g$, where ω_{ISCO} is the ISCO frequency and r_g the gravitational radius. *Right panel* : fractional deviation of the dimensionless product $\omega_{\text{ISCO}} r_g$ in khronometric theory. Both figures were extracted from [133]. There, the fractional deviation away from general relativity of two astrophysically-measurable parameters are plotted for the allowed parameter space.

percent, meaning that they would not be detectable with present data.

Inside the metric horizon however, the structure is more complex, as we have already discussed the presence of the spin-0 horizon and its implications on the regularity of the solution. Moreover, as in GR, the geometry at the center of the black hole is singular, as can be observed by computing the Kretschmann scalar and checking that it diverges as we approach $r = 0$. In between the spin-0 horizon and the origin singularity there is another peculiar surface, the universal horizon. In order to understand its appearance we will focus on the orientation of the æther field inside the metric horizon. More precisely, we will consider the boost angle between the æther and the normal to the constant- r hypersurfaces

$$\theta_r = \arccos \left(\mathbf{u} \cdot \frac{dr}{\sqrt{g^{rr}}} \right). \quad (2.86)$$

From the numerical solutions it is observed that θ_r generically vanishes on a constant radius surface $r = r_{\text{uh}}$ close to the metric horizon, and many times again further as shown in the left panel of figure 2.2.

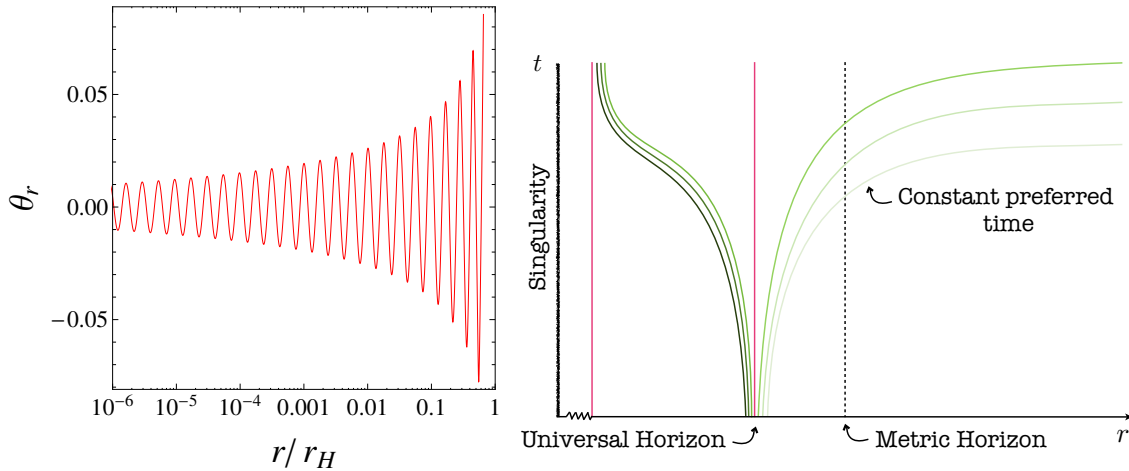


FIGURE 2.2 – *Left panel* : the boost angle θ_r between the æther field and the normal to the $r=\text{constant}$ hypersurfaces, in terms of the variable r/r_H , where r_H is the location of the metric horizon. The numerical solutions were obtained for æ-theory with $c_+ = 0.8$, $c_- = 0.01$. As r decreases, θ_r vanishes soon after crossing the metric horizon ($r/r_H < 1$), meaning that the æther becomes normal to an $r=\text{constant}$ hypersurface. This happens infinitely many times while approaching the center of the black hole, as indicated by the many oscillations of θ_r . The first crossing corresponds to the location of the universal horizon. *Right panel* : schematic representation of the spacetime for a Lorentz violating black hole. In green are the constant preferred-time hypersurfaces, darker lines corresponding to later preferred times T . The universal horizon is represented by the indicated red line, and for a smaller radius there is the next horizon where the boost angle vanishes again. The figure is truncated between these two horizons. The curves spanning the exterior of the universal horizon do not cross it. The curves spanning the region in between the red lines do not cross any of these horizons, and in particular they do not extend into the exterior of the universal horizon. Thus, as we require that signals must travel into the future, any signal emitted in the interior of the universal horizon will be trapped. Both figures were extracted from [133].

This is a result of great importance and it allows to answer the troubling question of arbitrarily high propagation speeds raised earlier on this section. In fact, by construction, the æther field defines a preferred foliation (this is intrinsically true for Hořava gravity and a consequence of spherical symmetry and the static Ansatz for Einstein-æther theory) by singling out hypersurfaces orthogonal to it. Also, we saw that by choosing adapted coordinates these hypersurfaces can be taken to be hypersurfaces of constant preferred time T . Thus the æther orientation defines unambiguously the future time direction of the foliation. It is clear then that hypersurfaces of constant preferred time T cannot intersect, and this means that if a hypersurface of constant $T = T_u$ is also a constant radius hypersurface $r = r_u$, then any hypersurface of constant $T > T_u$ cannot extend outside $r \geq r_u$. This is precisely what happens when $\theta_r = 0$: the æther field is parallel to the 1-form dr and thus orthogonal to the surface $r = \text{constant}$ where the θ_r angle vanishes. This is shown graphically in the right panel of figure 2.2. The outmost surface for which θ_r becomes zero is what has been called the universal horizon. As a consequence of this, no signal can escape the interior of the uni-

versal horizon, no matter how large its propagation speed (hence its name). This surface is, in Lorentz violating gravity, a causal boundary separating the black hole's inner region from its exterior region, in the same way in which the metric horizon does in general relativity.

The radial position r_{uh} of the universal horizon can be found by using the fact that, if the æther vector is orthogonal to $r_{\text{uh}} = \text{constant}$, then it is proportional to dr . In particular, this means that $u_v = 0$, or more explicitly (cf. equation (2.78))

$$1 + f(r_{\text{uh}})A(r_{\text{uh}})^2 = 0. \quad (2.87)$$

Within Eddington-Finkelstein coordinates, the universal horizon is located at the largest radial position r_{uh} where the previous equation is satisfied.

These results are the basis on which the work of next chapter relies. Hereafter, we will refer to the set of functions $f(r)$, $A(r)$ and $B(r)$ defining the static metric (2.77) and the static æther (2.78) as to the “background solution”, while the first order solution corresponding to a slowly moving black hole with respect to the æther will be referred as to the “perturbed solution”. Let us stress one more time that, although the static spherically symmetric black hole solution was derived for khronometric theory, the results are also valid for Einstein-æther theory.

2.A Derivation of the field equations

The gravitational action of Einstein-æther theory is given by

$$S_G = \frac{-1}{16\pi G} \int (R + L + l(g^{\mu\nu}u_\mu u_\nu - 1))\sqrt{-g}d^4x, \quad (2.88)$$

where l is a Lagrange multiplier enforcing the unitary condition and where

$$L = (c_1 g^{\mu\nu} g_{\alpha\beta} + c_2 \delta_\alpha^\mu \delta_\beta^\nu + c_3 \delta_\beta^\mu \delta_\alpha^\nu + c_4 u^\mu u^\nu g_{\alpha\beta}) \nabla_\mu u^\alpha \nabla_\nu u^\beta. \quad (2.89)$$

Khronometric theory is recovered by setting

$$u_\mu = \frac{\partial_\mu T}{\sqrt{g^{\rho\sigma} u_\rho u_\sigma}}, \quad (2.90)$$

and mapping the coupling coefficients

$$\alpha \equiv c_1 + c_4, \beta \equiv c_1 + c_3, \lambda \equiv c_2. \quad (2.91)$$

Then the total action of the theory is simply given by

$$S_{\text{total}} = S_G + S_{\text{matter}}[\mathbf{g}, \Psi]. \quad (2.92)$$

Variation of the gravitation part yields

$$\delta S_G = \frac{-1}{16\pi G} \int \left\{ \left(G_{\mu\nu} + \frac{\partial L}{\partial g^{\mu\nu}} - \frac{1}{2} g_{\mu\nu} L + l u_\mu u_\nu \right) \delta g^{\mu\nu} + \left(\frac{\partial L}{\partial u_\mu} + 2l u^\mu \right) \delta u_\mu + \delta l (u^2 - 1) \right\} \sqrt{-g} d^4x, \quad (2.93)$$

which gives the field equations

$$G_{\mu\nu} + \frac{\partial L}{\partial g^{\mu\nu}} - \frac{1}{2} g_{\mu\nu} L + l u_\mu u_\nu - 8\pi G T_{\mu\nu}^{\text{matter}} = 0, \quad (2.94a)$$

$$\frac{\partial L}{\partial u_\mu} + 2l u^\mu = 0, \quad (2.94b)$$

$$u^2 - 1 = 0, \quad (2.94c)$$

where $T_{\mu\nu}^{\text{matter}}$ comes from the matter action S_{matter} . We can solve for $l = -\frac{1}{2} u_\mu \frac{\partial L}{\partial u_\mu}$ and insert this back to obtain

$$G_{\mu\nu} - T_{\mu\nu}^U - 8\pi G T_{\mu\nu}^{\text{matter}} = 0, \quad (2.95a)$$

$$\mathbb{E}^\mu = 0, \quad (2.95b)$$

$$u^2 = 1. \quad (2.95c)$$

where we introduced

$$-T_{\mu\nu}^U \equiv \frac{\partial L}{\partial g^{\mu\nu}} - \frac{1}{2} g_{\mu\nu} L - \frac{1}{2} u_\rho \frac{\partial L}{\partial u_\rho} u_\mu u_\nu, \quad (2.96)$$

which differs for Einstein-æther theory and khronometric gravity due to the extra $g^{\mu\nu}$ contribution of (2.90) and

$$\mathbb{E}^\mu \equiv \frac{\partial L}{\partial u_\mu} - u_\rho \frac{\partial L}{\partial u_\rho} u^\mu = 0, \quad (2.97)$$

From (2.89) we can directly compute

$$\begin{aligned} T_{\mu\nu}^{\text{kh}} &\equiv \nabla_\rho \left[J_{(\mu}{}^\rho u_{\nu)} - J^\rho{}_{(\mu} u_{\nu)} - J_{(\mu\nu)} u^\rho \right] + \left[u_\sigma \nabla_\rho J^{\rho\sigma} - \alpha a^2 \right] u_\mu u_\nu \\ &\quad + \alpha a_\mu a_\nu + \frac{1}{2} (\lambda \theta^2 + \beta \nabla_\mu u^\nu \nabla_\nu u^\mu + \alpha a^2) g_{\mu\nu} + 2\mathbb{E}_{(\mu} u_{\nu)}, \end{aligned} \quad (2.98)$$

and

$$\mathbb{E}_\mu \equiv \gamma_{\mu\nu} \left(\nabla_\rho J^{\rho\nu} - \alpha a_\rho \nabla^\nu u^\rho \right) = 0, \quad (2.99)$$

where we introduced $J^\rho{}_\mu \equiv \lambda \theta \delta_\mu^\rho + \beta \nabla_\mu u^\rho + \alpha a_\nu u^\mu$.

2.B Bianchi identity in khronometric theory

The action of khronometric theory is given by

$$S_{\text{kh}} = -\frac{1}{16\pi G} \int d^4x \sqrt{-g} \left(R + \lambda (\nabla_\mu u^\mu)^2 + \beta \nabla_\mu u^\nu \nabla_\nu u^\mu + \alpha a_\mu a^\mu \right) + S_{\text{matter}}[g_{\mu\nu}, \Psi], \quad (2.100)$$

Its variation with respect to the metric $g^{\mu\nu}$ gives the modified Einstein equations

$$E_{\mu\nu} = 0, \quad (2.101)$$

while variation with respect to the khronon gives the khronon equation, which we do not need to compute yet. Ignoring the matter component, the variation of the action can be expressed as

$$\begin{aligned} \delta S &= \int \left(\frac{\delta S}{\delta g^{\mu\nu}} \delta g^{\mu\nu} + \frac{\delta S}{\delta T} \delta T \right) d^4x, \\ &= \int \left(E_{\mu\nu} \sqrt{-g} \delta g^{\mu\nu} + \frac{\delta S}{\delta T} \delta T \right) d^4x. \end{aligned} \quad (2.102)$$

In particular, if we make an infinitesimal change of coordinates given by a 4-vector ϵ^μ , the action (2.100) will change as

$$\delta_\epsilon S_{\text{kh}} = \frac{-1}{16\pi G_{\text{EA}}} \int \left[E_{\mu\nu} \mathcal{L}_\epsilon g^{\mu\nu} + \left(\frac{1}{\sqrt{-g}} \frac{\delta S}{\delta T} \right) \mathcal{L}_\epsilon T \right] \sqrt{-g} d^4x, \quad (2.103)$$

where \mathcal{L}_ϵ is the Lie derivative with respect to the vector ϵ^μ . After inserting the given Lie derivatives

$$\begin{aligned} \mathcal{L}_\epsilon g^{\mu\nu} &= -2\nabla^{(\mu} \epsilon^{\nu)}, \\ \mathcal{L}_\epsilon T &= \epsilon^\nu \nabla_\nu T, \end{aligned} \quad (2.104)$$

we can proceed to integration by parts in order to obtain the relation

$$\delta_\epsilon S_{\text{kh}} = \frac{-1}{16\pi G_{\text{EA}}} \int \left[2\nabla_\mu E^{\mu\nu} + \left(\frac{1}{\sqrt{-g}} \frac{\delta S}{\delta T} \right) \nabla^\nu T \right] \epsilon_\nu \sqrt{-g} d^4x, \quad (2.105)$$

From this equation (and diffeomorphism invariance) we deduce the Bianchi identity

$$\nabla_\mu E^{\mu\nu} = -\frac{1}{2} \left(\frac{1}{\sqrt{-g}} \frac{\delta S}{\delta T} \right) \|\nabla T\| u^\nu, \quad (2.106)$$

which shows that the divergence of $E^{\mu\nu}$ is proportional to u^ν by a term that includes the khronon equation. In fact, we can do better and compute explicitly the variation of S with respect to T . The easiest way to do so is by noticing that

$$\frac{\delta S}{\delta T} = \frac{\delta S}{\delta u_\nu} \Big|_{g^{\mu\nu}} \times \frac{\delta u_\nu}{\delta T} \Big|_{g^{\mu\nu}}, \quad (2.107)$$

where we keep $g^{\mu\nu}$ fixed, and using the fact that

$$\frac{\delta u_\nu}{\delta T} \Big|_{g^{\mu\nu}} = (\delta_\nu^\mu - u^\mu u_\nu) \partial_\mu \delta T. \quad (2.108)$$

Then after integrating by parts one finds that

$$\begin{aligned} \delta S \Big|_{g^{\mu\nu}} &= \int \left(\frac{\delta S}{\delta T} \delta T \right) d^4x \\ &= \int \nabla_\mu \left(\frac{(g^{\mu\nu} - u^\mu u^\nu)(\nabla_\rho J^\rho{}_\nu - \alpha a_\rho \nabla_\nu u^\rho)}{\|\nabla T\|} \right) \delta T \sqrt{-g} d^4x. \end{aligned} \quad (2.109)$$

Clearly then what we obtained is precisely the khronon equation (2.25)

$$\nabla_\mu \left(\frac{\mathbb{E}^\mu}{\|\nabla T\|} \right) = 0, \quad (2.110)$$

where we recall that we introduced

$$J^\rho{}_\mu \equiv \lambda (\nabla_\sigma u^\sigma) \delta_\mu^\rho + \beta \nabla_\mu u^\rho + \alpha a_\mu u^\rho \quad (2.111)$$

$$\mathbb{E}_\mu \equiv \gamma_{\mu\nu} (\nabla_\rho J^{\rho\nu} - \alpha a_\rho \nabla^\nu u^\rho), \quad (2.112)$$

$$\gamma_{\mu\nu} = g_{\mu\nu} - u_\mu u_\nu. \quad (2.113)$$

We can therefore express the khronometric Bianchi identity as

$$\nabla_\mu E^{\mu\nu} = \kappa u^\nu, \quad (2.114)$$

where we introduced

$$\kappa \equiv -\frac{1}{2} \left(\frac{1}{\sqrt{-g}} \frac{\delta S}{\delta T} \right) \|\nabla T\| = -\frac{1}{2} \|\nabla T\| \nabla_\mu \left(\frac{\mathbb{E}^\mu}{\|\nabla T\|} \right). \quad (2.115)$$

3 – Dipole emission in Lorentz-violating Gravity

In this chapter we will see how the preferred-frame effects introduced in the gravity sector affect the motion of a binary black hole system. We will also see how this leads to detectable changes in the gravitational wave fluxes the binary emits. In order to do so, we will first review the general physical principles that lead to these modifications in section 3.1, in particular the strong equivalence principle and its violations. Based on this motivation, in section 3.2 we will introduce a point-particle model containing parameters quantifying these violations, which we will refer to as “sensitivities”. Using a post-Newtonian approximation for the binary dynamics, we will show how this scheme naturally leads to a semi-analytic prescription to compute the sensitivities in section 3.3. Indeed, we will see that these can be read off from the asymptotic metric of a single slowly moving black hole. The formalism developed will be extended to describe the modified gravitational radiation in section 3.4. The main results of this chapter are based on the work of [?], and are the motivation for the work developed in the next chapter. Finally, the possibility of observing modifications to the gravitational wave flux will be discussed in section 3.5.

3.1 Strong equivalence principle and its violations

As explained in the previous chapter, the Einstein equivalence principle has been thoroughly tested in the limit of small gravitational binding energy. Moreover, we can show that in general relativity the equivalence principle is still valid for bodies whose gravitational binding energy is not negligible. That is, general relativity satisfies the strong equivalence principle (SEP). To clarify what we mean by this, let us suppose that we carry out any test experiment within a sufficiently small spacetime region \mathcal{U} , in the presence of an external gravitational field, and we record the results. Then the strong equivalence principle states that we can always find a suitable reference frame \mathcal{U}' , in the absence of a background gravitational field, where the observers will record the same results when performing the same experiment.

In order to see how this remarkable feature appears in general relativity, let us suppose we are given a gravitating system to study. Let us then consider a local, freely falling frame large enough to encompass one of the gravitating bodies (or experimental set-up), yet small enough so that we can neglect the inhomogeneities of the external gravitational field throughout its volume. On the one hand, the dynamics of the local system will be determined by the metric, which in turn will be generated both by the local and external systems. More precisely, when

solving the field equations for the gravitational field generated by the local system we must take into account, not only the matter distribution of the local system, but also the boundary conditions established by the external system. On the other hand, from general covariance it is always possible to find a coordinate system where the metric \mathbf{g} reduces to Minkowski's metric at the boundary between the local and the external systems. That is, if we denote \mathcal{R} the radius of curvature of spacetime due to the external fields (if the body were removed from it), then we can construct Riemann normal coordinates to describe our system, leading to the metric

$$g_{\mu\nu} = \eta_{\mu\nu} + \mathcal{O}\left(\frac{|x|^2}{\mathcal{R}^2}\right), \quad (3.1)$$

where x is the distance to the body (or test experiment). This leads thus to free falling motion for the local system in general relativity. It is capital to remark that this simple conclusion ceases to be valid in the presence of more than one gravitational field. Indeed, although it will always be possible to find a reference frame where equation (3.1) holds, the asymptotic values of the other gravitational fields will be determined by the external system. These asymptotic boundary conditions must be taken into account when solving the field equations for the internal gravitational field, and this leads to a reference frame-dependent dynamics.

Another way to state the strong equivalence principle is that self-gravitating objects also follow geodesics. Let us consider, for instance, the motion of a binary system. Then, as long as the binary's separation is sufficiently large compared to the size of its components, we are allowed to neglect finite size and tidal effects. For instance, the orbital motion of a celestial bodies such as the Earth and Sun, is the same as the orbital motion of any other couple of binary objects with the same mass and spin, save for tidal and finite size effects. This will hold true for any body regardless of its gravitational binding energy, again up to corrections due to tidal forces.

It is enlightening to discuss this from a more quantitative perspective, using a point particle description where the equations of motion are written in terms of surface integrals, as proposed by Itoh and Futamase [141, 142, 143]. Let us suppose that we can define a set of disjoint volumes V_a covering the a -the body. This is possible since we suppose that the typical binary distance d is much larger than the sizes of the bodies. Let us further suppose that we can cover a sufficiently large region of spacetime using harmonics coordinates, i.e., such that we can write the Einstein equations in "relaxed form"

$$\square h^{\alpha\beta} = 16\pi G \tau^{\alpha\beta}, \quad (3.2)$$

where $h^{\alpha\beta} \equiv \sqrt{-g} g^{\alpha\beta} - \eta^{\alpha\beta}$ and

$$\tau^{\alpha\beta} \equiv (-g) \left(T_{\text{matter}}^{\alpha\beta} + t_{\text{LL}}^{\alpha\beta} \right) + \frac{1}{16\pi G} \left(\partial_\nu h^{\alpha\mu} \partial_\mu h^{\beta\nu} - h^{\mu\nu} \partial_\mu \partial_\nu h^{\alpha\beta} \right), \quad (3.3)$$

where $t_{\text{LL}}^{\alpha\beta}$ is the Landau-Lifshitz pseudo-tensor

$$\begin{aligned} 16\pi G (-g) t_{\text{LL}}^{\alpha\beta} &\equiv g_{\lambda\mu} g^{\nu\rho} \partial_\nu h^{\alpha\lambda} \partial_\rho h^{\beta\mu} + \frac{1}{2} g_{\lambda\mu} g^{\alpha\beta} \partial_\rho h^{\lambda\nu} \partial_h^{\rho\mu} \\ &\quad - g_{\mu\nu} \left(g^{\lambda\alpha} \partial_\rho h^{\beta\nu} + g^{\lambda\beta} \partial_\rho h^{\alpha\nu} \right) \partial_\lambda h^{\rho\mu} \\ &\quad + \frac{1}{8} \left(2g^{\alpha\lambda} g^{\beta\mu} - g^{\alpha\beta} g^{\lambda\mu} \right) \left(2g_{\nu\rho} g_{\sigma\tau} - g_{\rho\sigma} g_{\nu\tau} \right) \partial_\lambda h^{\nu\tau} \partial_\mu h^{\rho\sigma}. \end{aligned} \quad (3.4)$$

The harmonic condition must be added to the relaxed equations in order to have a set of equations equivalent to the full Einstein equations :

$$\partial_\alpha h^{\alpha\beta} = 0, \quad (3.5)$$

and this implies, together with the relaxed equations (3.2), the conservation law

$$\partial_\alpha \tau^{\alpha\beta} = 0. \quad (3.6)$$

Multipole moments of the bodies are defined in terms of $\tau^{\alpha\beta}$, and in particular its masses. We can define the ‘‘center of mass’’ coordinates of each particle $z_a(t)$ such that the dipole moment

$$D_a^i \equiv \int_{V_a} d^3y y^i \tau^{00}(t, \vec{z}_a(t) + \vec{y}), \quad (3.7)$$

is a constant. The velocity of the a -th body is defined then as $\vec{v}_a \equiv \frac{d\vec{z}}{dt}$. We can take the time derivative of equation (3.7) to obtain the identity

$$\begin{aligned} 0 &= \frac{d}{dt} D_a^i = \int_{V_a} d^3y y^i (\partial_0 \tau^{00} + v_a^j \partial_j \tau^{00}) \\ &= \int_{V_a} d^3y y^i (-\partial_j \tau^{j0} + v_a^j \partial_j \tau^{00}) \\ &= - \int_{V_a} d^3y \{ \partial_j [y^i \tau^{j0}] - \tau^{i0} \} + v_a^j \int_{V_a} d^3y \{ \partial_j [y^i \tau^{00}] - \delta_j^i \tau^{00} \} \\ &= - \int_{S_a} dS_j y^i \tau^{j0} + \int_{V_a} d^3y \tau^{i0} + v_a^j \int_{S_a} dS_j y^i \tau^{00} - v_a^j \int_{V_a} d^3y \tau^{00}, \end{aligned} \quad (3.8)$$

where we used the conservation law (3.6) to go from the first to the second line, and Gauss’ theorem for the last step. The surface S_a is the boundary of the volume V_a . This equation can be expressed more simply as

$$0 = P_a^i - v_a^i P_a^0 - Q_a^i, \quad (3.9)$$

where P_a^μ is the effective four-momentum

$$P_a^\mu \equiv \int_{V_a} d^3y \tau^{0\mu}(t, \vec{z}_a(t) + \vec{y}), \quad (3.10)$$

and Q_a^i is defined only in terms of surface integrals

$$Q_a^i(t) \equiv \int_{S_a} dS_j y^i \tau^{j0} - v_a^j \int_{S_a} dS_j y^i \tau^{00}. \quad (3.11)$$

Taking one more time derivative leads us to an equation of motion for $\vec{z}(t)$, given by

$$P_a^0 \frac{dv_a^i}{dt} = \frac{dP_a^i}{dt} - v_a^i \frac{dP_a^0}{dt} - \frac{dQ_a^i}{dt}, \quad (3.12)$$

or equivalently,

$$P_a^0 \frac{dv_a^i}{dt} = - \int_{S_a} dS_j \tau^{ji} + v_a^j \int_{S_a} dS_j \tau^{0i} + v_a^i \int_{S_a} dS_j \tau^{j0} - v_a^i v_a^j \int_{S_a} dS_j \tau^{00} - \frac{dQ_a^i}{dt}, \quad (3.13)$$

The quantity P_a^0 can be identified with the mass of the a -th body as it tends to the ADM-mass in the $v_a \rightarrow 0$ limit (or equivalently, in the $d \rightarrow \infty$ limit). Thus, all these quantities can be computed in terms of surface integrals, which hints towards the “effacement of the internal structure” principle. In the freely falling frame, the asymptotically measured quantities that determine the gravitational field are the body’s mass m and its spin \vec{J} (again, ignoring tidal effects). Thus, the binary’s dynamics will depend exclusively on the mass and the spin of its components, independently of their compositions and internal structures. This miraculous simplification is sometimes referred to as the “effacement principle”. More precisely, it is possible to show that the contribution of higher internal multipole moments to these surface integrals enters as a 5 PN effect, but a more careful study is required to prove this fact. We refer to [144, 141, 142, 143] and references therein for more details.

This leads thus to free falling motion for the local system in general relativity. However, this principle will not hold true when we introduce extra gravitational degrees of freedom. The physical origin of this effect comes from the coupling of the extra fields to the matter through the metric. Indeed, while it might still be possible to find a coordinate system which has Minkowski’s metric as an asymptotic value, the new field will have non-trivial boundary values which will affect the dynamics of the local system. Particularly, for both khronometric and Einstein-æ theory the local’s system dynamics will depend on the boundary value of æ vector \mathbf{u} as seen by the freely-falling frame. More precisely, when expressing the modified Einstein equations in relaxed form we must include the khronon/æther stress energy tensor. Let us say, for instance, that we focus in khronometric theory. Then the relaxed equations take the form

$$\square h^{\alpha\beta} = 16\pi G(\tau^{\alpha\beta} + \tau_{\text{kh}}^{\alpha\beta}), \quad (3.14)$$

where $\tau_{\text{kh}}^{\alpha\beta}$ is given in terms of the khronon stress energy tensor $T_{\text{kh}}^{\alpha\beta}$ by

$$\tau_{\text{kh}}^{\alpha\beta} \equiv \frac{1}{8\pi G}(-g)T_{\text{kh}}^{\alpha\beta}. \quad (3.15)$$

Therefore, following the same procedure outlined before lead us to an evolution equation similar to (3.13). However, now some of the surface integrals will be carried over $\tau_{\text{kh}}^{\alpha\beta}$, introducing thus a dependence on the relative velocity between the falling frame and the khronon/æther field. Moreover, we will also find volume integrals over the tensor $\tau_{\text{kh}}^{\alpha\beta}$ which simply cannot be converted to surface integrals. Evidently the same conclusion holds by trading $\tau_{\text{kh}}^{\alpha\beta}$ for $\tau_{\text{EA}}^{\alpha\beta}$ as the definitions of $T_{\text{kh}}^{\alpha\beta}$ and $T_{\text{EA}}^{\alpha\beta}$ are analogous (cf. sections 2.3 and 2.4). Thus, neither Einstein-æther nor khronometric theory are expected to satisfy the strong equivalence principle. Furthermore, the way this velocity-dependence appears will depend on the body’s internal structure instead of only the body’s mass and spin.

Another well-known example where violations of the strong equivalence principle appear is given by scalar-tensor theories [?, ?, 145, 72, 71, ?]. These theories contain a scalar field ϕ , besides the metric $g_{\mu\nu}$, a potential function $V(\phi)$ and a coupling function $A(\phi)$. Their action can be written as

$$S = \frac{1}{16\pi G} \int [\phi R - \phi^{-1} \omega(\phi) g^{\mu\nu} \partial_\mu \phi \partial_\nu \phi - \phi^2 V(\phi)] \sqrt{-g} d^4x + S_{\text{matter}}[\mathbf{g}, \Psi], \quad (3.16)$$

where ω is such that

$$3 + \omega(\phi) \equiv \alpha(\phi)^{-2}, \quad \alpha(\phi) \equiv \frac{d(\ln A(\phi))}{d\phi}. \quad (3.17)$$

The strong equivalence principle is violated in these theories because the value of the scalar field affects the local value of the gravitational constant G_N , introducing thus a position dependence on the body’s gravitational binding energy. This leads to a renormalization of the gravitational mass m_a (because the binding energy contributes to it), which becomes a function of the scalar field. We can therefore write the mass of the a -th body as

$$m_a = m_a(\phi), \quad (3.18)$$

which explicitly takes into account the position-dependence of the gravitational mass through the local value of the scalar field ϕ . The corresponding modification of the body’s motion has been long known in these theories and is referred to as the “Nordtvedt effect”. By extension, we will also use the same name for Lorentz-violating theories. Of course, here instead of a position dependence we will find that the gravitational binding energy of a body must depend on its speed relative to the æther field.

3.2 Point-particle approximation and the sensitivities

The previous discussion was intended to motivate the physics behind SEP violations, thus it was essentially conceptual. Now, if we want to make precise predictions we need to solve the field equations and compute the physical observables associated to the solutions. However, we do not have exact solutions neither in khronometric theory nor in general relativity. Thus we are forced to either look for numerical schemes to solve the field equations or to approximate schemes to obtain the binary evolution.

Throughout this work we will consider the post-Newtonian approximation to study the orbital decay of binary black holes. Thus, we will assume that the orbital speed of the black holes is a small parameter that can be used to expand the system’s dynamics (recall that we set $c = 1$). This corresponds to an early phase where the distance between the black holes is large compared to their size. Otherwise said, we deal with a phase much earlier than the coalescence. Moreover, we will assume that the relative speed of each black hole relative to the æther field is small as well. The latter hypothesis can be justified by recalling two facts. On the one hand, the æther must be almost aligned with the CMB frame in order to avoid non-viable effects on the cosmological evolution, and notably large deviations away from the GR predictions for the CMB spectrum [146]. On the other hand, the peculiar velocities of galaxies such as our Milky Way, relative to the CMB, are of the order of $\sim 10^{-3}$. From this, we conclude that the velocity of the center of mass of binary systems with respect to the æther must also be small, justifying our assumption.

Furthermore, considering that the black holes are sufficiently afar, we will model each of them using a point-particle prescription. In order to encode the Nordtvedt effect described in the previous discussion, the point-particle action must depend on new “æther charges” or “sensitivity parameters”. These sensitivities will effectively couple the particles to the æther field.

In general, modeling compact objects using point-particles requires a scheme to describe their dynamics. This scheme must include effects such as the self-force appearing in any

field theory [147], but also the modifications to the dynamics coming from violations of the strong equivalence principle. Let us first describe how the violations of the strong equivalence principle are parametrized for scalar-tensor theories as given by the action (3.16). We can make a point-particle model, using the gravitational mass (3.18), by writing the point-particle action $S_{\text{pp}A}^{\phi} = -\int m_A(\phi)d\tau_A$, where $d\tau_A$ is the proper time along the body's trajectory. As we are interested in a post-Newtonian regime, where all motion is slow compared to the speed of light, we expect that the variations of the scalar field are slow and small as well. Then we can consider the leading-order Taylor expansion of the mass $m_A(\phi)$ in terms of the field ϕ , and parametrize the violations of SEP through the sensitivity [148]

$$s_A^{\phi} \equiv \left. \frac{\partial \ln m_A}{\partial \ln \phi} \right|_{\phi=\phi_0}, \quad (3.19)$$

where ϕ_0 is the (constant) value of the scalar field far from the object. This procedure allows to take into account the renormalization of the binding energy due to the dependence of the value of the gravitational constant on the local value of the scalar field.

For Lorentz-violating gravity, we can make use of a similar strategy to model the modifications to the dynamics coming from violations of the strong equivalence principle. A simple way to describe the latter consists of characterizing each body A by a mass function $m_A(\gamma_A)$, depending on its relative velocity with respect to the æther frame. This introduces a dependence in the point-particle action $S_{\text{pp}A}$ on the particle's Lorentz factor with respect to the æther, $\gamma_A \equiv \mathbf{u}_A \cdot \mathbf{u}$, where \mathbf{u} is the æther field at the particle's position and \mathbf{u}_A its four-velocity. Thus, the particle's point-particle action becomes [149]

$$S_{\text{pp}A} = -\int m_A(\gamma_A)d\tau_A, \quad (3.20)$$

where $d\tau_A$ is the proper time along the body's trajectory. Let us denote the velocity of the A -th particle with respect to the æther field as v_A , i.e., $v_A = \sqrt{\gamma^2 - 1}/\gamma$, and the relative velocity between the bodies as v_{12} . Since we are considering a PN regime where both v_{12} and v_A are small parameters, we can express the mass function $m_A(\gamma_A)$ perturbatively near the static limit $\gamma_A = 1$ (corresponding to $v_A = 0$). Expanding we can write thus

$$S_{\text{pp}A} = -\tilde{m}_A \int d\tau_A \left\{ 1 + \sigma_A(1 - \gamma_A) + \frac{1}{2}\sigma'_A(1 - \gamma_A)^2 + \mathcal{O}[(1 - \gamma_A)^3] \right\}, \quad (3.21)$$

where $\tilde{m}_A \equiv m_A(1)$ is the body's mass while at rest with respect to the æther, and where we have introduced the *sensitivities* σ_A and σ'_A as

$$\begin{aligned} \sigma_A &\equiv - \left. \frac{d \ln m_A(\gamma_A)}{d \ln \gamma_A} \right|_{\gamma_A=1}, \\ \sigma'_A &\equiv \sigma_A + \sigma_A^2 + \left. \frac{d^2 \ln m_A(\gamma_A)}{d(\ln \gamma_A)^2} \right|_{\gamma_A=1}. \end{aligned} \quad (3.22)$$

Let us stress that the sensitivities, as defined above, will in principle depend on the body's composition and internal structure. Thus for instance, the sensitivity of a neutron star of mass m and spin \vec{J} has no reason to be the same as the sensitivity of a black hole of the same mass and spin. This is markedly different from GR, and means in particular that the

effacement principle is violated. Therefore we have to compute the sensitivities for each different type of object. In this chapter we aim to compute them for black holes.

When we model the interaction between the æther and a massive object with an effective action such as (3.21), we formally introduce a direct coupling between the matter and the æther. However, the field equations (2.24) and (2.25) were obtained from an action where the matter couples only to the metric. Consequently, when modeling the coupling between a point-particle and the æther we must modify the field equations in order to take into account the effect of the sensitivities. Variation of the total action (2.39) with respect to its degrees of freedom will notably differ for S_{matter} , where terms proportional to the sensitivities will appear. More precisely, in the modified Einstein equations (2.24) and (2.44) the stress energy tensor of matter picks up a contribution proportional to sensitivities. Thus, while the æther stress energy tensor remains unchanged (i.e., given by (2.47)) the matter stress energy tensor becomes [129]

$$T_{\text{ppA,EA}}^{\mu\nu} = \frac{\tilde{m}_A \delta^{(3)}(x^i - x_A^i)}{u_A^0 \sqrt{-g}} \left([1 + \sigma_A - \frac{\sigma'_A}{2}(1 - \gamma_A^2)] \times u_A^\mu u_A^\nu - [\sigma_A + \sigma'_A(1 - \gamma_A)] (2u^{(\mu} u^{\nu)} - \gamma_A u^\mu u^\nu) \right), \quad (3.23)$$

for Einstein-æther theory and

$$T_{\text{ppA,kh}}^{\mu\nu} = \frac{\tilde{m}_A \delta^{(3)}(x^i - x_A^i)}{u_A^0 \sqrt{-g}} \left([1 + \sigma_A - \frac{\sigma'_A}{2}(1 - \gamma_A^2)] \times u_A^\mu u_A^\nu - [\sigma_A + \sigma'_A(1 - \gamma_A)] \gamma_A u^\mu u^\nu \right), \quad (3.24)$$

for khronometric theory. Here, x_A is the A th point-particle's worldline and $\delta^{(3)}$ is the three-dimensional Dirac delta. The æther equation is similarly modified. In fact, both in Einstein-æther and khronometric theory the vector A^μ now includes a source term [129]

$$\tilde{A}^\mu \equiv A^\mu + \frac{8\pi G_{\text{EA}} \tilde{m}_A}{u_A^0 \sqrt{-g}} \delta^{(3)}(x^i - x_A^i) \times (\sigma_A + \sigma'_A(1 - \gamma_A))(u_A^\mu - \gamma_A u^\mu), \quad (3.25)$$

where A^μ is still given by (2.45). Note that σ_A is multiplied by terms of order v_A , whereas σ'_A appears next to terms proportional to v_A^3 .

Now that we know how the field equations are modified in order to take into account for the effective coupling between an compact body A and the æther, we would like to have a procedure allowing us to compute the sensitivities. In order to achieve this goal, let us obtain a post-Newtonian expansion of the metric of a point-particle using the effective field equations. Then, comparison to an asymptotic solution of the field equations will allow us to express the sensitivities in terms of a set of parameters defining the asymptotic solution.

3.3 Sensitivities and the asymptotic metric

The field equations for a binary black hole system can be solved within a post-Newtonian approximation, i.e., one where an expansion of the dynamics is made using the orbital speed as a small parameter $v_{12} \ll 1$. We will also impose that the speed of each black hole with respect to the æther field be small, i.e., $v_A \ll 1$. The 1PN solution has the same form in both Einstein-æther and khronometric theory. The results of this section were obtained in [129].

Let us consider two black holes of masses \tilde{m}_1, \tilde{m}_2 orbiting each other. In the standard post-Newtonian gauge, that is, using PN coordinates (t', x', y', z') such that the spatial part of the metric is diagonal and isotropic (see [9], section 4.2 for more details), and restoring the powers of $1/c$ to clarify the PN order counting, the 1PN metric reads [129]

$$\begin{aligned} g_{0'0'} &= 1 - \frac{1}{c^2} \frac{2G_N \tilde{m}_1}{r'_1} + \frac{1}{c^4} \left[\frac{2G_N^2 \tilde{m}_1^2}{r'^2_1} + \frac{2G_N^2 \tilde{m}_1 \tilde{m}_2}{r'_1 r'_2} + \frac{2G_N^2 \tilde{m}_1 \tilde{m}_2}{r'_1 r'_{12}} - \frac{3G_N^2 \tilde{m}_1}{r'_1} v_1'^2 (1 + \sigma_1) \right] \\ &\quad + 1 \leftrightarrow 2 + \mathcal{O}(1/c^6), \\ g_{0'i'} &= -\frac{1}{c^3} \left[B_1^- \frac{G_N \tilde{m}_1}{r'_1} v_1'^i + B_1^+ \frac{G_N \tilde{m}_1}{r'_1} v_1'^i \hat{n}_1^i \hat{n}_1'^j \right] + 1 \leftrightarrow 2 + \mathcal{O}(1/c^4), \\ g_{i'j'} &= -\left(1 + \frac{1}{c^2} \frac{2G_N \tilde{m}_1}{r'_1} \right) \delta_{ij} + 1 \leftrightarrow 2 + \mathcal{O}(1/c^4), \end{aligned} \tag{3.26}$$

where v_A^i is the velocity of the A -th black hole, r'_{12} the binary's separation, r'_A the distance from the field point to the A -th black hole, \hat{n}_A^i the unit vector associated with r'_A and the symbol $1 \leftrightarrow 2$ means that one has to duplicate the terms on the right-hand side exchanging body 1 and 2. In this scheme, a term proportional to $(|v_A^i|/c)^{2N}$ (or equivalently to $G(\tilde{m}_A/r'_A)^N$) with respect to the Newtonian solution is said to be of N -th PN order and will be denoted as $\mathcal{O}(1/c^{2N})$. In khronometric theory the coefficients B^\pm are given by

$$B_A^\pm \equiv \pm \frac{3}{2} - 2 \pm \frac{1}{4} (\alpha_1^{\text{kh}} - 2\alpha_2^{\text{kh}}) \left(1 + \frac{2 - \alpha}{2\beta - \alpha} \sigma_A \right) - 2\sigma_A - \frac{1}{4} \alpha_1^{\text{kh}} (1 + \sigma_A), \tag{3.27}$$

where the PPN parameters are, for khronometric theory, given by

$$\alpha_1^{\text{kh}} = \frac{4(\alpha - 2\beta)}{\beta - 1}, \tag{3.28}$$

$$\alpha_2^{\text{kh}} = \frac{(\alpha - 2\beta)[- \beta^2 + \beta(\alpha - 3) + \alpha + \lambda(-1 - 3\beta + 2\alpha)]}{(\beta - 1)(\lambda + \beta)(\alpha - 2)}. \tag{3.29}$$

Using the same notations, the æther field at 1PN has the form

$$U^0 = 1 + \frac{1}{c^2} \frac{G_N \tilde{m}_1}{r'_1} + 1 \leftrightarrow 2 + \mathcal{O}(1/c^4), \tag{3.30}$$

$$U^i = \frac{1}{c^3} \frac{G_N \tilde{m}_1}{r'_1} \left(C_1^- v_1'^i + C_1^+ v_1'^j \hat{n}_1^j \hat{n}_1'^i \right) + 1 \leftrightarrow 2 + \mathcal{O}(1/c^5), \tag{3.31}$$

where the coefficients C^\pm are

$$C_A^\pm \equiv \frac{8 + \alpha_1^{\text{kh}}}{4} (1 + \sigma_A) \pm \frac{2 - \alpha}{4} \left(\frac{2\alpha_2^{\text{kh}} - \alpha_1^{\text{kh}}}{(2\beta - \alpha)} + \frac{2\sigma_A}{\beta + \lambda} \right). \tag{3.32}$$

Note that at 1 PN order there is only one sensitivity parameter, σ_A , appearing in the metric, whereas σ'_A is expected to appear at higher PN orders. More precisely, $g_{t',t'}$ contains the sensitivity multiplied by a $\mathcal{O}(v^2)$ term, the frame dragging metric component $g_{t',i'}$ contains σ multiplied by a $\mathcal{O}(v)$ term and the spatial part of the metric $g_{i'j'}$ does not contain any term proportional to the sensitivities.

3.3.1 Extraction procedure

This result for the 1PN metric hints at an extraction prescription allowing us to compute the sensitivities from a single-body solution. Indeed, this procedure can be obtained from the following argument. Let us consider the limit where there is only one black hole, by placing ourselves within a buffer region such that $R_* \ll r \ll r'_{12}$, where R_* is the ‘‘horizon radius’’ of the black hole. The existence of this region is guaranteed by the conditions defining the PN scheme, particularly the fact that $r'_{12} \gg R_*$. In this buffer region we can set the other black hole’s mass to zero, ($\tilde{m}_2 = 0$, i.e., the effect of the second black hole is subdominant) or equivalently take the limit where r'_{12} goes to infinity, producing an expression that contains parameters relative to the first black hole only.

Let us remark that, while it is difficult to look for exact solutions for a binary system, we can still attempt to find such solutions for single bodies (provided that they are simple enough). The key observation here is that, if we are able to solve the exact strong-field equations without a point-particle approximation, then we can read the sensitivity from the asymptotic behavior of the exact solution, by comparing to equation (3.26). This is the extraction procedure that we will use to compute the black hole sensitivity in the following sections. More precisely, we will consider a single black hole moving slowly with respect to the æther field, so that its speed v will be taken as a small parameter, and then solve the field equations to the first order in its speed. Then we will compare the asymptotic behavior of the analytic solution to the frame dragging sector of the PN solution in order to read the $\mathcal{O}(v)$ term containing the sensitivity σ . Since we will work using spatial spherical coordinates it is useful to recast the 1 PN metric of equation (3.26) for a single body in spherical coordinates. Thus, dropping the A label since we work with a single body, the asymptotic solution for a slowly moving black hole is given, in a suitable gauge, by the metric [129]

$$\begin{aligned} ds^2 = dt^2 - dr^2 &+ \left\{ -\frac{2M_*}{r}(dt^2 + dr^2) - r^2(d\theta^2 + \sin^2\theta d\varphi^2) \right. \\ &\quad \left. -2v \left[(B^- + B^+ + 4)\frac{M_*}{r} \right] \cos\theta dt dr \right. \\ &\quad \left. +2vr \left[(3 + B^- - J)\frac{M_*}{r} \right] \sin\theta dt d\theta \right\} \times \left[1 + \mathcal{O}\left(v, \frac{1}{r}\right) \right], \end{aligned} \quad (3.33)$$

and the æther field

$$U_\mu dx^\mu = (dt + v \cos\theta dr - vr \sin\theta d\theta) \times \left[1 - \frac{M_*}{r} + \mathcal{O}\left(\frac{1}{r^2}\right) \right] + \mathcal{O}(v^2), \quad (3.34)$$

where $M_* = G_N \tilde{m}$. Here B^\pm takes the same form as before and J is defined as

$$B^\pm \equiv \pm \frac{3}{2} \pm \frac{1}{4}(\alpha_1^{\text{kh}} - 2\alpha_2^{\text{kh}}) \left(1 + \frac{2-\alpha}{2\beta-\alpha}\sigma \right) - \left(2 + \frac{1}{4}\alpha_1^{\text{kh}} \right) (1 + \sigma), \quad (3.35)$$

$$J \equiv \frac{(2 + 3\lambda + \beta)[2(\beta + \sigma) - \alpha(1 + \sigma)]}{2(\lambda + \beta)(\alpha - 2)}. \quad (3.36)$$

Clearly, the sensitivity can be read off a strong field solution from the asymptotic values of the g_{tr} and $g_{r\theta}$ components of the metric, through the combinations $3 + B^- - J$ and $B^- + B^+ + 4$, respectively. Both readings must give the same value. This is indeed a consistency condition that we use to validate our computations.

3.4 Dipolar radiation

Before tackling the problem of finding exact solutions to the field equations, we will review the observable effects produced by the sensitivities. First, let us recall that the sensitivities were introduced in order to quantify deviations from geodesic motion, thus encoding the violations of the strong equivalence principle. Indeed, they characterize how the structure of a compact object, such as a black hole or a neutron star, changes with its motion relative to the ambient (extra) field in which it is immersed, i.e., the æther field. They are also determined by the composition and nature (black hole or neutron star) of the body, so different objects will respond differently to the ambient field. This is dependence on composition and nature of the body is a manifest breaking of the universality of free fall.

The sensitivities affect both the conservative and dissipative sectors. Indeed, in the conservative sector the sensitivities modify Newton’s universal gravitation law [149], so that the motion of a binary is described, at Newtonian order, by

$$\dot{v}_A^i = -\frac{G_N \tilde{m}_B \hat{n}_{AB}^i}{(1 + \sigma_A) r_{AB}^2}, \quad (3.37)$$

where $r_{AB} = |\mathbf{x}_A - \mathbf{x}_B|$ and $\hat{n}_{AB}^i = (x_A^i - x_B^i)/r_{AB}$.

This relation can be written in a more symmetrical way as

$$\dot{v}_A^i = -\frac{\mathcal{G} m_B \hat{n}_{AB}^i}{r_{AB}^2}, \quad (3.38)$$

where we introduced the *active* gravitational masses

$$m_B \equiv \tilde{m}_B (1 + \sigma_B) \quad (3.39)$$

and the “strong field” gravitational constant

$$\mathcal{G} \equiv \frac{G_N}{(1 + \sigma_A)(1 + \sigma_B)}. \quad (3.40)$$

The sensitivities also modify the equations of motion at higher PN order in the conservative sector in a similar fashion [149].

3.4.1 Dissipative PN dynamics

Regarding the dissipative sector, we expect to lose binary gravitational energy not only to the tensor modes, as in general relativity, but also to the scalar modes present in khronometric theory (and also to the vector modes in Einstein-æther). Furthermore, the sensitivities allow for dipolar radiation, which is absent in general relativity due to conservation of linear momentum (cf. section 1.5, see also [10]). This modifies in turn the gravitational wave flux.

From the corrections to the conservative sector at Newtonian order, we have that the binary’s binding energy E_b will be defined as in Newtonian mechanics, but written instead in terms of the strong field gravitational constant \mathcal{G} and the active gravitational masses m_A :

$$E_b = -\frac{\mathcal{G} \mu m}{2a}, \quad (3.41)$$

where a is the semi-major axis, $\mu \equiv m_1 m_2 / m$ is the reduced (active) mass and $m \equiv m_1 + m_2$ is the total (active) mass. The energy carried away from the system can be related to the rate of change of the gravitational binding energy through the balance law [124, 149]

$$\dot{E}_b = -\mathcal{F}, \quad (3.42)$$

where \mathcal{F} is the gravitational wave flux. In khronometric and Einstein-æther theory, this energy is carried away from the source by the tensor and scalar modes, as well as vector modes for Einstein-æther theory. The gravitational wave flux was first computed in [149, 124] for weak-field sources and later generalized to strong-field sources in [129], both for khronometric and Einstein-æther theory. From here on we will only discuss about the radiation problem in khronometric theory. We refer to [129] for a detailed discussion of gravitational radiation in Einstein-æther theory.

In order to compute the flux \mathcal{F} , we can place ourselves in the radiation zone and express the metric and khronon field as perturbations of the flat background and of a future time direction, respectively. Thus, we choose coordinates such that the background metric is the Minkowski metric and the æther background is aligned with the future direction. In this way, we can define $g_{\mu\nu} = \eta_{\mu\nu} + h_{\mu\nu}$ and $u^\mu = \delta_t^\mu + U^\mu$. Furthermore, we can choose a gauge [124] where $U^0 = 0$, by making an infinitesimal gauge transformation redefining the time coordinate t . In fact we have that

$$U^0 \rightarrow U^0 - \partial_t \xi \quad \text{if} \quad T \rightarrow T + \xi, \quad (3.43)$$

so that we can choose ξ so as to eliminate U^0 . Decomposing the metric and æther perturbations as irreducible transverse and longitudinal components, the perturbations can be written as

$$\begin{aligned} h_{0i} &= \gamma_i^h + \gamma_{,i}^h, & U^i &= \nu^i + \nu_{,i}, \\ h_{ij} &= \phi_{ij} + \frac{1}{2\Delta} \left(\delta_{ij} \Delta F^h - F_{,ij}^h \right) + 2\phi_{(i,j)} + \phi_{,ij}^h, \end{aligned} \quad (3.44)$$

where Δ is the Laplacian differential operator defined as $\Delta \equiv \partial_i \partial_i$, and

$$\gamma_{i,i}^h = \nu_{,i}^i = \phi_{ii} = \phi_{i,ij} = \phi_{i,i} = 0. \quad (3.45)$$

Thus, γ^h and $\partial_i \gamma^h$ are the transverse and longitudinal parts of h_{0i} , a similarly ν^i and $\partial_i \nu$ are the transverse and longitudinal pieces of U^i . The functions ϕ_{ij} and F correspond to the spin-2 and spin-0 far-zone fields, as it will become clear in equations (3.48) and (3.49), while the other metric terms correspond to longitudinal modes that do not radiate in khronometric theory. Let us denote by $x_A(t)$ the trajectories of the A -th point-particle and $v_A^i(t) = \dot{x}_A^i$ its 3-velocity. Our goal is to obtain the perturbation fields at a distance r far away from the source, $r \gg |x_A^i|$, i.e., in the radiation zone. Then, the transverse-traceless projector is

built using the unit-norm vector $\hat{n}^i \equiv \frac{r^i}{r}$, where the r^i are the coordinates of the field point. Inserting the metric and æther decomposition into the field equations, as derived from in the point-particle model, allows us to obtain the behavior by the far-zone fields. Following the methods described in [124], the gravitational wave flux can be computed as

$$\langle \mathcal{F} \rangle = -\frac{1}{32\pi G_{\text{EA}}} \oint_S d\Omega r^2 \left\langle \frac{1}{c_t} \dot{\phi}_{ij} \dot{\phi}_{ij} - \frac{(\alpha-2)}{2\alpha c_s} \dot{F} \dot{F} \right\rangle, \quad (3.46)$$

where the angled-brackets indicate an average over several wavelengths. Also, the propagation speed of the tensor modes is $c_t^{-2} = 1 - \beta$, and the propagation speed of the scalar modes is given by

$$c_s^2 = \frac{(\alpha - 2)(\beta + \lambda)}{\alpha(\beta - 1)(2 + \beta + 3\lambda)}, \quad (3.47)$$

cf. section 2.5. The far-zone fields are found to be [124] given by the expressions

$$\phi_{ij} = -\frac{2G_{\text{EA}}}{r} \ddot{Q}_{ij}^{TT}(t - r/c_t), \quad (3.48)$$

in the case of the tensor modes, which must be evaluated at the retarded time $t - r/c_t$, and

$$F = \frac{4G_{\text{EA}}\alpha}{(\alpha - 2)r} \left[\frac{3}{2}(\mathcal{Z} - 1)\hat{n}^i\hat{n}^j\ddot{Q}_{ij} + \frac{1}{2}\mathcal{Z}\ddot{I}_{kk} - \frac{\hat{n}^i\hat{n}^j}{\alpha c_s^2}(\ddot{Q}_{ij} + \frac{1}{3}\delta_{ij}\ddot{I}_{kk}) + \frac{2}{\alpha c_s}\hat{n}^i\Sigma^i \right], \quad (3.49)$$

in the case of the scalar modes. Here, Q_{ij} is the traceless quadrupole tensor, defined as

$$Q_{ij} = I_{ij} - \frac{1}{3}\delta_{ij}I_{kk}, \quad (3.50)$$

where the tensor of inertia I_{ij} of a system of A point-particles is given by

$$I_{ij} = \sum_A m_A x_A^i x_A^j \left[1 + \mathcal{O}(1/c^2) \right]. \quad (3.51)$$

We have also introduced the trace-free part of the rescaled mass quadrupole tensor \mathcal{Q}_{ij} , related to the rescaled mass inertia tensor

$$\mathcal{I}_{ij} = \sum_A \sigma_A \tilde{m}_A x_A^i x_A^j \left[1 + \mathcal{O}(1/c^2) \right], \quad (3.52)$$

by the relation

$$\mathcal{Q}_{ij} = \mathcal{I}_{ij} - \frac{1}{3}\delta_{ij}\mathcal{I}_{kk}, \quad (3.53)$$

as well as the vector

$$\Sigma^i = -\sum_A \sigma_A \tilde{m}_A v_A^i \left[1 + \mathcal{O}(1/c^2) \right], \quad (3.54)$$

and the constant \mathcal{Z} is given by

$$\mathcal{Z} \equiv \frac{(\alpha_1^{kh} - 2\alpha_2^{kh})(1 - \beta)}{3(2\beta - \alpha)}. \quad (3.55)$$

Let us stress that the different quantities defining F are to be evaluated at the retarded time $t - r/c_s$.

The flux can then be evaluated for a binary system in terms of the (Newtonian) center-of-mass coordinates $X_{CM}^i \equiv (m_1 x_1^i + m_2 x_2^i)/m$. The energy lost by the binary system is finally given by the formula [129]

$$\begin{aligned} \frac{\dot{E}_b}{E_b} &= 2 \left\langle \left(\frac{\mathcal{G}G_{\text{EA}}a\mu m}{r_{12}^4} \right) \left\{ \frac{8}{15}(\mathcal{A}_1 + \mathcal{S}\mathcal{A}_2 + \mathcal{S}^2\mathcal{A}_3)(12v_{12}^2 - 11\dot{r}_{12}^2) + 4(\mathcal{B}_1 + \mathcal{S}\mathcal{B}_2 + \mathcal{S}^2\mathcal{B}_3)\dot{r}_{12}^2 \right. \right. \\ &\quad \left. \left. + (s_1 - s_2)^2 \left(\mathcal{C} + \frac{18}{5}\mathcal{A}_3 V_{CM}^j V_{CM}^j + \left(\frac{6}{5}\mathcal{A}_3 + 36\mathcal{B}_3 \right) (V_{CM}^i \hat{n}_{12}^i)^2 \right) \right. \right. \\ &\quad \left. \left. + (s_1 - s_2) \left[12(\mathcal{B}_2 + 2\mathcal{S}\mathcal{B}_3)V_{CM}^i \hat{n}_{12}^i v_{12}^j \hat{n}_{12}^j + \frac{8}{5}(\mathcal{A}_2 + 2\mathcal{S}\mathcal{A}_3)V_{CM}^i (3v_{12}^i - 2\hat{n}_{12}^i v_{12}^j \hat{n}_{12}^j) \right] \right\} \right\rangle, \quad (3.56) \end{aligned}$$

where $V_{CM}^i \equiv \dot{X}_{CM}^i$ is the center of mass velocity of the system relative to the æther and $v_{12}^i \equiv \dot{r}_{12}^i$ is the relative 3-velocity of the binary. Also, we have introduced the coefficients

$$\mathcal{A}_1 \equiv \frac{c}{c_t} + \frac{3\alpha(\mathcal{Z}-1)^2c}{2c_s(2-\alpha)}, \quad \mathcal{A}_2 \equiv \frac{2(\mathcal{Z}-1)c^3}{(\alpha-2)c_s^3}, \quad (3.57)$$

$$\mathcal{A}_3 \equiv \frac{2c^5}{3\alpha(2-\alpha)c_s^5}, \quad \mathcal{B}_1 \equiv \frac{\alpha \mathcal{Z}^2c}{4c_s(2-\alpha)}, \quad (3.58)$$

$$\mathcal{B}_2 \equiv \frac{\mathcal{Z}c^3}{3c_s^3(\alpha-2)}, \quad \mathcal{B}_3 \equiv \frac{c^5}{9\alpha c_s^5(2-\alpha)}, \quad (3.59)$$

$$\mathcal{C} \equiv \frac{4c^3}{3c_s^3 \alpha(2-\alpha)} \quad (3.60)$$

where we reintroduced the powers of c for later power-counting, and the shorthand $\mathcal{S} \equiv s_1 m_2/m + s_2 m_1/m$. Finally, the sensitivities are represented by the parameter

$$s_A \equiv \frac{\sigma_A}{1 + \sigma_A}. \quad (3.61)$$

Let us remark first that in the limit where the khronometric coupling coefficients α, β, λ go to zero, the flux and the rate of energy loss formulae reduce to the GR result (provided that the sensitivities vanish in that limit), that is, we recover the quadrupole formula and there is no dipolar radiation. The preferred frame effect can be observed in these formulae through the presence of V_{CM} , the velocity of the center of mass with respect to the æther, whereas secular term depending directly on X_{CM} can be neglected [149]. Most importantly, let us stress that, provided that the difference of the bodies' sensitivities $|s_1 - s_2|$ and the coupling constants are large enough, the khronometric terms can dominate the GR ones, even for small coupling. Indeed, the leading order terms in the khronometric result enter at an absolute order of $\mathcal{O}(1/c^8)$, whereas the quadrupole formula in GR does it at $\mathcal{O}(1/c^{10})$. These dominant terms are proportional to the difference of the sensitivity parameters squared. Thus, this scaling given by fewer powers of \tilde{m}/r_{12} corresponds to a -1 PN correction and is therefore dominant during inspiral. This new emission mode, besides the standard quadrupole emission, enhances the energy loss rate of the binary, and consequently it will tend to shorten the duration of the orbital phase of binary systems and lead them to a faster coalescence (cf. section 1.6.2).

3.5 Chapter conclusions

We have seen that in modified theories of gravity, there is, generically, violations of the strong equivalence principle, that is, the universality of free fall does not extend into self-gravitating objects. This effect can be parametrized by a set of parameters called the *sensitivities*, as can be seen by introducing an effective point particle model, as explained in 3.2. The modification to the orbital dynamics induced by the sensitivities also modifies the gravitational wave flux, and in the case of Lorentz violating gravity the dominant emission mode now appears to be dipolar, as discussed in 3.4. The strength of this dipolar emission is proportional to the difference of the sensitivities squared. The apparition of a new emission channel leads to a faster binary energy loss, and therefore to a faster evolution towards coalescence. In particular, this would differ from predictions using multi-band GW detections as mentioned in section 1.6.2. Therefore the computation of the sensitivity for different

compact objects is of capital importance. This has been done in reference [?] in the case of neutron stars, and the purpose of the next chapter is to compute the sensitivity for binary black holes. More precisely, in section 3.3 we have seen that the sensitivities can be extracted from a solution slowly moving with respect to the Lorentz violating field, as it was done in [?], and the next chapter will tackle the computation of slowly moving black holes.

4 – Slowly moving black holes in Lorentz-violating Gravity

In this chapter we will see how the preferred-frame effects introduced in the gravity sector affect the motion of a binary black hole system. We will also see how this leads to detectable changes in the gravitational wave fluxes the binary emits. In order to do so, we will first review the general physical principles that lead to these modifications in section 3.1, in particular the strong equivalence principle and its violations. Based on this motivation, in section 3.2 we will introduce a point-particle model containing parameters quantifying these violations, which we will refer to as “sensitivities”. Using a post-Newtonian approximation for the binary dynamics, we will show how this scheme naturally leads to a semi-analytic prescription to compute the sensitivities in section 3.3. Indeed, we will see that these can be read off from the asymptotic metric of a single slowly moving black hole. The formalism developed will be extended to describe the modified gravitational radiation in section 3.4. Up to that point, we do not pretend showing any new result. Indeed, new results are postponed to the end of this chapter, starting in section 4.1. There we will describe solutions for black holes slowly moving with respect to a Lorentz-violating field. We will show that some of these solutions are not regular. Moreover, we will conclude that imposing regularity reduces the parameter space of Lorentz-violating theories in a way that is in agreement with experimental constraints. Finally, with these results at hand, the possibility of observing modifications to the gravitational wave flux will be discussed in section 4.4.

4.1 Slowly moving black holes

In section 3.3.1, we highlighted a prescription allowing us to measure the sensitivities of a compact object, which appear when modeling a binary system through the point-particle approximation, by taking the limit where the system is composed of a single object moving relative to the khronon field. In this section, we will construct such a solution in the case of a non-spinning black hole in khronometric theory, slowly moving with respect to the ambient khronon field. In order to do so, we will begin by presenting the metric and khronon Ansatz as composed by a static background and a perturbation scaling with the relative velocity v between the khronon and the black hole. Expanding the field equations at zeroth order in v will give the static solution described in section 2.6.1. Solving the first order equations will be the core of this section.

4.1.1 Construction of the Ansatz

We have formulated the physical system as composed by a stationary æther background and a non-spinning black hole in slow motion with respect to it. Equivalently, we can choose to describe the system as given by a black hole at rest and a moving æther¹ whose asymptotic behavior corresponds to a constant flow. Both pictures are related by a gauge transformation. Here we choose the latter point of view, as it avoids the need of a time-dependent description of the black hole's position. For definiteness, we will set the motion of the æther flow along the z axis, and let v be its asymptotic speed.

4.1.1.a) Symmetries and the perturbation potentials

We want to choose our coordinates in such a way that, at zeroth order in v , the solution will be described by the metric (2.77) and the khronon (2.78). Those solutions are given Ansatz using Eddington-Finkelstein coordinates (cf. section 2.6). However, for our goals it is easier to write the metric's and the æther's first order perturbations using isotropic cylindrical coordinates, $x^\mu = \{t, \rho, \phi, z\}$. In these coordinates, the black hole is located at the origin and its four-velocity is given by $u_{\text{bh}}^\mu = (1/\sqrt{g_{tt}}, 0, 0, 0)$ (black hole at rest). The background metric can be written as

$$ds^2 = f(\tilde{r})dt^2 - b^2(\tilde{r})(d\rho^2 + \rho^2 d\phi^2 + dz^2), \quad (4.1)$$

where $\tilde{r} = \sqrt{\rho^2 + z^2}$ is the isotropic radial coordinate. Note that \tilde{r} is different from the areal coordinate r used in Eddington-Finkelstein coordinates. They are simply related by the relation $r = \tilde{r}b(\tilde{r})$. Also, $b(\tilde{r})$ is related to $B(r)$ by the relation

$$\frac{B(r)}{\sqrt{f(r)}} = \frac{b(\tilde{r})}{b(\tilde{r}) + \tilde{r} db(\tilde{r})/d\tilde{r}}. \quad (4.2)$$

The background æther field is given by

$$u_\mu^{\mathbf{b}} dx^\mu = A(r)dt + \tilde{u}_r d\tilde{r}, \quad (4.3)$$

where \tilde{u}_r is determined by the normalization condition $u_\mu^{\mathbf{b}} u_{\mathbf{b}}^\mu = 1$. Note that $\tilde{u}_r \neq 0$, in contrast to a star where the æther cannot have any r component at $\mathcal{O}(v^0)$ (in which case we must set $u_\mu^{\mathbf{b}} = \delta_\mu^t \sqrt{f(\tilde{r})}$), see [150] where this is proved by direct resolution of the field equations². The advantage of using isotropic coordinates, instead of directly using Eddington-Finkelstein coordinates, comes from the fact that in the former the spatial part of the metric becomes conformally flat, thus simplifies our treatment in the following. Moreover, the use of cylindrical coordinates rather than spherical coordinates allows for an easier treatment of the

1. Let us recall that now the æther field is not a fundamental quantity, but is rather derived from the khronon field. We choose to speak of the æther field derived from the khronon, instead of the khronon field itself, as it allows for a simple geometrical description in terms of a vector field flow.

2. The physical reason behind this fact is that in stars we must impose regularity of the æther field at the center. More precisely, spherical symmetry implies that the radial part of the æther must vanish at $r = 0$. Imposing this boundary condition together with asymptotical flatness leads to the vanishing of the radial component everywhere. In contrast, for black holes the æther flow can be singular at the center and in fact it *flows* towards the center.

perturbed system. Indeed, our physical system exhibits cylindrical invariance with respect to the axis of the æther flow, i.e., the z axis. This implies that physical perturbations must transform, under rotations of the z axis, as scalar, vector, or tensor quantities. Also, due to cylindrical symmetry we have that physical quantities cannot depend on the azimuthal coordinate ϕ .

Let us consider the symmetry properties of the first order perturbation, i.e., carrying v . We note that the simultaneous coordinate reversal

$$\begin{aligned} t &\mapsto -t, \\ z &\mapsto -z, \end{aligned} \tag{4.4}$$

must leave the physics unchanged. This transformation can also be interpreted as a simultaneous time and motion reversal, which is clearly a symmetry of the system. It follows that the only metric components allowed for the perturbations are g_{tt} , $g_{t\rho}$, g_{tz} , $g_{\rho\rho}$, $g_{\rho z}$ and g_{zz} . With respect to spatial rotations, the metric perturbations will decompose as

$$\begin{aligned} \delta(ds^2) = & \quad v \delta g_{tt} dt^2 && \text{scalar} \\ & + 2v (\delta g_{t\rho} d\rho + \delta g_{tz} dz) dt && \text{vector} \\ & + v (\delta g_{\rho\rho} d\rho^2 + 2\delta g_{\rho z} d\rho dz + \delta g_{zz} dz^2) && \text{tensor}. \end{aligned} \tag{4.5}$$

The total metric would be then

$$\begin{aligned} ds^2 = & f(\tilde{r}) dt^2 - b^2(\tilde{r}) (d\rho^2 + \rho^2 d\phi^2 + dz^2) \\ & + v (\delta g_{tt} dt^2 + 2\delta g_{t\rho} dt d\rho + 2\delta g_{tz} dz dt + \delta g_{\rho\rho} d\rho^2 + 2\delta g_{\rho z} d\rho dz + \delta g_{zz} dz^2) + \mathcal{O}(v^2). \end{aligned} \tag{4.6}$$

The same symmetry considerations applied to the æther field imply that the only components that can be perturbed are δu^t , δu^ρ and δu^z . This leads to the æther Ansatz

$$u^\mu = u_{\mathbf{b}}^\mu + \delta u^t (\partial_t)^\mu + \delta u^\rho (\partial_\rho)^\mu + \delta u^z (\partial_z)^\mu. \tag{4.7}$$

Clearly, the only 3-vectors we have in order to construct the perturbations belong to the (ρ, z) plane and are given by $\vec{v} = (0, v)$ and $\vec{n} = (\rho, z)/\tilde{r} = (\sin \theta, \cos \theta)$, which provides a basis in the (ρ, z) plane. Thus, we must construct scalar, vector and tensor perturbations of order $\mathcal{O}(v)$ by means of \vec{v} and \vec{n} . This means, for instance, that the scalar terms must be expressed as the product of an arbitrary function of the radius \tilde{r} times the scalar $\vec{n} \cdot \vec{v}$. Thus, we can express the metric perturbations as

$$\begin{aligned} \delta g_{tt} &\equiv \tilde{\psi}(\tilde{r}) (\vec{n} \cdot \vec{v}) = v \cos \theta \tilde{\psi}(\tilde{r}), \\ \begin{pmatrix} \delta g_{t\rho} \\ \delta g_{tz} \end{pmatrix} &\equiv \alpha_1(\tilde{r}) (\vec{n} \cdot \vec{v}) \vec{n} + \alpha_2(\tilde{r}) \vec{v} \\ &= v \begin{pmatrix} \sin \theta \cos \theta \alpha_1(\tilde{r}) \\ \cos^2 \theta \alpha_1(\tilde{r}) + \alpha_2(\tilde{r}) \end{pmatrix}, \\ \begin{pmatrix} \delta g_{\rho\rho} & \delta g_{\rho z} \\ \delta g_{z\rho} & \delta g_{zz} \end{pmatrix} &\equiv \alpha_3(\tilde{r}) (\vec{n} \cdot \vec{v}) n^i n^j + \alpha_4(\tilde{r}) n^{(i} v^{j)}, \\ &= v \begin{pmatrix} \cos \theta \sin^2 \theta \alpha_3(\tilde{r}) & \sin \theta (\cos^2 \theta \alpha_3(\tilde{r}) + \alpha_4(\tilde{r})) \\ \sin \theta (\cos^2 \theta \alpha_3(\tilde{r}) + \alpha_4(\tilde{r})) & \cos \theta (\cos^2 \theta \alpha_3(\tilde{r}) + \alpha_4(\tilde{r})) \end{pmatrix}, \end{aligned} \tag{4.8}$$

where we have introduced the unknown functions $\tilde{\psi}(\tilde{r})$ and $\alpha_i(\tilde{r})$ for $i = 1, 2, 3, 4$. We will refer to them as the “metric perturbation potentials”. Along the same lines, we observe that the time component δu^t must transform as a scalar under spatial rotations while $(\delta u^\rho, \delta u^z)$ must transform as a vector. Thus, we must express the æther perturbations as

$$\delta u^t = \beta_1(\tilde{r}) \vec{n} \cdot \vec{v} = v \cos \theta \beta_1(\tilde{r}), \quad (4.9)$$

$$\begin{aligned} \begin{pmatrix} \delta u^\rho \\ \delta u^z \end{pmatrix} &= \beta_2(\tilde{r}) (\vec{n} \cdot \vec{v}) \vec{n} + \gamma(\tilde{r}) \vec{v} \\ &= v \begin{pmatrix} \cos \theta \sin \theta \beta_2(\tilde{r}) \\ \cos^2 \theta \beta_2(\tilde{r}) + \gamma(\tilde{r}) \end{pmatrix}, \end{aligned} \quad (4.10)$$

where we have introduced the arbitrary functions $\beta_{1,2}(\tilde{r})$ and $\gamma(\tilde{r})$, and we will refer to them as to the “khronon perturbation potentials”. Notice that a functional dependence on ρ or z would require another projection using the vector \vec{v} , and as such it would be a $\mathcal{O}(v^2)$ effect. Thus, the perturbation potentials are functions only of $\tilde{r} = \sqrt{\rho^2 + z^2}$ and not of ρ nor z .

4.1.1.b) Asymptotic æther flow condition

At this juncture we find it convenient to remark that, from the khronon Ansatz, we can immediately foresee the asymptotic behavior that we are looking for in the perturbation potentials. Indeed, an asymptotic æther flow in slow uniform motion along the z axis would correspond to $(\partial_t - v\partial_z)/\sqrt{1-v^2}$ in Cartesian coordinates, or equivalently to $(\partial_v v - v \cos \theta \partial_r + v \sin \theta / r \partial_\theta)/\sqrt{1-v^2}$ in Eddington-Finkelstein coordinates. Thus, inspection of equations (4.9) and (4.10) allows us to conclude that we must impose

$$\beta_{1,2}(\tilde{r}) \longrightarrow 0 \quad \text{as} \quad \tilde{r} \longrightarrow \infty, \quad (4.11a)$$

$$\gamma(\tilde{r}) \longrightarrow -1 \quad \text{as} \quad \tilde{r} \longrightarrow \infty, \quad (4.11b)$$

as this guarantees that the potentials are such that the $\mathcal{O}(v)$ æther field asymptotes to $(\partial_t - v\partial_z)$.

4.1.1.c) From isotropic cylindrical coordinates to Eddington-Finkelstein coordinates

Now that we obtained the Ansätze (4.6) and (4.7) with their explicit functional form, we can transform them to Eddington-Finkelstein coordinates $\{v, r, \theta, \phi\}$. Let us warn the reader that two typographies for “v” will be present from now on. First, the letter v corresponding to the small relative velocity between the black hole and the æther field. Second, the letter v which appears as a coordinate in Eddington-Finkelstein coordinates. In these coordinates the background metric is given by

$$ds^2 = f(r)dv^2 - 2B(r)dvdr + r^2d\Omega^2, \quad (4.12)$$

and the background æther field is

$$u_\mu dx^\mu = \frac{1 + A(r)^2 f(r)}{2A(r)} dv - A(r)B(r)dr. \quad (4.13)$$

After some straightforward algebra, on the one hand we can express the metric Ansatz as

$$\begin{aligned} g_{\mu\nu}dx^\mu dx^\nu = & (f + v \cos \theta f^2 \psi)dv^2 + 2\left(-B + v \cos \theta f (\eta_1 - B \psi)\right)dvdr \\ & + 2(-vf \sin \theta \eta_2)dv d\theta + \left(-v \cos \theta B (2\eta_1 + 2\eta_4 - B \psi)\right)dr^2 \\ & + \left(v \sin \theta (B \eta_2 - \eta_3)\right)dr d\theta - r^2 d\Omega^2 + \mathcal{O}(v^2), \end{aligned} \quad (4.14)$$

where we have introduced the new metric potentials $\psi(r)$ and $\eta_i(r)$ for $i = 1, 2, 3, 4$, and we have omitted the r -dependence of the functions $f(r)$, $A(r)$, and $B(r)$ as well as of the perturbations $\eta_{1,2,3}(r)$, and $\psi(r)$ in order to facilitate the reading. The æther Ansatz becomes

$$u_\mu dx^\mu = \left(\frac{1 + A(r)^2 f(r)}{2A(r)} + v \zeta_1(r) \cos \theta\right)dv + \left(-A(r)B(r) + v \zeta_2(r) \cos \theta\right)dr - v \zeta_3(r) \sin \theta d\theta, \quad (4.15)$$

where we have introduced the new potentials $\zeta_i(r)$ with $i = 1, 2, 3$.

4.1.1.d) Infinitesimal gauge transformations

The procedure outlined can be extended to simplify our Ansätze even further, however. Indeed, we can still perform an infinitesimal gauge transformation and simplify some of the potentials. In particular, we can choose to set u_θ to zero within a suitable gauge. In order to achieve this, we propose a coordinate transformation of the form³

$$v' = v + v H_1(r) \cos \theta + \mathcal{O}(v^2), \quad (4.16)$$

which gives $dv = dv' - v H_1'(r) \cos \theta dr + v H_1(r) \sin \theta d\theta$. Thus, for the 1-form u_μ this transformation gives

$$u_\mu dx^\mu = (u_v + v \zeta_1(r) \cos \theta)dv' + \left(u_r + (v \zeta_2(r) - v u_v H_1'(r)) \cos \theta\right)dr + \left(-v \zeta_3(r) + v u_v H_1(r)\right) \sin \theta d\theta. \quad (4.17)$$

Clearly, by choosing $H_1(r) = \frac{\zeta_3(r)}{u_v}$ we obtain $u_\theta = 0$. Henceforth we will drop the prime in the v' of this coordinate system and simply refer to it as the Eddington-Finkelstein coordinates $\{v, r, \theta, \phi\}$.

There is still another gauge transformation we can make to reduce the number of free potentials. Indeed, the infinitesimal coordinate transformation

$$r \mapsto r + v H_2(r) \cos \theta, \quad \theta \mapsto \theta - v \frac{H_2(r)}{r} \sin \theta, \quad (4.18)$$

allow us to remove *any* of the metric potentials in 4.14. We here choose to set $\eta_4(r) = 0$ without any loss of generality.

Moreover, the khronon potentials are not completely free though, because the æther flow must be both hypersurface-orthogonal and of unity norm. Thus, we need to restrain

3. Attention to the different “v”s...

the functions $\zeta_1(r)$ and $\zeta_2(r)$ further by imposing the normalization and the orthogonality conditions, namely $g_{\mu\nu}u^\mu u^\nu = 1$ and

$$\omega^\mu \equiv \epsilon^{\mu\alpha\beta\gamma} u_\alpha \nabla_\beta u_\gamma = 0, \quad (4.19)$$

where $\epsilon^{\mu\alpha\beta\gamma}$ is the Levi-Civita tensor, in agreement with Frobenius theorem. These relations completely determine the æther potentials $\zeta_{1,2}$ in terms of the metric potentials.

Therefore, after a few re-definitions we can express the metric Ansatz as

$$\begin{aligned} g_{\mu\nu}dx^\mu dx^\nu = & \left(f(r)dv^2 - 2B(r)drdv - r^2d\Omega^2 \right) + v \left\{ \cos\theta f(r)^2 \psi(r)dv^2 \right. \\ & + B(r) \cos\theta [\psi(r) - 2\delta(r)]dr^2 + 2f(r) \cos\theta [\delta(r) - B(r)\psi(r)]dvdr \\ & \left. - 2\sin\theta \chi(r)dv d\theta + 2\sin\theta [B(r)\chi(r) - \Sigma(r)]dr d\theta \right\} + \mathcal{O}(v^2). \end{aligned} \quad (4.20)$$

The final form of the æther Ansatz is then

$$\begin{aligned} u_\mu dx^\mu = & \frac{1 + f(r)A(r)^2}{2A(r)}dv - A(r)B(r)dr \\ & + v \cos\theta \frac{(1 + f(r)A(r)^2)h(r)}{8A(r)^3B(r)}dv - v \cos\theta \frac{h(r)}{4A(r)}dr + \mathcal{O}(v^2), \end{aligned} \quad (4.21)$$

where $h(r) \equiv (A(r)^4 f(r)^2 - 1)\delta(r) + 2A(r)^4 B(r)\psi(r)$. From now on, we will refer to $\delta(r)$, $\chi(r)$, $\psi(r)$ and $\Sigma(r)$ which appear in equations (4.20) and (4.21) as to the ‘‘perturbation potentials’’. All these transformations are shown in a recapitulative manner in figure 4.1.

Let us remark that, since the metric and khronon potentials depend only on one variable, r , the field equations *must* reduce to a system of *ordinary* differential equations for the potentials. However, the fact that this Ansatz yield separable equations is a highly non-trivial result. Indeed, instead of using the vectors \vec{n} and \vec{v} to express our potentials, we could have expressed the metric and æther perturbations as sums of Legendre polynomials, e.g.,

$$\delta g_{tt} = \sum_n k_n(r) P_n(\cos\theta), \quad (4.22)$$

where P_n is the n -th Legendre polynomial, and so on for the other perturbations. We can perform this decomposition because of the symmetries of our physical system. Plugging this form of Ansatz into the field equation yields a set of differential equations which must be solved order by order. On the one hand, each equation couples in general different modes (e.g., different k_n), meaning that, in principle, they are not independent (reflecting that the system is governed by *partial* differential equations). On the other hand, the fact that we can express our perturbations as in equations (4.20) and (4.21) means that only the first modes ($n = 1$) of the Legendre decomposition are necessary to characterize the order $\mathcal{O}(v)$ solution. Thus, the separability of the field equations is a consequence of the symmetries of the system that lead us to the decomposition given by (4.20) and (4.21).

Let us recall that, in order to obtain an asymptotic æther flow corresponding to our physical description, the potentials from the original æther Ansatz in isotropic cylindrical coordinates (see equations (4.10), (4.10)) must satisfy the conditions (4.11a), (4.11b). In

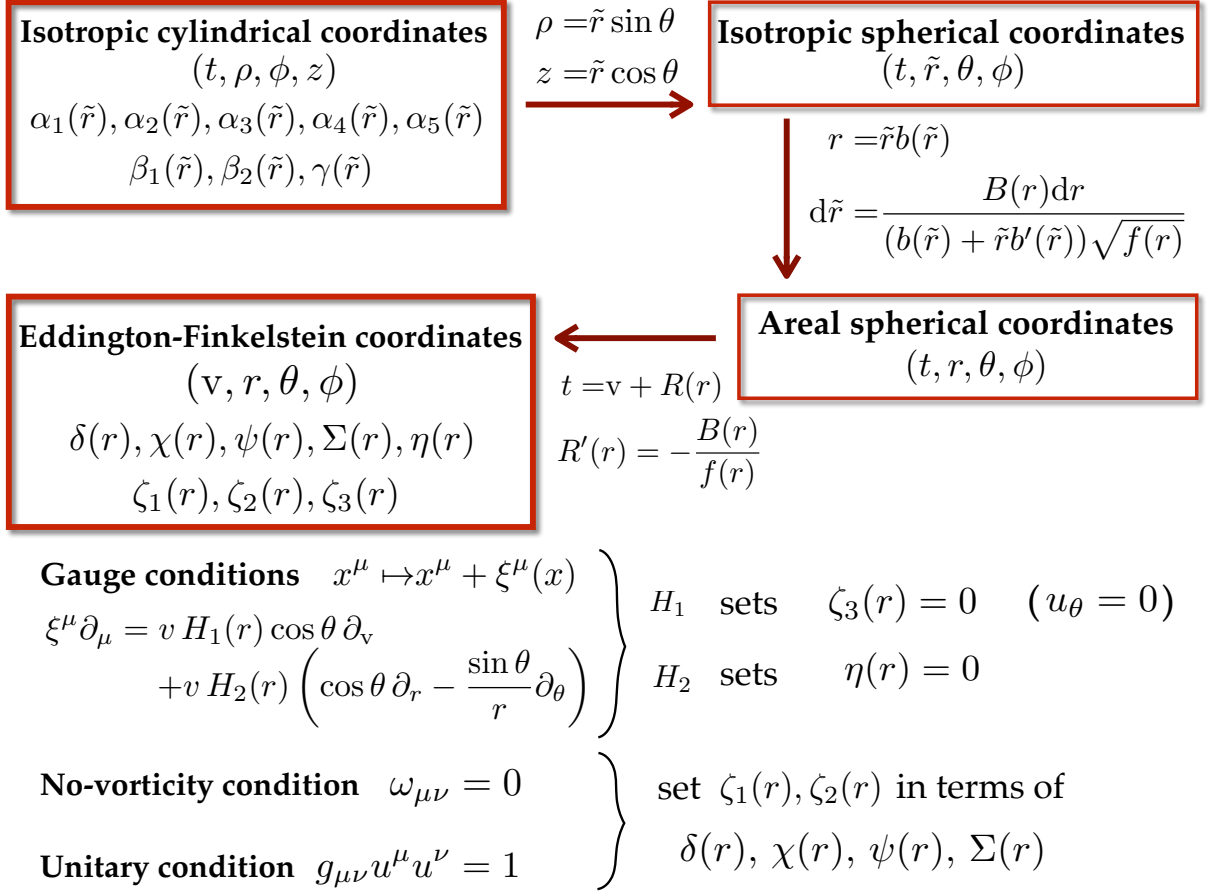


FIGURE 4.1 – Schematic representation of the coordinate transformations leading from the geometrical Ansatz in isotropic cylindrical coordinates to Eddington-Finkelstein coordinates, as well as the infinitesimal gauge conditions allowing to set two of the 8 initial potentials to zero, and the geometrical conditions that set two of the 6 remaining potentials in terms of the other four, which we call $\delta(r), \chi(r), \psi(r), \Sigma(r)$, the *perturbation potentials*.

particular, $\gamma(r)$ must asymptote to -1 for large r , so it is convenient to recast this function in terms of the new potentials introduced above

$$\gamma(r) = \frac{B(r)(1 + A^2(r)f(r))\chi(r) - (1 - A^2(r)f(r))\Sigma(r)}{2rA(r)B(r)}. \quad (4.23)$$

Later in this work, this relation will give us asymptotic conditions to be imposed on the potentials $\chi(r)$ and $\Sigma(r)$.

4.2 Structure of the field equations

We shall now tackle the problem of solving the field equations for a black hole slowly moving with respect to the æther field. Plugging the metric and æther Ansätze, (4.20) and (4.21) into the field equations and expanding in $\mathcal{O}(v)$ gives us zeroth and first order

equations for the potentials. The former involve only the background functions f , A and B , and correspond to the set of equations defining the static spherically symmetric background discussed in (2.6.1), while the latter are linear in the perturbations potentials $\delta(r)$, $\chi(r)$, $\psi(r)$ and $\Sigma(r)$, and depend also on the background potentials f , A and B . The piece of the modified Einstein tensor $E^\mu{}_\nu$ that scales linearly with v is composed of 7 non-zero components, two of them being proportional to each other. In principle, this means that there are 6 equations of motion, which we can write schematically as

$$\tilde{P}_n \equiv \sum_{i=1}^{11} p_{n,i}(r) w_i = 0, \quad \text{for } n \in \{1, 2, 3, 4, 5, 6\} \quad (4.24)$$

where the $p_{n,i}(r)$ are algebraic expressions of the radial coordinate r , the coupling coefficients α , β and λ , and of the background functions $f(r)$, $A(r)$ and $B(r)$ as well. The vector \mathbf{w} is defined in terms of the perturbations potentials as

$$\mathbf{w} = \left(\delta(r), \chi(r), \psi(r), \Sigma(r), \delta'(r), \chi'(r), \psi'(r), \Sigma'(r), \delta''(r), \chi''(r), \psi''(r) \right). \quad (4.25)$$

In the same way as we did in section 2.6, we can make use of the Bianchi identity

$$\nabla_\mu E^\mu{}_\nu = \kappa(r) u_\nu, \quad (4.26)$$

to show that not all 6 equations are dynamical equations. Let us first recall that the zeroth order piece of these identities lead in fact to the evolution equation (2.84) for the background constraint equation (2.82), cf. section 2.6. The piece proportional to v has 3 non-trivial relations obtained by setting $\nu = v$, r and θ . We can combine these relations to obtain

$$u_r \nabla_\mu E^\mu{}_\nu v - u_\nu v \nabla_\mu E^\mu{}_r = \kappa u_r u_\nu - \kappa u_r u_\nu v = 0, \quad (4.27a)$$

$$u_\theta \nabla_\mu E^\mu{}_r - u_r \nabla_\mu E^\mu{}_\theta = \kappa u_\theta u_r - \kappa u_r u_\theta = 0. \quad (4.27b)$$

Note that there are only two independent identities, since the analogous combination between the v and θ components can be deduced from these two. On the one hand, the first equation can be written as

$$\nabla_\mu (u_r E^\mu{}_v - u_\nu v E^\mu{}_r) = E^\mu{}_v v \nabla_\mu u_r - E^\mu{}_r \nabla_\mu u_\nu v, \quad (4.28)$$

while on the other hand, since $u_\theta = 0$ in our gauge, the second equation is simply

$$\nabla_\mu E^\mu{}_\theta = \nabla_r E^r{}_\theta + \nabla_\theta E^\theta{}_\theta = 0. \quad (4.29)$$

More important for us is the first order part of these identities. Expanding them, and performing a few algebraic manipulations, we find

$$\frac{dC_1}{dr} = a_1(r) C_1 + b_1(r) C_2 + \sum_{n=1}^4 d_{1,n}(r) P_n, \quad (4.30)$$

$$\frac{dC_2}{dr} = a_2(r) C_1 + b_2(r) C_2 + \sum_{n=1}^4 d_{2,n}(r) P_n, \quad (4.31)$$

where C_1 can be identified with the combination $u_r^{\mathbf{b}} \tilde{P}_4 - u_\nu^{\mathbf{b}} v \tilde{P}_5$, the term C_2 can be identified with \tilde{P}_6 , and $\mathbf{P} = (\tilde{P}_1, \tilde{P}_2, \tilde{P}_3, \tilde{P}_4)$. Here, the functions $a_i(r)$, $b_i(r)$ and $d_{i,j}(r)$ are algebraic

expressions of the radial coordinate r , of the background functions $f(r)$, $A(r)$ and $B(r)$ and the coupling coefficients α , β , and λ . From the identities (4.30) we deduce that, if all the modified Einstein equations $E^\mu{}_\nu = 0$ are satisfied at some initial point r_i , then it is enough to solve the equations $\mathbf{P} = \mathbf{0}$ to move to $r = r_i + \Delta r$, in order to satisfy the equations $C_1 = C_2 = 0$ there as well. We conclude that the equations (4.24) for $n = 1, 2, 3, 4$, that is, $\mathbf{P} = \mathbf{0}$, are indeed evolution equations for the perturbation potentials, while C_1 and C_2 are constraints to be imposed at the initial integration radius r_i .

More precisely, assuming the background potentials $\mathcal{O}(v)$ solve the zeroth order equations, then the modified Einstein equations reduce to a system of ordinary differential equations of second order in $\delta(r)$, $\chi(r)$, and $\psi(r)$ and of first order in $\Sigma(r)$, plus two initial value equations. The evolution equations can be diagonalized and put into the form

$$\delta''(r) = \delta''(\delta(r), \chi(r), \psi(r), \Sigma(r), \delta'(r), \chi'(r), \psi'(r)), \quad (4.32a)$$

$$\chi''(r) = \chi''(\delta(r), \chi(r), \psi(r), \Sigma(r), \delta'(r), \chi'(r), \psi'(r)), \quad (4.32b)$$

$$\psi''(r) = \psi''(\delta(r), \chi(r), \psi(r), \Sigma(r), \delta'(r), \chi'(r), \psi'(r)), \quad (4.32c)$$

$$\Sigma'(r) = \Sigma'(\delta(r), \chi(r), \psi(r), \Sigma(r), \delta'(r), \chi'(r), \psi'(r)), \quad (4.32d)$$

where each of these expressions is linear on the perturbed potentials and their derivatives. This is the system we will solve numerically in the following sections.

In practice, small errors appear since we solve for the field equations numerically, and these errors leak into the constraints. Nonetheless, we checked that the sign of the functions $a_i(r)$ and $b_i(r)$ are negative for large values of the radial coordinate r , meaning that the constraint evolution equations behave as an asymptotically damped system. This property guaranties that the constraints are stable near zero, and numerical errors tend to remain small at spatial infinity.

4.2.1 Boundary conditions

To obtain a numerical solution to our differential equations (4.32) we would like to set some initial conditions at given initial radius r_i and then numerically integrate the equations to all other radii. From the number of derivatives present in the equations of motion (7), and from the number of constraint equations (2), one would expect $7-2=5$ free initial conditions to be needed at any point in order to integrate the system. This would be the case if the equations were regular everywhere. Unfortunately, inspection of these equations shows possible singularities at the metric, spin-0 and universal horizon, together with spatial infinity. Let us consider for instance the equation (4.32a). If we Taylor expand it near the metric horizon r_h , we find

$$\delta''(r) = \frac{R_2}{(r - r_h)^2} + \frac{R_1}{(r - r_h)} + \mathcal{O}\left((r - r_h)^0\right), \quad (4.33)$$

where R_1 and R_2 are algebraic expressions on the potentials $\delta(r_h)$, $\chi(r_h)$, $\psi(r_h)$, $\Sigma(r_h)$ and their derivatives, evaluated at the metric horizon. Therefore, in order to have a regular equation for $\delta''(r)$ at $r = r_h$, both R_1 and R_2 must vanish at that point. Similar expressions appear when studying the equations of motion for the other potentials $\chi(r)$, $\psi(r)$ and $\Sigma(r)$,

for each of the singular points aforementioned. From a theoretical point of view, these singular points simply impose new conditions on the perturbation potentials. Yet from a numerical point of view they make the numerical solution unstable since the regularity condition is never perfectly satisfied if $r_i \neq r_{\text{singular}}$. Thus, from a practical point of view we found it more convenient to begin our numerical integration on an irregular point and impose regularity there through the initial conditions.

If one starts at the metric horizon for instance, regularity reduces the number of “free” initial conditions from 5 to 2. In practice, this is achieved by solving perturbatively the field equations near the singular point. This procedure give us a series expansion of the form

$$\begin{aligned}
\delta(r) &= \delta_{0,h} + \sum_{k=1}^{\infty} \delta_{k,h}(\delta_{0,h}, \Sigma_{0,h}) (r - r_h)^k, \\
\chi(r) &= \sum_{k=0}^{\infty} \chi_{k,h}(\delta_{0,h}, \Sigma_{0,h}) (r - r_h)^k, \\
\psi(r) &= \sum_{k=0}^{\infty} \psi_{k,h}(\delta_{0,h}, \Sigma_{0,h}) (r - r_h)^k, \\
\Sigma(r) &= \Sigma_{0,h} + \sum_{k=1}^{\infty} \Sigma_{k,h}(\delta_{0,h}, \Sigma_{0,h}) (r - r_h)^k,
\end{aligned} \tag{4.34}$$

where all the coefficients in the expansion can be expressed in terms of the two initial conditions $\delta_{0,h} \equiv \delta(r_h)$ and $\Sigma_{0,h} \equiv \Sigma(r_h)$. In this notation, the series coefficients, such as $\chi_{0,h}(\delta_{0,h}, \Sigma_{0,h}) = \chi(r_h)$ for instance, also depend on the free parameters of the background solution (see discussion in 2.6.2) and the coupling coefficients α , β , λ . Here we are assuming that the potentials are regular at the metric horizon. Indeed, it can be shown that analyticity of the potentials δ , χ , ψ and Σ is required to ensure finiteness of the invariants constructed with the metric, the æther vector, and the Killing vectors ∂_v and ∂_ϕ (e.g. R , $R_{\mu\nu}R^{\mu\nu}$, $R_{\mu\nu\alpha\beta}R^{\mu\nu\alpha\beta}$, and scalars obtained by contracting among themselves curvature tensors, Killing vectors and the æther). See Appendix 4.B for a proof of this fact.

Furthermore, the field equations at first order are linear in the perturbation potentials and their derivatives, thus they are invariant under a global rescaling. More precisely, if the set of potentials $\{\delta(r), \chi(r), \psi(r), \Sigma(r)\}$ is a solution of the field equations, then for any given $\lambda \in \mathbb{R}$, the set $\{\lambda\delta(r), \lambda\chi(r), \lambda\psi(r), \lambda\Sigma(r)\}$ will also be a solution. This is clear since the scaling factor λ appears simply as an overall factor in the field equations. We can make use of this rescaling freedom and choose λ to fix any one parameter of the initial conditions. Without loss of generality, we will set $\Sigma(r_h) = \Sigma_{0,h} = 1$. We can make use of the series expansion of equations (4.34), truncated at some finite order n , to integrate the system to a distance ϵ away from the singular point (the metric horizon in this case). In doing this, we are introducing a numerical error of the order $\mathcal{O}(\epsilon^{n+1})$, which can be made arbitrarily small by increasing n and decreasing ϵ . This procedure allows us to integrate numerically outwards or inwards the equations of motion, avoiding numerical instabilities at the metric horizon. To recapitulate, we found that constraints, regularity and scaling gives us just one initial condition parameter, $\delta_{0,h}$, to integrate from the metric horizon r_h .

4.2.2 Integration to spatial infinity

Let us consider the integration of the equations of motion from the metric horizon to spatial infinity. If the initial condition $\delta_{0,h}$ were a free parameter of the solution, then it would be a ‘‘hair’’ of the theory. We will soon show that this is not the case however, and in fact $\delta_{0,h}$ must get fixed by imposing asymptotical flatness.

Indeed, generic values for the parameter $\delta_{0,h}$ lead to solutions that are not asymptotically flat. However, for the cases that we studied we could always find a value of $\delta_{0,h}$ that gives an asymptotically flat solution. This special value can be found through a bisection procedure, where the free parameter is used as a shooting parameter. In order to implement this method, one must first understand the structure of asymptotically flat solutions. Solving perturbatively the field equations near spatial infinity give

$$\begin{aligned} \delta(r) = & \delta_0 - \frac{(\beta + \lambda)(F_1\delta_0 - 4\chi_0)}{(1 - 3\beta - 2\lambda)r} + \frac{\delta_2(\delta_0, \chi_0)}{r^2} + \frac{\delta_3(\delta_0, \chi_0, \chi_2) + \delta_{3,L}(\delta_0, \chi_0) \log(r)}{r^3} \\ & + \sum_{k=4}^{\infty} \left(\frac{\delta_k(\delta_0, \chi_0, \chi_2, \Sigma_1) + \delta_{k,L}(\delta_0, \chi_0, \chi_2, \Sigma_1) \log(r)}{r^k} \right), \end{aligned} \quad (4.35a)$$

$$\begin{aligned} \chi(r) = & \delta_0 r + \chi_0 + \left(\frac{F_1^2 (\alpha(\lambda + 1)(3\beta + 2\lambda - 1) - 11\beta^2 + \beta(7 - 15\lambda) + \lambda(7 - 4\lambda))}{16(\beta + \lambda)(3\beta + 2\lambda - 1)} \delta_0 + \frac{F_1(11\beta + 4\lambda - 7)}{12\beta + 8\lambda - 4} \chi_0 \right) \frac{1}{r} \\ & + \frac{\chi_2 + \chi_{2,L}(\delta_0, \chi_0) \log(r)}{r^2} \\ & + \sum_{k=3}^{\infty} \left(\frac{\chi_k(\delta_0, \chi_0, \chi_2, \Sigma_1) + \chi_{k,L}(\delta_0, \chi_0, \chi_2, \Sigma_1) \log(r)}{r^k} \right), \end{aligned} \quad (4.35b)$$

$$\psi(r) = \frac{3\beta(3F_1^2 - 8A_2)\delta_0 - 8\Sigma_1}{12r^2} + \frac{\psi_3(\delta_0, \chi_0, \Sigma_1)}{r^3} + \sum_{k=4}^{\infty} \frac{\psi_k(\delta_0, \chi_0, \chi_2, \Sigma_1)}{r^k}, \quad (4.35c)$$

$$\begin{aligned} \Sigma(r) = & \frac{\Sigma_1}{r} + \left\{ F_1(3F_1^2 - 8A_2) \left(\frac{\alpha^2(1 - \beta)}{16(2 - \alpha)} + \frac{\alpha(28\beta^2 + \beta(17\lambda - 52) - 25\lambda + 16) + 22\beta^2 + 6\beta(2\lambda - 1) + 4\lambda}{16(\alpha - 2)(3\beta + 2\lambda - 1)} \right) \delta_0 \right. \\ & - \frac{(8A_2 - 3F_1^2) ((13\alpha + 10)\beta^2 + 3\beta(\alpha(4\lambda - 5) + 4\lambda - 2) - 2(7\alpha + 4)\lambda)}{8(2 - \alpha)(1 - 3\beta - 2\lambda)} \chi_0 \\ & \left. - \frac{1}{6}(\alpha + 3)F_1 \Sigma_1 \right\} \frac{1}{r^2} + \sum_{k=3}^{\infty} \frac{\Sigma_k(\delta_0, \chi_0, \chi_2, \Sigma_1)}{r^k}, \end{aligned} \quad (4.35d)$$

where, due to regularity conditions at infinity, there are only 4 independent coefficients, δ_0 , χ_0 , χ_2 and Σ_1 which, together with the free parameters of the background solution, F_1 and A_2 , enable us to express the rest of the series. Let us remark the presence of logarithmic terms in the asymptotic development of $\delta(r)$ and $\chi(r)$, equations (4.35a) and (4.35b). Logarithmic terms are also present in post-Newtonian expansions of general relativity (see [144]), and they can be understood by noticing that the radial variable r is not really the propagation variable for light cones. The latter is rather related to the tortoise coordinate r^* , which

indeed relates to r through logarithmic terms.

Let us recall that spatial infinity is a singular point of the differential equations (4.32). The only condition imposed in order to get the result (4.35) is that the solution be regular at infinity (cf. discussion around equation (4.33)). Moreover, we did not need to solve for the constraint equations $C_1 = C_2 = 0$, as these equations were identically solved by the regular solution. Thus the reduction from 7 to 4 initial data is uniquely due to 3 regularity conditions. Let us remark, however, that this does not seem to be so until we solve the field equations (4.32) up to order $\mathcal{O}(1/r^3)$. More precisely, if we iterate only up to order $\mathcal{O}(1/r^2)$, then the solution contains some additional free parameters with respect to (4.35), which vanish once we solve the $\mathcal{O}(1/r^3)$ equations. In particular,

$$\psi(r) = \psi_p r + \psi_0 + \psi_1/r + \dots \quad (4.36)$$

at this order. However, we find that the constraints C_1 and C_2 are proportional to ψ_p , and therefore they do not vanish by merely solving the field equations up to order $\mathcal{O}(1/r^2)$. This subtlety will be of great importance later on (section 4.2.4) when interpreting our numerical solutions.

Inspection of the asymptotic behavior of the metric and æther Ansätze (4.20) and (4.21) given by the solution (4.35) shows that this is an asymptotically flat solution. Therefore we conclude that regularity near spatial infinity implies asymptotical flatness as well. However, generic solutions obtained by integration of the equations of motion, starting from the metric horizon, are not asymptotically flat and thus do not satisfy the relations (4.35) at infinity. More precisely, we have checked that for arbitrary values of the initial condition $\delta(r_h) = \delta_{0,h}$, the function $\delta(r)$ diverges at infinity. Together with the observation that, in general numerical solutions (empirically) satisfy $|\psi(r)| \ll |\delta(r)|$, this would imply that the g_{rr} component of the metric diverges as well, which is unacceptable. The subordination of $\psi(r)$ with respect to $\delta(r)$ can be understood from (4.35), where we observe that regular solutions have a $\mathcal{O}\left(\frac{1}{r^2}\right)$ relative order between these two functions⁴. We therefore conclude that we cannot accept arbitrary values of the parameter $\delta_{0,h}$ and we have to find the correct initial conditions to ensure that equations (4.35) are satisfied. As previously anticipated, we will determine the correct initial data via a bisection procedure.

4.2.3 Bisection procedure

We said in the previous section that generically numerical solution are not asymptotically flat, and one way to observe this fact is from the divergent behavior of $\delta(r)$ (which should in fact asymptote to a constant value, as seen in equation (4.35a)). For instance, the numerical solutions obtained using a given set of initial conditions $\delta_{0,h}^+$ and $\delta_{0,h}^-$ such that $|\delta_{0,h}^+ - \delta_{0,h}^-| = 1$ are shown in figure 4.2. They have an asymptotic divergence that goes as $\sim r^2$ and $\sim -r^2$, respectively.

Starting from an arbitrary numerical solution one can extract an asymptotic deviation

4. Note however that there is no special reason for irregular solutions to behave similarly to regular solutions. Therefore this is only a heuristic argument.

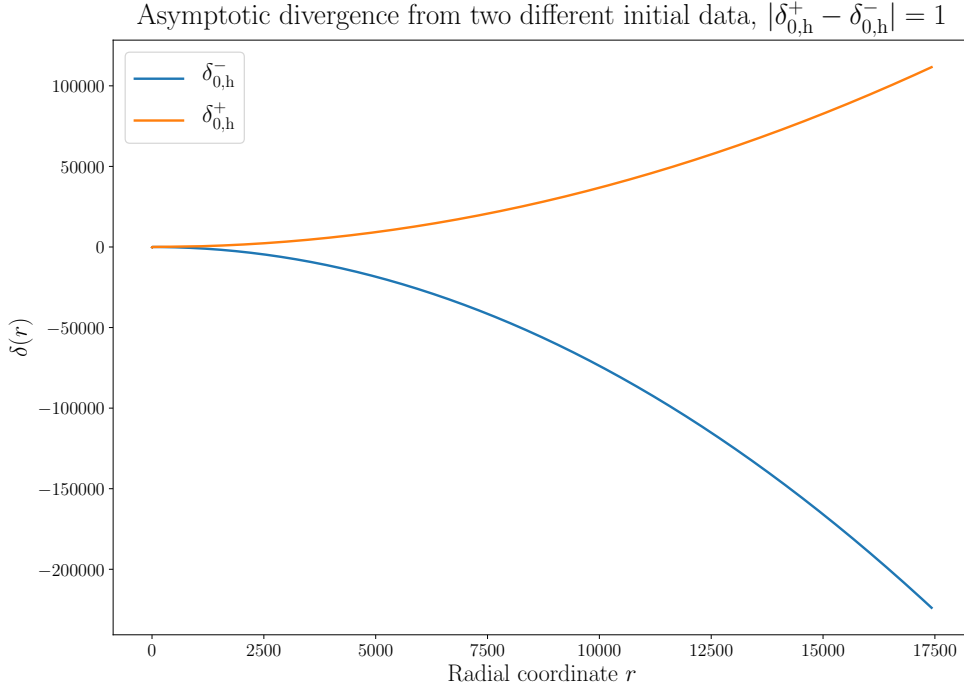


FIGURE 4.2 – Numerical solutions obtained using two initial conditions $\delta_{0,h}^+$ and $\delta_{0,h}^-$ such that $|\delta_{0,h}^+ - \delta_{0,h}^-| = 1$. The best asymptotic fit for both curves is actually of the form $\delta(r) \sim \delta_p r^2$. The fit using the form (4.37) represents the qualitatively divergent behavior as well. Numerical solution obtained for the coupling coefficients $\alpha = 0.02$, $\beta = 0.01$ and $\lambda = 0.1$.

parameter δ_p , defined in terms of the effective fit

$$\delta(r) \approx \delta_p r + \delta_0 + \frac{\delta_1}{r} + \frac{\delta_2}{r^2} + \frac{\delta_3 + \delta_{3,L} \log(r)}{r^3} + \mathcal{O}\left(\frac{1}{r^4}\right). \quad (4.37)$$

We do not presume that the function $\delta(r)$ grows indeed linearly with r , and in fact there are higher powers of r that dominate the expansion when the initial parameter $\delta_{0,h}$ is too “far” from the value giving asymptotical flatness.

Thus, the aim of describing these solutions as in equation (4.37) is to provide an operational prescription allowing us to determine if the solution diverges towards plus or minus infinity. The important point here is that, even for solutions diverging as a higher power of r (such as those in figure 4.2), the sign of the deviation parameter δ_p evaluated through the fit (4.37) truthfully represents the divergence towards plus or minus infinity. Compared to a more complex choice of the fitting function, such as $\delta(r) \approx \delta_{pp} r^2 + \delta_p r + \delta_0 + \delta_1/r + \delta_2/r^2 + (\delta_3 + \delta_{3,L} \log(r))/r^3 + \mathcal{O}(1/r^4)$, the fit (4.37) has the advantage of remaining stable when the deviation parameter becomes small, i.e., as we approach the asymptotically flat solution. Evidently, the coefficients δ_0 , δ_1 , δ_2 , etc. of the series (4.37) do not necessarily satisfy the same relations obtained for the regular solution (4.35).

By exploring the parameter space of the initial condition $\delta_{0,h}$, we find that it can be

neatly decomposed in a set of values for which the asymptotic deviation parameter δ_p is positive and another for which δ_p is negative. In order to make this statement more clear, let us call these sets \mathcal{D}^+ and \mathcal{D}^- , respectively. More precisely, we will say that $\delta_{0,h}^+ \in \mathcal{D}^+$ if the integrated solution using $\delta_{0,h}^+$ as the initial condition is such that the extracted deviation parameter is positive $\delta_p > 0$. Conversely, we will say that $\delta_{0,h}^- \in \mathcal{D}^-$ if the integrated solution is such that the extracted deviation parameter is negative $\delta_p < 0$. Then, we observed the following property. Let us suppose we have a pair of initial conditions $\delta_{0,h}^-$ and $\delta_{0,h}^+$ satisfying $\delta_{0,h}^- < \delta_{0,h}^+$, and another arbitrary initial condition $\delta_{0,h}$. On the one hand, if $\delta_{0,h}$ is such that $\delta_{0,h} > \delta_{0,h}^+$, then $\delta_{0,h}$ belongs to \mathcal{D}^+ . On the other hand, if $\delta_{0,h}$ is such that $\delta_{0,h} < \delta_{0,h}^-$, then it will belong to \mathcal{D}^- . The same discussion applies with the appropriate change in the inequalities if the initial pair $\delta_{0,h}^-$ and $\delta_{0,h}^+$ satisfied instead the relation $\delta_{0,h}^- > \delta_{0,h}^+$. In this case $\delta_{0,h} > \delta_{0,h}^+$ implies $\delta_{0,h} \in \mathcal{D}^-$ while $\delta_{0,h} < \delta_{0,h}^-$ implies $\delta_{0,h} \in \mathcal{D}^+$. This property implies the existence of a parameter $\delta_{0,h}^* \in \mathbb{R}$ such that the ensembles \mathcal{D}^- and \mathcal{D}^+ are simply given by the open intervals $] -\infty, \delta_{0,h}^*)$ and $(\delta_{0,h}^*, \infty [$. But more importantly for us, the initial condition at the metric horizon $\delta_{0,h}^*$ is such that, after integration, the asymptotic deviation parameter δ_p is zero, meaning that we found an asymptotically flat solution.

Starting from any pair $(\delta_{0,h}^-, \delta_{0,h}^+) \in \mathcal{D}^- \times \mathcal{D}^+$ we can approach $\delta_{0,h}^*$ through a bisection procedure. Indeed, let us suppose that we have found such a pair $(\delta_{0,h}^-, \delta_{0,h}^+)$. Let us then define

$$\delta_{0,h} = \frac{\delta_{0,h}^- + \delta_{0,h}^+}{2}, \quad (4.38)$$

and integrate using this value as the new initial condition. Obviously then, we have that either $\delta_{0,h} \in \mathcal{D}^-$ or $\delta_{0,h} \in \mathcal{D}^+$. If the former condition is satisfied, we define the new bisecting interval by setting $\delta_{0,h}^- \equiv \delta_{0,h}$ and letting $\delta_{0,h}^+$ unchanged, if the latter condition is satisfied then we set $\delta_{0,h}^+ \equiv \delta_{0,h}$ and $\delta_{0,h}^-$ remains unchanged. This procedure give us a new interval $(\delta_{0,h}^-, \delta_{0,h}^+) \in \mathcal{D}^- \times \mathcal{D}^+$ whose length is half the initial interval. Iteration then allows us to approach as much as desired the initial condition $\delta_{0,h}^*$ that we seek. An example of these iterations is given in figure 4.3. Since it is numerically impossible to reach the precise value of $\delta_{0,h}^*$, the best we can do is to iterate until the two branches given by $\delta_{0,h}^- \in \mathcal{D}^-$ and $\delta_{0,h}^+ \in \mathcal{D}^+$ are close enough so that we can neglect their difference. Let us define the relative error between the solutions $\delta^+(r)$ and $\delta^-(r)$, corresponding respectively to the initial conditions $\delta_{0,h}^- \in \mathcal{D}^-$ and $\delta_{0,h}^+ \in \mathcal{D}^+$, by

$$\text{relative error}(r) \equiv 2 \left| \frac{\delta^+(r) - \delta^-(r)}{\delta^+(r) + \delta^-(r)} \right| \quad (4.39)$$

This error function is plotted in figure 4.4 using a pair of solutions whose initial conditions are such that $|\delta_{0,h}^+ - \delta_{0,h}^-| = 125/140737488355328 \sim 10^{-12}$. As can be seen in that figure, the error function tends to grow as we get away from the initial radius r_h . We can use this error function to set a criterion qualifying our solution. Indeed, we choose to trust the solutions $\delta^+(r)$ and $\delta^-(r)$ only for radii such that the relative difference (4.39) is less than a certain threshold $\tilde{\epsilon}$. Then, we can determine a maximum radius \bar{r} such that $\text{relative error}(r) \leq \tilde{\epsilon}$ for all $r \leq \bar{r}$. On the one hand, we would like to have a large value of \bar{r} where we can trust our solutions. On the other hand, for any given threshold $\tilde{\epsilon}$, a larger value of \bar{r} generically implies more bisections to perform. We choose to set $\tilde{\epsilon}$ to 10^{-6} , and we find $\bar{r} \sim 2r_{\text{max}}/3$ for the

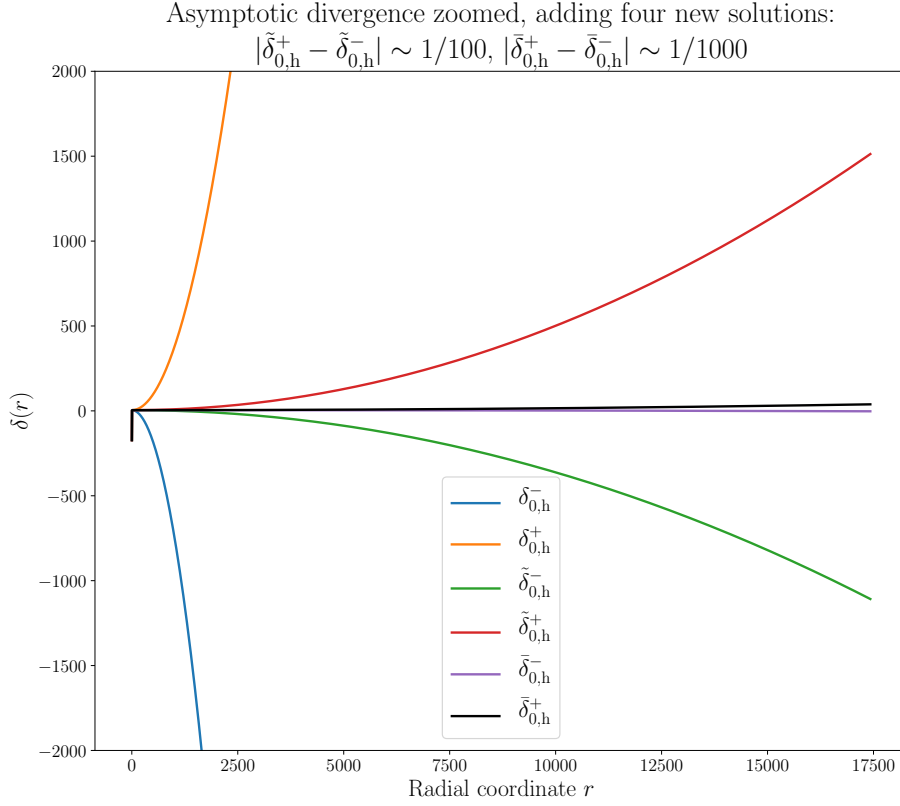


FIGURE 4.3 – To the previous plot of figure 4.2 we have added four new numerical solutions obtained through bisection of the interval defined by $\delta_{0,h}^+$ and $\delta_{0,h}^-$. The new pair of solutions were obtained by a bisection procedure, and their respective $\delta_{0,h}$ parameters are such that $|\tilde{\delta}_{0,h}^+ - \tilde{\delta}_{0,h}^-| = \frac{125}{16384}$ and $|\bar{\delta}_{0,h}^+ - \bar{\delta}_{0,h}^-| = \frac{125}{1048576}$. Numerical solution obtained for the coupling coefficients $\alpha = 0.02$, $\beta = 0.01$ and $\lambda = 0.1$.

solutions, where r_{\max} is the maximum radius up to which the background solution was solved.

Finally, we adopt as a proxy to the asymptotically flat solution the average potentials

$$\tilde{\delta}(r) \equiv \frac{\delta^+(r) + \delta^-(r)}{2}, \quad (4.40a)$$

$$\tilde{\chi}(r) \equiv \frac{\chi^+(r) + \chi^-(r)}{2}, \quad (4.40b)$$

$$\tilde{\psi}(r) \equiv \frac{\psi^+(r) + \psi^-(r)}{2}, \quad (4.40c)$$

$$\tilde{\Sigma}(r) \equiv \frac{\Sigma^+(r) + \Sigma^-(r)}{2}, \quad (4.40d)$$

defined only for r less than \bar{r} (that is, we discard the regions where $r > \bar{r}$). An example of the averaged solution is shown in the case of $\tilde{\delta}(r)$, in figure 4.5. On the one hand, we know

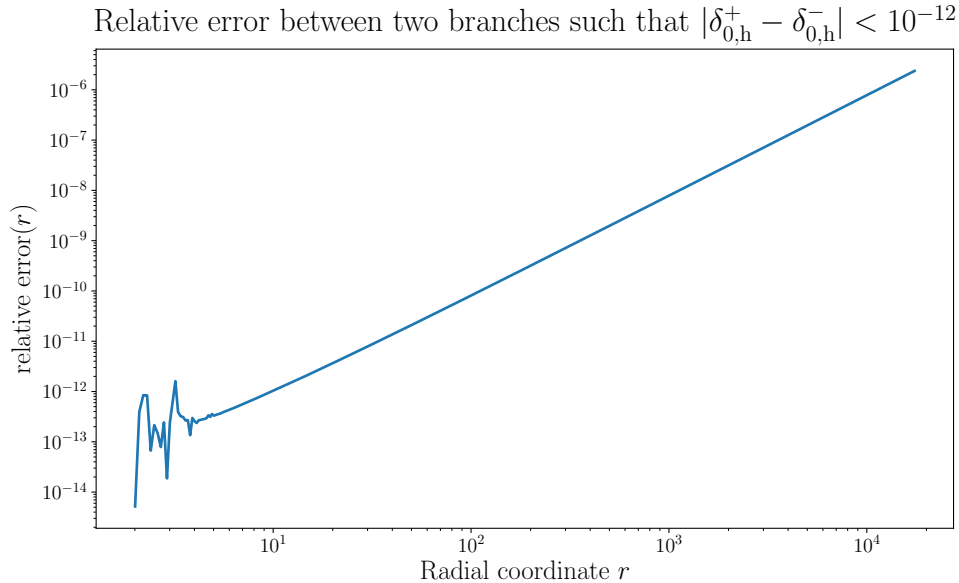


FIGURE 4.4 – The relative error function defined using the solutions corresponding to $\delta_{0,h}^+$ and $\delta_{0,h}^-$ obtained by bisection. Notice that the relative difference grows with the distance from the original integration point, i.e., the metric horizon. In the case shown, the threshold $\tilde{\epsilon} = 10^{-6}$ is crossed at $\bar{r} \simeq 11305$. Numerical solution obtained for the coupling coefficients $\alpha = 0.02$, $\beta = 0.01$ and $\lambda = 0.1$.

that the true asymptotically flat solution lies in between the plus and minus solutions, and on the other we have that these solutions do not differ in more than one part in a million throughout the domain of definition. Therefore we expect the solution defined in (4.40) to be close to one satisfying equations (4.35). Thus one must check that the potentials $\tilde{\delta}(r)$, $\tilde{\chi}(r)$, $\tilde{\psi}(r)$ and $\tilde{\Sigma}(r)$ thus obtained satisfy the regularity conditions associated to the asymptotic expansion (4.35). This will be done in the following section.

4.2.4 Consistency relations

In this section we will explain how we can make use of two numerical solutions, corresponding to the example shown in figure 4.5. We will refer to the solution given by $\delta^+(r)$, $\chi^+(r)$, $\psi^+(r)$, and $\Sigma^+(r)$ to as the “plus” solution, and the solution given by $\delta^-(r)$, $\chi^-(r)$, $\psi^-(r)$, and $\Sigma^-(r)$ to as the “minus” solution. We fitted each of the branches, plus and minus,

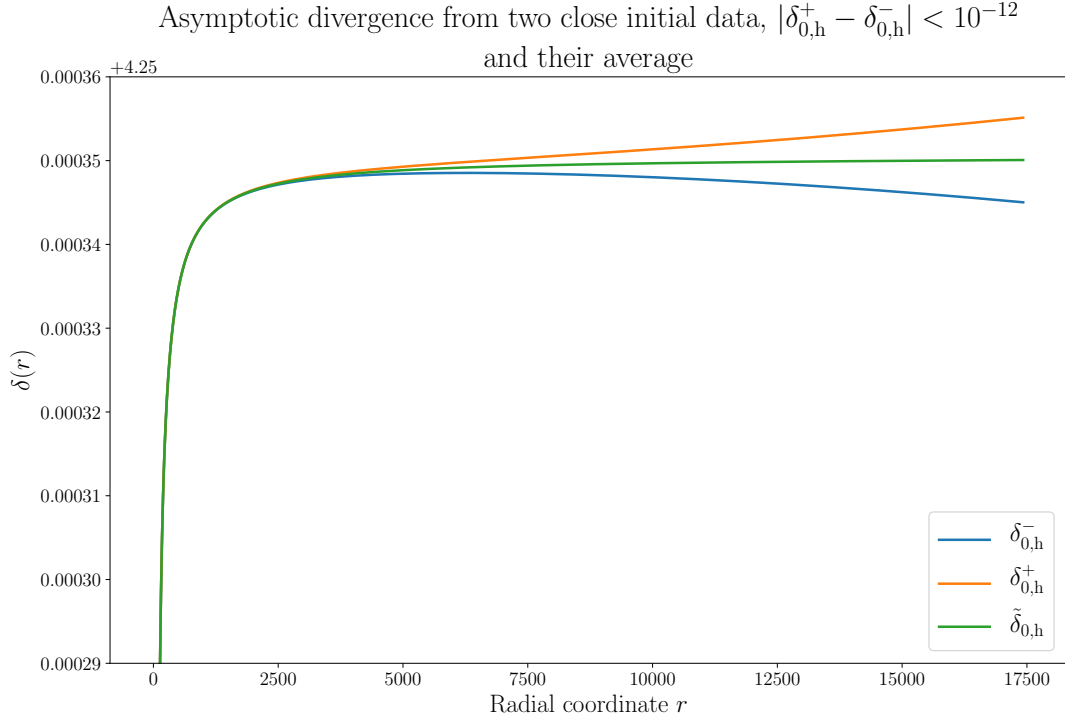


FIGURE 4.5 – Numerical solutions obtained using two very close initial conditions that we call again $\delta_{0,h}^+$ and $\delta_{0,h}^-$. In green we show the average of these solutions. Note that the latter function will correspond to some other intermediate value ($\tilde{\delta}_{0,h}$, not necessarily $(\delta_{0,h}^+ + \delta_{0,h}^-)/2$).

by the functions

$$\delta_{\text{fit}}(r) = \tilde{\delta}_{p2}r^2 + \tilde{\delta}_p r + \tilde{\delta}_0 + \frac{\tilde{\delta}_1}{r} + \frac{\tilde{\delta}_2}{r^2}, \quad (4.41a)$$

$$\chi_{\text{fit}}(r) = \tilde{\chi}_{p3}r^3 + \tilde{\chi}_{p2}r^2 + \tilde{\chi}_p r + \tilde{\chi}_0 + \frac{\tilde{\delta}_1}{r}, \quad (4.41b)$$

$$\psi_{\text{fit}}(r) = \tilde{\psi}_p r + \tilde{\psi}_0 + \frac{\tilde{\psi}_1}{r} + \frac{\tilde{\delta}_2}{r^2} + \frac{\tilde{\delta}_3}{r^3}, \quad (4.41c)$$

$$\Sigma_{\text{fit}}(r) = \tilde{\Sigma}_{p2}r^2 + \tilde{\Sigma}_p r + \tilde{\Sigma}_0 + \frac{\tilde{\Sigma}_1}{r} + \frac{\tilde{\Sigma}_2}{r^2} + \frac{\tilde{\Sigma}_3}{r^3}, \quad (4.41d)$$

and from these fits we estimated the value of the asymptotically flat coefficients. For instance, for the function $\delta(r)$ the fitted coefficients are

$$\begin{aligned} \tilde{\delta}_{p2}^+ &= 1.68 \times 10^{-14}, & \tilde{\delta}_{p2}^- &= -1.64 \times 10^{-14}, & \tilde{\delta}_p &= 1.19 \times 10^{-16}, \\ \tilde{\delta}_p^+ &= 1.63 \times 10^{-13}, & \tilde{\delta}_p^- &= 6.52 \times 10^{-14}, & \tilde{\delta}_p &= 1.14 \times 10^{-13}, \\ \tilde{\delta}_0^+ &= 4.250, & \tilde{\delta}_0^- &= 4.250, & \tilde{\delta}_0 &= 4.250, \\ \tilde{\delta}_1^+ &= -0.00812, & \tilde{\delta}_1^- &= -0.00812, & \tilde{\delta}_1 &= -0.00812, \\ \tilde{\delta}_2^+ &= 0.156, & \tilde{\delta}_2^- &= 0.156, & \tilde{\delta}_2 &= 0.156. \end{aligned}$$

In the first column we have the fitted coefficients for the plus branch, in the second column those of the minus branch, and in the third column we show the inferred value for the asymptotically flat solution defined as

$$\tilde{\delta}_{p2} = \frac{\tilde{\delta}_{p2}^+ + \tilde{\delta}_{p2}^-}{2}, \quad (4.42a)$$

$$\tilde{\delta}_p = \frac{\tilde{\delta}_p^+ + \tilde{\delta}_p^-}{2}, \quad (4.42b)$$

$$\tilde{\delta}_0 = \frac{\tilde{\delta}_0^+ + \tilde{\delta}_0^-}{2}, \quad (4.42c)$$

$$\tilde{\delta}_1 = \frac{\tilde{\delta}_1^+ + \tilde{\delta}_1^-}{2}, \quad (4.42d)$$

$$\tilde{\delta}_2 = \frac{\tilde{\delta}_2^+ + \tilde{\delta}_2^-}{2}. \quad (4.42e)$$

It could seem contradictory that the value of $\tilde{\delta}_p^-$ (4.42a) is positive, as it comes from the fit for a function whose deviation parameter δ_p is negative (see figure 4.5). Let us remark, however, that the fit (4.41) contains now a quadratic term, r^2 , which does indeed have a negative value. In any case, both coefficients are of the order of 10^{-14} and their sign is unstable if we change the number of functions we use as a base for fitting. This is why, we choose to keep just the linear term in r in the fit to determine whether the function $\delta(r)$ is positive or negative divergent. In this manner, the estimated values for the other potential's coefficients are the following :

$$\begin{array}{lll} \tilde{\chi}_{p3} = 9.8 \times 10^{-17}, & \tilde{\psi}_p = 4.8 \times 10^{-8}, & \tilde{\Sigma}_p = -4.7 \times 10^{-10}, \\ \tilde{\chi}_{p2} = 4.4 \times 10^{-14}, & \tilde{\psi}_0 = 1.4 \times 10^{-7}, & \tilde{\Sigma}_0 = -4.9 \times 10^{-10}, \\ \tilde{\chi}_p = 4.250, & \tilde{\psi}_1 = 1.9 \times 10^{-7}, & \tilde{\Sigma}_1 = 0.110, \\ \tilde{\chi}_0 = -2.110, & \tilde{\psi}_2 = 0.0404, & \tilde{\Sigma}_2 = -0.557, \\ \tilde{\chi}_1 = -0.152, & \tilde{\psi}_3 = 0.299, & \tilde{\Sigma}_3 = -0.5 \pm 4.5, \\ \tilde{\chi}_2 = 9.19. & & \end{array}$$

Thus we obtained an asymptotic fit for the data shown in figure 4.5, given by the potentials (4.41) and using the numerical values in (4.42a) and (4.43a). Let us recall that the independent coefficients of the series given by equation (4.35) are δ_0 , χ_0 , χ_2 and Σ_1 . From the numerical solution we can extract thus

$$\tilde{\delta}_0 = 4.250, \quad (4.43a)$$

$$\tilde{\chi}_0 = -2.110, \quad (4.43b)$$

$$\tilde{\chi}_2 = 9.19, \quad (4.43c)$$

$$\tilde{\Sigma}_1 = 0.110. \quad (4.43d)$$

Then we can check if the series coefficients correspond indeed to the expected values given by the relations (4.35). We can do so by computing the relative differences between the expected and the fitted coefficients. Thus, let us denote the former using the upper index "th", that is, the theoretical value given in equations (4.35) are δ_1^{th} , δ_2^{th} , and so on and so forth. Each of

these theoretical values depend on the three independent coefficients of (4.43), whose error are known. Thus we find

$$\left| \frac{\delta_1^{\text{th}}}{\tilde{\delta}_1} - 1 \right| = 1.9 \times 10^{-5}, \quad \left| \frac{\delta_2^{\text{th}}}{\tilde{\delta}_2} - 1 \right| = 1.5 \times 10^{-3}, \quad (4.44a)$$

$$\left| \frac{\chi_p^{\text{th}}}{\tilde{\chi}_p} - 1 \right| = 4.8 \times 10^{-11}, \quad \left| \frac{\chi_1^{\text{th}}}{\tilde{\chi}_1} - 1 \right| = 9.8 \times 10^{-4}, \quad (4.44b)$$

$$\left| \frac{\psi_2^{\text{th}}}{\tilde{\psi}_2} - 1 \right| = 3.0 \times 10^{-4}, \quad \left| \frac{\psi_3^{\text{th}}}{\tilde{\psi}_3} - 1 \right| = 0.012, \quad (4.44c)$$

$$\left| \frac{\Sigma_2^{\text{th}}}{\tilde{\Sigma}_2} - 1 \right| = 0.005, \quad \left| \frac{\Sigma_3^{\text{th}}}{\tilde{\Sigma}_3} - 1 \right| = 0.04 \quad (4.44d)$$

where we recall that the tilde stands for quantities fitted from the averaged numerical solution. The lower index “p” stands for the linear coefficient in the expansion of $\chi(r)$, that is to say, it appears as $\chi_p r$ in the series (4.35). The last of these consistency terms is the larger of all of them and it corresponds to a relative difference between the expected theoretical relation (4.35) and the fitted value of no more than 4 percent. We conclude that we can safely make use of our averaged solution to extract the first terms of the series (4.35). In particular, the “free parameters” δ_0 and χ_0 are the only required to compute the sensitivity σ (see equation (4.47) below).

Let us remark that, if we consider exclusively the errors associated with the fitting of the coefficients (4.42a) and (4.43a), and the corresponding propagation, we find that the terms (4.44) are not zero within the numerical errors. In fact, it can be argued that the small errors in the expressions (4.44) come from the violation of the constraint equations $C_i = 0$. Indeed, as previously discussed the asymptotic expansion (4.35) can be carried out without imposing the constraint equations and allowing for a larger set of solutions (cf. discussion around equation (4.36)). Therefore, solving perturbatively up to order $\mathcal{O}\left(\frac{1}{r^2}\right)$ in the equations of motion allows for a term $\sim \psi_p r$, which can account for the small linear term in (4.41c). This coefficient in turn it can be related to the other small coefficients in the series, as well as accounting for a small correction to the leading terms of the fit.

On the one hand, however, the $\mathcal{O}\left(\frac{1}{r^2}\right)$ field equations together with the constraint equations necessarily imply $\psi_p = 0$. On the other hand, we saw that imposing the constraints at the initial data and solving for the equations of motion implied the constraint equations through the constraint evolution equation (4.30). Nevertheless, when we solve the field equations numerically we introduce some errors to the solution, which lead to non-vanishing constraints. We therefore conclude that the small violations of the constraints, due to the numerical resolution scheme, are due to the small errors in the numerical scheme solving for the equations of motion. The thorough study of this issue constitutes a work in progress...

4.2.5 Extraction of the sensitivities

An appropriate gauge transformation allows us to compare the post-Newtonian solution (3.33) containing the sensitivity Σ to the asymptotic solution (4.35). Indeed, in our gauge

the metric (4.20) is given by

$$\begin{aligned} ds^2 = & \left(1 - \frac{2M}{r}\right) dt^2 - \left(1 + \frac{2M}{r}\right) dr^2 - r^2 d\Omega^2 \\ & + v \left\{ 2\delta_0 \cos\theta dt dr - 2\delta_0 \sin\theta dt d\theta \left[r \left(1 - \frac{2M}{r}\right) \delta_0 + \chi_0 \right] \right\} + \mathcal{O}\left(\frac{1}{r^2}, v^2\right). \end{aligned} \quad (4.45)$$

Therefore we have that this metric can match the form given by equation (3.33) if we make an infinitesimal change of coordinates

$$t \rightarrow t + vr \cos\theta. \quad (4.46)$$

In principle, this is enough to extract the sensitivity, since it is contained in two different pieces of the metric. Indeed, we find that the sensitivity σ is given by

$$\sigma = \frac{\alpha - \beta - 3\alpha\beta + 5\beta^2 + \lambda - 2\alpha\lambda + 3\beta\lambda}{(2 - \alpha)(1 - 3\beta - 2\lambda)} + 2 \frac{(1 - \beta)(\beta + \lambda)}{1 - 3\beta - 2\lambda} \frac{\chi_0}{R_0 \delta_0}, \quad (4.47)$$

where $R_0 \equiv \frac{2G_{\text{EA}}M}{(1 - \alpha/2)}$ is the gravitational radius associated to the mass M , and δ_0, χ_0 are the constant terms appearing in the asymptotic series for $\delta(r)$ and $\chi(r)$, cf. equations (4.35a-4.35b).

There is yet another way to get the same result (4.47). Indeed, we can solve the modified Einstein equations

$$G^{\mu\nu} - T_{\text{kh}}^{\mu\nu} = 8\pi G T_{\text{matter}}^{\mu\nu}, \quad (4.48)$$

where we use a point particle prescription for the stress-energy tensor as in equation (3.24). Thus the right-hand side contains the sensitivity σ in its piece proportional to v , while the left-hand side is constructed using the zeroth and first order potentials $f, A, B, \delta, \chi, \psi$, and Σ , as usual. We can expand the modified Einstein equations in powers of $1/c^2$, that is, we express the potentials as

$$\begin{aligned} f(r) &= f_0(r) + \frac{f_1(r)}{c^2} + \frac{f_2(r)}{c^4} + \mathcal{O}\left(\frac{1}{c^6}\right), \\ A(r) &= A_0(r) + \frac{A_1(r)}{c^2} + \frac{A_2(r)}{c^4} + \mathcal{O}\left(\frac{1}{c^6}\right), \\ B(r) &= B_0(r) + \frac{B_1(r)}{c^2} + \frac{B_2(r)}{c^4} + \mathcal{O}\left(\frac{1}{c^6}\right), \end{aligned} \quad (4.49)$$

as well as the analogous expressions for the first order potentials $\delta(r), \chi(r), \psi(r)$ and $\Sigma(r)$. Thus we obtain a set of Poisson-type equations with a source. Solving these equations allows us to find the direct functional dependence of the potential's coefficients on the source terms. In particular, we find δ_0 and χ_0 as a functions of σ , and inverting these relations we recovered the result (4.47).

This means that, for any set of coupling coefficients $\{\alpha, \beta, \lambda\}$, we can extract the associated sensitivity from the asymptotic values of the numerically computed functions $\delta(r)$ and $\chi(r)$. For the example presented in the previous section, we had $\beta = 1/100 = \alpha/2$ and $\lambda = 1/10$, the gravitational radius $R_0 = -F_1 = m$ was set to 2.002, and the fitted values for δ_0 and χ_0 obtained in (4.43) give us $\chi_0/\delta_0 = -0.497$. The formula (4.47) give us then

$$\Sigma \sim 0.00125, \quad (4.50)$$

for this special case. Note that the sensitivity is a dimensionless quantity, as it is simple to check that χ_0 scales as a length. This is an illustration of how the methods presented can be used to extract the sensitivities describing a compact object such as a black hole in Lorentz violating gravity.

4.2.6 Interior solution and the spin-0 frame

Until now we have been focused on finding a numerical solution valid from the metric horizon outwards to spatial infinity. However, the solution must be completed by integrating also from the metric horizon inwards, at least up to the universal horizon. There the situation is more delicate because of the inner structure of the black hole and the singular points. Thus, before describing how we solve the field equations inside the metric horizon, it will be useful to analyze the functional form of the different scalar curvature invariants near the singular points inside the metric horizon.

4.2.6.a) Curvature invariants

Curvature invariants are essential to determine, at any putative singular point, whether or not we are facing a physical singularity, or if we deal instead with a coordinate singularity. Let us consider as an example the case of a non-spinning static black hole in general relativity. If we express the solution in Schwarzschild coordinates, then one might suspect the presence of a physical singularity at the event horizon and another one at the center of the black hole. On the one hand, the former turns out to be simply a coordinate singularity. This is readily seen as none of the curvature invariants diverges at the event horizon. Furthermore, this singularity can be made to disappear by an appropriate coordinate transformation, as can be seen by choosing Eddington-Finkelstein coordinates. Thus the Schwarzschild metric for a black hole of mass M becomes

$$ds^2 = \left(1 - \frac{r_0}{r}\right) dv^2 + 2dvdr - r^2 d\Omega^2, \quad (4.51)$$

where $r_0 = 2GM$ is the Schwarzschild radius. It is clear then that the metric is indeed regular at the event horizon, $r = r_0$. On the other hand, it is impossible to get rid of the $r = 0$ singularity. Indeed, by computing the curvature invariants one realizes that the origin of the coordinates is actually a physical singularity. For instance, the Kretschmann invariant scales as $R_{\mu\nu\alpha\beta} R^{\mu\nu\alpha\beta} \sim M^2/r^6$, thus it clearly blows up while approaching $r = 0$.

In our case, there are several quantities of interest which ought to be computed. In particular, unlike in general relativity, the field equations (2.24) and (2.44) do not necessarily imply a vanishing Ricci tensor in the absence of matter fields, since the contribution of the æther stress-energy tensor (2.47) does not vanish. Furthermore, although we impose regularity at the metric horizon, nothing guarantees that our solutions will be regular at the spin-0 or universal horizon. Indeed, the field equations (4.32a) can be shown to present a possible singularity there (cf. equation (4.33)). Thus, in the following we will investigate the regularity of these hypersurfaces. First, the volume invariant $\sqrt{-g} dx^4$ is regular everywhere

$$\sqrt{-g} dx^4 = \left(r^2 B(r) \sin \theta + \frac{v}{4} r^2 f(r) B(r) \sin 2\theta \psi(r) + \mathcal{O}(v^2)\right) dv dr d\theta d\phi, \quad (4.52)$$

so it will not be further discussed. Using the Ansatz (4.20-4.21), the Ricci scalar R can be expressed schematically as

$$R = \frac{a_1(r)}{r^2} + v \frac{b_1(r)}{r^3} \cos \theta + \mathcal{O}(v^2), \quad (4.53)$$

where $a_1(r)$ stands for an algebraic expression given in terms of the zeroth order potentials f , A and B and their derivatives, and $b_1(r)$ stands for an algebraic expression given in terms of zeroth and first order potentials f , A , B , δ , χ , ψ , Σ and their derivatives. Similarly, the Ricci tensor contracted with itself is

$$R_{\alpha\beta} R^{\alpha\beta} = \frac{a_2(r)}{r^4} + v \frac{b_2(r)}{r^5} \cos \theta + \mathcal{O}(v^2), \quad (4.54)$$

the Kretschmann invariant is

$$R_{\mu\nu\alpha\beta} R^{\mu\nu\alpha\beta} = \frac{a_3(r)}{r^4} + v \frac{b_3(r)}{r^5} \cos \theta + \mathcal{O}(v^2), \quad (4.55)$$

and the two Killing scalars coming from the contraction of the Riemann tensor with the Killing vectors (∂_v) and (∂_ϕ) read

$$k_1 = R_{\mu\nu\alpha\beta} u^\mu u^\alpha (\partial_v)^\nu (\partial_v)^\beta = a_4(r) + v b_4(r) \cos \theta + \mathcal{O}(v^2), \quad (4.56)$$

$$k_2 = R_{\mu\nu\alpha\beta} u^\mu u^\alpha (\partial_\phi)^\nu (\partial_\phi)^\beta = a_5(r) \sin^2 \theta + v b_5(r) \cos \theta \sin^2 \theta + \mathcal{O}(v^2). \quad (4.57)$$

The combinations $R_{\mu\nu\alpha\beta} u^\mu u^\alpha (\partial_v)^\nu (\partial_\phi)^\beta$ and $R_{\mu\nu\alpha\beta} u^\mu u^\alpha (\partial_\phi)^\nu (\partial_v)^\beta$ are identically zero, so they will not be considered. Again, $a_i(r)$ and $b_i(r)$ are functions of the zeroth and first order potentials f , A , B , δ , χ , ψ , Σ and their derivatives.

Thus, most curvature invariants are singular at the center of the black hole $r = 0$. We recover then the same result as in general relativity. Regarding the different horizon surfaces, at zeroth order in v all curvature invariant are regular [127]. Indeed, the key observation here is that, since the background functions $f(r)$, $A(r)$ and $B(r)$ can be integrated inwards up to $r = 0$ with no singularity, then the terms $a_i(r)$ are everywhere regular. At first order however, the terms $b_i(r)$ depend on the perturbed potentials $\delta(r)$, $\chi(r)$, $\psi(r)$ and $\Sigma(r)$ as well. This means that, the $\mathcal{O}(v)$ part of the curvature invariants can become singular depending on the behavior of the first order solution (i.e., if the field equations present singularities at $r = r_{s0}$ or r_{uh} and as a result δ , χ , ψ , and Σ diverge, then the curvature invariants diverge as well).

4.2.6.b) The spin-0 horizon

Let us then go back to the completion of the solution inside the black hole. Empirically we observed that, in general, the system cannot be fully integrated inwards as the solution blows up while approaching the spin-0 horizon. We here recall that, by definition, the spin-0 horizon radius r_{s0} is such that

$$g_{\text{vv}}^{(0)} = g_{\text{vv}} + (s_0^2 - 1)u_v u_v, \quad (4.58)$$

where s_0 is the spin-0 speed as given by equation (2.62a). Then we find that the field equations can be integrated numerically until the spin-0 radius $r_{s0} \in (r_{\text{uh}}, r_{\text{h}})$ instead of r_{h} as required. In order to verify that this is due to a physical irregularity and not simply due to the stiffness

of the system at that point we checked two things. We computed the curvature invariants and studied their behavior as the solution approaches the spin-0 horizon. Denoting CI any of the curvature invariants previously defined, we find

$$CI \sim \frac{a}{(r - r_{s0})^b} \quad (4.59)$$

for some constant $a \in \mathbb{R}$ and where $b \simeq 2$. This is exemplified in figure 4.6.

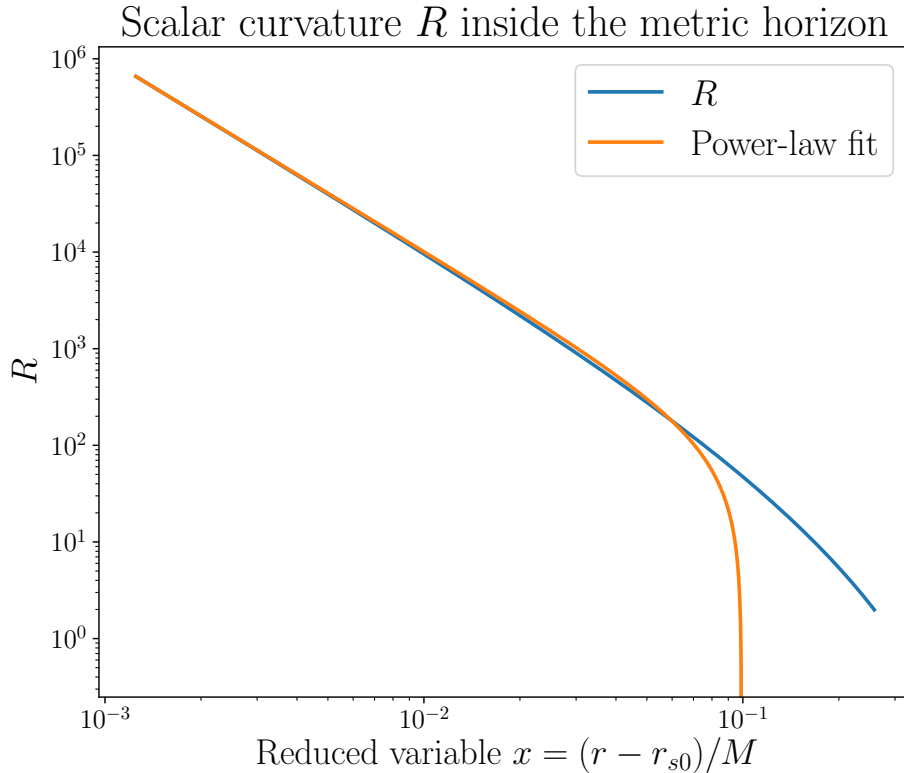


FIGURE 4.6 – The first order component of the scalar curvature, corresponding to the term $b_1(r)$ in (4.53), is plotted against the distance to the spin-0 horizon defined as $x = (r - r_{s0})/M$. The data comes from a numerical solution obtained for $\beta = 1/100 = \alpha/2$ and $\lambda = 1/10$. In orange there is the best power law fit to represent the divergence. The power-law is given by $R \sim (-103.4 + 1/x^{2.004})M$.

One could argue, however, that this argument is not conclusive. Indeed, the divergence of the scalar invariants could be due to numerical instabilities while approaching a regular but apparently singular point of the differential equations. More precisely, the solution could be such that the terms collectively denoted by “ a ” in equation (4.59) go to zero as they approach the spin-0 horizon. If we have $a \sim (r - r_{s0})^b$, then the curvature invariants would tend to a finite value and the solution would be regular there. However, even if the solution were to be regular, numerical instabilities would make this division unstable and the system could diverge anyway. Fortunately, there is another way to study this problem based on a

field redefinition. In order to see how this method comes about, let us note that the action (2.39) is invariant under the transformation [151]

$$\begin{aligned} g_{\mu\nu} &\rightarrow g'_{\mu\nu} = g_{\mu\nu} + (\zeta - 1)u_\mu u_\nu, \\ T &\rightarrow T' = T \end{aligned} \quad (4.60)$$

ζ being a constant, provided that the original values α , β and λ are replaced by the following alongside the re-definitions

$$\begin{aligned} \alpha' &= \alpha, \\ \beta' + \lambda' &= \zeta(\beta + \lambda), \\ \beta' - 1 &= \zeta(\beta - 1). \end{aligned} \quad (4.61)$$

It is easy to see that the æther vector transforms as $u^\mu \rightarrow u'^\mu = u^\mu/\sqrt{\zeta}$. From this symmetry we conclude that for every “physical” solution corresponding to a set of allowed coefficients α , β and λ in the theory’s parameter space, one can generate an additional one-parameter family of “mathematical” solutions given by equation (4.60), corresponding to the one-parameter family of coefficients α' , β' and λ' given by equation (4.61). Note that the new set of coefficients does not need to be necessarily physically allowed in parameter space. Also note that if $\zeta = s_0^2$, then the primed metric g' coincides with the spin-0 metric. Therefore, by performing the field redefinition given by equations (4.60) and (4.61), we can solve the original problem in a “frame” (the so-called spin-0 frame) in which the metric and spin-0 horizon coincide. In this way, the two spin-0 and metric singularities in the field equations (4.32) get to coincide and therefore our numerical treatment is simplified. Indeed, we can impose regularity by solving the equations perturbatively there. Let us stress that precisely the same trick was used to find the static, spherically symmetric black hole solutions (see [136, 127, 133]).

In order to solve the field equations within the spin-0 frame we must repeat the procedure described starting in section 4.2.1. That is, we expand the equations near the singular point and we count how many free parameters we have to set our initial data after we impose regularity. The first thing that we note in doing so concerns the background solution. In section 2.6.2 we mentioned that regularity left three initial conditions at the metric horizon, as it was already known and exposed in [133]. More precisely, for the “physical” system, i.e., where $s_0 \neq 1$, we have at the metric horizon

$$\left. \begin{array}{ll} f(r_h) & = 0, \\ f'(r_h) & \text{free}, \\ A(r_h) & \text{free}, \\ A'(r_h) & \text{free}, \\ B(r_h) & \text{fixed by the constraint.} \end{array} \right\} \quad (4.62)$$

Thus, when solving the equations perturbatively near r_h the solution could be expressed in terms of $f_1 \equiv f'(r_h)$, $A_0 \equiv A(r_h)$ and $A_1 \equiv A'(r_h)$. This way, we can obtain an analytic

formula for $B_0 \equiv B(r_h)$ in the form $B_0 = B_0(f_1, A_0, A_1)$, and in general we will have

$$f(r) = f_1(r - r_h) + \sum_{k=2}^{\infty} \frac{f_k(f_1, A_0, A_1)}{k!} (r - r_h)^k, \quad (4.63a)$$

$$A(r) = A_0 + A_1(r - r_h) + \sum_{k=2}^{\infty} \frac{A_k(f_1, A_0, A_1)}{k!} (r - r_h)^k, \quad (4.63b)$$

$$B(r) = \sum_{k=0}^{\infty} \frac{B_k(f_1, A_0, A_1)}{k!} (r - r_h)^k, \quad (4.63c)$$

where all the series are determined by f_1 , A_0 and A_1 . Let us stress that these expressions f_{k+2} , A_{k+2} or B_k for $k \geq 0$ depend on the coupling coefficients as well, and more importantly for us, they happen to diverge in when $s_0 \rightarrow 1$ (i.e., in the spin-0 frame). Indeed, the combination $s_0^2 - 1$ appears in the denominator of these expressions. Therefore, in the spin-0 frame we can no longer make use of the same formulae for the background series that we obtained in the physical frame, because those formulae were obtained under the hypothesis that $s_0 \neq 1$. Instead, we have to solve again for the series expansion near the metric horizon (which coincides with the spin-0 horizon) for the particular value of the coupling coefficients predicted by (4.61), and generically we will have

$$\text{in the spin} - 0 \text{ frame} \left\{ \begin{array}{ll} f(r_h) & = 0, \\ f'(r_h) & \text{fixed by regularity,} \\ A(r_h) & \text{free,} \\ A'(r_h) & \text{free,} \\ B(r_h) & \text{fixed by the constraint.} \end{array} \right\} \quad (4.64)$$

This translates into a new counting of the regularity conditions for the perturbed potentials at the metric horizon, because the series expansion (4.34) depends on the form of the background potentials and thus was also obtained under the assumption that $s_0 \neq 1$. The initial data for the potentials δ , χ , ψ and Σ changes when we go to the spin-0 frame in a similar fashion to the passage from the initial data (4.62) to the new (4.64) for the background potentials f , A and B . Indeed, while in the general case we had $7 - 2(\text{constraints}) - 3(\text{regularity}) = 2$ initial conditions to input at the metric horizon, one of which can be set to 1 by rescaling, we now have $7 - 2(\text{constraints}) - 4(\text{regularity}) = 1$ condition which can be fixed to any value by rescaling. Thus, the parameter δ_0 which we used as a bisection parameter in the previous scheme can be now set to 1 without any lose of generality.

4.2.6.c) Integration outside the black hole

It follows then, that we can just integrate the equations of motion using of the unique (up to a rescaling factor) set of initial conditions at the metric/spin-0 horizon. The fact that we can implement the field redefinition as discussed above shows that the singularity at the spin-0 horizon can be removed using the spin-0 frame. This procedure is known to give regular, asymptotically flat solutions at $\mathcal{O}(v^0)$ [133]. Unfortunately, then we find that the solutions are no longer asymptotically flat at $\mathcal{O}(v)$. Indeed, we see in figure 4.7 that, asymptotically, $\delta(r)$ diverges as $\sim r^2$. As discussed earlier in section 4.2.2, this means that the solution thus obtained is not flat at infinity.

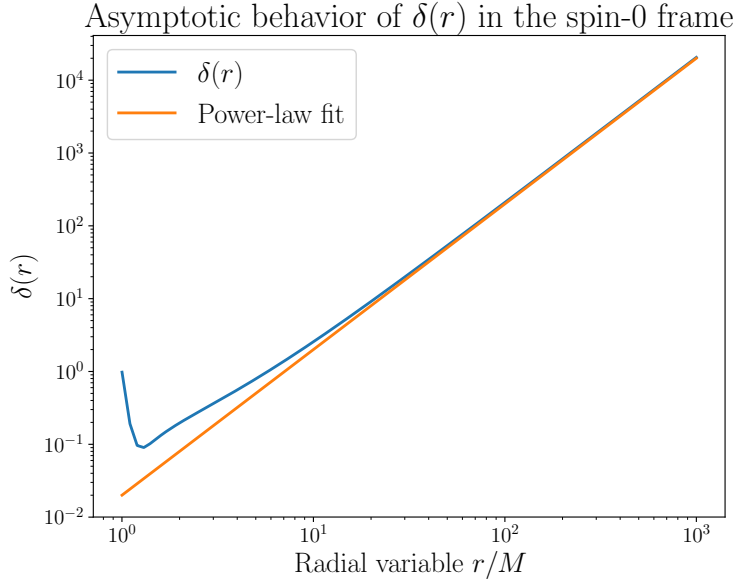


FIGURE 4.7 – Log-log plot of the potential $\delta(r)$ integrated from the metric/spin-0 horizon outwards using the unique set of initial data available at that point (cf. section 4.2.6.b)). The data comes from a numerical solution computed in the spin-0 frame, corresponding to the values $\beta = 0.01 = \alpha/2$ and $\lambda = 0.2$ in the physical frame. An orange line denotes the best power law fit to represent the divergence, given by $\delta(r) \sim r^2/50$.

4.2.6.d) Integration inside the black hole

At this stage, ignoring the issue of asymptotic flatness at infinity, the only problem left is the regularity of the solution at the universal horizon. Since $r = r_{\text{uh}}$ is a singular point of the equations of motion, the integrated solution will inevitably diverge there due to numerical instabilities. Again, we would like to assess if this divergence is physical or not. One way to avoid numerical instabilities is to integrate the equations of motion twice, once starting from the universal horizon up to a middle point $r^* = (r_{\text{uh}} + r_{\text{h}})/2$, and another starting from the metric horizon down to the middle point. That is, we impose regularity by solving perturbatively at both r_{h} and r_{uh} , and then we check whether the two solutions match at the middle point. The solution coming from the metric horizon inwards is uniquely determined, because it has a unique set of initial data up to rescaling freedom (the discussion is analogous to the previous section). In order to set our initial data at the universal horizon r_{uh} we must consider how many conditions are imposed by regularity in the same way as we have done before for the metric horizon. Thus we find that regularity conditions reduce the number of free parameters from 7 to 3, and after rescaling one of them we find that there are only two free parameters that define the initial conditions. We choose to express our initial conditions

in terms of $\delta_{0,\text{uh}} \equiv \delta(r_{\text{uh}})$ and $\chi_{0,\text{uh}} \equiv \chi(r_{\text{uh}})$ so that

$$\begin{aligned}
\delta(r) &= \delta_{0,\text{uh}} + \sum_{k=1}^{\infty} \delta_{k,\text{uh}}(\delta_{0,\text{uh}}, \chi_{0,\text{uh}}) (r - r_{\text{uh}})^k, \\
\chi(r) &= \chi_{0,\text{uh}} + \sum_{k=1}^{\infty} \chi_{k,\text{uh}}(\delta_{0,\text{uh}}, \chi_{0,\text{uh}}) (r - r_{\text{uh}})^k, \\
\psi(r) &= \sum_{k=0}^{\infty} \psi_{k,\text{uh}}(\delta_{0,\text{uh}}, \chi_{0,\text{uh}}) (r - r_{\text{uh}})^k, \\
\Sigma(r) &= \sum_{k=0}^{\infty} \Sigma_{k,\text{uh}}(\delta_{0,\text{uh}}, \chi_{0,\text{uh}}) (r - r_{\text{uh}})^k.
\end{aligned} \tag{4.65}$$

Summarizing, the branch coming from the metric/spin-0 horizon is known, and we want to determine if there exists a couple $(\delta_{0,\text{uh}}, \chi_{0,\text{uh}})$ such that the solution coming from the universal horizon matches the former.

The matching of these solutions would imply, for instance, that the derivative at midpoint $\delta'_h(r)$ computed when $r \rightarrow r^*$ from the metric horizon must be equal to the derivative $\delta'_{\text{uh}}(r)$ computed when $r \rightarrow r^*$ from the universal horizon. However, we know each solution only up to a global scaling coefficient. One way to get rid of the unknown scaling parameter is by taking the ratios $\delta'_h(r)/\delta_h(r)$ and $\delta'_{\text{uh}}(r)/\delta_{\text{uh}}(r)$, where the unknown scaling parameter simplifies. Therefore, we require that the differences

$$\begin{aligned}
\Delta \left(\frac{\delta'(r)}{\delta(r)} \right) &\equiv \left(\left[\frac{\delta'(r^*)}{\delta(r^*)} \right]_{\text{uh}} - \left[\frac{\delta'(r^*)}{\delta(r^*)} \right]_{\text{h}} \right), \\
\Delta \left(\frac{\chi'(r)}{\chi(r)} \right) &\equiv \left(\left[\frac{\chi'(r^*)}{\chi(r^*)} \right]_{\text{uh}} - \left[\frac{\chi'(r^*)}{\chi(r^*)} \right]_{\text{h}} \right), \\
\Delta \left(\frac{\psi'(r)}{\psi(r)} \right) &\equiv \left(\left[\frac{\psi'(r^*)}{\psi(r^*)} \right]_{\text{uh}} - \left[\frac{\psi'(r^*)}{\psi(r^*)} \right]_{\text{h}} \right), \\
\Delta \left(\frac{\Sigma'(r)}{\Sigma(r)} \right) &\equiv \left(\left[\frac{\Sigma'(r^*)}{\Sigma(r^*)} \right]_{\text{uh}} - \left[\frac{\Sigma'(r^*)}{\Sigma(r^*)} \right]_{\text{h}} \right),
\end{aligned} \tag{4.66}$$

where the subscript 'uh' (resp. 'h') indicates that the quantity is evaluated using the numerical solution integrated from the universal horizon (resp. from the metric horizon), vanish. Let us stress that, in each of these terms, the fraction corresponding to the metric horizon branch is fixed. Thus we integrate from the point $r_{\text{uh}} + \epsilon$, where $\epsilon = 10^{-3}$ up to r^* , exploring a grid of initial conditions given by $(\delta_{0,\text{uh}}, \chi_{0,\text{uh}}) \in [-10000, 10000] \times [-10000, 10000]$, spaced by intervals of 1000 in each dimension. This rather coarse grid allows us to observe the main features of the differences (4.66). Thus, in figure 4.8 we show the sum of the squares

$$\bar{\Delta} \equiv \left[\Delta \left(\frac{\delta'(r)}{\delta(r)} \right) \right]^2 + \left[\Delta \left(\frac{\chi'(r)}{\chi(r)} \right) \right]^2 + \left[\Delta \left(\frac{\psi'(r)}{\psi(r)} \right) \right]^2 + \left[\Delta \left(\frac{\Sigma'(r)}{\Sigma(r)} \right) \right]^2, \tag{4.67}$$

and we note that there is a “valley” where the differences (4.66) are minimized. We increased the resolution of our grid to a few thousand of points in order to analyze the reduced area represented in figure 4.9. However, we found that the lowest value for $\bar{\Delta}$ was of the order of

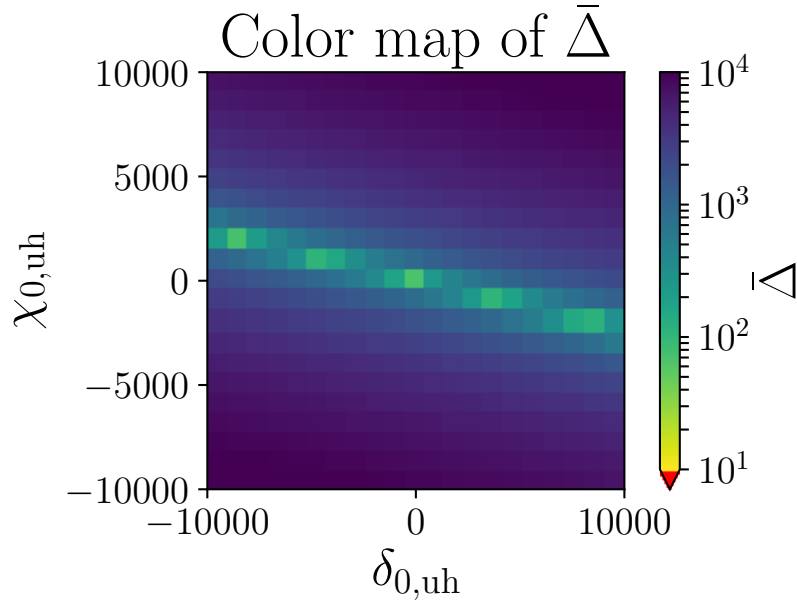


FIGURE 4.8 – Color map of $\bar{\Delta}$ as a function of $(\delta_{0,\text{uh}}, \chi_{0,\text{uh}})$. The colors were chosen so as to show that $\bar{\Delta}$ is positive everywhere. Indeed, the minimal value set for the color-bar is 10, and any value under 10 would be indicated in red. This coarse grid suggest a more detailed analysis around a reduced area.

~ 20 , and indeed we investigated with an increased precision in the region where we found the local minimum. The plot corresponding to that region is shown in figure 4.10. The fact that $\bar{\Delta}$ never goes below a threshold of the order of 20 shows that the different terms in squares in (4.67) never vanish simultaneously. Consequently, we conclude that neither the differences (4.66) do so, and this means that there is no pair of initial conditions $(\delta_{0,\text{uh}}, \chi_{0,\text{uh}})$ at the universal horizon such that the solution matches that one from the metric horizon. From this we conclude that it is not possible to find a solution regular both at the spin-0 horizon and at the universal horizon, i.e., our regular solution at the metric/spin-0 horizon is not regular at the universal horizon.

In conclusion, going to the spin-0 frame allowed us to enforce regularity at the spin-0 horizon. However, the solution was found to be unique and we lost the shooting parameter to bisect. Outside the metric horizon, the solution thus obtained was found to be singular at spatial infinity and not asymptotically flat. Inside the metric horizon the solution is singular at the universal horizon.

4.3 The $\alpha = \beta = 0$ case

From the results of the last section one would conclude that, in khronometric theory, black holes are not regular at order $\mathcal{O}(v)$. We reach this conclusion because the spin-0 horizon is between the universal horizon and the metric horizon, and we need to impose regularity at

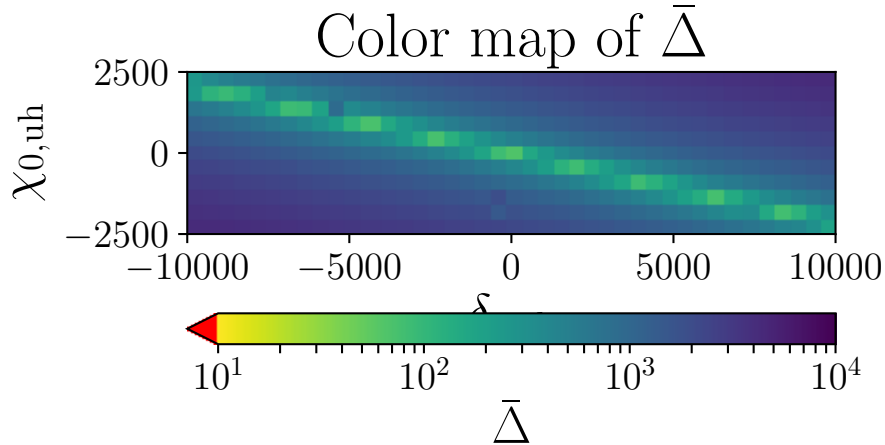


FIGURE 4.9 – Color map of $\bar{\Delta}$ as a function of $(\delta_{0,\text{uh}}, \chi_{0,\text{uh}})$. The colors were chosen so as to show that $\bar{\Delta}$ is positive everywhere. Indeed, the minimal value set for the color-bar is 10, and any value under 10 would be indicated in red. Although the grid still seems to be coarse, there is in fact much more data which we could not include in the figure. This was due to the use of an irregular grid and the problems to interpolate under such conditions.

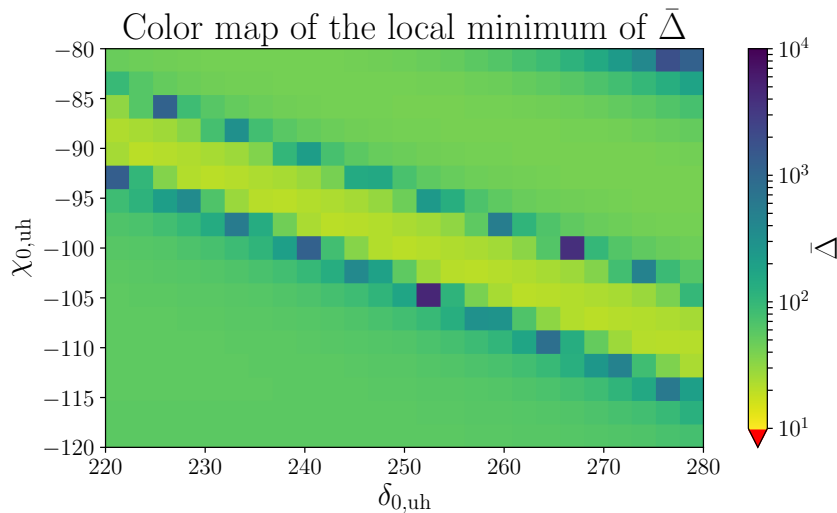


FIGURE 4.10 – Color map of $\bar{\Delta}$ as a function of $(\delta_{0,\text{uh}}, \chi_{0,\text{uh}})$. The colors were chosen so as to show that $\bar{\Delta}$ is positive everywhere. Indeed, the minimal value set for the color-bar is 10, and any value under 10 would be indicated in red. This is the valley where the minimal values are reached. The lowest value of all is of the order of ~ 20 .

each of these surfaces separately. However, there may exist a set of parameters α , β , λ for which the spin-0 horizon coincides with the universal horizon, so that enforcing regularity at the former is sufficient to ensure the existence of a regular solution. For this to be true, we would need to have the conditions defining the radial position of the spin-0 horizon (2.75) and the universal horizon (2.87) both being satisfied at a single point $r^* = r_{\text{uh}} = r_{s_0}$. More explicitly, as long as the spin-0 speed s_0 is finite, this would mean that the radius r^* is such that

$$f(r^*) + (s_0^2 - 1) \left(\frac{1 + f(r^*)A(r^*)^2}{2A(r^*)} \right)^2 = 0, \quad (4.68a)$$

$$1 + f(r^*)A(r^*)^2 = 0. \quad (4.68b)$$

The first equation is the relation defining the spin-0 horizon r_{s_0} and the second defines the universal horizon r_{uh} . Plugging (4.68b) into (4.68a) gives $f(r^*) = 0$, which is then incompatible with equation (4.68b). There is yet another way to merge the spin-0 horizon with the universal horizon without lose all Lorentz violating effects : we can make the spin-0 speed s_0 diverge so that equation (4.68a) reduces to equation (4.68b). This can be achieved by setting $\alpha = 0$. The special case where α is set to zero as been worked out in [152] in static, spherically symmetric configurations. Even though the exact form of the functions $f(r)$, $B(r)$ and $A(r)$ can in general be given only numerically, in the special case $\alpha = 0$ analytic solutions exist for the background functions :

$$f(r) = 1 - \frac{2G_N \tilde{m}}{r} - \frac{\beta r_{\text{kr}}^4}{r^4}, \quad B(r) = 1, \quad (4.69a)$$

$$A(r) = \frac{1}{f} \left(-\frac{r_{\text{kr}}^2}{r^2} + \sqrt{f + \frac{r_{\text{kr}}^4}{r^4}} \right), \quad (4.69b)$$

$$r_{\text{kr}} = \frac{G_N \tilde{m}}{2} \left(\frac{27}{1 - \beta} \right)^{1/4} \quad (4.69c)$$

It can be easily checked that the universal horizon and the spin-0 horizon coincide in this particular case, since when $\alpha \rightarrow 0$ the spin-0 speed given by eq. (2.62a) diverges, and are both located at $r_{\text{uh}} = \frac{3}{2}G_N \tilde{m}$. Indeed, as the spin-0 speed increases, the location of the spin-0 horizon moves further into the black hole. Moreover, since the universal horizon is such that it traps modes propagating at any arbitrary speed, we conclude that in this limit the spin-0 horizon merges with the universal horizon. This statement can also be mathematically proved, noting that if s_0 becomes infinite then $1 + f(r^*)A(r^*)^2 = 0$ becomes a necessary condition in equation (4.68a), leading precisely to equation (4.68b). This procedure has the evident advantage that it does not impose $f(r^*) = 0$ as well, so that the metric and universal horizons do not merge.

Note also that this solution does not depend on the coupling parameter λ , even though that is *not* assumed to vanish.

This limit is particularly attractive as $|\alpha| \lesssim 10^{-7}$ experimentally (c.f. Sec. 2.5). Assuming $\alpha = 0$ alone, however, does not avoid the appearance of finite-area singularities at the universal/metric horizon, as can be seen from figure 4.11, where we show the divergence of the curvature invariants of the asymptotically flat solution regular at the matter horizon.

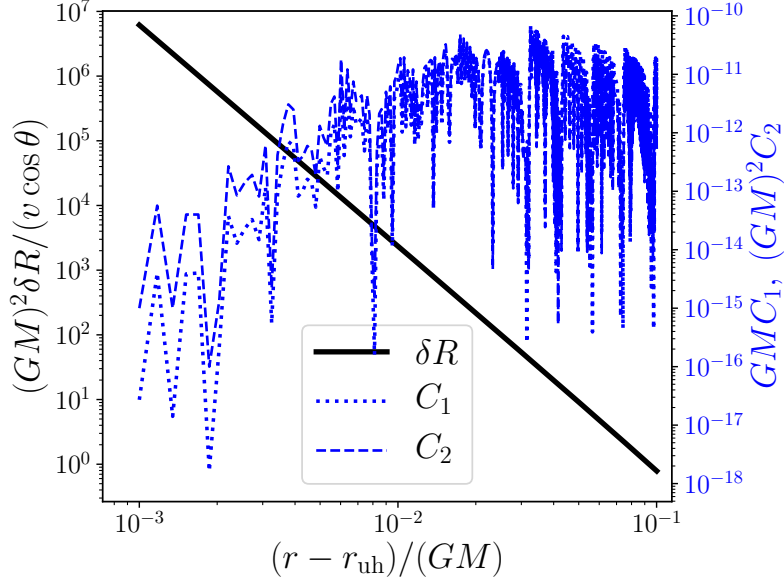


FIGURE 4.11 – $\mathcal{O}(v)$ contribution to the Ricci scalar near the universal/spin-0 horizon, for the asymptotically flat solution regular at the matter horizon, and for $\alpha = 0$, $\beta = 0.01$ and $\lambda = 0.1$.

However, from the experimental limits presented in Sec. 2.5, it follows that $|\beta| \lesssim 10^{-15}$, so it is attractive to also set $\beta = 0$ exactly. Indeed, from the experimental bounds discussed in 2.5.2 and in 2.5.3, α is zero up to 10^{-7} and β is zero up to 10^{-15} (indeed, as the spin-2 mode speed is given by $s_2^2 = 1/(1 - \beta)$, the nearly coincident arrival of gravitational and electromagnetic radiation constraints β to be very small. Then, this result together with the solar system constraints bounding α to be close to 2β gives a tight bound due to the very tight bound on β). Spherical black hole solutions for $\alpha = \beta = 0$ are very simple and known analytically in this limit, and are given by

$$f(r) = 1 - \frac{2\mu}{r}, \quad (4.70a)$$

$$A(r) = \frac{1}{1 - 2\mu/r} \left(\sqrt{f(r) + \left(\frac{r_{\text{EA}}}{r}\right)^4} - \left(\frac{r_{\text{EA}}}{r}\right)^2 \right), \quad (4.70b)$$

$$B(r) = 1, \quad (4.70c)$$

where $r_{\text{EA}} = \frac{3^{3/4}}{2}\mu$. Again, the coupling coefficient λ does not appear in the solution for the background potentials, nor any other coupling coefficient. Furthermore, the solution for the metric corresponds precisely to a Schwarzschild black hole in general relativity. Since $\alpha = 0$ implies that $G_N = G_{\text{EA}}$, then the gravitational radius coincides with the Schwarzschild radius. From these considerations it follows that the parameter λ cannot be constrained by static stationary black holes, as they are indistinguishable from GR black holes.

For the slowly moving black hole, the sensitivity of equation (4.47) reduces to

$$\sigma = \frac{\lambda}{2(1-2\lambda)} \left(1 + 4 \frac{\chi_0}{R_0 \delta_0} \right), \quad (4.71)$$

where χ_0 is the asymptotic constant defined in (4.35b), and R_0 is the gravitational radius of the black hole and is equal to 2μ . Thus, in principle λ may be constrained by black hole dipole flux emission [68].

In the previous paragraphs we have shown the order $\mathcal{O}(v^0)$ black hole solution as determined by the metric potentials f , A and B , which are greatly simplified. Let us now tackle the $\mathcal{O}(v^0)$ system and solve for the perturbed potentials $\delta(r)$, $\chi(r)$, $\psi(r)$ and $\Sigma(r)$. First, one can show that, for $\alpha = \beta = 0$, both the functions $\psi(r)$ and $\Sigma(r)$ vanish identically. Indeed, this can be proven by inserting a null Ansatz for both ψ and Σ into the field equations, and showing that $\delta(r)$ and $\chi(r)$ satisfy a system of 2 ordinary differential equations, i.e., that the problem is not over-determined. In more detail, setting $\psi \equiv 0$ and $\Sigma \equiv 0$ allows us to solve the two constraint equations C_1 and C_2 in terms of $\delta'(r)$ and $\chi'(r)$. Taking derivatives of these equations, one obtains the remaining equations of motion (4.32a) and (4.32b). Another way to obtain this result, is to perform a perturbative expansion near some given initial point. One can then show by recursion that all the series coefficients for ψ and Σ must vanish.

As a consequence of this result, we can make use of the constraint equations $C_1 = C_2 = 0$ (cf. equations (4.30)) instead of the equations of motion (4.32a) and (4.32b), as both sets of equations happen to be equivalent. This procedure is simpler, as the constraints involve fewer derivatives in the potentials than the equations of motion. Thus, setting $\psi(r)$ and $\Sigma(r)$ to zero the constraint equations simply become

$$\delta'(r) + \frac{4(8r^4 + 4\mu r^3 - 27\mu^4)}{16r^5 - 21\mu r^4 + 27\mu^4 r} \delta(r) - \frac{32r^2}{16r^4 - 21\mu r^3 + 27\mu^4} \chi(r) = 0, \quad (4.72)$$

$$\chi'(r) - \delta(r) = 0. \quad (4.73)$$

Let us remark that these expressions do not involve the coupling coefficient λ , and therefore we will find solutions that do not depend on it. We thus expect that the solution to be also equivalent to a Schwarzschild black hole. Further on we will want to assess whether or not we find regular solutions to the system (4.72) and (4.73), so we will express now the functional form of the curvature invariants. They are now simply given by

$$R = \mathcal{O}(v^2), \quad (4.74a)$$

$$R_{\alpha\beta} R^{\alpha\beta} = \mathcal{O}(v^2), \quad (4.74b)$$

$$R_{\alpha\beta\mu\nu} R^{\alpha\beta\mu\nu} = \frac{48\mu^2}{r^6} + \mathcal{O}(v^2), \quad (4.74c)$$

$$k_1 = \frac{27\mu^5}{8r^7} + v \tilde{b}_1(r) \delta(r) \cos \theta + \mathcal{O}(v^2), \quad (4.74d)$$

$$k_2 = -\frac{\mu}{r} \sin^2 \theta + v \tilde{b}_2(r) (\delta(r) - \chi'(r)) \cos \theta \sin^2 \theta + \mathcal{O}(v^2), \quad (4.74e)$$

where $\tilde{b}_1(r)$ and $\tilde{b}_2(r)$ are algebraic expressions on the background functions. Thus, up to order $\mathcal{O}(v^2)$, the curvature invariants not involving the æther are the same as for a Schwarzschild black hole in general relativity. The $\mathcal{O}(v)$ piece comes as no surprise since we know

that the metric is Schwarzschild, however the $\mathcal{O}(v)$ is not a trivial result. Also, due to the equation of motion (4.73), the $\mathcal{O}(v)$ part of the killing invariant k_2 vanishes.

We can express $\chi(r)$ in terms of $\delta(r)$ and $\delta'(r)$ using equation (4.72)

$$\chi(r) = \frac{27\mu^4 + 16r^4 - 32\mu r^3}{32r^2} \delta'(r) + \frac{8r^4 - 4\mu r^3 - 27\mu^4}{8r^3} \delta(r). \quad (4.75)$$

Taking the derivative of equation (4.75) and replacing $\chi'(r)$ into equation (4.73) we obtain a second order differential equation for $\delta(r)$,

$$\left(\frac{r^2}{2} - \mu r + \frac{27\mu^4}{32r^2} \right) \delta''(r) + \left(2r - \frac{3\mu}{2} - \frac{81\mu^4}{16r^3} \right) \delta'(r) + \frac{81\mu^4}{8r^4} \delta(r) = 0. \quad (4.76)$$

From this, it follows that we can simply focus on solving equation (4.76), as it is enough to get all the information on the system.

Solving equation (4.76) near spatial infinity gives

$$\delta(r) = \delta_0 + \frac{\delta_3}{r^3} + \mathcal{O}\left(\frac{1}{r^4}\right), \quad (4.77)$$

where δ_0 and δ_3 are integration constants. This in turn implies through equation (4.75) that $\chi(r)$ behaves asymptotically as

$$\chi(r) = \delta_0 r + \chi_0 - \frac{\delta_3}{2r^2} + \mathcal{O}\left(\frac{1}{r^4}\right), \quad (4.78)$$

where $\chi_0 = -\frac{\mu}{2}\delta_0 = -\frac{R_0}{4}\delta_0$ (let us recall that R_0 is the gravitational radius) is fixed in terms of δ_0 . It follows that $\frac{\chi_0}{R_0\delta_0} = -\frac{1}{4}$, and from this we obtain that the sensitivity σ vanishes. Indeed, equation (4.71) give us

$$\sigma = 0, \quad (4.79)$$

irrespective for the value for λ . This result was to be expected, since the equations of motion do not actually depend on the coupling coefficient λ (cf. equations (4.72) and (4.73)).

In fact, we found an infinitesimal gauge transformation that brings the perturbed stationary metric of equation (4.20) to the Schwarzschild solution in Eddington-Finkelstein coordinates. To see this, let us note that for $\alpha = \beta = 0$ the metric Ansatz of equation (4.20) can be recast as

$$\begin{aligned} ds^2 = & \left(1 - \frac{2\mu}{r} \right) dv^2 - 2dvdr - r^2 d\Omega \\ & + v \left[2 \left(1 - \frac{2\mu}{r} \right) \left(\cos \theta \delta(r) dr - \sin \theta \chi(r) d\theta \right) dv - 2 \cos \theta \delta(r) dr^2 + 2 \sin \theta \chi(r) d\theta dr \right] \\ & + \mathcal{O}(v^2), \end{aligned} \quad (4.80)$$

and the $\mathcal{O}(v)$ piece can be removed by the time coordinate redefinition

$$v' = v + v \chi(r) \cos \theta, \quad (4.81)$$

leaving us with the Schwarzschild solution in Eddington-Finkelstein coordinates

$$ds^2 = \left(1 - \frac{2\mu}{r}\right) dv'^2 - 2dv'dr - r^2 d\Omega + \mathcal{O}(v^2). \quad (4.82)$$

This means that at first order in v , the geometry of the spacetime is not affected by the presence of the æther field. In particular, since the metric is equivalent to the Schwarzschild solution up to a gauge transformation, all invariants constructed only using the metric are automatically regular outside the origin $r = 0$. Nonetheless, the æther field still might have a non-trivial profile (different from the background solution) which must be solved for, even after the gauge transformation is performed.

Inspection of equations (4.76) and (4.73) reveals that, besides $r = 0$, the only singular point of the equations of motion corresponds to the universal horizon, located at $r_{\text{uh}} = 3\mu/2^5$. Near the universal horizon, the equation (4.76) for $\delta(r)$ takes the form

$$x^2 \delta''(x) + 5x \delta'(x) + 2\delta(x) \simeq 0. \quad (4.83)$$

where $x = r - r_{\text{uh}}$ is the distance to the universal horizon, and we have taken only the leading orders in x . Then, we find that the solution to this equation is made of two divergent modes, namely

$$\delta(x) \simeq C_{\text{h}} x^{-\sqrt{2}(1+\sqrt{2})} + C_{\text{s}} x^{\sqrt{2}(1-\sqrt{2})}. \quad (4.84)$$

where C_{h} and C_{s} are integration constants. We can call the first mode the “hard” mode and the second the “soft” mode. Indeed, though in both cases the function $\delta(r)$ diverges while approaching the universal horizon, for the soft mode we can make again a coordinate redefinition absorbing this divergence. To show this, let us write the metric Ansatz again using the coordinate x instead of r as

$$ds^2 = f(x) dv^2 - 2dvdx - (x + r_{\text{uh}})^2 d\Omega + v \left[2f(x) \cos \theta \delta(x) dv dx - 2f(x) \sin \theta \chi(x) d\theta dv - 2 \cos \theta \delta(x) dx^2 + 2 \sin \theta \chi(x) d\theta dx \right] + \mathcal{O}(v^2). \quad (4.85)$$

We want to show that the terms proportional to $\delta(x)$ and $\chi(x)$ can be made regular at $x = 0$. Let us define the coordinate $\bar{x} = x\delta(x)$, so that we find

$$dx = \left(1 + x \frac{\delta'(x)}{\delta(x)}\right)^{-1} \frac{d\bar{x}}{\delta(x)}. \quad (4.86)$$

If, near $x = 0$, we have $\delta(x) \sim x^n$, where n is one of the powers in (4.84), then the product $x \frac{\delta'(x)}{\delta(x)}$ converges to a constant as we approach $x = 0$. We note that, in terms of \bar{x} , each of

5. To be more precise, the equations of motion do present a singularity at spatial infinity, however it is a removable singularity and therefore the solutions are always regular at infinity. This can be seen from equation (4.77), which has the maximum number of free parameters (as there are only two derivatives in the equations (4.76) and (4.73)), meaning that regularity does not impose any condition on the initial data, and is always asymptotically flat.

the coefficients of the metric are now automatically regular except for the $g_{v\theta}$ component of the metric. Indeed, if we expand this term near $x = 0$ we find that it becomes

$$g_{v\theta} = -2vf(x) \sin \theta \chi(x) d\theta dv \simeq -2(n+3)f(x) \sin(\theta) x^{n+1} dv d\theta, \quad (4.87)$$

and this will be finite at $x = 0$ only if $n + 1 \geq 0$. This is indeed true for the soft mode, as $n \simeq -0.5$. However, the hard mode as a power $n \simeq -3$, so that the $g_{v\theta}$ component of the metric diverges.

Therefore we were not able to absorb the metric singularity of the hard mode, and by computing the killing scalar k_1 we confirm that that mode produces a curvature singularity. Indeed, to leading order in the auxiliary variable $x = r - r_{\text{uh}}$, the $\mathcal{O}(v)$ part of the killing scalar k_1 goes as

$$k_1 \propto \cos(\theta) (r - r_{\text{uh}})^3 \delta(r). \quad (4.88)$$

Thus, expressing $\delta(r)$ as a superposition of the two modes we have

$$k_1 \propto \cos(\theta) (C_h x^m + C_s x^n), \quad (4.89)$$

with $m = 1 - \sqrt{2} < 0$ and $n = 1 + \sqrt{2} > 0$. As we can see, the hard mode produces a curvature singularity as it approaches the universal horizon, while the soft mode is physically well behaved. This result is in agreement with the fact that we can make a redefinition of the perturbations such as to absorb the divergence of the function $\delta(r)$ when it contains only a soft mode, while this is no longer possible if $\delta(r)$ contains a hard mode as well.

We therefore conclude that we can integrate the system of equations (4.76) and (4.73) starting from the universal horizon, using initial data such that only the soft mode is excited. As there are no other singular points we can obtain a solution everywhere else. Such a solution is shown in figure 4.12, for the potential $\delta(r)$. Also, the $\mathcal{O}(v)$ part of the killing scalar k_1 is plotted. Both quantities are plotted in absolute value.

4.4 Chapter conclusions

On the one hand, the study of slowly moving black holes in section 4.1 revealed that regular black hole solutions do not exist when the coupling coefficients α and β are different from zero (cf. sections 4.2.6 to 4.2.6.d). We therefore conclude that, even without the LIGO-Virgo/FERMI detection, or even without the parametrized post-Newtonian constraints, we would still have to set $\alpha = \beta = 0$.

On the other hand, setting $\alpha = \beta = 0$ led us to a unique slowly moving black hole solution, independent of the coupling constant λ . This solution is identical to a Schwarzschild black hole in its metric, but has a non-trivial khronon-field. Moreover, the associated sensitivity vanishes for all values of λ , meaning that the simple prescription adopted in section 3.4 is not sufficient to constraint λ through dipolar radiation constraints. Indeed, to describe the dipolar radiation our methods must be extended to include effects coming from higher order sensitivities, such as described in section 3.2.

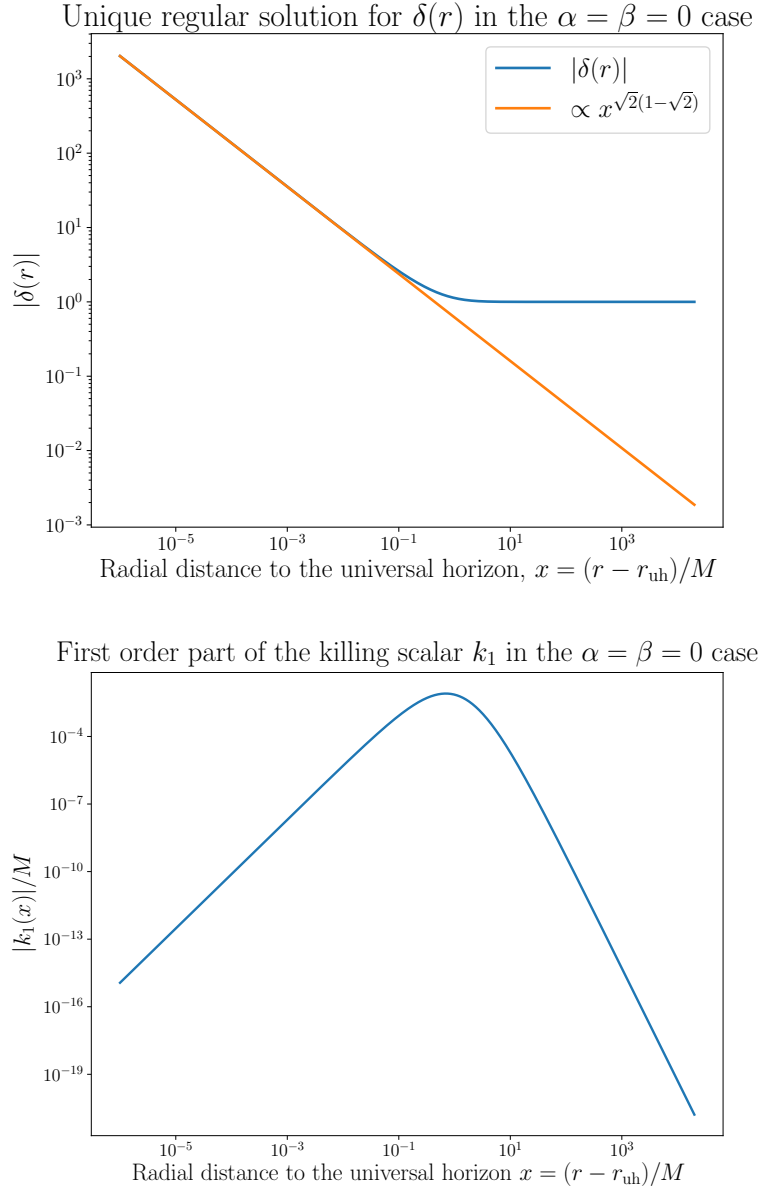


FIGURE 4.12 – *Upper panel* : The (absolute value of the) unique solution that is physically regular is plotted in log scale. Near the universal horizon the solution goes as $\delta(x) \simeq C_s x^{\sqrt{2}(1-\sqrt{2})}$, where $C_s \sim -1.618$ in order to have $\delta(r) \sim -1$ as r goes to infinity. *Lower panel* : The killing scalar \tilde{k} is shown to be finite everywhere for this solution.

4.A Explicit form of the field equations

Let us express the modified Einstein tensor E^μ_ν in the form

$$E^\mu_\nu = \begin{pmatrix} Q_1 + v \cos \theta S_1(r) & Q_2 + v \cos \theta S_2(r) & 0 & v \sin \theta S_3(r) \\ Q_4 + v \cos \theta S_4(r) & Q_5 + v \cos \theta S_5(r) & 0 & v \sin \theta S_6(r) \\ 0 & 0 & Q_7 + v \cos \theta S_7(r) & 0 \\ v \sin \theta S_8(r) & v \sin \theta S_9(r) & 0 & Q_{10} + v \cos \theta S_{10}(r) \end{pmatrix} + \mathcal{O}(v^2), \quad (4.90)$$

where Q_i, P_i for $i = 1, \dots, 10$ are respectively, the background and perturbed equations (i.e., the $\mathcal{O}(v^0)$ and $\mathcal{O}(v)$ equations). Then the explicit form of these equations are

$$\begin{aligned} Q_1 = & \frac{1}{8r^2 A[r]^4 B[r]^3} \left(3r^2 (-\alpha + \beta + \lambda) B[r] A'[r]^2 - 2A[r]^2 (B[r] (-\lambda + r^2 (4\alpha + 3(-\alpha + \beta) + 3\lambda) f[r] A'[r]^2) + r\lambda B'[r]) + r(4\alpha + 3(-\alpha + \beta) + 3\lambda) \right. \\ & A[r]^3 f[r] (-rA'[r] B'[r] + B[r] (2A'[r] + rA''[r])) + rA[r] (r(-\alpha + \beta + \lambda) A'[r] B'[r] - B[r] (2(-\alpha + \beta + 3\lambda) A'[r] + r(-\alpha + \beta + \lambda) A''[r])) + \\ & r(-\alpha + \beta + \lambda) A[r]^7 f[r]^2 (-r f[r] A'[r] B'[r] + B[r] (2rA'[r] f'[r] + f[r] (2A'[r] + rA''[r]))) + rA[r]^5 f[r] \\ & (r(-4\alpha - 5(-\alpha + \beta) - 5\lambda) f[r] A'[r] B'[r] + B[r] (2r(2\alpha + 5(-\alpha + \beta) + 5\lambda) A'[r] f'[r] + f[r] (2(4\alpha + 5(-\alpha + \beta) + 7\lambda) A'[r] + r(4\alpha + 5(-\alpha + \beta) + 5\lambda) A''[r]))) - \\ & A[r]^8 f[r]^2 (rB'[r] (2\lambda f[r] + r(-\alpha + \beta + \lambda) f'[r]) + B[r] (2(\beta + \lambda) f[r] - r(-\alpha + \beta + \lambda) (2f'[r] + rf''[r]))) + \\ & A[r]^4 (8B[r]^3 + rB'[r] (2(8 + 5\lambda) f[r] + r(\alpha + \beta + \lambda) f'[r]) - \\ & B[r] (-2(-4 + 3\alpha + 3(-\alpha + \beta) + \lambda) f[r] + r^2(3\alpha + \beta + \lambda) f[r]^2 A'[r]^2 + r(2(4\alpha + \beta + 3\lambda) f'[r] + r(\alpha + \beta + \lambda) f''[r]))) + \\ & A[r]^6 (-2rf[r] B'[r] (3\lambda f[r] + r(\alpha + 2(-\alpha + \beta) + 2\lambda) f'[r]) + \\ & B[r] (-2(2\alpha + 2(-\alpha + \beta) + \lambda) f[r]^2 + r^2(-\alpha + \beta + \lambda) f'[r]^2 + 2rf[r] (2(\alpha + 2(-\alpha + \beta) + 3\lambda) f'[r] + r(\alpha + 2(-\alpha + \beta) + 2\lambda) f''[r]))) \left. \right) \\ Q_2 = & -\frac{1}{4r^2 B[r]^2} \\ & \left(8rB'[r] - \frac{1}{A[r]^2} (2r^2(4\alpha + 3(-\alpha + \beta) + 3\lambda) B[r] A'[r]^2 + 2A[r]^2 (B[r] (-3(\beta + \lambda) + r^2(\alpha + \beta + \lambda) f[r] A'[r]^2) - 3r\lambda B'[r]) + r(4\alpha + 3(-\alpha + \beta) + 3\lambda) A[r] \right. \\ & (rA'[r] B'[r] - B[r] (2A'[r] + rA''[r])) - r(-\alpha + \beta + \lambda) A[r]^5 f[r] (-rf[r] A'[r] B'[r] + B[r] (2rA'[r] f'[r] + f[r] (2A'[r] + rA''[r]))) - \\ & 2rA[r]^3 (-2r(\beta + \lambda) f[r] A'[r] B'[r] + B[r] (r(2\alpha + 3(-\alpha + \beta) + 3\lambda) A'[r] f'[r] + 2(\beta + \lambda) f[r] (2A'[r] + rA''[r]))) + \\ & A[r]^6 f[r] (rB'[r] (2\lambda f[r] + r(-\alpha + \beta + \lambda) f'[r]) + B[r] (2(\beta + \lambda) f[r] - r(-\alpha + \beta + \lambda) (2f'[r] + rf''[r]))) + \\ & \left. A[r]^4 (rB'[r] (4\lambda f[r] + r(2\alpha + 3(-\alpha + \beta) + 3\lambda) f'[r]) + B[r] (4(\beta + \lambda) f[r] - r(2\alpha + 3(-\alpha + \beta) + 3\lambda) (2f'[r] + rf''[r]))) \right) \\ Q_4 = & -\frac{1}{16r^2 A[r]^6 B[r]^4} \left((1 + A[r]^2 f[r])^2 (2r^2(-\alpha + \beta + \lambda) B[r] A'[r]^2 + 2A[r]^2 (B[r] (-\beta - \lambda + r^2(\alpha + \beta + \lambda) f[r] A'[r]^2) - r\lambda B'[r]) + \right. \\ & r(-\alpha + \beta + \lambda) A[r] (rA'[r] B'[r] - B[r] (2A'[r] + rA''[r])) - 2r(\alpha + \beta + \lambda) A[r]^3 (-rf[r] A'[r] B'[r] + B[r] (rA'[r] f'[r] + f[r] (2A'[r] + rA''[r]))) - \\ & r(-\alpha + \beta + \lambda) A[r]^5 f[r] (-rf[r] A'[r] B'[r] + B[r] (2rA'[r] f'[r] + f[r] (2A'[r] + rA''[r]))) + r(\alpha + \beta + \lambda) A[r]^4 (rB'[r] f'[r] - B[r] (2f'[r] + rf''[r])) + \\ & \left. A[r]^6 f[r] (rB'[r] (2\lambda f[r] + r(-\alpha + \beta + \lambda) f'[r]) + B[r] (2(\beta + \lambda) f[r] - r(-\alpha + \beta + \lambda) (2f'[r] + rf''[r]))) \right) \\ Q_5 = & -\frac{1}{8r^2 B[r]^3} \\ & \left(8B[r] (-B[r]^2 + f[r] + rf'[r]) - \frac{1}{A[r]^4} (3r^2(-\alpha + \beta + \lambda) B[r] A'[r]^2 + 2A[r]^2 (B[r] (\lambda + r^2(4\alpha + 3(-\alpha + \beta) + 3\lambda) f[r] A'[r]^2) - r\lambda B'[r]) + r(4\alpha + 3(-\alpha + \beta) + 3\lambda) \right. \\ & A[r]^3 f[r] (rA'[r] B'[r] - B[r] (2A'[r] + rA''[r])) + rA[r] (r(-\alpha + \beta + \lambda) A'[r] B'[r] - B[r] (2(-\alpha + \beta + 3\lambda) A'[r] + r(-\alpha + \beta + \lambda) A''[r])) - \\ & r(-\alpha + \beta + \lambda) A[r]^7 f[r]^2 (-rf[r] A'[r] B'[r] + B[r] (2rA'[r] f'[r] + f[r] (2A'[r] + rA''[r]))) - \\ & rA[r]^5 f[r] (-r(4\alpha + 3(-\alpha + \beta) + 3\lambda) f[r] A'[r] B'[r] + B[r] (2r(\alpha + \beta + \lambda) A'[r] f'[r] + f[r] (2(4\alpha + 3(-\alpha + \beta) + \lambda) A'[r] + r(4\alpha + 3(-\alpha + \beta) + 3\lambda) A''[r]))) + \\ & A[r]^8 f[r]^2 (rB'[r] (2\lambda f[r] + r(-\alpha + \beta + \lambda) f'[r]) + B[r] (2(\beta + \lambda) f[r] - r(-\alpha + \beta + \lambda) (2f'[r] + rf''[r]))) + \\ & A[r]^6 (2rf[r] B'[r] (\lambda f[r] + r(\beta + \lambda) f'[r]) + B[r] ((4\alpha + 4(-\alpha + \beta) + 6\lambda) f[r]^2 + r^2(-\alpha + \beta + \lambda) f'[r]^2 - 2rf[r] (2\beta f'[r] + r(\beta + \lambda) f''[r]))) + \\ & \left. A[r]^4 (rB'[r] (-2\lambda f[r] + r(\alpha + \beta + \lambda) f'[r]) + \right. \\ & \left. B[r] (-2(3\alpha + 3(-\alpha + \beta) + 5\lambda) f[r] + r^2(4\alpha + 3(-\alpha + \beta) + 3\lambda) f[r]^2 A'[r]^2 - r(2(\alpha + \beta + 3\lambda) f'[r] + r(\alpha + \beta + \lambda) f''[r]))) \right) \\ Q_7 = & \frac{1}{8rA[r]^4 B[r]^3} \left(r(\alpha - \beta + 5\lambda) B[r] A'[r]^2 - 2A[r]^2 (r(\alpha + \beta + \lambda) B[r] f[r] A'[r]^2 + (\beta + 2\lambda) B'[r]) - \right. \\ & 2r(\alpha + \beta + \lambda) A[r]^3 B[r] A'[r] f'[r] - 2A[r] (-r\lambda A'[r] B'[r] + B[r] (2(\beta + 2\lambda) A'[r] + r\lambda A''[r])) + \\ & 2A[r]^5 f[r] (-r\lambda f[r] A'[r] B'[r] + B[r] (r(\alpha - \beta + 3\lambda) A'[r] f'[r] + f[r] (2(\beta + 2\lambda) A'[r] + r\lambda A''[r]))) + \\ & A[r]^6 (-2(\beta + 2\lambda) f[r]^2 B'[r] + r(\alpha - \beta + \lambda) B[r] f'[r]^2 + 2f[r] (-r\lambda B'[r] f'[r] + B[r] (2(\beta + 2\lambda) f'[r] + r\lambda f''[r]))) + \\ & \left. A[r]^4 (2B'[r] (2(2\beta + 2\lambda) f[r] + r(2\lambda) f'[r]) + B[r] (r(\alpha - \beta + \lambda) f[r]^2 A'[r]^2 - 2(2(2\beta + 2\lambda) f'[r] + r(2\lambda) f''[r]))) \right) \\ Q_{10} = Q_7 \end{aligned}$$

for the background equations, while for the perturbed equations we have

$$\begin{aligned}
S_1 = & \frac{1}{64 r^3 A[r]^6 B[r]^5} (16 r^3 (-\alpha + \beta + \lambda) B[r]^2 (-2 \delta[r] + B[r] \psi[r]) A'[r]^2 - \\
& 2 r^2 A[r] B[r] (10 r (-\alpha + \beta + \lambda) \delta[r] A'[r] B'[r] - B[r] (r (-\alpha + \beta + \lambda) A'[r] (\psi[r] B'[r] + 8 \delta'[r]) + 2 \delta[r] (2 (-\alpha + \beta + 5 \lambda) A'[r] + r (-\alpha + \beta + \lambda) A''[r])) + \\
& B[r]^2 (4 r (-\alpha + \beta + \lambda) A'[r] \psi'[r] + \psi[r] (2 (-\alpha + \beta + 5 \lambda) A'[r] + r (-\alpha + \beta + \lambda) A''[r]))) + \\
& 6 r^2 (-\alpha + \beta + \lambda) A[r]^{11} B[r] f[r]^4 (-4 r f[r] \delta[r] A'[r] B'[r] + B[r]^2 (4 r \psi[r] A'[r] f'[r] + f[r] (2 \psi[r] A'[r] + r A'[r] \psi'[r] + r \psi[r] A''[r]))) + \\
& B[r] (8 r \delta[r] A'[r] f'[r] + f[r] (r A'[r] (-\psi[r] B'[r] + 2 \delta'[r]) + 2 \delta[r] (2 A'[r] + r A''[r]))) + \\
& 4 r A[r]^5 B[r] f[r] (4 (-\alpha + \beta + \lambda) B[r]^3 \chi[r] A'[r] + 6 r^2 (4 \alpha + 3 (-\alpha + \beta) + 3 \lambda) f[r] \delta[r] A'[r] B'[r] - \\
& r (4 \alpha + 3 (-\alpha + \beta) + 3 \lambda) B[r] (4 r \delta[r] A'[r] f'[r] + f[r] (r A'[r] (\psi[r] B'[r] + 4 \delta'[r]) + 2 \delta[r] (2 A'[r] + r A''[r]))) - \\
& (4 \alpha + 3 (-\alpha + \beta) + 3 \lambda) B[r]^2 (4 \Sigma[r] A'[r] - r (2 r \psi[r] A'[r] f'[r] + f[r] (2 \psi[r] A'[r] + 2 r A'[r] \psi'[r] + r \psi[r] A''[r]))) + \\
& 4 r A[r]^7 B[r] f[r]^2 (-4 (-\alpha + \beta + 5 \lambda) B[r]^3 \chi[r] A'[r] - 4 r^2 (3 \alpha + 5 (-\alpha + \beta) + 5 \lambda) f[r] \delta[r] A'[r] B'[r] + \\
& r B[r] (r A'[r] ((8 \alpha + 7 (-\alpha + \beta) + 7 \lambda) \delta[r] A'[r] f'[r] + f[r] (-r A'[r] ((4 \alpha + 3 (-\alpha + \beta) + 5 \lambda) \psi[r] B'[r] - 2 (2 \alpha + 5 (-\alpha + \beta) + 5 \lambda) \delta'[r]) + \\
& 2 \delta[r] (2 (4 \alpha + 5 (-\alpha + \beta) + 7 \lambda) A'[r] + r (4 \alpha + 5 (-\alpha + \beta) + 5 \lambda) A''[r]))) + B[r]^2 (-4 (4 \alpha + 5 (-\alpha + \beta) + 7 \lambda) \Sigma[r] A'[r] + \\
& r (2 r (5 \alpha + 6 (-\alpha + \beta) + 6 \lambda) \psi[r] A'[r] f'[r] + f[r] (3 r (2 \alpha + 3 (-\alpha + \beta) + 3 \lambda) A'[r] \psi'[r] + (4 \alpha + 3 (-\alpha + \beta) + 3 \lambda) \psi[r] (2 A'[r] + r A''[r])))) + \\
& 2 r A[r]^3 B[r] (-8 (-\alpha + \beta + 3 \lambda) B[r]^3 \chi[r] A'[r] + 20 r^2 (\alpha + \beta + \lambda) f[r] \delta[r] A'[r] B'[r] - r B[r] (4 r (3 \alpha - \beta - \lambda) \delta[r] A'[r] f'[r] + \\
& f[r] (r A'[r] ((8 \alpha + 7 (-\alpha + \beta) + 7 \lambda) \psi[r] B'[r] + 2 (12 \alpha + 5 (-\alpha + \beta) + 5 \lambda) \delta'[r]) + 2 \delta[r] (2 (8 \alpha + 5 (-\alpha + \beta) + 5 \lambda) A'[r] + r (8 \alpha + 5 (-\alpha + \beta) + 5 \lambda) A''[r]))) + \\
& B[r]^2 (8 (-\alpha + \beta + 3 \lambda) \Sigma[r] A'[r] + r (4 r (2 \alpha - \beta - \lambda) \psi[r] A'[r] f'[r] + f[r] (3 r (3 \alpha + \beta + \lambda) A'[r] \psi'[r] + (8 \alpha + 7 (-\alpha + \beta) + 7 \lambda) \psi[r] (2 A'[r] + r A''[r])))) + \\
& 2 r A[r]^9 B[r] f[r]^3 (-8 (-\alpha + \beta + \lambda) B[r]^3 \chi[r] A'[r] - 2 r^2 (16 \alpha + 29 (-\alpha + \beta) + 29 \lambda) f[r] \delta[r] A'[r] B'[r] + \\
& r B[r] (16 r (3 \alpha + 7 (-\alpha + \beta) + 7 \lambda) \delta[r] A'[r] f'[r] + f[r] (r A'[r] (-8 \alpha + 11 (-\alpha + \beta) + 11 \lambda) \psi[r] B'[r] + 16 (\alpha + 2 (-\alpha + \beta) + 2 \lambda) \delta'[r]) + \\
& 2 \delta[r] (2 (8 \alpha + 13 (-\alpha + \beta) + 17 \lambda) A'[r] + r (8 \alpha + 13 (-\alpha + \beta) + 13 \lambda) A''[r]))) + B[r]^2 (-8 (-\alpha + \beta + \lambda) \Sigma[r] A'[r] + r (4 r (6 \alpha + 13 (-\alpha + \beta) + 13 \lambda) \\
& \psi[r] A'[r] f'[r] + f[r] (8 r (\alpha + 2 (-\alpha + \beta) + 2 \lambda) A'[r] \psi'[r] + \psi[r] (2 (8 \alpha + 11 (-\alpha + \beta) + 15 \lambda) A'[r] + r (8 \alpha + 11 (-\alpha + \beta) + 11 \lambda) A''[r]))) + \\
& r A[r]^2 (-6 r^2 (-\alpha + \beta + \lambda) \delta[r] B'[r]^2 + 2 r B[r] (3 r (-\alpha + \beta + \lambda) B'[r] \delta'[r] + \delta[r] (2 (-\alpha + \beta + 3 \lambda) B'[r] + r (-\alpha + \beta + \lambda) B''[r])) + \\
& B[r]^2 (4 \delta[r] (-2 (\beta + 2 \lambda) + 3 r^2 (8 \alpha + 5 (-\alpha + \beta) + 5 \lambda) f[r] A'[r]^2) - r (4 (-\alpha + \beta + 3 \lambda) \delta'[r] + r (-\alpha + \beta + \lambda) (B'[r] \psi'[r] + 2 \delta''[r]))) + \\
& B[r]^3 (\psi[r] (4 (\beta + 2 \lambda) - 6 r^2 (8 \alpha + 7 (-\alpha + \beta) + 7 \lambda) f[r] A'[r]^2) + r (2 (-\alpha + \beta + 3 \lambda) \psi'[r] + r (-\alpha + \beta + \lambda) \psi''[r])) + \\
& 2 A[r]^8 f[r] (12 r \alpha B[r]^5 f[r] \psi[r] + 6 r^3 (6 \alpha + 7 (-\alpha + \beta) + 7 \lambda) f[r]^2 \delta[r] B'[r]^2 + \\
& 8 B[r]^4 (-2 r (\beta + 3 \lambda) \chi[r] f'[r] + f[r] (r \alpha \delta[r] + (8 \alpha + 8 (-\alpha + \beta) + 6 \lambda) \chi[r] - r (4 \alpha + 4 (-\alpha + \beta) + 5 \lambda) \chi'[r])) - 2 r^2 B[r] f[r] (6 r (5 \alpha + 7 (-\alpha + \beta) + 7 \lambda) \\
& \delta[r] B'[r] f'[r] + f[r] (3 r (6 \alpha + 7 (-\alpha + \beta) + 7 \lambda) B'[r] \delta'[r] + \delta[r] (2 (6 \alpha + 7 (-\alpha + \beta) + 15 \lambda) B'[r] + r (6 \alpha + 7 (-\alpha + \beta) + 7 \lambda) B''[r]))) + \\
& r B[r]^2 (24 r^2 (-\alpha + \beta + \lambda) f[r]^3 \delta[r] A'[r]^2 + 2 r^2 (8 \alpha + 15 (-\alpha + \beta) + 15 \lambda) \delta[r] f'[r]^2 + 2 f[r] (12 \lambda \Sigma[r] B'[r] + r (r f'[r] \\
& (- (3 \alpha + 5 (-\alpha + \beta) + 5 \lambda) \psi[r] B'[r] + (20 \alpha + 27 (-\alpha + \beta) + 27 \lambda) \delta'[r]) + \delta[r] (2 (10 \alpha + 15 (-\alpha + \beta) + 21 \lambda) f'[r] + 5 r (2 \alpha + 3 (-\alpha + \beta) + 3 \lambda) f''[r]))) + \\
& f[r]^2 (-8 (2 \alpha + 2 (-\alpha + \beta) + \lambda) \delta[r] + r (4 (6 \alpha + 7 (-\alpha + \beta) + 9 \lambda) \delta'[r] + r (-2 \alpha + 7 (-\alpha + \beta) + 7 \lambda) B'[r] \psi'[r] + 2 (6 \alpha + 7 (-\alpha + \beta) + 7 \lambda) \delta''[r]))) + \\
& B[r]^3 (12 r^3 (-\alpha + \beta + \lambda) f[r]^3 \psi[r] A'[r]^2 + r f'[r] (-16 (\alpha + 2 (-\alpha + \beta) + 3 \lambda) \Sigma[r] + r^2 (8 \alpha + 15 (-\alpha + \beta) + 15 \lambda) \psi[r] f'[r]) + f[r] (16 (2 \alpha + 2 (-\alpha + \beta) + \lambda) \Sigma[r] + \\
& r (-24 \lambda \Sigma'[r] + r^2 (12 \alpha + 29 (-\alpha + \beta) + 29 \lambda) f'[r] \psi'[r] + 2 r \psi[r] (2 (3 \alpha + 5 (-\alpha + \beta) + 4 \lambda) f'[r] + r (3 \alpha + 5 (-\alpha + \beta) + 5 \lambda) f''[r]))) + \\
& r^2 f[r]^2 (2 (2 \alpha + 7 (-\alpha + \beta) + 5 \lambda) \psi[r] + r (2 \alpha + 7 (-\alpha + \beta) + 7 \lambda) \psi''[r])) + r A[r]^{12} f[r]^3 (6 r^2 (-\alpha + \beta + \lambda) f[r]^2 \delta[r] B'[r]^2 - \\
& 2 r B[r] f[r] (12 r (-\alpha + \beta + \lambda) \delta[r] B'[r] f'[r] + f[r] (3 r (-\alpha + \beta + \lambda) B'[r] \delta'[r] + \delta[r] (2 (-\alpha + \beta + 5 \lambda) B'[r] + r (-\alpha + \beta + \lambda) B''[r]))) + \\
& B[r]^2 (12 r^2 (-\alpha + \beta + \lambda) \delta[r] f'[r]^2 + 6 r (-\alpha + \beta + \lambda) f[r] (r f'[r] (-\psi[r] B'[r] + 2 \delta'[r]) + 2 \delta[r] (2 f'[r] + r f''[r])) - \\
& f[r]^2 (16 (\beta + \lambda) \delta[r] + r (8 \lambda \psi[r] B'[r] - (-\alpha + \beta + \lambda) (4 \delta'[r] - r B'[r] \psi'[r] + 2 r \delta''[r]))) + B[r]^3 \\
& (6 r^2 (-\alpha + \beta + \lambda) \psi[r] f'[r]^2 + 6 r (-\alpha + \beta + \lambda) f[r] (r f'[r] \psi'[r] + \psi[r] (2 f'[r] + r f''[r])) + f[r]^2 (-8 (\beta + \lambda) \psi[r] + r (-\alpha + \beta + \lambda) (2 \psi'[r] + r \psi''[r]))) - \\
& 2 A[r]^6 (-4 r (5 \alpha + 2 (-\alpha + \beta)) B[r]^5 f[r] \psi[r] - 6 r^3 (6 \alpha + 5 (-\alpha + \beta) + 5 \lambda) f[r]^2 \delta[r] B'[r]^2 + \\
& 8 B[r]^4 (r (\alpha + \beta + \lambda) \chi[r] f'[r] + f[r] (r (-4 + 3 \alpha + 2 (-\alpha + \beta)) \delta[r] - 6 (\beta + \lambda) \chi[r] + r (4 + 3 \lambda) \chi'[r])) + 2 r^2 B[r] f[r] \\
& (12 r (\beta + \lambda) \delta[r] B'[r] f'[r] + f[r] (3 r (6 \alpha + 5 (-\alpha + \beta) + 5 \lambda) B'[r] \delta'[r] + \delta[r] (2 (6 \alpha + 5 (-\alpha + \beta) + 7 \lambda) B'[r] + r (6 \alpha + 5 (-\alpha + \beta) + 5 \lambda) B''[r]))) + r \\
& B[r]^2 f[r] (4 r^2 (3 \alpha + \beta + \lambda) f[r]^2 \delta[r] A'[r]^2 - \\
& 2 (-4 (8 + 5 \lambda) \Sigma[r] B'[r] + r (r f'[r] ((7 \alpha + 6 (-\alpha + \beta) + 6 \lambda) \psi[r] B'[r] + (10 \alpha + 9 (-\alpha + \beta) + 9 \lambda) \delta'[r]) + (2 \alpha + 3 (-\alpha + \beta) + 3 \lambda) \delta[r] (2 f'[r] + r f''[r]))) + \\
& f[r] (8 (\beta + \lambda) \delta[r] - r (8 \lambda \psi[r] B'[r] + 4 (6 \alpha + 5 (-\alpha + \beta) + 5 \lambda) \delta'[r] + r ((18 \alpha + 13 (-\alpha + \beta) + 13 \lambda) B'[r] \psi'[r] + 2 (6 \alpha + 5 (-\alpha + \beta) + 5 \lambda) \delta''[r]))) + \\
& B[r]^3 (2 r^3 (4 \alpha + 3 (-\alpha + \beta) + 3 \lambda) f[r]^3 \psi[r] A'[r]^2 + 4 r f'[r] (-2 (4 \alpha + \beta + 3 \lambda) \Sigma[r] + r^2 (3 \alpha + 2 (-\alpha + \beta) + 2 \lambda) \psi[r] f'[r]) + \\
& f[r] (16 (-4 + 3 \alpha + 3 (-\alpha + \beta) + \lambda) \Sigma[r] + r (-8 (8 + 5 \lambda) \Sigma'[r] + r^2 (46 \alpha + 33 (-\alpha + \beta) + 33 \lambda) f'[r] \psi'[r] + 2 r \psi[r] \\
& (2 (7 \alpha + 6 (-\alpha + \beta) + 7 \lambda) f'[r] + r (7 \alpha + 6 (-\alpha + \beta) + 6 \lambda) f''[r]))) + r f[r]^2 (-4 \beta \psi[r] + r (18 \alpha + 13 (-\alpha + \beta) + 13 \lambda) (2 \psi'[r] + r \psi''[r]))) + \\
& A[r]^{10} f[r]^2 (-8 r (\alpha + 2 (-\alpha + \beta)) B[r]^5 f[r] \psi[r] + 6 r^3 (4 \alpha + 7 (-\alpha + \beta) + 7 \lambda) f[r]^2 \delta[r] B'[r]^2 - 16 B[r]^4 \\
& (r (-\alpha + \beta + \lambda) \chi[r] f'[r] + f[r] (r (\alpha + 2 (-\alpha + \beta)) \delta[r] - 2 (\beta + \lambda) \chi[r] + r \lambda \chi'[r])) - 2 r^2 B[r] f[r] (32 r (\alpha + 2 (-\alpha + \beta) + 2 \lambda) \delta[r] B'[r] f'[r] + \\
& f[r] (3 r (4 \alpha + 7 (-\alpha + \beta) + 7 \lambda) B'[r] \delta'[r] + \delta[r] (2 (4 \alpha + 7 (-\alpha + \beta) + 21 \lambda) B'[r] + r (4 \alpha + 7 (-\alpha + \beta) + 7 \lambda) B''[r]))) + \\
& r B[r]^2 (12 r^2 (-\alpha + \beta + \lambda) f[r]^3 \delta[r] A'[r]^2 + 8 r^2 (4 \alpha + 9 (-\alpha + \beta) + 9 \lambda) \delta[r] f'[r]^2 + 4 f[r] (4 \lambda \Sigma[r] B'[r] + r (r f'[r] (-3 (\alpha + 2 (-\alpha + \beta) + 2 \lambda) \psi[r] B'[r] + \\
& (10 \alpha + 19 (-\alpha + \beta) + 19 \lambda) \delta'[r]) + \delta[r] (2 (6 \alpha + 13 (-\alpha + \beta) + 17 \lambda) f'[r] + r (6 \alpha + 13 (-\alpha + \beta) + 13 \lambda) f''[r]))) - f[r]^2 (8 (5 \alpha + 5 (-\alpha + \beta) + 4 \lambda) \\
& \delta[r] + r (16 \lambda \psi[r] B'[r] - 4 (4 \alpha + 7 (-\alpha + \beta) + 9 \lambda) \delta'[r] + r ((4 \alpha + 9 (-\alpha + \beta) + 9 \lambda) B'[r] \psi'[r] - 2 (4 \alpha + 7 (-\alpha + \beta) + 7 \lambda) \delta''[r]))) + \\
& B[r]^3 (6 r^3 (-\alpha + \beta + \lambda) f[r]^3 \psi[r] A'[r]^2 + 4 r f'[r] (-4 (-\alpha + \beta + \lambda) \Sigma[r] + r^2 (4 \alpha + 9 (-\alpha + \beta) + 9 \lambda) \psi[r] f'[r]) + \\
& 2 f[r] (16 (\beta + \lambda) \Sigma[r] + r (-8 \lambda \Sigma'[r] + r^2 (10 \alpha + 21 (-\alpha + \beta) + 21 \lambda) f'[r] \psi'[r] + 2 r \psi[r] (2 (3 \alpha + 6 (-\alpha + \beta) + 7 \lambda) f'[r] + 3 r (\alpha + 2 (-\alpha + \beta) + 2 \lambda) f''[r]))) + \\
& r f[r]^2 (-4 (3 \alpha + 3 (-\alpha + \beta) + 2 \lambda) \psi[r] + r (2 (4 \alpha + 9 (-\alpha + \beta) + 7 \lambda) \psi'[r] + r (4 \alpha + 9 (-\alpha + \beta) + 9 \lambda) \psi''[r]))) + \\
& A[r]^4 (8 r \alpha B[r]^5 \psi[r] + 6 r^3 (3 \alpha + \beta + \lambda) f[r] \delta[r] B'[r]^2 - 16 B[r]^4 (r \alpha \delta[r] - \lambda (2 \chi[r] + r \chi'[r])) - \\
& 2 r^2 B[r] (-4 r (\alpha + 2 (-\alpha + \beta) + 2 \lambda) \delta[r] B'[r] f'[r] + f[r] (3 r (3 \alpha + \beta + \lambda) B'[r] \delta'[r] + \delta[r] (2 (3 \alpha + \beta - 3 \lambda) B'[r] + r (3 \alpha + \beta + \lambda) B''[r]))) + \\
& r B[r]^2 (16 r^2 (4 \alpha + 3 (-\alpha + \beta) + 3 \lambda) f[r]^2 \delta[r] A'[r]^2 - \\
& 2 (-8 \lambda \Sigma[r] B'[r] + r (r f'[r] ((2 \alpha + 3 (-\alpha + \beta) + 3 \lambda) \psi[r] B'[r] + 4 (-\alpha + \beta + \lambda) \delta'[r]) + 4 \delta[r] (2 (\beta + 2 \lambda) f'[r] + r (\beta + \lambda) f''[r]))) + \\
& f[r] (-16 (\beta + 2 \lambda) \delta[r] + r (8 \lambda \psi[r] B'[r] + 4 (3 \alpha + \beta - 3 \lambda) \delta'[r] + r ((5 \alpha - \beta - \lambda) B'[r] \psi'[r] + 2 (3 \alpha + \beta + \lambda) \delta''[r]))) + \\
& B[r]^3 (-32 \lambda \Sigma[r] + r (-8 r^2 (4 \alpha + 3 (-\alpha + \beta) + 3 \lambda) f[r]^2 \psi[r] A'[r]^2 + 2 (4 (-2 \lambda \Sigma'[r] + r^2 (-\alpha + \beta + \lambda) f'[r] \psi'[r]) + r \psi[r] \\
& (2 (2 \alpha + 3 (-\alpha + \beta) + 5 \lambda) f'[r] + r (2 \alpha + 3 (-\alpha + \beta) + 3 \lambda) f''[r])) + f[r] (8 (\beta + \lambda) \psi[r] + r (-2 (5 \alpha - \beta - 5 \lambda) \psi'[r] + r (-5 \alpha + \beta + \lambda) \psi''[r])))
\end{aligned}$$

$$\begin{aligned}
S_2 = & \frac{1}{32r^3B[x]^4} \left(-32rB[x]^2 (-2B[x]^3\psi[x] - 2(\Sigma[x]B'[x] + f[x](\delta[x] + r\psi[x]B'[x]) + r\delta[x]f'[x]) + \right. \\
& B[x]^2(4\delta[x] - 2\chi'[x]) + B[x](2(r\psi[x]f'[x] + \Sigma'[x]) + f[x](\psi[x] + r\psi'[x])) + 8rB[x]f[x](\delta[x] - B[x]\psi[x]) \\
& \left. \left(8rB'[x] - \frac{1}{A[x]^2} (2r^2(4\alpha+3(-\alpha+\beta)+3\lambda)B[x]A'[x]^2 + 2A[x]^2(B[x](-3(\beta+\lambda) + r^2(\alpha+\beta+\lambda)f[x]A'[x]^2) - 3r\lambda B'[x]) + r(4\alpha+3(-\alpha+\beta)+3\lambda) \right. \right. \\
& A[x](rA'[x]B'[x] - B[x](2A'[x] + rA''[x])) - r(-\alpha+\beta+\lambda)A[x]^5f[x](-rf[x]A'[x]B'[x] + B[x](2rA'[x]f'[x] + f[x](2A'[x] + rA''[x]))) - \\
& 2rA[x]^3(-2r(\beta+\lambda)f[x]A'[x]B'[x] + B[x](r(2\alpha+3(-\alpha+\beta)+3\lambda)A'[x]f'[x] + 2(\beta+\lambda)f[x](2A'[x] + rA''[x]))) + \\
& A[x]^6(2rf[x]B'[x](\lambda f[x] + r(\beta+\lambda)f'[x]) + B[x](2(\beta+\lambda)f[x] - r(-\alpha+\beta+\lambda)(2f'[x] + rf''[x]))) \left. \right) + \\
& A[x]^4(rB'[x](4\lambda f[x] + r(2\alpha+3(-\alpha+\beta)+3\lambda)f'[x]) + B[x](4(\beta+\lambda)f[x] - r(2\alpha+3(-\alpha+\beta)+3\lambda)(2f'[x] + rf''[x]))) \left. \right) + \\
& 4rB[x](-2\delta[x] + B[x]\psi[x]) \left(8B[x](-B[x]^2 + f[x] + rf'[x]) - \frac{1}{A[x]^4} (3r^2(-\alpha+\beta+\lambda)B[x]A'[x]^2 + \right. \\
& 2A[x]^2(B[x](\lambda + r^2(4\alpha+3(-\alpha+\beta)+3\lambda)f[x]A'[x]^2) - r\lambda B'[x]) + r(4\alpha+3(-\alpha+\beta)+3\lambda)A[x]^3f[x](rA'[x]B'[x] - B[x](2A'[x] + rA''[x]))) + \\
& rA[x](r(-\alpha+\beta+\lambda)A'[x]B'[x] - B[x](2(-\alpha+\beta+3\lambda)A'[x] + r(-\alpha+\beta+\lambda)A''[x])) - \\
& r(-\alpha+\beta+\lambda)A[x]^7f[x]^2(-rf[x]A'[x]B'[x] + B[x](2rA'[x]f'[x] + f[x](2A'[x] + rA''[x]))) - rA[x]^5f[x] \\
& (-r(4\alpha+3(-\alpha+\beta)+3\lambda)f[x]A'[x]B'[x] + B[x](2r(\alpha+\beta+\lambda)A'[x]f'[x] + f[x](2(4\alpha+3(-\alpha+\beta)+\lambda)A'[x] + r(4\alpha+3(-\alpha+\beta)+3\lambda)A''[x]))) + \\
& A[x]^8f[x]^2(rB'[x](2\lambda f[x] + r(-\alpha+\beta+\lambda)f'[x]) + B[x](2(\beta+\lambda)f[x] - r(-\alpha+\beta+\lambda)(2f'[x] + rf''[x]))) + \\
& A[x]^6(2rf[x]B'[x](\lambda f[x] + r(\beta+\lambda)f'[x]) + B[x](4(\alpha+4(-\alpha+\beta)+6\lambda)f[x]^2 + r^2(-\alpha+\beta+\lambda)f'[x]^2 - 2rf[x](2\beta f'[x] + r(\beta+\lambda)f''[x]))) + \\
& A[x]^4(rB'[x](-2\lambda f[x] + r(\alpha+\beta+\lambda)f'[x]) + \\
& B[x](-2(3\alpha+3(-\alpha+\beta)+5\lambda)f[x] + r^2(4\alpha+3(-\alpha+\beta)+3\lambda)f[x]^2A'[x]^2 - r(2(\alpha+\beta+3\lambda)f'[x] + r(\alpha+\beta+\lambda)f''[x]))) \left. \right) - \\
& \frac{1}{A[x]^4} (-2r^3(20\alpha+21(-\alpha+\beta)+21\lambda)B[x]^2(-2\delta[x] + B[x]\psi[x])A'[x]^2 + 2r^2A[x]B[x](4r(8\alpha+7(-\alpha+\beta)+7\lambda)\delta[x]A'[x]B'[x] - \\
& B[x](rA'[x](4(\alpha+5(-\alpha+\beta)+5\lambda)\psi[x]B'[x] + 6(4\alpha+3(-\alpha+\beta)+3\lambda)\delta'[x]) + 2\delta[x](2(4\alpha+5(-\alpha+\beta)+9\lambda)A'[x] + r(4\alpha+5(-\alpha+\beta)+5\lambda)A''[x])) + \\
& B[x]^2(3r(4\alpha+3(-\alpha+\beta)+3\lambda)A'[x]\psi'[x] + \psi[x](2(4\alpha+5(-\alpha+\beta)+9\lambda)A'[x] + r(4\alpha+5(-\alpha+\beta)+5\lambda)A''[x]))) + \\
& 6r^2(-\alpha+\beta+\lambda)A[x]^9B[x]f[x]^3(-4rf[x]\delta[x]A'[x]B'[x] + B[x]^2(4r\psi[x]A'[x]f'[x] + f[x](2\psi[x]A'[x] + rA'[x]\psi'[x] + r\psi[x]A''[x]))) + \\
& B[x](8r\delta[x]A'[x]f'[x] + f[x](rA'[x](-\psi[x]B'[x] + 2\delta'[x]) + 2\delta[x](2A'[x] + rA''[x]))) + 4r(4\alpha+3(-\alpha+\beta)+3\lambda)A[x]^3B[x] \\
& (4B[x]^3\chi[x]A'[x] + 6r^2f[x]\delta[x]A'[x]B'[x] - rB[x](2r\delta[x]A'[x]f'[x] + f[x](rA'[x](-\psi[x]B'[x] + 4\delta'[x]) + 2\delta[x](2A'[x] + rA''[x]))) + \\
& B[x]^2(-4\Sigma[x]A'[x] + r(r\psi[x]A'[x]f'[x] + f[x](2rA'[x]\psi'[x] - \psi[x](2A'[x] + rA''[x]))) + \\
& 4rA[x]^7B[x]f[x]^2(-4(-\alpha+\beta+\lambda)B[x]^3\chi[x]A'[x] - 2r^2(8\alpha+11(-\alpha+\beta)+11\lambda)f[x]\delta[x]A'[x]B'[x] + \\
& rB[x](2r(2\alpha+19(-\alpha+\beta)+19\lambda)\delta[x]A'[x]f'[x] + f[x](-rA'[x](4\alpha+3(-\alpha+\beta)+3\lambda)\psi[x]B'[x] - 4(2\alpha+3(-\alpha+\beta)+3\lambda)\delta'[x]) + \\
& 2(4\alpha+5(-\alpha+\beta)+5\lambda)\delta[x](2A'[x] + rA''[x]))) + B[x]^2(-4(-\alpha+\beta+\lambda)\Sigma[x]A'[x] + \\
& r(3r(4\alpha+5(-\alpha+\beta)+5\lambda)\psi[x]A'[x]f'[x] + f[x](2r(2\alpha+3(-\alpha+\beta)+3\lambda)A'[x]\psi'[x] + (4\alpha+3(-\alpha+\beta)+3\lambda)\psi[x](2A'[x] + rA''[x]))) + \\
& 8rA[x]^5B[x]f[x](-4(\alpha-\beta+\lambda)B[x]^3\chi[x]A'[x] + 2r^2(-2\alpha-3(-\alpha+\beta)-3\lambda)f[x]\delta[x]A'[x]B'[x] + \\
& rB[x](2r(2\alpha+5(-\alpha+\beta)+5\lambda)\delta[x]A'[x]f'[x] + f[x](rA'[x](\alpha+2(-\alpha+\beta)+2\lambda)\psi[x]B'[x] + (2\alpha+3(-\alpha+\beta)+3\lambda)\delta'[x]) + \\
& \delta[x](2(2\alpha+3(-\alpha+\beta)+5\lambda)A'[x] + r(2\alpha+3(-\alpha+\beta)+3\lambda)A''[x]))) - B[x]^2(8(\beta+\lambda)\Sigma[x]A'[x] + \\
& r(2r(-2\alpha+\beta+\lambda)\psi[x]A'[x]f'[x] + f[x](-3r(\beta+\lambda)A'[x]\psi'[x] + \psi[x](2(\alpha+2(-\alpha+\beta)+3\lambda)A'[x] + r(\alpha+2(-\alpha+\beta)+2\lambda)A''[x]))) + rA[x]^2 \\
& (6r^2(4\alpha+3(-\alpha+\beta)+3\lambda)\delta[x]B'[x]^2 - 2rB[x](3r(4\alpha+3(-\alpha+\beta)+3\lambda)B'[x]\delta'[x] + \delta[x](2(4\alpha+3(-\alpha+\beta)+7\lambda)B'[x] + r(4\alpha+3(-\alpha+\beta)+3\lambda)B''[x])) + \\
& B[x]^2(8\delta[x](2\lambda+3r^2(4\alpha+3(-\alpha+\beta)+3\lambda)f[x]A'[x]^2) + r(8\lambda\psi[x]B'[x] + (4\alpha+3(-\alpha+\beta)+3\lambda)(4\delta'[x] + rB'[x]\psi'[x] + 2r\delta''[x]))) + \\
& B[x]^3(4\psi[x](-2\lambda+r^2(4\alpha+3(-\alpha+\beta)+3\lambda)f[x]A'[x]^2) - r(4\alpha+3(-\alpha+\beta)+3\lambda)(2\psi'[x] + r\psi''[x]))) + \\
& 2A[x]^8f[x](-4r(\alpha+2(-\alpha+\beta))B[x]^5f[x]\psi[x] + 6r^3(2\alpha+3(-\alpha+\beta)+3\lambda)f[x]^2\delta[x]B'[x]^2 - \\
& 8B[x]^4(r(-\alpha+\beta+\lambda)\chi[x]f'[x] + f[x](r(\alpha+2(-\alpha+\beta))\delta[x] - 2(\beta+\lambda)\chi[x] + r\lambda\chi'[x])) - 2r^2B[x]f[x](r(16\alpha+25(-\alpha+\beta)+25\lambda)\delta[x]B'[x]f'[x] + \\
& f[x](3r(2\alpha+3(-\alpha+\beta)+3\lambda)B'[x]\delta'[x] + \delta[x](2(2\alpha+3(-\alpha+\beta)+7\lambda)B'[x] + r(2\alpha+3(-\alpha+\beta)+3\lambda)B''[x]))) + \\
& rB[x]^2(6r^2(-\alpha+\beta+\lambda)f[x]^3\delta[x]A'[x]^2 + 8r^2(2\alpha+3(-\alpha+\beta)+3\lambda)\delta[x]f'[x]^2 + \\
& f[x](8\lambda\Sigma[x]B'[x] + r(rf'[x]((-6\alpha-7(-\alpha+\beta)-7\lambda)\psi[x]B'[x] + 10(2\alpha+3(-\alpha+\beta)+3\lambda)\delta'[x]) + 4(3\alpha+5(-\alpha+\beta)+5\lambda)\delta[x](2f'[x] + rf''[x]))) - \\
& 2f[x]^2(8(\beta+\lambda)\delta[x] + r(-2(2\alpha+3(-\alpha+\beta)+3\lambda)\delta'[x] + r(\alpha+2(-\alpha+\beta)+2\lambda)B'[x]\psi'[x] + (-2\alpha-3(-\alpha+\beta)-3\lambda)\delta''[x]))) + \\
& B[x]^3(3r^3(-\alpha+\beta+\lambda)f[x]^3\psi[x]A'[x]^2 + 4rf'[x](-2(-\alpha+\beta+\lambda)\Sigma[x] + r^2(2\alpha+3(-\alpha+\beta)+3\lambda)\psi[x]f'[x]) + \\
& f[x](16(\beta+\lambda)\Sigma[x] + r(-8\lambda\Sigma'[x] + r^2(10\alpha+17(-\alpha+\beta)+17\lambda)f'[x]\psi'[x] + r\psi[x](2(6\alpha+7(-\alpha+\beta)+5\lambda)f'[x] + r(6\alpha+7(-\alpha+\beta)+7\lambda)f''[x])) + \\
& 2r^2f[x]^2(2(\alpha+2(-\alpha+\beta)+\lambda)\psi'[x] + r(\alpha+2(-\alpha+\beta)+2\lambda)\psi''[x])) + rA[x]^{10}f[x]^2(6r^2(-\alpha+\beta+\lambda)f[x]^2\delta[x]B'[x]^2 - \\
& 2rB[x]f[x](12r(-\alpha+\beta+\lambda)\delta[x]B'[x]f'[x] + f[x](3r(-\alpha+\beta+\lambda)B'[x]\delta'[x] + \delta[x](2(-\alpha+\beta+5\lambda)B'[x] + r(-\alpha+\beta+\lambda)B''[x]))) + \\
& B[x]^2(12r^2(-\alpha+\beta+\lambda)\delta[x]f'[x]^2 + 6r(-\alpha+\beta+\lambda)f[x](rf'[x](-\psi[x]B'[x] + 2\delta'[x]) + 2\delta[x](2f'[x] + rf''[x])) - \\
& f[x]^2(16(\beta+\lambda)\delta[x] + r(8\lambda\psi[x]B'[x] - (\alpha+\beta+\lambda)(4\delta'[x] - rB'[x]\psi'[x] + 2r\delta''[x]))) + B[x]^3 \\
& (6r^2(-\alpha+\beta+\lambda)\psi[x]f'[x]^2 + 6r(-\alpha+\beta+\lambda)f[x](rf'[x]\psi'[x] + \psi[x](2f'[x] + rf''[x])) + f[x]^2(-8(\beta+\lambda)\psi[x] + r(-\alpha+\beta+\lambda)(2\psi'[x] + r\psi''[x]))) + \\
& 2A[x]^6(8r\alpha B[x]^5f[x]\psi[x] + 36r^3(\beta+\lambda)f[x]^2\delta[x]B'[x]^2 + 8B[x]^4(-r(\alpha+\beta+3\lambda)\chi[x]f'[x] + 4(\beta+\lambda)f[x](2\chi[x] - r\chi'[x])) - \\
& 4r^2B[x]f[x](2r(7\alpha+8(-\alpha+\beta)+8\lambda)\delta[x]B'[x]f'[x] + f[x](9r(\beta+\lambda)B'[x]\delta'[x] + \delta[x](2(3\alpha+3(-\alpha+\beta)+5\lambda)B'[x] + 3r(\beta+\lambda)B''[x]))) + \\
& rB[x]^2(12r^2(-\alpha+\beta+\lambda)f[x]^3\delta[x]A'[x]^2 + 2r^2(8\alpha+11(-\alpha+\beta)+11\lambda)\delta[x]f'[x]^2 + f[x](16\lambda\Sigma[x]B'[x] + \\
& r(rf'[x](3(-\alpha+\beta+\lambda)\psi[x]B'[x] + 2(20\alpha+21(-\alpha+\beta)+21\lambda)\delta'[x]) + 2\delta[x](2(8\alpha+11(-\alpha+\beta)+15\lambda)f'[x] + r(8\alpha+11(-\alpha+\beta)+11\lambda)f''[x]))) + \\
& f[x]^2(-8\beta\delta[x] + r(16\lambda\psi[x]B'[x] + 24(\beta+\lambda)\delta'[x] + r(-2\alpha+5(-\alpha+\beta)+5\lambda)B'[x]\psi'[x] + 12(\beta+\lambda)\delta''[x]))) + \\
& B[x]^3(6r^3(-\alpha+\beta+\lambda)f[x]^3\psi[x]A'[x]^2 + rf'[x](-8(2\alpha+3(-\alpha+\beta)+3\lambda)\Sigma[x] + r^2(8\alpha+7(-\alpha+\beta)+7\lambda)\psi[x]f'[x]) + \\
& f[x](32(\beta+\lambda)\Sigma[x] + r(-16\lambda\Sigma'[x] + r^2(12\alpha+19(-\alpha+\beta)+19\lambda)f'[x]\psi'[x] - r\psi[x](6(-\alpha+\beta)+22\lambda)f'[x] + 3r(-\alpha+\beta+\lambda)f''[x]))) + \\
& rf[x]^2(4(3\alpha+3(-\alpha+\beta)+2\lambda)\psi[x] + r(2(2\alpha+5(-\alpha+\beta)+\lambda)\psi'[x] + r(2\alpha+5(-\alpha+\beta)+5\lambda)\psi''[x]))) + \\
& 2A[x]^4(4r(3\alpha+2(-\alpha+\beta))B[x]^5\psi[x] + 6r^3(6\alpha+5(-\alpha+\beta)+5\lambda)f[x]\delta[x]B'[x]^2 - 8B[x]^4(r(3\alpha+2(-\alpha+\beta))\delta[x] - 6(\beta+\lambda)\chi[x] + 3r\lambda\chi'[x]) - \\
& 2r^2B[x](r(12\alpha+13(-\alpha+\beta)+13\lambda)\delta[x]B'[x]f'[x] + \\
& f[x](3r(6\alpha+5(-\alpha+\beta)+5\lambda)B'[x]\delta'[x] + \delta[x](2(6\alpha+5(-\alpha+\beta)+9\lambda)B'[x] + r(6\alpha+5(-\alpha+\beta)+5\lambda)B''[x]))) + \\
& rB[x]^2(-8r^2\alpha f[x]^2\delta[x]A'[x]^2 - 24\lambda\Sigma[x]B'[x] + r(rf'[x](6\alpha+7(-\alpha+\beta)+7\lambda)\psi[x]B'[x] + 2(10\alpha+9(-\alpha+\beta)+9\lambda)\delta'[x]) +
\end{aligned}$$

$$\begin{aligned}
S_5 = & \frac{1}{64 r^3 B[x]^5} \\
& \left(-64 B[x]^2 (-r B[x]^3 f[x] \psi[x] - r f[x] \delta[x] (f[x] + r f'[x]) + r B[x]^2 f[x] (2 \delta[x] - \chi'[x]) + B[x] (-r \Sigma[x] f'[x] + f[x] (-2 \Sigma[x] + r^2 \psi[x] f'[x]) + r^2 f[x]^2 \psi'[x])) + \right. \\
& 4 r B[x] (-2 \delta[x] + B[x] \psi[x]) \left(16 B[x] f[x] (-B[x]^2 + f[x] + r f'[x]) - \frac{1}{A[x]^6} \right. \\
& (-2 r^2 (-\alpha + \beta + \lambda) B[x] A'[x]^2 + 2 A[x]^2 (B[x] (\beta + \lambda - 2 r^2 \alpha f[x] A'[x]^2) + r \lambda B'[x]) + 2 r^2 (4 \alpha + 3 (-\alpha + \beta) + 3 \lambda) A[x]^5 B[x] f[x] A'[x] f'[x] + r (-\alpha + \beta + \lambda) \\
& A[x] (-r A'[x] B'[x] + B[x] (2 A'[x] + r A''[x])) - r (-\alpha + \beta + \lambda) A[x]^9 f[x]^3 (-r f[x] A'[x] B'[x] + B[x] (2 r A'[x] f'[x] + f[x] (2 A'[x] + r A''[x]))) - \\
& 2 r A[x]^7 f[x]^2 (-r (\alpha + \beta + \lambda) f[x] A'[x] B'[x] + B[x] (r (3 \alpha - \beta - \lambda) A'[x] f'[x] + f[x] (2 (\alpha + \beta - \lambda) A'[x] + r (\alpha + \beta + \lambda) A''[x]))) + \\
& 2 r A[x]^3 (-r (\alpha + \beta + \lambda) f[x] A'[x] B'[x] + B[x] (r (\alpha + \beta + \lambda) A'[x] f'[x] + f[x] (2 (\alpha + \beta - \lambda) A'[x] + r (\alpha + \beta + \lambda) A''[x]))) + \\
& A[x]^{10} f[x]^3 (r B'[x] (2 \lambda f[x] + r (-\alpha + \beta + \lambda) f'[x]) + B[x] (2 (\beta + \lambda) f[x] - r (-\alpha + \beta + \lambda) (2 f'[x] + r f''[x]))) + \\
& A[x]^4 (-r^2 (\alpha + \beta + \lambda) B'[x] f'[x] + B[x] (4 (\beta + 2 \lambda) f[x] + 2 r^2 (4 \alpha + 3 (-\alpha + \beta) + 3 \lambda) f[x]^2 A'[x]^2 + r (\alpha + \beta + \lambda) (2 f'[x] + r f''[x]))) + A[x]^6 f[x] \\
& (-r B'[x] (4 \lambda f[x] + r (-\alpha + \beta + \lambda) f'[x]) + B[x] (-4 (3 \alpha + 3 (-\alpha + \beta) + 5 \lambda) f[x] + 4 r^2 (\beta + \lambda) f[x]^2 A'[x]^2 + r (-2 (\alpha - \beta + 3 \lambda) f'[x] + r (-\alpha + \beta + \lambda) f''[x]))) + \\
& A[x]^8 f[x] (r^2 (\alpha + \beta + \lambda) f[x] B'[x] f'[x] + B[x] (4 (\beta + 2 \lambda) f[x]^2 + 2 r^2 (-\alpha + \beta + \lambda) f'[x]^2 - r f[x] (2 (\alpha + \beta - 3 \lambda) f'[x] + r (\alpha + \beta + \lambda) f''[x]))) \left. \right) + \\
& 8 r B[x] f[x] (\delta[x] - B[x] \psi[x]) \left(8 B[x] (-B[x]^2 + f[x] + r f'[x]) - \frac{1}{A[x]^4} (3 r^2 (-\alpha + \beta + \lambda) B[x] A'[x]^2 + \right. \\
& 2 A[x]^2 (B[x] (\lambda + r^2 (4 \alpha + 3 (-\alpha + \beta) + 3 \lambda) f[x] A'[x]^2) - r \lambda B'[x]) + r (4 \alpha + 3 (-\alpha + \beta) + 3 \lambda) A[x]^3 f[x] (r A'[x] B'[x] - B[x] (2 A'[x] + r A''[x])) + \\
& r A[x] (r (-\alpha + \beta + \lambda) A'[x] B'[x] - B[x] (2 (-\alpha + \beta + 3 \lambda) A'[x] + r (-\alpha + \beta + \lambda) A''[x])) - \\
& r (-\alpha + \beta + \lambda) A[x]^7 f[x]^2 (-r f[x] A'[x] B'[x] + B[x] (2 r A'[x] f'[x] + f[x] (2 A'[x] + r A''[x]))) - r A[x]^5 f[x] \\
& (-r (4 \alpha + 3 (-\alpha + \beta) + 3 \lambda) f[x] A'[x] B'[x] + B[x] (2 r (\alpha + \beta + \lambda) A'[x] f'[x] + f[x] (2 (4 \alpha + 3 (-\alpha + \beta) + \lambda) A'[x] + r (4 \alpha + 3 (-\alpha + \beta) + 3 \lambda) A''[x]))) + \\
& A[x]^8 f[x]^2 (r B'[x] (2 \lambda f[x] + r (-\alpha + \beta + \lambda) f'[x]) + B[x] (2 (\beta + \lambda) f[x] - r (-\alpha + \beta + \lambda) (2 f'[x] + r f''[x]))) + \\
& A[x]^6 (2 r f[x] B'[x] (\lambda f[x] + r (\beta + \lambda) f'[x]) + B[x] ((4 \alpha + 4 (-\alpha + \beta) + 6 \lambda) f[x]^2 + r^2 (-\alpha + \beta + \lambda) f'[x]^2 - 2 r f[x] (2 \beta f'[x] + r (\beta + \lambda) f''[x]))) + \\
& A[x]^4 (r B'[x] (-2 \lambda f[x] + r (\alpha + \beta + \lambda) f'[x]) + \\
& B[x] (-2 (3 \alpha + 3 (-\alpha + \beta) + 5 \lambda) f[x] + r^2 (4 \alpha + 3 (-\alpha + \beta) + 3 \lambda) f[x]^2 A'[x]^2 - r (2 (\alpha + \beta + 3 \lambda) f'[x] + r (\alpha + \beta + \lambda) f''[x]))) \left. \right) - \\
& \frac{1}{A[x]^6} (-16 r^3 (-\alpha + \beta + \lambda) B[x]^2 (-2 \delta[x] + B[x] \psi[x]) A'[x]^2 + 2 r^2 A[x] B[x] (10 r (-\alpha + \beta + \lambda) \delta[x] A'[x] B'[x] - \\
& B[x] (r (-\alpha + \beta + \lambda) A'[x] (\psi[x] B'[x] + 8 \delta'[x]) + 2 \delta[x] (2 (-\alpha + \beta + 5 \lambda) A'[x] + r (-\alpha + \beta + \lambda) A''[x])) + \\
& B[x]^2 (4 r (-\alpha + \beta + \lambda) A'[x] \psi'[x] + \psi[x] (2 (-\alpha + \beta + 5 \lambda) A'[x] + r (-\alpha + \beta + \lambda) A''[x]))) + \\
& 6 r^2 (-\alpha + \beta + \lambda) A[x]^{11} B[x] f[x]^4 (-4 r f[x] \delta[x] A'[x] B'[x] + B[x]^2 (4 r \psi[x] A'[x] f'[x] + f[x] (2 \psi[x] A'[x] + r A'[x] \psi'[x] + r \psi[x] A''[x])) + \\
& B[x] (8 r \delta[x] A'[x] f'[x] + f[x] (r A'[x] (-\psi[x] B'[x] + 2 \delta'[x]) + 2 \delta[x] (2 A'[x] + r A''[x]))) + \\
& 4 r A[x]^5 B[x] f[x] (4 (8 \alpha + 5 (-\alpha + \beta) + 5 \lambda) B[x]^3 \chi[x] A'[x] + 4 r^2 (4 \alpha + 3 (-\alpha + \beta) + 3 \lambda) f[x] \delta[x] A'[x] B'[x] + r^2 (4 \alpha + 3 (-\alpha + \beta) + 3 \lambda)
\end{aligned}$$

$$\begin{aligned}
S7 = & -\frac{1}{32r^3 B[x]^5} \left(8rB[x]^2 (-2B[x]^3 f[x] \psi[x] - 2f[x] B'[x] (-2\Sigma[x] + r^2 (\psi[x] f'[x] + f[x] \psi'[x]))) + \right. \\
& B[x] (-4\Sigma[x] f'[x] + 3r^2 \psi[x] f'[x]^2 + f[x] (-4\Sigma'[x] + 7r^2 f'[x] \psi'[x] + 2r\psi[x] (f'[x] + rf''[x])) + 2rf[x]^2 (\psi'[x] + r\psi''[x])) - \\
& \left. \frac{1}{A[x]^6} (-32r\lambda A[x]^5 B[x]^4 f[x] \chi[x] A'[x] + 20r^3 \lambda B[x]^2 (-2\delta[x] + B[x] \psi[x]) A'[x]^2 - \right. \\
& B[x] (3r^3 (-\alpha + \beta + \lambda) B[x] (-2\delta[x] + B[x] \psi[x]) A'[x]^2 + 2rA[x]^5 f[x] A'[x] (-16\lambda B[x]^3 \chi[x] - 2r^2 (4\alpha + 3(-\alpha + \beta) + 3\lambda) f[x] \delta[x] B'[x] + \\
& r^2 (-\alpha + \beta + \lambda) B[x]^2 \psi[x] f'[x] + 2r^2 (4\alpha + 3(-\alpha + \beta) + 3\lambda) B[x] (\delta[x] f'[x] + f[x] \delta'[x])) + 2rA[x]^2 \\
& (2r\lambda \delta[x] B'[x] - 2B[x] (\delta[x] (\beta + 2\lambda + r^2 (4\alpha + 3(-\alpha + \beta) + 3\lambda) f[x] A'[x]^2) + r\lambda \delta'[x]) + B[x]^2 (\psi[x] (\beta + 2\lambda + 2r^2 (\alpha + \beta + \lambda) f[x] A'[x]^2) + r\lambda \psi'[x])) - \\
& r^2 A[x] A'[x] (2r(-\alpha + \beta + \lambda) \delta[x] B'[x] - 2B[x] (8\lambda \delta[x] + r(-\alpha + \beta + \lambda) \delta'[x]) + B[x]^2 (8\lambda \psi[x] + r(-\alpha + \beta + \lambda) \psi'[x])) + \\
& r^2 A[x]^9 f[x]^3 A'[x] (-2r(-\alpha + \beta + \lambda) f[x] \delta[x] B'[x] + 2B[x] (6r(-\alpha + \beta + \lambda) \delta[x] f'[x] + f[x] (8\lambda \delta[x] + r(-\alpha + \beta + \lambda) \delta'[x])) + \\
& B[x]^2 (6r(-\alpha + \beta + \lambda) \psi[x] + f[x] (8\lambda \psi[x] + r(-\alpha + \beta + \lambda) \psi'[x]))) + rA[x]^{10} f[x]^2 (-2rf[x] \delta[x] B'[x] + r(-\alpha + \beta + \lambda) f'[x]) + \\
& 2B[x] (3r^2 (-\alpha + \beta + \lambda) \delta[x] f'[x]^2 + 2f[x]^2 ((\beta + 2\lambda) \delta[x] + r\lambda \delta'[x]) + rf[x] f'[x] (8\lambda \delta[x] + r(-\alpha + \beta + \lambda) \delta'[x])) + \\
& B[x]^2 (3r^2 (-\alpha + \beta + \lambda) \psi[x] f'[x]^2 + 2f[x]^2 ((\beta + 2\lambda) \psi[x] + r\lambda \psi'[x]) + rf[x] f'[x] (8\lambda \psi[x] + r(-\alpha + \beta + \lambda) \psi'[x])) - \\
& 2rA[x]^3 A'[x] (8\lambda B[x]^3 \chi[x] + 4r^2 (\beta + \lambda) f[x] \delta[x] B'[x] - 4rB[x] (-r\alpha \delta[x] f'[x] + f[x] (2\lambda \delta[x] + r(\beta + \lambda) \delta'[x])) + \\
& B[x]^2 (-8\lambda \Sigma[x] + r^2 ((-3\alpha + \beta + \lambda) \psi[x] f'[x] + (2\alpha + 3(-\alpha + \beta) + 3\lambda) f[x] \psi'[x]))) + \\
& 2rA[x]^7 f[x]^2 A'[x] (-8\lambda B[x]^3 \chi[x] - 4r^2 (\beta + \lambda) f[x] \delta[x] B'[x] + 4rB[x] (3r(\beta + \lambda) \delta[x] f'[x] + f[x] (2\lambda \delta[x] + r(\beta + \lambda) \delta'[x])) + \\
& B[x]^2 (-8\lambda \Sigma[x] + r^2 ((6\alpha + 5(-\alpha + \beta) + 5\lambda) \psi[x] f'[x] + (2\alpha + 3(-\alpha + \beta) + 3\lambda) f[x] \psi'[x]))) - A[x]^4 (-16(\beta + 2\lambda) B[x]^3 \chi[x] + \\
& 2r^2 \delta[x] B'[x] (-4\lambda f[x] + r(\alpha + \beta + \lambda) f'[x]) - 2rB[x] ((\beta + 2\lambda) \delta[x] + r\lambda \delta'[x]) + rf[x] (-4\lambda \delta[x] + r(\alpha + \beta + \lambda) \delta'[x])) + \\
& B[x]^2 (16(\beta + 2\lambda) \Sigma[x] + r^2 (-2r(-\alpha + \beta + \lambda) f[x]^2 \psi[x] A'[x]^2 - 8\lambda f[x] \psi'[x] + f'[x] (-8\lambda \psi[x] + r(\alpha + \beta + \lambda) \psi'[x]))) + \\
& A[x]^8 f[x] (-16B[x]^3 \chi[x] ((\beta + 2\lambda) f[x] + r\lambda f'[x]) - 2r^2 f[x] \delta[x] B'[x] (4\lambda f[x] + r(2\alpha + 3(-\alpha + \beta) + 3\lambda) f'[x]) + \\
& 2rB[x] (3r^2 (-\alpha + \beta + \lambda) f[x]^3 \delta[x] A'[x]^2 + 2r^2 (2\alpha + 3(-\alpha + \beta) + 3\lambda) \delta[x] f'[x]^2 + 4f[x]^2 ((\beta + 2\lambda) \delta[x] + r\lambda \delta'[x]) + rf[x] f'[x] \\
& (12\lambda \delta[x] + r(2\alpha + 3(-\alpha + \beta) + 3\lambda) \delta'[x])) + B[x]^2 (3r^3 (-\alpha + \beta + \lambda) f[x]^3 \psi[x] A'[x]^2 + 2rf[x] (-8\lambda \Sigma[x] + r^2 (2\alpha + 3(-\alpha + \beta) + 3\lambda) \psi[x] f'[x]) + \\
& 8r^2 \lambda f[x]^2 \psi'[x] + f[x] (-16(\beta + 2\lambda) \Sigma[x] + r^2 f'[x] (8\lambda \psi[x] + r(2\alpha + 5(-\alpha + \beta) + 5\lambda) \psi'[x]))) + \\
& A[x]^6 (-16r\lambda B[x]^3 \chi[x] f'[x] - 2r^3 (4\alpha + 3(-\alpha + \beta) + 3\lambda) f[x] \delta[x] B'[x] f'[x] + 2r^3 (4\alpha + 3(-\alpha + \beta) + 3\lambda) B[x] (2f[x]^3 \delta[x] A'[x]^2 + \\
& \delta[x] f'[x]^2 + f[x] f'[x] \delta'[x]) + B[x]^2 (4r^3 (\alpha + \beta + \lambda) f[x]^3 \psi[x] A'[x]^2 - rf[x] (-16\lambda \Sigma[x] + r^2 (8\alpha + 5(-\alpha + \beta) + 5\lambda) \psi[x] f'[x]) - 4 \\
& rf[x]^2 ((\beta + 2\lambda) \psi[x] + 5r\lambda \psi'[x]) + f[x] (32(\beta + 2\lambda) \Sigma[x] - r^2 f'[x] (24\lambda \psi[x] + r(8\alpha + 5(-\alpha + \beta) + 5\lambda) \psi'[x]))) - \\
& 4r^2 A[x] B[x] (6r\lambda \delta[x] A'[x] B'[x] - B[x] (r\lambda A'[x] (\psi[x] B'[x] + 4\delta'[x]) + 2\delta[x] (2(\beta + 3\lambda) A'[x] + r\lambda A''[x]))) + \\
& B[x]^2 (2r\lambda A'[x] \psi[x] + \psi[x] (2(\beta + 3\lambda) A'[x] + r\lambda A''[x]))) + \\
& 4rA[x]^3 B[x] (-4(\beta + 3\lambda) B[x]^3 \chi[x] A'[x] - 6r^2 \lambda f[x] \delta[x] A'[x] B'[x] + B[x]^2 A'[x] (4(\beta + 3\lambda) \Sigma[x] - 3r^2 \lambda (\psi[x] f'[x] + f[x] \psi'[x])) + \\
& 2rB[x] (2r\lambda \delta[x] A'[x] f'[x] + f[x] (2r\lambda A'[x] \delta'[x] + \delta[x] (2(\beta + 3\lambda) A'[x] + r\lambda A''[x]))) + \\
& 4rA[x]^7 B[x] f[x]^2 (-4(\beta + 3\lambda) B[x]^3 \chi[x] A'[x] - 6r^2 \lambda f[x] \delta[x] A'[x] B'[x] + B[x]^2 A'[x] (-4(\beta + 3\lambda) \Sigma[x] + 3r^2 \lambda (\psi[x] f'[x] + f[x] \psi'[x])) + \\
& 2rB[x] (6r\lambda \delta[x] A'[x] f'[x] + f[x] (2r\lambda A'[x] \delta'[x] + \delta[x] (2(\beta + 3\lambda) A'[x] + r\lambda A''[x]))) + 4r^2 A[x]^9 B[x] f[x]^3 \\
& (-6r\lambda f[x] \delta[x] A'[x] B'[x] + B[x] (16r\lambda \delta[x] A'[x] f'[x] + f[x] (r\lambda A'[x] (-\psi[x] B'[x] + 4\delta'[x]) + 2\delta[x] (2(\beta + 3\lambda) A'[x] + r\lambda A''[x]))) + \\
& B[x]^2 (8r\lambda \psi[x] A'[x] f'[x] + f[x] (2r\lambda A'[x] \psi'[x] + \psi[x] (2(\beta + 3\lambda) A'[x] + r\lambda A''[x]))) + \\
& rA[x]^2 (-6r^2 \lambda \delta[x] B'[x]^2 + 2rB[x] (3r\lambda B'[x] \delta'[x] + \delta[x] (2(2\alpha + 2(-\alpha + \beta) + 5\lambda) B'[x] + r\lambda B''[x])) - \\
& B[x]^2 (4\delta[x] (\beta + 2\lambda + 6r^2 \lambda f[x] A'[x]^2) + r(2(\beta + 2\lambda) \psi[x] B'[x] + 4(\beta + 3\lambda) \delta'[x] + r\lambda (B'[x] \psi'[x] + 2\delta''[x])) + \\
& B[x]^3 (2(\beta + 2\lambda) \psi[x] + r(2(\beta + 3\lambda) \psi'[x] + r\lambda \psi''[x]))) + \\
& 4A[x]^8 f[x] (3r^3 \lambda f[x]^2 \delta[x] B'[x]^2 - 2B[x]^4 (2r(\beta + 3\lambda) \chi[x] f'[x] + (\beta + 2\lambda) f[x] (2\chi[x] + r\chi'[x])) - \\
& r^2 B[x] f[x] (9r\lambda \delta[x] B'[x] f'[x] + f[x] (3r\lambda B'[x] \delta'[x] + \delta[x] (2(2\alpha + 2(-\alpha + \beta) + 5\lambda) B'[x] + r\lambda B''[x]))) + rB[x]^2 (6r^2 \lambda f[x]^3 \delta[x] A'[x]^2 + \\
& 6r^2 \lambda \delta[x] f'[x]^2 + f[x] (2(\beta + 2\lambda) \Sigma[x] B'[x] + r(r\lambda f'[x] (-\psi[x] B'[x] + 6\delta'[x]) + 3\delta[x] (2(\beta + 3\lambda) f'[x] + r\lambda f''[x])) + f[x]^2 \\
& (2(\beta + 2\lambda) \delta[x] + r(2(\beta + 3\lambda) \delta'[x] + r\lambda (-B'[x] \psi'[x] + \delta''[x]))) + B[x]^3 (3r^3 \lambda f[x]^3 \psi[x] A'[x]^2 + rf[x] (-4(\beta + 3\lambda) \Sigma[x] + 3r^2 \lambda \psi[x] f'[x]) + \\
& f[x] (-4(\beta + 2\lambda) \Sigma[x] + r(-2(\beta + 2\lambda) \Sigma'[x] + 5r^2 \lambda f'[x] \psi'[x] + r\psi[x] ((\beta + 4\lambda) f'[x] + r\lambda f''[x]))) + r^2 f[x]^2 ((\beta + 4\lambda) \psi'[x] + r\lambda \psi''[x])) + \\
& rA[x]^{10} f[x]^2 (6r^2 \lambda f[x]^2 \delta[x] B'[x]^2 - 2rB[x] f[x] (12r\lambda \delta[x] B'[x] f'[x] + f[x] (3r\lambda B'[x] \delta'[x] + \delta[x] (2(2\alpha + 2(-\alpha + \beta) + 5\lambda) B'[x] + r\lambda B''[x]))) + \\
& B[x]^2 (24r^2 \lambda \delta[x] f'[x]^2 + 4rf[x] (r\lambda f'[x] (-\psi[x] B'[x] + 4\delta'[x]) + 2\delta[x] (2(\beta + 3\lambda) f'[x] + r\lambda f''[x])) + \\
& f[x]^2 (4(\beta + 2\lambda) \delta[x] + r(-2(\beta + 2\lambda) \psi[x] B'[x] + 4(\beta + 3\lambda) \delta'[x] + r\lambda (-B'[x] \psi'[x] + 2\delta''[x]))) + \\
& B[x]^3 (12r^2 \lambda \psi[x] f'[x]^2 + 4rf[x] (2r\lambda f'[x] \psi'[x] + \psi[x] (2(\beta + 3\lambda) f'[x] + r\lambda f''[x])) + f[x]^2 (2(\beta + 2\lambda) \psi[x] + r(2(\beta + 3\lambda) \psi'[x] + r\lambda \psi''[x]))) - \\
& 2A[x]^6 B[x]^2 (8r\lambda B[x]^2 \chi[x] f'[x] - rf[x] (4r^2 \lambda f[x]^2 \delta[x] A'[x]^2 - 2B'[x] (4(\beta + 2\lambda) \Sigma[x] - 3r^2 \lambda \psi[x] f'[x]) + \\
& rf[x] B'[x] (2(\beta + 2\lambda) \psi[x] + 5r\lambda \psi'[x])) + B[x] (-8rf[x] ((\beta + 3\lambda) \Sigma[x] - r^2 \lambda \psi[x] f'[x]) - \\
& 2f[x] (8(\beta + 2\lambda) \Sigma[x] - r(-4(\beta + 2\lambda) \Sigma'[x] + 9r^2 \lambda f'[x] \psi'[x] + r\psi[x] (2(2\alpha + 2(-\alpha + \beta) + 7\lambda) f'[x] + 3r\lambda f''[x]))) + \\
& rf[x]^2 (2(\beta + 2\lambda) \psi[x] + r((6\alpha + 6(-\alpha + \beta) + 22\lambda) \psi'[x] + 5r\lambda \psi''[x]))) + 4A[x]^4 (-3r^3 \lambda f[x] \delta[x] B'[x]^2 + 2(\beta + 2\lambda) B[x]^4 (2\chi[x] + r\chi'[x]) + \\
& r^2 B[x] (3r\lambda \delta[x] B'[x] f'[x] + f[x] (3r\lambda B'[x] \delta'[x] + \delta[x] (2(2\alpha + 2(-\alpha + \beta) + 5\lambda) B'[x] + r\lambda B''[x]))) - rB[x]^2 (-2(\beta + 2\lambda) \Sigma[x] B'[x] + \\
& r(r\lambda f'[x] (\psi[x] B'[x] + 2\delta'[x]) + \delta[x] (2(\beta + 3\lambda) f'[x] + r\lambda f''[x])) + f[x] (2(\beta + 2\lambda) \delta[x] + r(2(\beta + 3\lambda) \delta'[x] + r\lambda (B'[x] \psi'[x] + \delta''[x]))) + \\
& B[x]^3 (-4(\beta + 2\lambda) \Sigma[x] + r(-2(\beta + 2\lambda) \Sigma'[x] + r\psi[x] ((\beta + 4\lambda) f'[x] + r\lambda f''[x]) + r(2r\lambda f'[x] \psi'[x] + f[x] ((\beta + 4\lambda) \psi'[x] + r\lambda \psi''[x])))) \Big)
\end{aligned}$$

$$\begin{aligned}
S8 = & -\frac{1}{32r^4 A[x]^6 B[x]^4} \left(4r^2(-\alpha+\beta+\lambda) B[x] (-\Sigma[x] + B[x] \chi[x]) A'[x]^2 + \right. \\
& A[x]^2 \left(4r\lambda \Sigma[x] B'[x] - 2B[x] (\Sigma[x] (-2(\beta+\lambda) + 2r^2(2\alpha+3(-\alpha+\beta)+3\lambda) f[x] A'[x]^2) + r\lambda(r\delta[x] + 2\chi[x]) B'[x]) + \right. \\
& 2B[x]^2 (2r(\beta+\lambda)\delta[x] + 2\chi[x](-\beta-\lambda+r^2(2\alpha+7(-\alpha+\beta)+\lambda) f[x] A'[x]^2) + r^2\lambda\delta'[x]) - rB[x]^3 (2(\beta+\lambda)\psi[x] + r\lambda\psi'[x]) \left. \right) + \\
& 2rA[x]^5 f[x] \left(r(-\alpha+\beta+\lambda) B[x]^3 f[x] \psi[x] A'[x] - 2r(4\alpha+3(-\alpha+\beta)+3\lambda) f[x] \Sigma[x] A'[x] B'[x] - 2r(-\alpha+\beta+\lambda) B[x]^2 \chi[x] A'[x] f'[x] + \right. \\
& 2(4\alpha+3(-\alpha+\beta)+3\lambda) B[x] \Sigma[x] (rA'[x] f'[x] + f[x] (2A'[x] + rA''[x])) \left. \right) + \\
& rA[x] \left(r(\alpha-\beta+3\lambda) B[x]^3 \psi[x] A'[x] - 2r(-\alpha+\beta+\lambda) \Sigma[x] A'[x] B'[x] + 2(-\alpha+\beta+\lambda) B[x] (r\chi[x] A'[x] B'[x] + \Sigma[x] (2A'[x] + rA''[x])) - \right. \\
& 2B[x]^2 (r(\alpha-\beta+3\lambda)\delta[x] A'[x] + (-\alpha+\beta+\lambda)\chi[x] (2A'[x] + rA''[x])) \left. \right) + rA[x]^9 f[x]^3 \left(r(\alpha-\beta+3\lambda) B[x]^3 f[x] \psi[x] A'[x] - \right. \\
& 2r(-\alpha+\beta+\lambda) f[x] \Sigma[x] A'[x] B'[x] + 2(-\alpha+\beta+\lambda) B[x] (2r\Sigma[x] A'[x] f'[x] + f[x] (-r\chi[x] A'[x] B'[x] + \Sigma[x] (2A'[x] + rA''[x]))) \left. \right) + \\
& 2B[x]^2 (2r(-\alpha+\beta+\lambda)\chi[x] A'[x] f'[x] + f[x] (r(\alpha-\beta+3\lambda)\delta[x] A'[x] + (-\alpha+\beta+\lambda)\chi[x] (2A'[x] + rA''[x]))) \left. \right) + \\
& 4rA[x]^3 \left(r(2\alpha+2(-\alpha+\beta)+\lambda) B[x]^3 f[x] \psi[x] A'[x] - 2r(\beta+\lambda) f[x] \Sigma[x] A'[x] B'[x] + \right. \\
& B[x] (r(\alpha+\beta+\lambda) \Sigma[x] A'[x] f'[x] + f[x] (r(2\alpha+3(-\alpha+\beta)+\lambda)\chi[x] A'[x] B'[x] + 2(\beta+\lambda)\Sigma[x] (2A'[x] + rA''[x]))) - \\
& B[x]^2 (r(\alpha+\beta+\lambda)\chi[x] A'[x] f'[x] + f[x] (r(4\alpha+5(-\alpha+\beta)+3\lambda)\delta[x] A'[x] + \chi[x] (2(-\alpha+\beta+\lambda) A'[x] + r(2\alpha+3(-\alpha+\beta)+\lambda) A''[x]))) \left. \right) + \\
& 4rA[x]^7 f[x]^2 \left(r(2\alpha+2(-\alpha+\beta)+\lambda) B[x]^3 f[x] \psi[x] A'[x] - 2r(\beta+\lambda) f[x] \Sigma[x] A'[x] B'[x] + \right. \\
& B[x] (r(2\alpha+3(-\alpha+\beta)+3\lambda)\Sigma[x] A'[x] f'[x] + f[x] (-r(2\alpha+3(-\alpha+\beta)+\lambda)\chi[x] A'[x] B'[x] + 2(\beta+\lambda)\Sigma[x] (2A'[x] + rA''[x]))) + \\
& B[x]^2 (r(2\alpha+9(-\alpha+\beta)+\lambda)\chi[x] A'[x] f'[x] + f[x] (r(4\alpha+5(-\alpha+\beta)+3\lambda)\delta[x] A'[x] + \chi[x] (2(-\alpha+\beta+\lambda) A'[x] + r(2\alpha+3(-\alpha+\beta)+\lambda) A''[x]))) \left. \right) + \\
& A[x]^{10} f[x]^3 \left(-2r\Sigma[x] B'[x] (2\lambda f[x] + r(-\alpha+\beta+\lambda) f'[x]) + rB[x]^3 (r(\alpha-\beta+3\lambda)\psi[x] f'[x] + f[x] (2(\beta+\lambda)\psi[x] + r\lambda\psi'[x])) - \right. \\
& 2B[x] (f[x] (2(\beta+\lambda)\Sigma[x] + r\lambda(r\delta[x] + 2\chi[x]) B'[x]) + r(-\alpha+\beta+\lambda) (r\chi[x] B'[x] f'[x] - \Sigma[x] (2f'[x] + rf''[x]))) \left. \right) + \\
& 2B[x]^2 (f[x] (2r(\beta+\lambda)\delta[x] - 2(\beta+\lambda)\chi[x] + r^2\lambda\delta'[x]) + r(r(\alpha-\beta+3\lambda)\delta[x] f'[x] + (-\alpha+\beta+\lambda)\chi[x] (2f'[x] + rf''[x]))) \left. \right) - \\
& A[x]^4 \left(8(\beta+2\lambda) B[x]^4 \chi[x] + 2r\Sigma[x] B'[x] (-4\lambda f[x] + r(\alpha+\beta+\lambda) f'[x]) + B[x]^3 \right. \\
& (-8(\beta+2\lambda)\Sigma[x] + r(r(\alpha+\beta+5\lambda)\psi[x] f'[x] + f[x] (4(2\alpha+2(-\alpha+\beta)+\lambda)\psi[x] + 2r(2\alpha+2(-\alpha+\beta)+3\lambda)\psi'[x]))) + 2B[x] (2r^2(4\alpha+3(-\alpha+\beta)+3\lambda) \\
& f[x]^2 \Sigma[x] A'[x]^2 - 4f[x] ((\beta+\lambda)\Sigma[x] - r(r(\beta+\lambda)\delta[x] - \beta\chi[x]) B'[x]) - r(\alpha+\beta+\lambda) (r\chi[x] B'[x] f'[x] + \Sigma[x] (2f'[x] + rf''[x]))) - 2B[x]^2 \\
& (-2r^2(-\alpha+\beta+\lambda) f[x]^2 \chi[x] A'[x]^2 + 4f[x] (2r(\beta+\lambda)\delta[x] - \beta\chi[x] + r^2(\beta+\lambda)\delta'[x]) + r(r(\alpha+\beta+3\lambda)\delta[x] f'[x] - (\alpha+\beta+\lambda)\chi[x] (2f'[x] + rf''[x]))) \left. \right) + \\
& A[x]^8 f[x] \left(-8(\beta+2\lambda) B[x]^4 f[x] \chi[x] - 2rf[x] \Sigma[x] B'[x] (4\lambda f[x] + r(2\alpha+3(-\alpha+\beta)+3\lambda) f'[x]) + \right. \\
& B[x]^3 f[x] (-8(\beta+2\lambda)\Sigma[x] + r(r(10\alpha+9(-\alpha+\beta)+9\lambda)\psi[x] f'[x] + f[x] (4(2\alpha+2(-\alpha+\beta)+\lambda)\psi[x] + 2r(2\alpha+2(-\alpha+\beta)+3\lambda)\psi'[x]))) - 2B[x] f[x] \\
& (4f[x] ((\beta+\lambda)\Sigma[x] + r(r(\beta+\lambda)\delta[x] - \beta\chi[x]) B'[x]) + r(2\alpha+5(-\alpha+\beta)+\lambda)\chi[x] B'[x] f'[x] - (2\alpha+3(-\alpha+\beta)+3\lambda)\Sigma[x] (2f'[x] + rf''[x]))) + \\
& 2B[x]^2 (4r^2(-\alpha+\beta)\chi[x] f'[x]^2 + 4f[x]^2 (2r(\beta+\lambda)\delta[x] - \beta\chi[x] + r^2(\beta+\lambda)\delta'[x]) + \\
& rf[x] (r(10\alpha+11(-\alpha+\beta)+9\lambda)\delta[x] f'[x] + \chi[x] (2(-3\alpha+\beta+\lambda) f'[x] + r(2\alpha+5(-\alpha+\beta)+\lambda) f''[x]))) \left. \right) - \\
& A[x]^6 f[x] \left(16(\beta+2\lambda) B[x]^4 \chi[x] - r^2(-\alpha+\beta+\lambda) B[x]^3 \psi[x] f'[x] + 2r^2(4\alpha+3(-\alpha+\beta)+3\lambda)\Sigma[x] B'[x] f'[x] + \right. \\
& 2rB[x] (2r(\alpha+\beta+\lambda) f[x]^2 \Sigma[x] A'[x]^2 - r(-3(-\alpha+\beta)+\lambda)\chi[x] B'[x] f'[x] + \\
& 2f[x] B'[x] (r(4+3\lambda)\delta[x] - 2((2\alpha+2(-\alpha+\beta)+\lambda)\chi[x] - 2r(-1+\beta)\chi'[x])) - (4\alpha+3(-\alpha+\beta)+3\lambda)\Sigma[x] (2f'[x] + rf''[x])) + \\
& 2B[x]^2 (2r^2(3\alpha-\beta+\lambda) f[x]^2 \chi[x] A'[x]^2 + r(r(-16+4\alpha+3(-\alpha+\beta)-9\lambda)\delta[x] f'[x] - 16r(-1+\beta) f'[x] \chi'[x] + \\
& \chi[x] (2(3\alpha+\beta+\lambda) f'[x] + r(-3(-\alpha+\beta)+\lambda) f''[x])) - 2f[x] (6r(\beta+\lambda)\delta[x] - 2(\beta-\lambda)\chi[x] + r^2((4+3\lambda)\delta'[x] + 4(-1+\beta)\chi''[x]))) \left. \right) \\
S9 = & \frac{1}{16r^4 B[x]^3} \left(2r(-\Sigma[x] + B[x] \chi[x]) \left(\frac{r(-\alpha+\beta-5\lambda) B[x] A'[x]^2}{A[x]^4} + \frac{2(r(\alpha+\beta+\lambda) B[x] f[x] A'[x]^2 + (\beta+2\lambda) B'[x])}{A[x]^2} + \right. \right. \\
& \frac{2r(\alpha+\beta+\lambda) B[x] A'[x] f'[x]}{A[x]} - 2B'[x] (2(2+\beta+2\lambda) f[x] + r(2+\lambda) f'[x]) + \frac{-2r\lambda A'[x] B'[x] + 2B[x] (2(\beta+2\lambda) A'[x] + r\lambda A''[x])}{A[x]^3} - \\
& \frac{2A[x] f[x] (-r\lambda f[x] A'[x] B'[x] + B[x] (r(\alpha-\beta+3\lambda) A'[x] f'[x] + f[x] (2(\beta+2\lambda) A'[x] + r\lambda A''[x])))}{A[x]^3} + \\
& \left. \left. B[x] (-r(\alpha-\beta+\lambda) f[x]^2 A'[x]^2 + 4(2+\beta+2\lambda) f'[x] + 2r(2+\lambda) f''[x]) + \right. \right. \\
& \left. \left. A[x]^2 (2(\beta+2\lambda) f[x]^2 B'[x] - r(\alpha-\beta+\lambda) B[x] f'[x]^2 - 2f[x] (-r\lambda B'[x] f'[x] + B[x] (2(\beta+2\lambda) f'[x] + r\lambda f''[x]))) \right) \right) - \\
& 4B[x] \left(r(3rB[x]^2 \psi[x] f'[x] - 2(2\Sigma[x] + r\chi[x] B'[x]) f'[x] + B[x] (-4r\delta[x] f'[x] + 4\chi[x] f'[x] + 4rf'[x] \chi'[x] + 2r\chi[x] f''[x])) - \right. \\
& 2f[x] (2\Sigma[x] + r(B'[x] (-r\delta[x] + 2\chi[x] + r\chi'[x]) + B[x]^2 (\psi[x] - r\psi'[x] + rB[x] (\delta'[x] - \chi''[x]))) \left. \right) + \frac{1}{A[x]^4} (6r^2(-\alpha+\beta+\lambda) B[x] (-\Sigma[x] + B[x] \chi[x]) \\
& A'[x]^2 - A[x]^2 (-4r\lambda \Sigma[x] B'[x] + 2B[x] (2\Sigma[x] (\lambda + r^2(4\alpha+3(-\alpha+\beta)+3\lambda) f[x] A'[x]^2) + r(r(2\alpha+2(-\alpha+\beta)+\lambda)\delta[x] + 2\lambda\chi[x]) B'[x]) + \\
& 2B[x]^2 (-2r(\beta+\lambda)\delta[x] + 2\chi[x] (-\lambda + r^2(4\alpha+3(-\alpha+\beta)+3\lambda) f[x] A'[x]^2) - r^2(2\alpha+2(-\alpha+\beta)+\lambda)\delta'[x]) + \\
& rB[x]^3 (2(\beta+\lambda)\psi[x] + r(2\alpha+2(-\alpha+\beta)+\lambda)\psi'[x])) + rA[x]^3 f[x] \\
& (r(-\alpha+\beta+\lambda) B[x]^3 \psi[x] A'[x] - 2r(4\alpha+3(-\alpha+\beta)+3\lambda)\Sigma[x] A'[x] B'[x] + 2(4\alpha+3(-\alpha+\beta)+3\lambda) B[x] (-r\chi[x] A'[x] B'[x] + \Sigma[x] (2A'[x] + rA''[x])) - \\
& 2(4\alpha+3(-\alpha+\beta)+3\lambda) B[x]^2 (r\delta[x] A'[x] - \chi[x] (2A'[x] + rA''[x]))) + rA[x] (r(6\alpha+7(-\alpha+\beta)+3\lambda) B[x]^3 \psi[x] A'[x] - \\
& 2r(-\alpha+\beta+\lambda)\Sigma[x] A'[x] B'[x] + 2B[x] (r(-\alpha+\beta+\lambda)\chi[x] A'[x] B'[x] + \Sigma[x] (2(-\alpha+\beta+3\lambda) A'[x] + r(-\alpha+\beta+\lambda) A''[x])) - \\
& 2B[x]^2 (r(6\alpha+7(-\alpha+\beta)+3\lambda)\delta[x] A'[x] + \chi[x] (2(-\alpha+\beta+3\lambda) A'[x] + r(-\alpha+\beta+\lambda) A''[x]))) + rA[x]^7 f[x]^2 (r(\alpha-\beta+3\lambda) B[x]^3 f[x] \psi[x] A'[x] - \\
& 2r(-\alpha+\beta+\lambda) f[x] \Sigma[x] A'[x] B'[x] + 2(-\alpha+\beta+\lambda) B[x] (2r\Sigma[x] A'[x] f'[x] + f[x] (-r\chi[x] A'[x] B'[x] + \Sigma[x] (2A'[x] + rA''[x]))) + \\
& 2B[x]^2 (2r(-\alpha+\beta+\lambda)\chi[x] A'[x] f'[x] + f[x] (r(\alpha-\beta+3\lambda)\delta[x] A'[x] + (-\alpha+\beta+\lambda)\chi[x] (2A'[x] + rA''[x]))) \left. \right) + \\
& rA[x]^5 f[x] \left(r(\alpha+\beta+\lambda) B[x]^3 f[x] \psi[x] A'[x] - 2r(4\alpha+3(-\alpha+\beta)+3\lambda) f[x] \Sigma[x] A'[x] B'[x] + 2B[x] (2r(\alpha+\beta+\lambda)\Sigma[x] A'[x] f'[x] + \right. \\
& f[x] (r(-4\alpha-5(-\alpha+\beta)-5\lambda)\chi[x] A'[x] B'[x] + \Sigma[x] (2(4\alpha+3(-\alpha+\beta)+\lambda) A'[x] + r(4\alpha+3(-\alpha+\beta)+3\lambda) A''[x]))) + 2B[x]^2 (2r(2\alpha+5(-\alpha+\beta)+5\lambda)
\end{aligned}$$

$$\begin{aligned}
& \chi[\mathbf{r}] \mathbf{A}'[\mathbf{r}] \mathbf{f}'[\mathbf{r}] + \mathbf{f}[\mathbf{r}] (\mathbf{r} (2\alpha + 3(-\alpha + \beta) + 3\lambda) \delta[\mathbf{r}] \mathbf{A}'[\mathbf{r}] + \chi[\mathbf{r}] (2(4\alpha + 5(-\alpha + \beta) + 7\lambda) \mathbf{A}'[\mathbf{r}] + \mathbf{r} (4\alpha + 5(-\alpha + \beta) + 5\lambda) \mathbf{A}''[\mathbf{r}])) + \\
& \mathbf{A}[\mathbf{r}]^8 \mathbf{f}[\mathbf{r}]^2 (-2\mathbf{r} \Sigma[\mathbf{r}] \mathbf{B}'[\mathbf{r}] (2\lambda \mathbf{f}[\mathbf{r}] + \mathbf{r} (-\alpha + \beta + \lambda) \mathbf{f}'[\mathbf{r}]) + \mathbf{r} \mathbf{B}[\mathbf{r}]^3 (\mathbf{r} (\alpha - \beta + 3\lambda) \psi[\mathbf{r}] \mathbf{f}'[\mathbf{r}] + \mathbf{f}[\mathbf{r}] (2(\beta + \lambda) \psi[\mathbf{r}] + \mathbf{r} \lambda \psi'[\mathbf{r}])) - \\
& 2\mathbf{B}[\mathbf{r}] (\mathbf{f}[\mathbf{r}] (2(\beta + \lambda) \Sigma[\mathbf{r}] + \mathbf{r} \lambda (\mathbf{r} \delta[\mathbf{r}] + 2\chi[\mathbf{r}]) \mathbf{B}'[\mathbf{r}]) + \mathbf{r} (-\alpha + \beta + \lambda) (\mathbf{r} \chi[\mathbf{r}] \mathbf{B}'[\mathbf{r}] \mathbf{f}'[\mathbf{r}] - \Sigma[\mathbf{r}] (2\mathbf{f}'[\mathbf{r}] + \mathbf{r} \mathbf{f}''[\mathbf{r}])) + \\
& 2\mathbf{B}[\mathbf{r}]^2 (\mathbf{f}[\mathbf{r}] (2\mathbf{r} (\beta + \lambda) \delta[\mathbf{r}] - 2(\beta + \lambda) \chi[\mathbf{r}] + \mathbf{r}^2 \lambda \delta'[\mathbf{r}]) + \mathbf{r} (\mathbf{r} (\alpha - \beta + 3\lambda) \delta[\mathbf{r}] \mathbf{f}'[\mathbf{r}] + (-\alpha + \beta + \lambda) \chi[\mathbf{r}] (2\mathbf{f}'[\mathbf{r}] + \mathbf{r} \mathbf{f}''[\mathbf{r}])) + \\
& \mathbf{A}[\mathbf{r}]^6 (-8(\beta + 2\lambda) \mathbf{B}[\mathbf{r}]^4 \mathbf{f}[\mathbf{r}] \chi[\mathbf{r}] - 4\mathbf{r} \mathbf{f}[\mathbf{r}] \Sigma[\mathbf{r}] \mathbf{B}'[\mathbf{r}] (\lambda \mathbf{f}[\mathbf{r}] + \mathbf{r} (\beta + \lambda) \mathbf{f}'[\mathbf{r}]) + \\
& \mathbf{B}[\mathbf{r}]^3 \mathbf{f}[\mathbf{r}] (-8(\beta + 2\lambda) \Sigma[\mathbf{r}] + \mathbf{r} (2\mathbf{r} (\alpha + \beta + 3\lambda) \psi[\mathbf{r}] \mathbf{f}'[\mathbf{r}] + \mathbf{f}[\mathbf{r}] (2(3\alpha + 3(-\alpha + \beta) + \lambda) \psi[\mathbf{r}] + \mathbf{r} (2\alpha + 2(-\alpha + \beta) + 5\lambda) \psi'[\mathbf{r}])) - \\
& 2\mathbf{B}[\mathbf{r}] (\mathbf{f}[\mathbf{r}]^2 ((4\alpha + 4(-\alpha + \beta) + 6\lambda) \Sigma[\mathbf{r}] + \mathbf{r} (\mathbf{r} (2\alpha + 2(-\alpha + \beta) + 3\lambda) \delta[\mathbf{r}] + 6\lambda \chi[\mathbf{r}]) \mathbf{B}'[\mathbf{r}]) + \\
& \mathbf{r}^2 (-\alpha + \beta + \lambda) \Sigma[\mathbf{r}] \mathbf{f}'[\mathbf{r}]^2 - 2\mathbf{r} \mathbf{f}[\mathbf{r}] (-\mathbf{r} (\alpha + 2(-\alpha + \beta) + 2\lambda) \chi[\mathbf{r}] \mathbf{B}'[\mathbf{r}] \mathbf{f}'[\mathbf{r}] + \Sigma[\mathbf{r}] (2\beta \mathbf{f}'[\mathbf{r}] + \mathbf{r} (\beta + \lambda) \mathbf{f}''[\mathbf{r}])) + \\
& 2\mathbf{B}[\mathbf{r}]^2 (\mathbf{r}^2 (-\alpha + \beta + \lambda) \chi[\mathbf{r}] \mathbf{f}'[\mathbf{r}]^2 + \mathbf{f}[\mathbf{r}]^2 (6\mathbf{r} (\beta + \lambda) \delta[\mathbf{r}] - 2(2\alpha + 2(-\alpha + \beta) + \lambda) \chi[\mathbf{r}] + \mathbf{r}^2 (2\alpha + 2(-\alpha + \beta) + 3\lambda) \delta'[\mathbf{r}]) + \\
& 2\mathbf{r} \mathbf{f}[\mathbf{r}] (\mathbf{r} (2\alpha + 2(-\alpha + \beta) + 3\lambda) \delta[\mathbf{r}] \mathbf{f}'[\mathbf{r}] + \chi[\mathbf{r}] (2(\alpha + 2(-\alpha + \beta) + 3\lambda) \mathbf{f}'[\mathbf{r}] + \mathbf{r} (\alpha + 2(-\alpha + \beta) + 2\lambda) \mathbf{f}''[\mathbf{r}])) + \\
& \mathbf{A}[\mathbf{r}]^4 (-8(\beta + 2\lambda) \mathbf{B}[\mathbf{r}]^4 \chi[\mathbf{r}] - 2\mathbf{r} \Sigma[\mathbf{r}] \mathbf{B}'[\mathbf{r}] (-2\lambda \mathbf{f}[\mathbf{r}] + \mathbf{r} (\alpha + \beta + \lambda) \mathbf{f}'[\mathbf{r}]) + \\
& \mathbf{B}[\mathbf{r}]^3 (8(\beta + 2\lambda) \Sigma[\mathbf{r}] + \mathbf{r} (\mathbf{r} (4\alpha + 3(-\alpha + \beta) - 5\lambda) \psi[\mathbf{r}] \mathbf{f}'[\mathbf{r}] - \mathbf{f}[\mathbf{r}] (2(3\alpha + 3(-\alpha + \beta) + \lambda) \psi[\mathbf{r}] + 5\mathbf{r} \lambda \psi'[\mathbf{r}])) + \\
& 2\mathbf{B}[\mathbf{r}] (-\mathbf{r}^2 (4\alpha + 3(-\alpha + \beta) + 3\lambda) \mathbf{f}[\mathbf{r}]^2 \Sigma[\mathbf{r}] \mathbf{A}'[\mathbf{r}]^2 + \mathbf{f}[\mathbf{r}] (2(3\alpha + 3(-\alpha + \beta) + 5\lambda) \Sigma[\mathbf{r}] + \mathbf{r} \mathbf{B}'[\mathbf{r}] (-3\mathbf{r} \lambda \delta[\mathbf{r}] + 2(4\alpha + 4(-\alpha + \beta) + 5\lambda) \chi[\mathbf{r}] - 4\mathbf{r} \beta \chi'[\mathbf{r}])) + \\
& \mathbf{r} (\mathbf{r} (-2\alpha - 3(-\alpha + \beta) + \lambda) \chi[\mathbf{r}] \mathbf{B}'[\mathbf{r}] \mathbf{f}'[\mathbf{r}] + \Sigma[\mathbf{r}] (2(\alpha + \beta + 3\lambda) \mathbf{f}'[\mathbf{r}] + \mathbf{r} (\alpha + \beta + \lambda) \mathbf{f}''[\mathbf{r}])) - 2\mathbf{B}[\mathbf{r}]^2 \\
& (\mathbf{r}^2 (3\alpha + \beta + \lambda) \mathbf{f}[\mathbf{r}]^2 \chi[\mathbf{r}] \mathbf{A}'[\mathbf{r}]^2 + \mathbf{r} (\mathbf{r} (4\alpha + 3(-\alpha + \beta) - 3\lambda) \delta[\mathbf{r}] \mathbf{f}'[\mathbf{r}] - 8\mathbf{r} \beta \mathbf{f}'[\mathbf{r}] \chi'[\mathbf{r}] + \chi[\mathbf{r}] (2(\alpha + \beta + 3\lambda) \mathbf{f}'[\mathbf{r}] + \mathbf{r} (-2\alpha - 3(-\alpha + \beta) + \lambda) \mathbf{f}''[\mathbf{r}])) - \\
& \mathbf{f}[\mathbf{r}] (6\mathbf{r} (\beta + \lambda) \delta[\mathbf{r}] - 2(\beta - \lambda) \chi[\mathbf{r}] + \mathbf{r}^2 (3\lambda \delta'[\mathbf{r}] + 4\beta \chi''[\mathbf{r}]))))
\end{aligned}$$

S10 = S7

Note however that not all of these components are independent, as the modified Einstein tensor is symmetric : $E^{\mu\nu} = E^{\nu\mu}$, and from this we deduce the following relations

$$Q_5 = Q_1 + \frac{Q_2 f(r)}{B(r)}, \quad (4.91)$$

$$S_2 = \frac{B(r)^2 (-2Q_4 \delta(r) - S_1 + S_5) + B(r)^3 Q_4 \psi(r) - Q_2 f(r)^2 \delta(r)}{B(r) f(r)}, \quad (4.92)$$

$$S_8 = \frac{B(r)(Q_4 \chi(r) + S_6) - f(r)(\chi(r)(Q_1 - Q_7) + S_3) - Q_4 \Sigma(r)}{r^2}, \quad (4.93)$$

$$S_9 = \frac{B(r)^2 (\chi(r)(Q_1 - Q_7) + S_3) + B(r) \Sigma(r) (Q_7 - Q_1) - Q_2 f(r) \Sigma(r)}{r^2 B(r)}. \quad (4.94)$$

Furthermore, the generalized Bianchi identity implies that the combinations

$$C_0 \equiv -A(r)B(r)Q_4 - \frac{Q_5 (A(r)^2 f(r) + 1)}{2A(r)}, \quad (4.95)$$

$$C_1 \equiv -\frac{S_6 (A(r)^2 f(r) + 1)}{2A(r)}, \quad (4.96)$$

$$\begin{aligned}
C_2 \equiv & -\frac{1}{16A(r)^3} \left\{ 2A(r)^2 Q_4 (A(r)^2 f(r) + 1) (B(r) \psi(r) (A(r)^2 f(r) + 1) + 2\delta(r) (A(r)^2 f(r) - 1)) \right. \\
& + \frac{Q_5 (A(r)^2 f(r) + 1)^2 (B(r) \psi(r) (A(r)^2 f(r) + 1) + 2\delta(r) (A(r)^2 f(r) - 1))}{B(r)} \\
& \left. + 16A(r)^4 B(r) S_4 + 8A(r)^2 S_5 (A(r)^2 f(r) + 1) \right\}, \quad (4.97)
\end{aligned}$$

are initial constraint equations. Indeed, they satisfy the following identities

$$\begin{aligned}
\frac{dC_0}{dr} &= \frac{Q_2 (4f(r)A'(r) + A(r)^3 (-f(r))f'(r) + A(r)f'(r))}{4A(r)^2 B(r)} \\
&+ Q_1 \left(\frac{A'(r)}{A(r)^2} - \frac{1}{2} A(r) f'(r) \right) + C_0 \left(\frac{A'(r)}{A(r)} - \frac{2}{r} \right) - \frac{Q_7 (A(r)^2 f(r) + 1)}{r A(r)},
\end{aligned}$$

$$\begin{aligned}
\frac{dC_1}{dr} = & - \frac{C_1}{rA(r)^3B(r)f(r) + rA(r)B(r)} \left\{ -rA(r)^2B(r)f(r)A'(r) + rB(r)A'(r) + rA(r)^3f(r)B'(r) \right. \\
& \left. + rA(r)B'(r) - rA(r)^3B(r)f'(r) + 2A(r)^3B(r)f(r) + 2A(r)B(r) \right\} \\
& + \frac{Q_1 (A(r)^2f(r) + 1) (B(r)\psi(r) (3A(r)^2f(r) + 1) - 2\delta(r) (A(r)^2f(r) + 1))}{8A(r)^3B(r)} \\
& + \frac{Q_2 f(r) (A(r)^2f(r) + 1)^2 (B(r)\psi(r) - 2\delta(r))}{8A(r)^3B(r)^2} + \frac{C_0 (A(r)^2f(r) + 1) (B(r)\psi(r) - 2\delta(r))}{4A(r)^2B(r)} \\
& - \frac{Q_7 f(r)\psi(r) (A(r)^2f(r) + 1)}{4A(r)} - \frac{S_7 (A(r)^2f(r) + 1)}{2A(r)},
\end{aligned} \tag{4.98}$$

$$\begin{aligned}
\frac{dC_2}{dr} = & -\frac{4C_1A(r)^2B(r)^2}{r^2(f(r)A(r)^2+1)} + \frac{(1-A(r)^2f(r))S_3B(r)}{r^2A(r)} \\
& + \frac{S_4(f(r)(A(r)^3f'(r)-4A'(r))-A(r)f'(r))B(r)}{2f(r)(f(r)A(r)^2+1)} \\
& + \frac{Q_7}{8r^2A(r)^3} \left\{ 16B(r)f(r)\chi(r)A(r)^4 + 8(f(r)A(r)^2+1)(\Sigma(r)-B(r)\chi(r))A(r)^2 \right. \\
& \left. - \frac{r(f(r)A(r)^2+1)^2(2(A(r)^2f(r)-1)\delta(r)+B(r)(f(r)A(r)^2+1)\psi(r))}{B(r)} \right\} \\
& + C_2 \left(\frac{f'(r)A(r)^2}{f(r)A(r)^2+1} + \frac{f(r)A'(r)A(r)}{f(r)A(r)^2+1} - \frac{2}{r} - \frac{f'(r)}{2f(r)} - \frac{A'(r)}{f(r)A(r)^3+A(r)} \right) \\
& - \frac{Q_2(f(r)A(r)^2+1)}{32r^2A(r)^4B(r)^3} \left\{ r^2B(r)f(r)^2(2\delta(r)+B(r)\psi(r))f'(r)A(r)^5 \right. \\
& + 4f(r)(8\chi(r)B(r)^3+r^2(\psi(r)f'(r)+f(r)\psi'(r))B(r)^2 \\
& - r^2(3\delta(r)f'(r)+2f(r)\delta'(r))B(r)+2r^2f(r)\delta(r)B'(r))A(r)^3 \\
& - 4r^2B(r)f(r)^2(2\delta(r)+B(r)\psi(r))A'(r)A(r)^2 - 4r^2B(r)f(r)(B(r)\psi(r)-2\delta(r))A'(r) \\
& \left. + r^2(3B(r)(B(r)\psi(r)-2\delta(r))f'(r)+4f(r)(\psi'(r)B(r)^2-2\delta'(r)B(r)+2\delta(r)B'(r)))A(r) \right\} \\
& + \frac{Q_1}{16r^2A(r)^4B(r)^2f(r)} \left\{ 2r^2B(r)f(r)^3(2\delta(r)+B(r)\psi(r))A'(r)A(r)^4 \right. \\
& - r^2B(r)f(r)^3(2\delta(r)+B(r)\psi(r))f'(r)A(r)^7 \\
& - 2f(r)^2A(r)^5(16\chi(r)B(r)^3+r^2(4\psi(r)f'(r)+3f(r)\psi'(r))B(r)^2 \\
& - 2r^2(\delta(r)f'(r)+f(r)\delta'(r))B(r)+2r^2f(r)\delta(r)B'(r)) \\
& + r^2f(r)A(r)^3(B(r)(10\delta(r)-9B(r)\psi(r))f'(r)-8f(r)(\psi'(r)B(r)^2-\delta'(r)B(r)+\delta(r)B'(r))) \\
& \left. + 4r^2B(r)^2f(r)^2\psi(r)A'(r)A(r)^2+2r^2B(r)f(r)(B(r)\psi(r)-2\delta(r))A'(r) \right. \\
& \left. - 2r^2A(r)(B(r)(B(r)\psi(r)-2\delta(r))f'(r)+f(r)(\psi'(r)B(r)^2-2\delta'(r)B(r)+2\delta(r)B'(r))) \right\} \\
& + \frac{C_0}{16r^2A(r)^2B(r)^2f(r)} \left\{ 4r^2B(r)f(r)^3(2\delta(r)+B(r)\psi(r))A'(r)A(r)^3 \right. \\
& + 4r^2B(r)f(r)^2(2\delta(r)+B(r)\psi(r))A'(r)A(r) \\
& + r^2f(r)^2A(r)^4(3B(r)(2\delta(r)+B(r)\psi(r))f'(r)+f(r)(2\psi'(r)B(r)^2+4\delta'(r)B(r)-4\delta(r)B'(r))) \\
& - 4f(r)A(r)^2(8\chi(r)B(r)^3+2B(r)^2(r^2(\psi(r)f'(r)+f(r)\psi'(r))-4\Sigma(r)) \\
& - r^2(3\delta(r)f'(r)+2f(r)\delta'(r))B(r)+2r^2f(r)\delta(r)B'(r)) \\
& \left. + r^2(-3B(r)(B(r)\psi(r)-2\delta(r))f'(r)-2f(r)(\psi'(r)B(r)^2-2\delta'(r)B(r)+2\delta(r)B'(r))) \right\} \\
& - \frac{(f(r)A(r)^2+1)S_7}{rA(r)} - \frac{(f(r)A(r)^2+1)p_1(r)f'(r)}{4A(r)f(r)},
\end{aligned} \tag{4.99}$$

which are constraint evolution equations.

4.B Regularity of the potentials at the metric horizon

The Ricci tensor $R_{\alpha\beta}$ can be contracted twice with the killing vector $k^\mu = (\partial_v)^\mu$, that is, its time-time component R_{vv} must be an invariant. Its $\mathcal{O}(v)$ part can be expressed in term of the first order potentials as

$$\begin{aligned} \frac{R_{vv}}{\cos\theta} &= \frac{f(r)}{4r^2 B(r)^3} \left(-2r^2 f(r) B'(r) (2\psi(r) f'(r) + f(r) \psi'(r)) \right. \\ &\quad + B(r) \left(r(3r\psi(r) f'(r)^2 + f(r) (4r\psi(r) f''(r) + 7r f'(r) \psi'(r) + 8\psi(r) f'(r)) \right. \\ &\quad \left. \left. + 2f(r)^2 (r\psi''(r) + 2\psi'(r)) \right) - 4\Sigma(r) f'(r) \right) - 4B(r)^3 f(r) \psi(r). \end{aligned} \quad (4.100)$$

Near the metric horizon, for $\alpha = 2\beta = 1/100$ and $\lambda = 1/10$, R_{vv} becomes

$$\frac{R_{vv}}{\cos\theta} \sim x(0.094\psi(x) - 0.062\Sigma(x)) + \mathcal{O}(x^2), \quad (4.101)$$

where $x \equiv r - r_h$, r_h being the metric horizon, and where we neglected terms of order $\mathcal{O}(x^2)$. If we want R_{vv} to remain finite as we approach $x = 0$, then the difference $0.14\psi(x) - 0.32\Sigma(x)$ can diverge at most as $1/x$. More precisely, by setting $R_{vv} = \tilde{a}_1 + \tilde{b}_1 x + \mathcal{O}(x^2)$ for some $\tilde{a}_1, \tilde{b}_1 \in \mathbb{R}$, we get

$$\Sigma(x) = 1.5\psi(x) + \frac{a_1}{x} + b_1, \quad (4.102)$$

for some real numbers $a_1, b_1 \in \mathbb{R}$. Similarly, the $\mathcal{O}(v)$ part of the Ricci scalar R is given by

$$\begin{aligned} \frac{R}{\cos\theta} &= \frac{1}{2r^3 B(r)^3} \left(-2r f(r) B'(r) \left(r^2 (\psi(r) f'(r) + f(r) \psi'(r)) - 4\Sigma(r) \right) + \right. \\ &\quad B(r) \left(r f'(r) \left(3r^2 \psi(r) f'(r) - 8\Sigma(r) \right) \right. \\ &\quad \left. + f(r) \left[r \left(7r^2 f'(r) \psi'(r) + 2r\psi(r) (r f''(r) + 2f'(r)) - 8\Sigma'(r) \right) - 8\Sigma(r) \right] \right. \\ &\quad \left. + 2r^2 f(r)^2 (r\psi''(r) + 2\psi'(r)) \right) - 4r B(r)^3 f(r) \psi(r). \end{aligned} \quad (4.103)$$

Near the metric horizon R becomes

$$\begin{aligned} \frac{R}{\cos\theta} &\sim -0.5\Sigma(x) + 0.4\psi(x) + x \left[\psi(x) + 0.7\Sigma(x) + 1.2\psi'(x) - \Sigma'(x) + \right] + \mathcal{O}(x^2) \\ &= \left(\frac{8}{x} - 12 \right) a_1 + (8 - 12x)b_1 + (0.11x - 0.4)\psi(x) - 0.25x \psi'(x) + \mathcal{O}(x^2), \end{aligned} \quad (4.104)$$

where we have used in the second line the relation between $\Sigma(x)$ and $\psi(x)$ given by (4.102). In order to keep R finite, that is, $R \sim a_2 + b_2 x$ for some real numbers $a_2, b_2 \in \mathbb{R}$, $\psi(x)$ must be of the form

$$\psi(x) = \frac{e^{0.5x}}{x^{1.5}} \left((152a_1 + 13a_2 + 102b_1)\Gamma(1.5, x/2) + 47a_1\Gamma(0.5, 2x) + 330b_1\Gamma(2, x/2) + 28b_2\Gamma(2, x/2) + c_1 \right), \quad (4.105)$$

where $\Gamma(x, y)$ is the incomplete gamma function and c_1 is some integration constant. The same analysis shows that the $\mathcal{O}(v)$ part of $R_{\alpha\beta}R^{\alpha\beta}$ is given by

$$\begin{aligned} \frac{R_{\alpha\beta}R^{\alpha\beta}}{\cos\theta} = & \frac{1}{2r^5B(r)^6} \left\{ 2r^2f(r)B'(r)^2 \left(f(r) \left(r^2f'(r) (r\psi'(r) + 2\psi(r)) - 12\Sigma(r) \right) + 4rB(r)^6f(r)\psi(r) \right. \right. \\ & + rf'(r) \left(r^2\psi(r)f'(r) - 2\Sigma(r) \right) + 2r^2f(r)^2\psi'(r) \\ & + 2rB(r)^3f(r)B'(r) (r\psi(r) (rf'(r) + 2f(r)) - 4\Sigma(r)) \\ & - rB(r)B'(r) \left[r^2f'(r)^2(3r^2\psi(r)f'(r) - 4\Sigma(r)) + 4r^2f(r)^3 (r\psi''(r) + \psi'(r)) \right. \\ & + rf(r) \left(rf'(r) \left(7r^2f'(r)\psi'(r) + 4r\psi(r) (rf''(r) + 3f'(r)) - 4\Sigma'(r) \right) \right. \\ & \left. \left. - 4\Sigma(r)(rf''(r) + 8f'(r)) \right) \right. \\ & + 2f(r)^2 \left(r \left(r^2 (rf''(r)\psi'(r) + f'(r) (r\psi''(r) + 10\psi'(r))) \right. \right. \\ & \left. \left. + 2r\psi(r) (rf''(r) + f'(r)) - 12\Sigma'(r) - 12\Sigma(r) \right) \right. \\ & + B(r)^2 \left[r^2f'(r) \left(3r^2\psi(r)f'(r) (rf''(r) + 2f'(r)) - 4\Sigma(r) (rf''(r) + 4f'(r)) \right) \right. \\ & + rf(r) \left(r \left(-4rf''(r)\Sigma'(r) + 14r^2f'(r)^2\psi'(r) + f'(r) \left(7r^3f''(r)\psi'(r) - 16\Sigma'(r) \right) \right. \right. \\ & \left. \left. + 2r\psi(r) \left(r^2f''(r)^2 + 4f'(r)^2 + 3rf'(r)f''(r) \right) \right) \right. \\ & \left. \left. - 24\Sigma(r)f'(r) \right) + 4r^2f(r)^3\psi'(r) \right. \\ & + 2f(r)^2 \left(r \left(r^4f''(r)\psi''(r) + r^3f''(r)\psi'(r) + 2r^3f'(r)\psi''(r) + 4r^2f'(r)\psi'(r) \right. \right. \\ & \left. \left. + 2r\psi(r)f'(r) - 4\Sigma'(r) - 8\Sigma(r) \right) \right. \\ & \left. \left. - 2B(r)^4 \left(-4r\Sigma(r)f'(r) + f(r) \left(r (r\psi(r) (rf''(r) + 6f'(r)) - 4\Sigma'(r)) - 8\Sigma(r) \right) \right. \right. \right. \\ & \left. \left. \left. + 2rf(r)^2 (r\psi'(r) + \psi(r)) \right) \right\}. \end{aligned} \tag{4.106}$$

Near the metric horizon this expression in turns becomes

$$\frac{R_{\alpha\beta}R^{\alpha\beta}}{\cos\theta} \sim 0.0007\Sigma(x) - 0.0002\psi(x) + x(0.003\psi(x) - 0.004\Sigma(x) + 0.001\Sigma'(x) - 0.0007\psi'(x)) + \mathcal{O}(x^2). \tag{4.107}$$

In order to keep $R_{\alpha\beta}R^{\alpha\beta}$ finite as we approach $x = 0$, that is, setting $R_{\alpha\beta}R^{\alpha\beta} = a_3 + b_3x$ for some $a_3, b_3 \in \mathbb{R}$, then ψ must be of the form

$$\psi(x) = \frac{e^{2.6x}}{x^{0.6}} \left((28a_1 - 450a_2 - 4.8b_1)\Gamma(0.6, 2.6x) + 12a_1\Gamma(-0.4, 2.6x) + 11b_1\Gamma(1.6, 2.6x) - 170b_2\Gamma(1.6, 2.6x) + c_2 \right), \tag{4.108}$$

for some constant c_2 (we have again made use of (4.102) to express $\Sigma(x)$ in terms of $\psi(x)$). However the two conditions (4.105) and (4.108) are both satisfied only if $\psi(x)$ is finite as x goes to zero, that is, if we set $c_2 = c_1 = a_1 = 0$.

In fact, from equation (4.108) it follows that a_1 must be set to zero, so that (4.108) would yield a real-valued function. In any case, the set of functions

$$\left\{ \frac{e^{0.5x}}{x^{1.5}}, \frac{e^{0.5x}}{x^{1.5}} \Gamma(0.5, 0.5x), \frac{e^{0.5x}}{x^{1.5}} \Gamma(1.5, 0.5x), \frac{e^{0.5x}}{x^{1.5}} \Gamma(2, 0.5x) \right\}, \quad (4.109)$$

being linearly independent from the set

$$\left\{ \frac{e^{2.6x}}{x^{0.6}}, \frac{e^{2.6x}}{x^{0.6}} \Gamma(-0.4, 2.6x), \frac{e^{2.6x}}{x^{0.6}} \Gamma(0.6, 2.6x), \frac{e^{2.6x}}{x^{0.6}} \Gamma(1.6, 2.6x) \right\}, \quad (4.110)$$

then one must set each of the coefficients to zero. We therefore conclude that ∂ , and consequently Σ , must be regular at the metric horizon.

In a similar fashion, the $\mathcal{O}(v)$ piece of the Ricci tensor contracted with the Killing vector $k^\mu = (\partial_v)^\mu$ and the æther vector u^μ , near the metric horizon takes the form

$$\begin{aligned} R_{\mu\nu} k^\mu u^\nu &\sim 0.00001\delta(x) - 0.04\Sigma(x) + 0.06\psi(x) \\ &+ x(0.04\delta(x) - 0.09\psi(x) + 0.03\Sigma(x) \\ &+ 0.00001\delta'(x) - 0.04\Sigma'(x) - 0.04\chi'(x) + 0.2\psi'(x)) + \mathcal{O}(x^2), \end{aligned} \quad (4.111)$$

from which we deduce that δ must be regular at the metric horizon given that we already proved that both ψ and Σ are regular there. Finally, the $\mathcal{O}(v)$ piece of the Ricci tensor contracted twice with the æther vector u^μ , near the metric horizon takes the form

$$\begin{aligned} R_{\mu\nu} u^\mu u^\nu &\sim 0.06\delta(x) + 0.05\Sigma'(x) - 0.1\Sigma(x) - 0.06\chi'(x) + 0.2\psi(x) \\ &+ x(-0.04\delta(x) - 0.5\psi(x) + 0.3\Sigma(x) + 0.06\delta'(x) + 0.04\chi'(x) \\ &+ 0.7\psi'(x) - 0.3\Sigma'(x) + 0.05\Sigma''(x) - 0.06\chi''(x)) + \mathcal{O}(x^2), \end{aligned} \quad (4.112)$$

from which we deduce the regularity of χ' near the metric horizon, and therefore that of χ there.

5 – Open issues and conclusions

The aim of this thesis was to study the effect of Lorentz violations on the emission of the gravitational waves produced by binary black holes. More precisely, in chapter 2 we have presented two different phenomenological frameworks, namely khronometric theory and Einstein-æther theory, where Lorentz violations were introduced via a new gravitational field. Various aspects and constraints were presented in that chapter, and in particular we have reviewed the static spherically symmetric black hole solutions ([127, 133]) in section 2.6.

The main results of this thesis were presented in chapter 4. In sections 3.1 and 3.2 we have shown that the coupling of the Lorentz violating field to the metric induces a violation of the strong equivalence principle and the universality of free-fall. We have also shown that this can be quantified by new parameters within a point-particle approximation, the sensitivities. The great physical importance of the sensitivities was highlighted in section 3.4, where we have shown that the new dynamics leads to a modification of the gravitational wave flux, and in particular to the appearance of dipolar radiation proportional to the sensitivities squared, which could dominate over the quadrupolar flux if the sensitivities do not vanish.

Following the extraction procedure discussed in section 3.3, where we have shown that the sensitivities can be computed from the asymptotic metric of a single compact object moving slowly with respect to the Lorentz violating field, in section 4.1 we have begun the study of slowly moving black holes. This study has revealed some interesting phenomenology. First, we have found in section 4.2.6 that slowly moving black holes are inherently singular in most of the parameter space of the theory (where $\alpha \neq 0$ and $\beta \neq 0$). More precisely, we have found that either slowly moving black holes are singular at the spin-0 horizon or they can be made regular at the spin-0 horizon by exploiting a symmetry in the action. However, we have seen in sections 4.2.6.c) and 4.2.6.d) that regularity can only be achieved at the high cost of losing asymptotic flatness, and even then black holes are inevitably singular at the universal horizon. Consequently, $\alpha = \beta = 0$ is the only region in parameter space where we can have slowly moving black holes that are regular throughout the whole space time, without curvature singularities. As discussed in section 4.3, this region is special since the speed of the spin-0 modes goes to infinity as α and β go to zero, and from this it follows that the spin-0 horizon merges the universal horizon.

Black holes in this region are simpler because their spin-0 horizon coincides with the universal horizon. We have found that, up to $\mathcal{O}(v^2)$ corrections, slowly moving black holes are regular everywhere, as discussed in section 4.3. Indeed, at $\mathcal{O}(v^2)$ we have found that their metric is a Schwarzschild one, although the khronon field still presents a non trivial profile. From this slowly moving black hole solution, we have found that the sensitivity vanishes, re-

ardless of the value of λ , in agreement with the fact that the metric is the same as in general relativity. This result is of great importance, as it implies that binary black holes in the only non pathological region of the parameter space of the theory do not emit dipole radiation as expected. Indeed, this is a very surprising result, because in khronometric theory there is no symmetry preventing the emission of dipolar radiation, in contrast to general relativity where the conservation of momentum protects the dipole moment from radiating.

We have motivated the physical meaning of the sensitivities via the strong equivalence principle and its violations. Let us consider again one the arguments that we have given in section 3.1. We want to describe the motion of a binary system in their inspiral phase, when the typical binary distance d is much larger than the sizes of the bodies, and we can define a set of disjoint volumes V_a , covering the a -the body. Let us suppose that we can cover a sufficiently large region of spacetime using harmonics coordinates, and let us write the modified Einstein equations in the relaxed form

$$\square h^{\alpha\beta} = 16\pi G(\tau^{\alpha\beta} + \tau_{\text{kh}}^{\alpha\beta}), \quad \partial_\alpha h^{\alpha\beta} = 0, \quad (5.1)$$

where $\tau_{\text{kh}}^{\alpha\beta} \equiv \frac{1}{8\pi G}(-g)T_{\text{kh}}^{\alpha\beta}$. These equations imply the ‘‘conservation law’’

$$\partial_\alpha \tau^{\alpha\beta} + \partial_\alpha \tau_{\text{kh}}^{\alpha\beta} = 0. \quad (5.2)$$

In the same way as we did in section 3.1, we can define the a -the body’s position \vec{z}_a as such that the dipole moment

$$D_a^i \equiv \int_{V_a} d^3y y^i \tau^{00}(t, \vec{z}_a(t) + \vec{y}), \quad (5.3)$$

is a constant. Deriving this relation with respect to time gives us

$$\begin{aligned} 0 = \partial_0 D_a^i &= \int_{V_a} d^3y y^i (\partial_0 \tau^{00} + v_a^j \partial_j \tau^{00}) \\ &= \int_{V_a} d^3y y^i (-\partial_j \tau^{j0} - \partial_0 \tau_{\text{kh}}^{00} - \partial_j \tau_{\text{kh}}^{j0}) + v_a^j \int_{V_a} d^3y (\partial_j (y^i \tau^{00}) - \delta_j^i \tau^{00}) \\ &= - \int_{V_a} d^3y \left\{ \partial_j [y^i \tau^{j0} + y^i \tau_{\text{kh}}^{j0}] - \tau^{i0} - \tau_{\text{kh}}^{i0} + y^i \partial_0 \tau_{\text{kh}}^{00} \right\} + v_a^j \int_{S_a} dS_j y^i \tau^{00} - v_a^i \int_{V_a} d^3y \delta_j^i \tau^{00} \\ &= - \int_{S_a} dS_j y^i \tau^{j0} + \int_{V_a} d^3y \tau^{i0} + v_a^j \int_{S_a} dS_j y^i \tau^{00} - v_a^i \int_{V_a} d^3y \delta_j^i \tau^{00} \\ &\quad - \int_{S_a} dS_j y^i \tau_{\text{kh}}^{j0} + \int_{V_a} d^3y (\tau_{\text{kh}}^{i0} - y^i \partial_0 \tau_{\text{kh}}^{00}), \end{aligned} \quad (5.4)$$

where we used the conservation law (5.2) and Gauss’ theorem. We can rewrite this equation in a more compact form using the effective four-momentum P_a^μ and a boundary term, Q_a^i , defined in equation (3.11).

$$0 = P_a^i - v_a^i P_a^0 - Q_a^i + \int_{V_a} d^3y (\tau_{\text{kh}}^{i0} - y^i \partial_0 \tau_{\text{kh}}^{00}) - \int_{S_a} dS_j y^i \tau_{\text{kh}}^{j0}, \quad (5.5)$$

Taking one more time derivative leads us to the equation of motion

$$P_a^0 \frac{dv_a^i}{dt} = \frac{dP_a^i}{dt} - v_a^i \frac{dP_a^0}{dt} - \frac{dQ_a^i}{dt} + \frac{d}{dt} \int_{V_a} d^3y (\tau_{\text{kh}}^{i0} - y^i \partial_0 \tau_{\text{kh}}^{00}) - \frac{d}{dt} \int_{S_a} dS_j y^i \tau_{\text{kh}}^{j0}, \quad (5.6)$$

which generalizes the geodesic equation for a body in khronometric theory. In general relativity, all the right-hand side terms are defined in terms of surface integrals, and can be simplified using Riemann normal coordinates. In khronometric theory, however, some of the surface integrals depend on $\tau_{\text{kh}}^{\alpha\beta}$, introducing thus a dependence on the relative velocity between the falling frame and the khronon field. Moreover, we also find volume integrals which introduce a dependence on the fields at the interior of V_a . How can, under these general considerations, the movement of a black hole not depend on its relative motion with respect to the enviring khronon field? To answer this question we can express expand $\tau_{\text{kh}}^{\alpha\beta}$ in the relative velocity v , and use the results obtained in the previous chapter. In fact, we can easily show that, in the region where $\alpha = \beta = 0$, $T_{\text{kh}}^{\alpha\beta}$ depends exclusively on the æther's divergence $\nabla_\mu u^\mu$. Using the solution that we have found in section 4.3 we obtain that $\nabla_\mu u^\mu$ vanishes up to order $\mathcal{O}(v^2)$. In turn, this implies that $\tau_{\text{kh}}^{\alpha\beta}$ and the surface and volume integrals appearing in equation (5.6) vanish up to order $\mathcal{O}(v^2)$, in agreement with the vanishing of the sensitivity σ .

We have seen in section 2.5 that, on the one hand, solar system experiments [10, 122, 124] constraint the parameters α and β to satisfy $|\alpha - 2\beta| = 0$ to within one part in 10^7 . On the other hand, the multi-messenger observation of GW170817 [23, 28] bounds β to vanish up to one part in 10^{15} , otherwise the propagation speed of gravitational waves would significantly differ from that of light, in contradiction to the simultaneous arrival of the electromagnetic and gravitational signals from GW170817. Together, these experimental results bound α and β to satisfy $|\alpha| \lesssim 10^{-7}$ and $|\beta| \lesssim 10^{-15}$. The final shape of the parameter space, all bounds taken into account, corresponds to the segment $0 \leq \lambda \lesssim 0, 1$, as is shown in figure 5.1, where the parameter space is projected into the $\beta - \lambda$ plane.

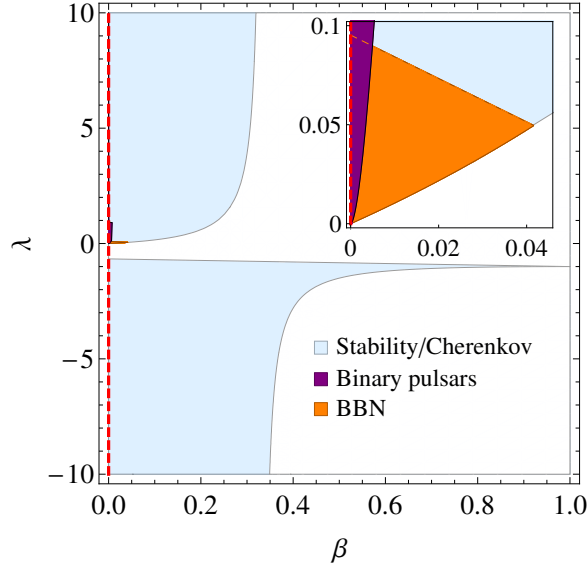


FIGURE 5.1 – Projection of the α , β , λ parameter space into the $\beta - \lambda$ plane. The light-blue shaded region corresponds to the allowed parameter space after imposing stability/Cherenkov considerations, the orange region to Big-Bang nucleosynthesis bounds, and the purple region to binary pulsar constraints. The current allowed parameter space is a one-dimensional set, which in this figure corresponds to the red line, i.e., to $\beta = 0$. Notice also that, due to BBN bounds, that line is restricted to the interval $0 \leq \lambda \lesssim 0, 1$. Figure adapted from [129].

In retrospective, the fact that LIGO-VIRGO found gravitational waves that propagate at the speed of light should not be surprising at all, as the spin-2 modes propagate at the same speed as the photon for $\alpha = \beta = 0$. Indeed, under the light of the results of this work it is clear that one would have reached the conclusion that $\alpha = \beta = 0$ was a special region even without these experimental constraints.

Altogether, $\alpha = \beta = 0$ is favored by empirical observations and by the aforementioned theoretical remarks. This leaves only one free parameter left for khronometric theory, namely λ . Pulsar constraints bound this parameter to be no more than 0.1, i.e., $|\lambda| < 0.1$ [129]. However, from the theoretical standpoint we have not been able to give further bounds to this coupling coefficient. Indeed, we have found that there is no dipole radiation at order $\mathcal{O}(v^2)$ in the relative motion between the black-holes and the khronon-field.

These results are of importance in the interpretation of Lorentz violations in gravity, particularly with upcoming missions such as LISA, as it tell us that dipolar emission is not present even when Lorentz symmetry is explicitly violated in the gravitational sector. Therefore, more studies are required in order to find the leading-order (if any) modifications to the GR gravitational wave fluxes produced by Lorentz violations. In particular, the derivative of the sensitivity with respect to the black hole velocity still could be non-zero in khronometric theory, in which case there would be a modification to the quadrupole formula of general relativity. Furthermore, this study does not consider slowly moving black holes in Einstein-æther theory, where it could still be possible to find $\sigma \neq 0$ and therefore a non-vanishing dipole contribution to the gravitational wave flux. Thus a natural path to extend the studies

of this thesis consist of testing both the regularity of black holes outside the available region of Einstein-æther theory, but more importantly to check whether the sensitivity vanishes for its allowed parameter space.

A – Appendix : academic paper

Finally, we here present the latest version of the academic paper where the research work highlighted in this thesis is resumed, to be published soon.

Constraints on Hořava gravity from binary black hole observations

Oscar Ramos^{1,2} and Enrico Barausse¹

¹ *Institut d’Astrophysique de Paris, CNRS & Sorbonne Universités,
UMR 7095, 98 bis bd Arago, 75014 Paris, France and*

² *Institut Lagrange de Paris (ILP), Sorbonne Universités, 98 bis bd Arago, 75014 Paris, France*
(Dated: November 6, 2018)

Hořava gravity breaks Lorentz symmetry by introducing a preferred spacetime foliation, which is defined by a timelike dynamical scalar field, the khronon. The presence of this preferred foliation makes black hole solutions more complicated than in General Relativity, with the appearance of multiple distinct event horizons: a matter horizon for light/matter fields; a spin-0 horizon for the scalar excitations of the khronon; a spin-2 horizon for tensorial gravitational waves; and even, at least in spherical symmetry, a universal horizon for instantaneously propagating modes appearing in the ultraviolet. We study how black hole solutions in Hořava gravity change when the black hole is allowed to move with low velocity relative to the preferred foliation. These slowly moving solutions are a crucial ingredient to compute black hole “sensitivities” and predict gravitational wave emission (and particularly dipolar radiation) from the inspiral of binary black hole systems. We find that for *generic* values of the theory’s three dimensionless coupling constants, slowly moving black holes present curvature singularities at the universal horizon. Singularities at the spin-0 horizon also arise unless one waives the requirement of asymptotic flatness at spatial infinity. Nevertheless, we have verified that at least in a one-dimensional subset of the (three-dimensional) parameter space of the theory’s coupling constants, slowly moving black holes are regular everywhere, even though they coincide with the general relativistic ones (thus implying in particular the absence of dipolar gravitational radiation). Remarkably, this subset of the parameter space essentially coincides with the one selected by the recent constraints from GW170817 and by solar system tests.

I. INTRODUCTION

Lorentz symmetry is believed to be a fundamental symmetry of Nature, and has been tested with high precision in a variety of settings. Indeed, violations of Lorentz symmetry are tightly constrained in the matter sector through particle physics experiments, and parametrized models such as the Standard Model Extension [1–3] efficiently bound such violations in the interaction sector between gravity and matter. Nevertheless, constraints in the gravitational sector (i.e. from purely gravitational systems) are much less compelling. Since Lorentz symmetry is a cornerstone of our current understanding of fundamental physics, it is worth exploring ways to improve these purely gravitational constraints. One may argue that the absence of Lorentz violations (LVs) in the matter and matter/gravity sectors probably points to small LVs in the purely gravitational sector, but that is not necessarily the case. Indeed, mechanisms allowing large LVs in gravity to co-exist with small LVs in matter have been put forward, and include e.g. the emergence of Lorentz symmetry at low energies as a result of renormalization group running [4–6] or accidental symmetries [7], or the suppression of the percolation of LVs from gravity to matter via a large energy scale [8].

In order to bound LVs in gravity, one has to set up a suitable phenomenological framework. In this paper we will focus not on LVs tout court, but rather on violations of boost symmetry (see e.g. [9] for violations of spatial rotation symmetry in gravity). A generic way to break boost symmetry is to introduce a dynamical timelike vector field (the æther) defining a preferred time direction at each spacetime event. Restricting the action to be covari-

ant and quadratic in the first derivatives of the æther, one obtains Einstein-Æther theory [10], which has been extensively used as a theoretical framework to understand how LVs may appear in gravitational experiments, so as to constrain them. If one further requires that the æther field not only defines a local preferred time direction, but also a preferred spacetime foliation, one ends up with a different Lorentz violating theory, khronometric gravity [11]. The action for this theory is the same as that of Einstein-Æther theory (which is indeed the most generic action one can write at quadratic order in the derivatives), but the æther field is constrained to be hypersurface orthogonal, i.e. parallel to the gradient of a timelike scalar field (the khronon) defining the preferred spacetime foliation.

Besides being interesting as a theoretical framework to effectively describe LVs in gravity at low energies, khronometric theory gains further interest from coinciding with the low energy limit of Hořava gravity [12, 13]. The latter is a theory of gravity that is power counting [12, 13] and also perturbatively renormalizable [14], thanks to the presence of an anisotropic scaling (Lifschitz scaling) between the time and spatial coordinates. Since this anisotropic scaling clearly breaks boost symmetry, Lorentz (and specifically boost) violations are crucial for the improved ultraviolet (UV) behavior of this theory.

Among the places where LVs play a major role is the structure of black holes (BHs). Indeed, in both Einstein-Æther and khronometric/Hořava gravity there exist additional graviton polarizations besides the spin-2 gravitons of General Relativity (GR). In more detail, the æther vector of Einstein-Æther theory can be decomposed into spin-1 and spin-0 degrees of freedom [15],

while the Lorentz violating khronon scalar of khronometric/Hořava gravity gives rise to a spin-0 polarization [16]. These additional graviton polarizations propagate with speed that is generally different from the speed of the spin-2 modes, which in turn does not necessarily match the speed of light.¹ As a result, BHs have multiple horizons, a matter horizon for light and other matter fields; a spin-2 horizon for tensor GWs; a spin-0 horizon for scalar modes; and a spin-1 horizons for the vector modes, if they are present. Moreover, at least in spherically symmetric, static and asymptotically flat configurations, BHs also possess a universal horizon for modes of arbitrary speed [19, 20]. Modes with propagation speed diverging in the UV do indeed appear in Hořava gravity when one moves away from its low energy limit (i.e. from khronometric gravity).

The regularity of these multiple event horizons has long proven a thorny issue in these theories. Already in spherical symmetry, there exists a one parameter family of BH solutions (parametrized by the mass, as in GR), but also a two parameter family of solutions (parametrized by the mass and a “hair” charge) that are singular at the spin-0 horizon [19, 21]. Numerical simulations seem to suggest that this second family of BHs is never produced in gravitational collapse [22], but regularity becomes even more of an issue when one moves away from spherical symmetry. For instance, while slowly rotating BHs in khronometric theory pose no particular problem [23, 24], ones in Einstein-æther theory present no universal horizon [25]. Moreover, they are singular at all but the outermost spin-1 horizon in regions of the parameter space of the theory’s couplings where multiple spin-1 horizons exist [25]. There are also suggestions that the universal horizon found in static spherically symmetric BHs may be non-linearly unstable, at least in the eikonal (i.e. small wavelength) limit and in Hořava gravity, thus forming a finite-area curvature singularity [20]. This may be related to the universal horizon being a Cauchy horizon in Hořava gravity [26].

To further investigate the stability and regularity of BH horizons in boost-violating gravity, we focus here on non-spinning BHs moving slowly relative to the preferred foliation in khronometric theory. This is a highly relevant physical configuration for understanding GW emission from binary systems including at least one BH. A generic feature of gravitational theories extending GR is the possible presence of dipolar gravitational radiation from quasicircular binary systems of compact objects, e.g. neutron stars [27–33] or BHs [34]. This is experimen-

tally very important because dipolar emission appears at -1PN order, i.e. it is enhanced by a factor $(v/c)^{-2}$ (with v being the binary’s relative velocity) compared to the usual quadrupolar emission of GR². As such, dipolar emission may in principle dominate the evolution of binary systems at large separations, a prediction that can be tested against binary pulsars data or the latest LIGO/Virgo detections.

In Einstein-Æther and khronometric/Hořava gravity, dipolar emission from systems of two neutron stars was studied and compared to binary pulsar observations in Ref. [27]. Ref. [27] also laid out the theoretical framework to compute dipolar gravitational emission in these theories, showing that the effect is proportional (as in Fierz-Jordan-Brans-Dicke theory [28, 29, 33, 36–38]) to the square of the difference of the “sensitivities” of the two binary components. Ref. [27] then went on to extract the sensitivities of neutron stars from solutions of isolated stars in slow motion relative to the æther/khronon. In this paper, we will follow the same program for BHs in Hořava gravity, extracting their sensitivities from slowly moving solutions and drawing the implications for dipolar GW emission.

A. Executive summary, layout and conventions

The calculation of BH sensitivities turns out to be much more complicated than for neutron stars, due to the presence of multiple BH horizons and their tendency to become singular. Our main findings and conclusions can be summarized as follows:

- For generic values of the three dimensionless coupling constants α , β , λ of khronometric theory, BHs slowly moving relative to the preferred foliation present finite area curvature singularities. In more detail, if one imposes that the solution is asymptotically flat and regular at the matter horizon (which turns out to be the outermost one once experimental constraints on the theory’s couplings are accounted for), a curvature singularity necessarily arises further in, at the spin-0 horizon. Giving up the requirement of asymptotic flatness allows one to obtain solutions that are regular at the spin-0 and matter horizons, but *not* further in, at the universal horizon, which becomes a finite-area curvature singularity.
- If the coupling parameters of the theory are such that the speed of the spin-2 modes *exactly* matches that of light and the predictions of the theory in

¹Note that the GW170817 coincident detection of a neutron star merger in gravitational waves (GWs) and gamma rays constrains the speed of the spin-2 mode to match almost exactly the speed of light. However, even if one includes this constraint, Lorentz violating gravity remains viable [17], and in particular the speed of the spin-0 mode can be very different from the speed of light [18]. We will examine in detail the experimental bounds on khronometric theory, including those from GW170817, in Sec. II.

²The post-Newtonian (PN) expansion [35] is one in v/c , v being the characteristic velocity of the system under consideration, with terms of order $(v/c)^{2n}$ relative to the leading one being referred to as terms of “nPN” order.

the solar system (i.e. at 1PN order) *exactly* match those of GR, one is still left with a one-dimensional parameter space. In more detail, these conditions set $\alpha = \beta = 0$ (which is quite natural since the experimental bounds on these two parameters are very tight, $|\alpha| \lesssim 10^{-7}$ and $|\beta| \lesssim 10^{-15}$), while λ can be as large as $\sim 0.01 - 0.1$ without violating any experimental bounds. In this one-dimensional subset of the parameter space, slowly moving BHs are regular everywhere outside the central singularity at $r = 0$, but coincide with the Schwarzschild solution (because the khronon profile, albeit non-trivial, has vanishing stress energy, i.e. the khronon is a stealth field). Therefore, BH sensitivities are zero and no dipolar emission is expected from systems of two BHs. This result confirms, at the order at which we are working, the conclusion of Refs. [39], namely that khronometric theories with $\alpha = \beta = 0$ only have general relativistic solutions in vacuum, if asymptotic flatness is imposed. We therefore expect GW emission to match the general relativistic predictions exactly even at higher PN orders (quadrupolar emission and higher) if $\alpha = \beta = 0$.

- Even if the finite area curvature singularities that we find were due to the breakdown of our approximation scheme, and moving BHs turned out to exit and be regular away from the central singularity at $r \neq 0$, deviations away from the GR predictions for GW emission should be expected to be of (fractional) order $\mathcal{O}[\max(\alpha, \beta)] \sim 10^{-7}$, since GW generation should be exactly the same as in GR for $\alpha = \beta = 0$ even at higher PN orders. Such small differences are unlikely to be observable with present and future GW detectors. However, if finite area curvature singularities exist (possibly smoothed by UV corrections to the low energy theory), they may give rise to “echos” in the post-ringdown GW signal and/or smoking-gun features in the stochastic GW background.

The paper is organized as follows. In Sec. II we will briefly review Hořava/khronometric gravity and the experimental constraints on its free parameters. In Sec. III we review how sensitivities of generic compact objects can be computed from slowly moving solutions, and how they are related to strong equivalence principle violations and more specifically to dipolar gravitational emission. In Sec. IV we review spherical BHs in Hořava/khronometric gravity, and introduce the ansatz for the metric and khronon field of slowly moving BHs. In Sec. V we write the field equations for slowly moving BHs and solve them for generic values of the coupling constants, while the $\alpha = \beta = 0$ case is discussed in Sec. VI. Our conclusions are drawn in Sec. VII.

Henceforth, we will set the speed of light $c = 1$, and adopt a metric signature $(+, -, -, -)$.

II. LORENTZ VIOLATING GRAVITY

In Hořava gravity [13], Lorentz symmetry is violated by introducing a dynamical scalar field T , the “khronon”, which defines a preferred time foliation. As such, the gradient of the khronon needs to be a timelike vector ($\nabla_\mu T \nabla^\mu T > 0$ in our notation), i.e. hypersurfaces of constant khronon (the preferred foliation) are spacelike. Using coordinates adapted to the khronon (i.e. using T as the time coordinate), the action for Hořava gravity can be written as [11, 13]

$$S = \frac{1-\beta}{16\pi G} \int dT d^3x N \sqrt{\gamma} \left(K_{ij} K^{ij} - \frac{1+\lambda}{1-\beta} K^2 + \frac{1}{1-\beta} {}^3R + \frac{\alpha}{1-\beta} a_i a^i + \frac{1}{M_*^2} L_4 + \frac{1}{M_*^4} L_6 \right) + S_{\text{matter}}[g_{\mu\nu}, \Psi], \quad (1)$$

where K^{ij} , 3R , and γ_{ij} are respectively the extrinsic curvature, 3-dimensional Ricci scalar and 3-metric of the $T = \text{const}$ hypersurfaces; $K = K^{ij} \gamma_{ij}$; N is the lapse; $a_i \equiv \partial_i \ln N$; α , β and λ are dimensionless coupling constants, and Latin (spatial) indices are raised/lowered with the 3-metric γ_{ij} . The bare gravitational constant G is related to the value measured locally (e.g. via Cavendish experiments) by [40, 41]

$$G_N = \frac{G}{1-\alpha/2}. \quad (2)$$

The terms L_4 and L_6 , suppressed by a mass scale M_* , contain respectively fourth and sixth order derivatives with respect to the spatial coordinates, but no T -derivatives. Their detailed form is not needed for our purposes, but note that their presence is needed to ensure power counting renormalizability of the theory. Note that this action is *not* invariant under generic 4-dimensional diffeomorphisms (exactly because it violates Lorentz symmetry) but only under foliation-preserving diffeomorphisms

$$T \rightarrow \tilde{T}(T), \quad x^i \rightarrow \tilde{x}^i(x, T). \quad (3)$$

The matter fields, collectively denoted as Ψ , are assumed to couple (at the level of the action) with the 4-metric $g_{\mu\nu}$ alone, so as to ensure that test particles move along geodesics and that no LVs appear in the matter sector (i.e. in the Standard Model of particle physics), at least at lowest order. LVs may still percolate to the matter sector from the gravitational one, and suitable mechanisms suppressing this effect have therefore to be put in place in order to satisfy the tight bounds on LVs in the Standard Model. Such mechanisms include for instance the possibility that Lorentz invariance in the matter sector might merely be an emergent feature at low energies [42, 43], due e.g. to renormalization group running [4–6] or to accidental symmetries [7]. Alternatively, as pointed out in [8], the matter sector and the gravitational sector could present different levels of LV,

provided that the interaction between them is suppressed by a high energy-scale.

According to the precise mechanism that prevents the aforementioned percolation of LVs from gravity to the Standard Model, the bounds on the mass scale M_* may vary. Assuming this percolation is efficiently suppressed, M_* needs to be $\gtrsim 10^{-2}$ eV to agree with experimental tests of Newton's law at sub-mm scales [44, 45], and needs to be bound from above ($M_* \lesssim 10^{16}$ GeV) so that the theory is perturbative at all scales [44], which is a necessary condition to apply the power-counting renormalizability arguments of [13] (see also [14]).

The effect of the higher-order terms L_2 and L_4 appearing in the action (1) is typically small for astrophysical objects. Simple dimensional arguments show indeed that the fractional error incurred as a result of neglecting those terms when studying objects of mass M is $\sim \mathcal{O}((G_N M M_*)^{-2}) = \mathcal{O}(M_P^4 / (M M_*)^2)$ (with M_P the Planck mass) [27]. Therefore, given the viable range for M_* , the error is $\lesssim 10^{-18} (10 M_\odot / M)^2$. For most (astrophysical) purposes, one can therefore neglect those terms, even though they are crucial for power counting renormalizability and for the definition of BH horizons (c.f. Refs. [46] and the discussion on universal horizons in Sec. IV).

For these reasons, in this paper we will focus on the low-energy limit of Hořava gravity, i.e. we will neglect the terms L_2 and L_4 in eq. (1). The resulting theory is often also referred to as khronometric theory [27]. For our purposes it will also be convenient to re-write the action covariantly, i.e. in a generic coordinate system not adapted to the khronon field, in terms of an “aether” timelike vector u^μ of unit norm,

$$u_\mu = \frac{\partial_\mu T}{\sqrt{\nabla^\alpha T \nabla_\alpha T}}. \quad (4)$$

Neglecting the L_2 and L_4 terms the action (1) then becomes

$$S_{\text{kh}} = -\frac{1}{16\pi G} \int d^4x \sqrt{-g} \left(R + \lambda (\nabla_\mu u^\mu)^2 + \beta \nabla_\mu u^\nu \nabla_\nu u^\mu + \alpha a_\mu a^\mu \right) + S_{\text{matter}}[g_{\mu\nu}, \Psi], \quad (5)$$

where g , R and ∇ are 4-dimensional quantities (the metric determinant, Ricci scalar and Levi-Civita connection respectively). Note that this action is invariant under 4-dimensional diffeomorphisms, but the theory is still Lorentz (i.e. boost) violating due to the presence of the timelike aether vector u^μ , which defines a preferred time direction.

The field equations of khronometric theory are obtained by varying the action (5) with respect to $g^{\mu\nu}$ and T . Variation with respect to the metric yields the generalized Einstein equations

$$G_{\mu\nu} - T_{\mu\nu}^{\text{kh}} = 8\pi G T_{\mu\nu}^{\text{matter}}, \quad (6)$$

where $G_{\mu\nu} = R_{\mu\nu} - R g_{\mu\nu}/2$ is the Einstein tensor, the

matter stress-energy tensor is defined as usual as

$$T_{\text{matter}}^{\mu\nu} = \frac{-2}{\sqrt{-g}} \frac{\delta S_{\text{matter}}}{\delta g_{\mu\nu}}, \quad (7)$$

and the khronon stress-energy tensor is given by

$$T_{\mu\nu}^{\text{kh}} \equiv \nabla_\rho [J_{(\mu}{}^\rho u_{\nu)} - J^\rho{}_{(\mu} u_{\nu)} - J_{(\mu\nu)} u^\rho] + \alpha a_\mu a_\nu + [u_\sigma \nabla_\rho J^{\rho\sigma} - \alpha a^2] u_\mu u_\nu + \frac{1}{2} L_{\text{kh}} g_{\mu\nu} + 2\mathbb{E}_{(\mu} u_{\nu)}, \quad (8)$$

with

$$J^\rho{}_\mu \equiv \lambda (\nabla_\sigma u^\sigma) \delta_\mu^\rho + \beta \nabla_\mu u^\rho + \alpha a_\mu u^\rho, \quad (9)$$

$$\mathbb{E}_\mu \equiv \gamma_{\mu\nu} (\nabla_\rho J^{\rho\nu} - \alpha a_\rho \nabla^\nu u^\rho), \quad (10)$$

$$\gamma_{\mu\nu} = g_{\mu\nu} - u_\mu u_\nu. \quad (11)$$

Variation with respect to T gives instead the scalar equation

$$\nabla_\mu \left(\frac{\mathbb{E}^\mu}{\sqrt{\nabla^\alpha T \nabla_\alpha T}} \right) = 0. \quad (12)$$

However, it can be shown that this equation actually follows from the generalized Einstein equations (6), from the Bianchi identity, and from the equations of motion of matter (which imply in particular $\nabla_\mu T_{\text{matter}}^{\mu\nu} = 0$). This fact is also obvious by considering diffeomorphism invariance of the covariant action (5), c.f. [41]. In the following, to derive moving BH solutions, we will therefore solve the generalized Einstein equations (6) only.

Moreover, in the same way in which diffeomorphism invariance implies the Bianchi identity in GR, diffeomorphism invariance of the covariant gravitational action (i.e. (5) without the matter contribution S_{matter}) implies the generalized Bianchi identity :

$$\nabla_\mu E^{\mu\nu} = \kappa u^\nu, \quad (13)$$

where we have defined

$$E^{\mu\nu} \equiv G_{\mu\nu} - T_{\mu\nu}^{\text{kh}}, \quad (14)$$

$$\kappa \equiv -\frac{1}{2} \sqrt{\nabla^\alpha T \nabla_\alpha T} \nabla_\mu \left(\frac{\mathbb{E}^\mu}{\sqrt{\nabla^\alpha T \nabla_\alpha T}} \right). \quad (15)$$

A. Experimental constraints

The coupling parameters α , β and λ of khronometric theory need to satisfy a number of theoretical and experimental constraints, which we will now review.

First, let us note that the theory has three propagating degrees of freedom, namely a spin-2 mode (with two polarizations) like in GR, and a spin-0 mode. The propagation speeds of these modes in flat spacetime are respectively given by

$$c_0^2 = \frac{(\alpha - 2)(\beta + \lambda)}{\alpha(\beta - 1)(2 + \beta + \lambda)}, \quad (16a)$$

$$c_2^2 = \frac{1}{1 - \beta}. \quad (16b)$$

To avoid classical (gradient) instabilities and to ensure positive energies (i.e. quantum stability, or absence of ghosts), one needs to impose $c_0^2 > 0$ and $c_2^2 > 0$ [47, 48]. Moreover, to avoid ultra-high energy cosmic rays to decay into these gravitational modes in a Cherenkov-like cascade, the propagation speeds must satisfy $c_0^2 \gtrsim 1 - 10^{-15}$ and $c_2^2 \gtrsim 1 - 10^{-15}$. Gravitational wave observations also constrain the coupling parameters and the propagation speeds. Binary pulsar observations bound the speed of the spin-2 mode to match the speed of light to within about 0.5% [27], while the recent coincident detection of GW170817 and GRB 170817A [49] constrains $-3 \times 10^{-15} < c_2 - 1 < 7 \times 10^{-16}$. Overall, all these constraints imply in particular

$$|\beta| \lesssim 10^{-15}. \quad (17)$$

Further bounds follow from solar system measurements, and specifically from the upper bounds on the preferred frame parameters α_1 and α_2 appearing in the parametrized PN expansion, i.e. $|\alpha_1| \lesssim 10^{-4}$ and $|\alpha_2| \lesssim 10^{-7}$ [45]. Indeed, in khronometric theory these parameters are functions of the coupling constants through [16]

$$\alpha_1 = 4 \frac{\alpha - 2\beta}{\beta - 1}, \quad (18a)$$

$$\alpha_2 = \frac{\alpha_1}{8 + \alpha_1} \left[1 + \frac{\alpha_1(1 + \beta + 2\lambda)}{4(\beta + \lambda)} \right]. \quad (18b)$$

Taking into account the multi-messenger constraint (17), solar system bounds thus become

$$4|\alpha| \lesssim 10^{-4}, \quad (19a)$$

$$\left| \frac{\alpha}{\alpha - 2} \right| \left| 1 - \alpha \frac{1 + 2\lambda}{\lambda} \right| \lesssim 10^{-7}. \quad (19b)$$

These constraints are satisfied by $|\alpha| \lesssim 10^{-7}$, at least if $\lambda \gg 10^{-7}$; or by $|\alpha| \lesssim 0.25 \times 10^{-4}$ and $\lambda \approx \alpha/(1 - 2\alpha)$. The latter case (together with Eq. (17)) would imply therefore very small values for the three coupling constants, $|\alpha| \sim |\lambda| \lesssim 10^{-5}$ and $|\beta| \lesssim 10^{-15}$, which seem unlikely to allow for large observable deviations away from the general-relativistic behavior. The former case, however, while tightly constraining α and β ($|\alpha| \lesssim 10^{-7}$, $|\beta| \lesssim 10^{-15}$), leaves λ essentially unconstrained.

Indeed, the only meaningful constraint on λ comes from cosmological observations. For khronometric theory, the Friedmann equations take the same form as in GR, but with a gravitational constant G_C different from the locally measured one (G_N) and related to it by

$$\frac{G_N}{G_C} = \frac{2 + \beta + 3\lambda}{2 - \alpha} \approx 1 + \frac{3}{2}\lambda, \quad (20)$$

where in the last equality we have used the aforementioned bounds on α and β . In order to correctly predict the abundance of primordial elements during Big Bang Nucleosynthesis (BBN), which is in turn very sensitive to the expansion rate of the Universe and thus to G_C , one

needs to impose $|G_C/G_N - 1| \lesssim 1/8$ [40]. This results in $0 \leq \lambda \lesssim 0.1$ (note that λ need to be positive to avoid ghosts, gradient instabilities and vacuum Cherenkov radiation, as discussed at the beginning of this section; c.f. also Ref. [27]). Further constraints may come from other cosmological observations (such as those of the large scale structure and the cosmic microwave background – CMB), but have not yet been worked out in detail. Ref. [50] performed some work in this direction, but requiring that the Lorentz violating field be the Dark Energy; the resulting bounds are therefore inapplicable to our case. Similarly, Ref. [39] constrained $0 \leq \lambda \lesssim 0.01$ by using CMB observations, but assume α and β to be exactly zero.

In summary, a viable region of the parameter space of khronometric gravity is given by $|\alpha| \lesssim 10^{-7}$, $|\beta| \lesssim 10^{-15}$ and $10^{-7} \ll \lambda \lesssim 0.01 - 0.1$. This is indeed the region that we will investigate in the following.

III. VIOLATIONS OF THE STRONG EQUIVALENCE PRINCIPLE

In theories of gravity beyond GR, the strong equivalence principle is typically violated. Indeed, such theories generally include additional degrees of freedom besides the spin-2 gravitons of GR. Even if these additional graviton polarizations do not couple directly to matter at the level of the action, they are typically coupled non-minimally to the spin-2 gravitons. As a result, effective interactions between these extra gravitational degrees of freedom and matter re-appear in strong-gravity regimes, mediated by the spin-2 field (i.e. by the perturbations of the metric). This effective coupling is responsible, in particular, for the Nordtvedt effect, i.e. the deviation of the motion of binary of strongly gravitating objects (such as neutron stars and BHs) away from the general-relativistic trajectories. In more detail, these deviations from GR can appear in both the conservative sector (where they can be thought of as “fifth forces”) as well as in the dissipative one (where they can be understood as due to the radiation reaction of the extra graviton polarizations), and they strongly depend on the nature of the compact objects under consideration (e.g. whether they are neutron stars or BHs) and their properties (e.g. compactness, spin, etc). The Nordtvedt effect has indeed been studied thoroughly in theories such as Fierz-Jordan-Brans-Dicke and other scalar tensor theories, and at least for neutron stars also in Einstein-æther theory and khronometric gravity. In this section, we will review the framework necessary to extend this treatment to the case of BHs in khronometric gravity. We refer the reader to Ref. [27] for more details.

A. The sensitivities and their physical effect

The dynamics of a compact object binary can be described in the PN approximation as long as the char-

acteristic velocity of the system is much lower than the speed of light. For khronometric gravity, one has to consider two velocities, the relative velocity of the binary v_{12} , and the velocity of the center of mass relative to the preferred frame V_{CM} . The former is $\ll 1$ in the low-frequency inspiral phase of the binary evolution. The latter can instead be estimated by noting that the preferred frame needs to be almost aligned with the cosmic microwave background [51], hence V_{CM} is comparable to the peculiar velocity of galaxies, i.e. $V_{\text{CM}} \sim 10^{-3}$.

The binary components are typically described in PN theory as point particles. To account for the effective coupling to matter due to the Nordtvedt effect, the point-particle action of GR is modified, in khronometric theory, by making the mass vary with the body's velocity relative to the preferred frame [52]:

$$S_{\text{pp}A} = - \int m_A(\gamma_A) d\tau_A, \quad (21)$$

where $d\tau_A$ is the proper time along the body's trajectory, $\gamma_A \equiv \mathbf{u}_A \cdot \mathbf{u}$ is the projection of the body's four-velocity \mathbf{u}_A on the "aether" vector \mathbf{u} , and $A = 1, 2$ is an index running on the binary components. Since both v_{12} and V_{CM} are $\ll 1$, we can expand the action in $\gamma_A - 1 \ll 1$ as

$$S_{\text{pp}A} = -\tilde{m}_A \int d\tau_A \left\{ 1 + \sigma_A(1 - \gamma_A) + \frac{1}{2} \sigma'_A(1 - \gamma_A)^2 + \mathcal{O}[(1 - \gamma_A)^3] \right\}, \quad (22)$$

where $\tilde{m}_A \equiv m_A(1)$ is the body's mass while at rest with respect to the khronon, and where

$$\sigma_A \equiv - \left. \frac{d \ln m_A(\gamma_A)}{d \ln \gamma_A} \right|_{\gamma_A=1} \quad (23)$$

$$\sigma'_A \equiv \sigma_A + \sigma_A^2 + \left. \frac{d^2 \ln m_A(\gamma_A)}{d(\ln \gamma_A)^2} \right|_{\gamma_A=1}.$$

are the *sensitivity parameters* [27]. These parameters encode the violations of the strong equivalence principle, and depend on the nature of the bodies and their properties (they can be viewed as additional "gravitational charges" distinct from the masses, or as "hairs" in the special case of BHs).

Letting aside for the moment the problem of *computing* the sensitivities, one can use the action (22), together with the modified Einstein equations (6) (expanded in PN orders, i.e. in $V_{\text{CM}}, v_{12} \ll 1$) to compute the binary's motion. In particular, the sensitivities modify the conservative gravitational dynamics already at Newtonian order, i.e. the Newtonian acceleration of body A is given by

$$\dot{v}_A^i = - \frac{\mathcal{G} m_B \hat{n}_{AB}^i}{r_{AB}^2}, \quad (24)$$

where $r_{AB} = |\mathbf{x}_A - \mathbf{x}_B|$, $\hat{n}_{AB}^i = (x_A^i - x_B^i)/r_{AB}$, and where we have introduced the *active* gravitational masses

$$m_B \equiv \tilde{m}_B(1 + \sigma_B) \quad (25)$$

and the "strong field" gravitational constant

$$\mathcal{G} \equiv \frac{G_N}{(1 + \sigma_A)(1 + \sigma_B)}. \quad (26)$$

The sensitivities also enter at higher PN orders in the conservative sector [27, 52].

Similarly, the sensitivities also enter in the dissipative sector, i.e. in the GW fluxes. For quasi-circular orbits, the sensitivities cause binaries of compact objects to emit dipole gravitational radiation. This effect, absent in GR (where the leading effect is quadrupole radiation), appears at -1 PN order, i.e. it is enhanced by a factor $(v/c)^{-2}$ relative to quadrupole radiation. In more detail, the gravitational binding energy of a binary is given (because of Eq. (24)) by

$$E_b = - \frac{\mathcal{G} \mu m}{2r_{12}}, \quad (27)$$

with r_{12} the binary separation, $\mu \equiv m_1 m_2 / m$ and $m \equiv m_1 + m_2$, and changes under GW emission according to the balance law

$$\frac{\dot{E}_b}{E_b} = 2 \left\langle \left(\frac{\mathcal{G} G_{\mathbb{E}} a \mu m}{r_{12}^4} \right) \left\{ \frac{32}{5} (\mathcal{A}_1 + \mathcal{S} \mathcal{A}_2 + \mathcal{S}^2 \mathcal{A}_3) v_{12}^2 + (s_1 - s_2)^2 \left[\mathcal{C} + \frac{18}{5} \mathcal{A}_3 V_{\text{CM}}^j V_{\text{CM}}^j + \left(\frac{6}{5} \mathcal{A}_3 + 36 \mathcal{B}_3 \right) (V_{\text{CM}}^i \hat{n}_{12}^i)^2 \right] + (s_1 - s_2) \left[12 (\mathcal{B}_2 + 2 \mathcal{S} \mathcal{B}_3) V_{\text{CM}}^i \hat{n}_{12}^i v_{12}^j \hat{n}_{12}^j + \frac{8}{5} (\mathcal{A}_2 + 2 \mathcal{S} \mathcal{A}_3) V_{\text{CM}}^i (3v_{12}^i - 2\hat{n}_{12}^i v_{12}^j \hat{n}_{12}^j) \right] \right\} \right\rangle, \quad (28)$$

where we have defined the rescaled sensitivities

$$s_A \equiv \frac{\sigma_A}{1 + \sigma_A}, \quad (29)$$

and we have introduced the coefficients

$$\mathcal{A}_1 \equiv \frac{1}{c_2} + \frac{3\alpha(\mathcal{Z} - 1)^2}{2c_0(2 - \alpha)}, \quad \mathcal{A}_2 \equiv \frac{2(\mathcal{Z} - 1)}{(\alpha - 2)c_0^3}, \quad (30)$$

$$\mathcal{A}_3 \equiv \frac{2}{3\alpha(2 - \alpha)c_0^5}, \quad \mathcal{B}_2 \equiv \frac{\mathcal{Z}}{3c_0^3(\alpha - 2)}, \quad (31)$$

$$\mathcal{B}_3 \equiv \frac{1}{9\alpha c_0^5(2 - \alpha)}, \quad \mathcal{C} \equiv \frac{4}{3c_0^3 \alpha(2 - \alpha)}, \quad (32)$$

$$\mathcal{Z} \equiv \frac{(\alpha_1 - 2\alpha_2)(1 - \beta)}{3(2\beta - \alpha)}, \quad \mathcal{S} \equiv s_1 \frac{m_2}{m} + s_2 \frac{m_1}{m}. \quad (33)$$

B. Extracting the sensitivities from the asymptotic metric

In principle, the actual values of the sensitivities for a given body (e.g. a neutron star or a BH) may be computed from their very definition, Eq. (23), provided that

one can obtain solutions to the field equations for bodies in motion relative to the preferred frame, through at least order $\gamma - 1 = \mathcal{O}(v^2)$, v being the body's velocity in the preferred frame (i.e. with respect to the æther vector). Ref. [27] proposed however a simpler procedure, inspired by a similar calculation in scalar-tensor theories [28], whereby the sensitivities can be extracted from a solution to the field equation that is accurate only through order $\mathcal{O}(v)$.

The idea is based on the fact that if one solves the field equations for a *single* point particle (as described by the action (22)) in motion relative to the preferred frame (or, equivalently, the point particle is at rest and the khronon moves), the sensitivities appear in the metric and in the khronon field near spatial infinity already at order $\mathcal{O}(v)$, i.e., in a suitable gauge,

$$\begin{aligned}
ds^2 = & dt^2 - dr^2 + \left\{ -\frac{2G_N \tilde{m}}{r}(dt^2 + dr^2) \right. \\
& - r^2 (d\theta^2 + \sin^2 \theta d\varphi^2) \\
& - 2v \left[(B^- + B^+ + 4) \frac{G_N \tilde{m}}{r} \right] \cos \theta dt dr \\
& \left. + 2vr \left[(3 + B^- - J) \frac{G_N \tilde{m}}{r} \right] \sin \theta dt d\theta \right\} \\
& \times \left[1 + \mathcal{O}\left(v, \frac{1}{r}\right) \right], \\
u_\mu dx^\mu = & \left(dt + v \cos \theta dr - vr \sin \theta d\theta \right) \\
& \times \left[1 - \frac{G_N \tilde{m}}{r} + \mathcal{O}\left(\frac{1}{r^2}\right) \right] + \mathcal{O}(v^2), \tag{34}
\end{aligned}$$

where B^\pm and J are defined as

$$\begin{aligned}
B^\pm \equiv & \pm \frac{3}{2} \pm \frac{1}{4}(\alpha_1 - 2\alpha_2) \left(1 + \frac{2 - \alpha}{2\beta - \alpha} \sigma \right) \\
& - \left(2 + \frac{1}{4} \alpha_1 \right) (1 + \sigma), \tag{36}
\end{aligned}$$

$$J \equiv \frac{(2 + 3\lambda + \beta)[2(\beta + \sigma) - \alpha(1 + \sigma)]}{2(\lambda + \beta)(\alpha - 2)}. \tag{37}$$

Therefore, the sensitivity can be read off a strong field solution valid through order $\mathcal{O}(v)$, i.e. a solution describing a body moving slowly relative to the khronon. Once such a strong-field solution is obtained, one can indeed extract them from the g_{tr} and $g_{r\theta}$ components of the metric, through the combinations $3 + B^- - J$ and $B^- + B^+ + 4$, respectively. Both readings must of course yield the same value, which we will use as a consistency check of our strong-field solution in Sec. IV.

This was indeed the procedure used in [27] to estimate the sensitivities of neutron stars. In the following, we will tackle the problem of finding strong-field solutions for BHs moving slowly relative to the preferred frame.

IV. BLACK HOLES IN LORENTZ VIOLATING GRAVITY

To construct the slowly moving BH solutions needed to extract the sensitivities, let us start from a static spherically symmetric solution at rest relative to the khronon. We will then perturb this solution to account for the (slow) motion of the BH relative to the preferred frame.

A. Spherical BHs at rest

Regular (outside the central singularity at $r = 0$), spherically symmetric, static and asymptotically flat BHs in khronometric theory coincide with those of Einstein-æther theory [41] and were extensively studied in Ref. [19]. Their metric and æther vector take, in Eddington-Finkelstein coordinates, the form

$$ds^2 = f(r)dv^2 - 2B(r)dvdr + r^2 d\Omega^2, \tag{38}$$

$$u_\mu dx^\mu = \frac{1 + f(r)A(r)^2}{2A(r)} dv - A(r)B(r)dr, \tag{39}$$

where the exact functional form of the ‘‘potentials’’ $f(r)$, $B(r)$ and $A(r)$ depends on the coupling constants α , β and λ and is obtained by solving (in general numerically) the field equations. Because of asymptotic flatness, all three potentials asymptote to 1 at large radii, i.e. their asymptotic solution is given by

$$f(r) = 1 - \frac{2G_N \tilde{m}}{r} - \frac{\alpha(G_N \tilde{m})^3}{6r^3} + \dots \tag{40}$$

$$B(r) = 1 + \frac{\alpha(G_N \tilde{m})^2}{4r^2} - \frac{2\alpha(G_N \tilde{m})^3}{3r^3} + \dots \tag{41}$$

$$\begin{aligned}
A(r) = & 1 + \frac{G_N \tilde{m}}{r} + \frac{a_2(G_N \tilde{m})^2}{r^2} + \\
& (24a_2 + \alpha - 6) \frac{(G_N \tilde{m})^3}{r^3} + \dots, \tag{42}
\end{aligned}$$

where the parameter a_2 is determined (numerically) once the mass \tilde{m} is fixed [19].

The causal structure of these solutions is highly non-trivial. Besides a ‘‘matter horizon’’ for photons (and in general for matter modes), defined as in GR by the condition $f = 0$, these BHs also possess distinct horizons for the gravitational spin-0 and spin-2 modes. Since the characteristics of the evolution equations for these modes correspond to null geodesics of the effective metrics

$$g_{\alpha\beta}^{(i)} = g_{\alpha\beta} + (c_i^2 - 1)u_\alpha u_\beta, \tag{43}$$

where c_i is the propagation speed of the mode under consideration (c.f. eq. (16)), the spin-0 and spin-2 horizons are defined by the conditions $g_{vv}^{(0)} = 0$ and $g_{vv}^{(2)} = 0$, respectively. These horizons are typically located inside the matter horizon since the Cherenkov bound implies $c_0^2, c_2^2 \gtrsim 1 - 10^{-15}$.

While UV corrections – due to the fourth and sixth order spatial derivative terms in the full Hořava gravity

action (1) – to the metric and æther solutions of Ref. [19] are negligible for astrophysical BHs (c.f. discussion of the L_4 and L_6 terms in Sec. II), their presence is crucial, at least conceptually, for the causal structure of the solutions. Indeed, because of the higher order spatial derivatives, the dispersion relation for the gravitational modes includes k^4 and k^6 terms (k being the wavenumber), i.e. their frequency ω is given by

$$\omega^2 = c_i^2 k^2 + a k^4 + b k^6, \quad (44)$$

where a and b are coefficients with the right dimensions. As a result, the phase velocity of these modes diverges in the UV. Since matter is coupled to the gravitational modes, similar non-linear dispersion relations will also appear in the matter sector.

It would therefore appear that no event horizons should exist in the UV limit. However, Ref. [19] identified the presence of a “universal horizon” for modes of arbitrarily large speed. This horizon appears because the preferred foliation of Hořava gravity becomes a compact hypersurface in the strong field of the BH. Modes of any speed need to move inwards at this hypersurface in order to move in the future preferred-time direction (defined by the preferred foliation). It can be shown that the location of this universal horizon, which lies within the matter, spin-0 and spin-2 horizons, is defined by the condition $u_v \propto 1 + fA^2 = 0$.

Even though the exact form of the functions $f(r)$, $B(r)$ and $A(r)$ can in general be given only numerically, analytic solutions exist in a few special cases, e.g. in the case $\alpha = 0$:

$$f(r) = 1 - \frac{2G_N \tilde{m}}{r} - \frac{\beta r_{\text{kr}}^4}{r^4}, \quad B(r) = 1, \quad (45a)$$

$$A(r) = \frac{1}{f} \left(-\frac{r_{\text{kr}}^2}{r^2} + \sqrt{f + \frac{r_{\text{kr}}^4}{r^4}} \right), \quad (45b)$$

$$r_{\text{kr}} = \frac{G_N \tilde{m}}{2} \left(\frac{27}{1 - \beta} \right)^{1/4} \quad (45c)$$

It can be easily checked that the universal horizon and the spin-0 horizon coincide in this particular case, since when $\alpha \rightarrow 0$ the spin-0 speed given by eq. (16a) diverges, and are both located at $r_{\text{uh}} = \frac{3}{2} G_N \tilde{m}$. Note also that this solution does not depend on the coupling parameter λ , even though that is *not* assumed to vanish.

In the following, we will use spherically symmetric, static and asymptotically flat BHs as as the starting point for the construction of our slowly moving solutions. These spherical BHs are either produced numerically as in Ref. [19], or are given by the explicit solution (45) for $\alpha = 0$.

B. Slowly moving BHs

Let us now construct ansätze for the metric and khronon field of a (non-spinning) BH moving slowly relative to the preferred frame, based on the symmetries

of the problem. Let us first place ourselves in the reference frame comoving with the BH, i.e. consider the physically equivalent situation where the BH is actually at rest, while the khronon (which determines the preferred frame) is moving relative to it with small velocity $-v^i$ (note the different script that differentiates this velocity from the coordinate time v) along the z -axis. In order for the metric to be asymptotically flat, one will therefore have to impose $g_{\mu\nu} = \eta_{\mu\nu} + \mathcal{O}(1/r)$ and $u^\mu \partial_\mu = \partial_t - v \partial_z + \mathcal{O}(v)^2$ in cartesian coordinates (t, x^i) .

To exploit the symmetry of the configuration under rotations around the z axis, it is convenient to adopt cylindrical isotropic coordinates (t, ρ, z, ϕ) , in which the background $\mathcal{O}(v)^0$ spherical BHs of Sec. IV A can be written as

$$ds^2 = f(r(\tilde{r})) dt^2 - b^2(\tilde{r}) (d\rho^2 + \rho^2 d\phi^2 + dz^2), \quad (46)$$

$$u_\mu dx^\mu = A(r(\tilde{r})) dt + u_r(\tilde{r}) d\tilde{r}. \quad (47)$$

Here, \tilde{u}_r is determined by the normalization condition $u_\mu u^\mu = 1$; $\tilde{r} = \sqrt{\rho^2 + z^2}$ is the radial isotropic coordinate, which is related to the areal radius r used in Eqs. (38) by the relation $r = \tilde{r} b(\tilde{r})$; and $b(\tilde{r})$ is related to $B(r)$ by the relation

$$\frac{B(r)}{\sqrt{f(r)}} = \frac{b(\tilde{r})}{b(\tilde{r}) + \tilde{r} db(\tilde{r})/d\tilde{r}}. \quad (48)$$

Also note that the time coordinate t is related to the Eddington-Finkelstein time coordinate v by $t = v - \int_{\tilde{r}}^{r(\tilde{r})} B(r)/f(r) dr$, where \tilde{r} is a reference radius.

The use of isotropic coordinates makes it now simple to construct the ansätze for the $\mathcal{O}(v)$ perturbations. Following the idea briefly outlined in Appedix A of Ref. [27] for stellar systems, we can observe that the perturbations δg_{tt} and δu_t transform as scalars under spatial rotations; δg_{ti} and u_i transform as vectors; and δg_{ij} transforms as a tensor. Since we only have two 3-vectors, v^i and $\vec{n}^i = x^i/|x|$, to construct these quantities, we can write, without loss of generality,

$$\delta g_{tt} = \alpha_1(\tilde{r}) \vec{n} \cdot \vec{v}, \quad (49a)$$

$$\delta u^t = \beta_1(\tilde{r}) \vec{n} \cdot \vec{v}, \quad (49b)$$

$$\begin{pmatrix} \delta g_{t\rho} \\ \delta g_{tz} \end{pmatrix} = \alpha_2(\tilde{r}) (\vec{n} \cdot \vec{v}) \vec{n} + \alpha_3(\tilde{r}) \vec{v}, \quad (49c)$$

$$\begin{pmatrix} \delta u^\rho \\ \delta u^z \end{pmatrix} = \beta_2(\tilde{r}) (\vec{n} \cdot \vec{v}) \vec{n} + \beta_3(\tilde{r}) \vec{v}, \quad (49d)$$

$$\begin{pmatrix} \delta g_{\rho\rho} & \delta g_{\rho z} \\ \delta g_{z\rho} & \delta g_{zz} \end{pmatrix} = \alpha_4(\tilde{r}) (\vec{n} \cdot \vec{v}) \vec{n} \otimes \vec{n} \\ + \alpha_5(\tilde{r}) (\vec{n} \otimes \vec{v} + \vec{v} \otimes \vec{n}), \quad (49e)$$

$$\delta g_{t\phi} = \delta g_{\phi\phi} = \delta g_{\rho\phi} = \delta g_{z\phi} = 0, \quad (49f)$$

where we have introduced the potentials $\alpha_i(\tilde{r})$ for $i = 1, 2, 3, 4, 5$ and β_i with $i = 1, 2, 3$, which must depend only on the radial coordinate \tilde{r} (and not on ρ and z singularly) to ensure the right transformation properties under rotations. Note that actually only six of these eight potentials

are independent, as the (perturbed) æther $\tilde{u}^\mu = u^\mu + \delta u^\mu$ must satisfy the normalization condition $\tilde{u}^\mu \tilde{u}_\mu = 1$ and be hypersurface orthogonal, i.e. $\epsilon^{\mu\nu\alpha\beta} \tilde{u}_\nu \partial_\alpha \tilde{u}_\beta = 0$ (c.f. eq. (4)). Also note that $\delta g_{t\phi}$, $\delta g_{\phi\phi}$, $\delta g_{\rho\phi}$ and $\delta g_{z\phi}$ must vanish because neither v^i nor n^i possess a tangential component in the ϕ direction. (One may in principle obtain non-zero values for these components by introducing the tangential pseudovector $\vec{n} \times \vec{v}$, but that would violate parity, which would be incompatible with the symmetries of the system, which does not rotate around the z -axis.)

Transforming now back to the original Eddington-Finkelstein coordinates that we will use in this paper, the most generic form of the metric and æther vector then becomes

$$\begin{aligned} \tilde{g}_{\mu\nu} dx^\mu dx^\nu = & f(r) dv^2 - 2B(r) dr dv - r^2 d\Omega^2 \\ & + v \left\{ dv^2 f(r)^2 \cos\theta \psi(r) \right. \\ & - 2d\theta dr \sin\theta [\Sigma(r) - B(r)\chi(r)] \\ & + 2dr dv f(r) \cos\theta [\delta(r) - B(r)\psi(r)] \\ & + dr^2 B(r) \cos\theta [B(r)\psi(r) - 2\delta(r) + 2\Delta(r)] \\ & \left. - 2d\theta dv f(r) \sin\theta \chi(r) \right\} + \mathcal{O}(v^2), \end{aligned} \quad (50)$$

$$\begin{aligned} \tilde{u}_\mu dx^\mu = & u_v(r) dv - A(r) B(r) dr + v \left\{ \frac{1}{2} f(r) \cos\theta \times \right. \\ & \left[2u^r(r) \left(\frac{B(r)\Delta(r)u^r(r)}{u_v(r)} + \delta(r) - \eta(r) \right) \right. \\ & \left. + \psi(r)u_v(r) \right] dv + \frac{1}{2} \cos\theta \times \\ & \left[B(r) \left(-\frac{2B(r)\Delta(r)(u^r(r))^2}{u_v(r)} - 2\delta(r)u^r(r) \right. \right. \\ & \left. \left. - \psi(r)u_v(r) \right) + 2A(r)f(r)\eta(r) \right] dr \\ & \left. - \sin\theta \Pi(r)u_v(r)d\theta \right\} + \mathcal{O}(v^2), \end{aligned} \quad (51)$$

where the background æther components u_v and u^r are given by Eq. (39), i.e. $u_v = (1 + fA^2)/(2A)$ and $u^r = (-1 + A^2 f)/(2AB)$,

$$\begin{aligned} \eta(r) = & -\frac{2(u^r(r))^3 B(r)^3 \Delta(r) - 2(u_v(r))^3 \Pi'(r)}{2f(r)u_v(r)} \\ & - \frac{B(r)^2 u_v(r) u^r(r) (2\delta(r)u^r(r) + \psi(r)u_v(r))}{2f(r)u_v(r)} \end{aligned} \quad (52)$$

to ensure hypersurface orthogonality, and the six independent potentials $\delta, \chi, \psi, \Delta, \Sigma, \Pi$ are algebraically related to the potentials α_i and β_i introduced above. This ansatz can then be further simplified by noting that a gauge transformation $v' = v - v \Pi(r) \cos\theta + \mathcal{O}(v^2)$ sends

$\Pi = 0$, while leaving the form of the ansatz (51) unchanged. A further gauge transformation with generator $\xi^\mu \partial_\mu = \Omega(r)(-r \cos\theta \partial_r + \sin\theta \partial_\theta)$ can be used, by choosing the function $\Omega(r)$ appropriately, to set any one of five remaining independent potentials to zero. In the following, we will therefore set $\Delta = 0$.

One is therefore left with four independent potentials $\delta, \chi, \psi, \Sigma$, which near spatial infinity ($r \rightarrow +\infty$) must satisfy the boundary conditions $\psi, \Sigma \rightarrow 0$, $\delta \rightarrow -1$ and $\chi/r \rightarrow -1$ in order to ensure asymptotic flatness. Indeed, it is easy to see that these conditions lead to $ds^2 \approx dt^2 - dr^2 - r^2 d\Omega^2 + 2v dt dz$, where we have changed time coordinate to $t \approx v - r$ and $z = r \cos\theta$. A further coordinate change $t' = t + vz$ transforms the line element to the flat one. As for the æther, the same coordinate transformations yield $\tilde{u}^\mu \partial_\mu \approx \partial_t - v \partial_z$ asymptotically, i.e. near spatial infinity the æther moves with velocity $-v$ relative to the flat asymptotic metric. Another way of checking these boundary conditions is to note that they correspond to $\beta_3 \rightarrow -1$ and $\beta_{1,2}, \alpha_{1,2,3,4,5} \rightarrow 0$ in terms of the potentials introduced in eqs. (49).

As expected from the symmetries of the problem (see also Appendix A of Ref. [27]) the field equations (6), when evaluated with these ansätze, become ordinary differential equations in the radial coordinate, i.e. the dependence on the polar angle θ drops out. This is a highly non-trivial fact which simplifies the search for solutions – to be compared for instance with the procedure followed by Ref. [27], which involved projecting the field equations onto Legendre polynomials – and which is also an a posteriori check of the procedure leading to the ansatz.

V. FIELD EQUATIONS AND NUMERICAL SOLUTIONS

In this section, we will first analyze the structure of the field equations for the $\mathcal{O}(v)$ potentials $\delta(r)$, $\chi(r)$, $\psi(r)$ and $\Sigma(r)$ introduced in the previous section. We will then analyze the boundary and regularity conditions that those potentials must satisfy, and obtain numerical solutions for them under various choices of those conditions.

A. Structure of the field equations

By replacing the metric and æther ansätze, (50) and (51), into the field equations and expanding in v , one obtains ordinary differential equations for the background potentials f , A and B at zeroth order, and for $\delta(r)$, $\chi(r)$, $\psi(r)$ and $\Sigma(r)$ at first order. Since the background solutions are known from previous work (c.f. Sec. IV), we will focus here on the first order equations.

Naively, there appear to be six non-trivial field equations at first order, coming from the perturbations δE^v_v , δE^v_θ , δE^r_v , δE^r_r , δE^r_θ , and δE^θ_θ of eq. (14). However, because of the generalized Bianchi identity eq. (13), only

four of these equations are actually independent, thus providing a closed problem for the potentials $\delta(r)$, $\chi(r)$, $\psi(r)$ and $\Sigma(r)$. In more detail, eq. (13) has three non-trivial components through linear order in v (the ϕ component being trivial since both sides of the identity are $\mathcal{O}(v^2)$). Since we are not solving the khronon equation (12) (because that is automatically implied by the modified Einstein equations (14), as discussed in Sec. II and as can also be seen, at least in vacuum, from the identity eq. (13) itself), it is convenient to eliminate κ from the three non-trivial components of eq. (13). This leads to the identities

$$u_r \nabla_\mu E^\mu{}_\nu - u_\nu \nabla_\mu E^\mu{}_r = \mathcal{O}(v^2), \quad (53a)$$

$$u_\theta \nabla_\mu E^\mu{}_r - u_r \nabla_\mu E^\mu{}_\theta = \mathcal{O}(v^2), \quad (53b)$$

which can in turn be rewritten as

$$\nabla_\mu (u_r E^\mu{}_\nu - u_\nu E^\mu{}_r) = E^\mu{}_\nu \nabla_\mu u_r - E^\mu{}_r \nabla_\mu u_\nu + \mathcal{O}(v^2), \quad (54)$$

$$\nabla_\mu E^\mu{}_\theta = \mathcal{O}(v^2). \quad (55)$$

where we have used (in the second equation) the fact that $u_\theta = \mathcal{O}(v^2)$ in our gauge.

By expanding the summations in these identities, it is clear that the $E^r{}_\theta$ and the combination $u_r E^r{}_\nu - u_\nu E^r{}_r$ and $E^r{}_\theta$ must depend on the potentials f , A and B (at zeroth order) and $\delta(r)$, $\chi(r)$, $\psi(r)$ and $\Sigma(r)$ (at first order) through *one less* radial derivative than the highest derivatives appearing in the rest of the field equations. Moreover, from the same (expanded) identities it follows that these two quantities are initial value constraints for evolutions in the radial coordinate, i.e. if they are set to zero at some radius, they remain zero at all other radii *if* the remaining field equations (the “evolution equations”) are solved. As can be seen, this follows from the generalized Bianchi identity in the same way in which in GR the Bianchi identity allows splitting initial value problems in energy and momentum constraints and evolution equations. The same procedure was also followed in Ref. [19] to split the field equations of Einstein-æther gravity into constraints and evolution equations (in the radial coordinate) in static spherically symmetric configurations.

The explicit form of the equations for $\delta(r)$, $\chi(r)$, $\psi(r)$ and $\Sigma(r)$ is too complicated to be given here, but its schematic form is given as follows. The evolution equations take the form

$$e_1 \equiv \delta''(r) - \sum_{n=1}^7 w_n^\delta(r) M_n = 0, \quad (56a)$$

$$e_2 \equiv \chi''(r) - \sum_{n=1}^7 w_n^\chi(r) M_n = 0, \quad (56b)$$

$$e_3 \equiv \psi''(r) - \sum_{n=1}^7 w_n^\psi(r) M_n = 0 \quad (56c)$$

$$e_4 \equiv \Sigma'(r) - \sum_{n=1}^7 w_n^\Sigma(r) M_n = 0, \quad (56d)$$

where $\vec{M} \equiv [\delta(r), \chi(r), \psi(r), \Sigma(r), \delta'(r), \chi'(r), \psi'(r)]$ and $w_n^\delta(r), w_n^\chi(r), w_n^\psi(r), w_n^\Sigma(r)$ (with $n = 1, 7$) are functions of the radial coordinate, the background solution f, A, B and the coupling constants. As for the constraints $C_1(\vec{M})$ and $C_2(\vec{M})$, they satisfy the conservation equations

$$\frac{dC_i}{dr} = \sum_{n=1}^2 w_n^{C_i}(r) C_n + \sum_{n=1}^4 w_n^{e, C_i}(r) e_n, \quad i = 1, 2, \quad (57)$$

where again the coefficients $w_n^{C_i}(r)$ and $w_n^{e, C_i}(r)$ (with $i = 1, 2$ and $n = 1, 4$) depend on the background solution and the coupling constants. Note that at least at large radii, the coefficients $w_n^{C_i}(r)$ are negative, which contributes to damping potential violations of the constraints during our radial evolutions.

Finally, let us also note that because eqs. (56)–(57) are linear and homogeneous, one is free to rescale any one solution by a constant factor, i.e. given a solution $[\delta(r), \chi(r), \psi(r), \Sigma(r)]$, also $\Lambda[\delta(r), \chi(r), \psi(r), \Sigma(r)]$, with $\Lambda = \text{const}$, is a solution. We will use this fact when setting the initial/boundary conditions for the system given by eqs. (56) in the next section.

B. Solutions regular at the matter horizon

Before solving the system given by eqs. (56), let us comment on the boundary/initial conditions that the solution needs to satisfy. Close inspection of the coefficients $w_n^\delta(r), w_n^\chi(r), w_n^\psi(r), w_n^\Sigma(r)$ shows that the system presents at least three singular points (with $r \neq 0$) at which at least one of the coefficients diverges. These three singularities are located at the matter horizon, at the spin-0 horizon, and at the universal horizon. Regularity at these radial positions need therefore to be enforced. On top of this, physically relevant solutions should asymptote to flat space and to a khronon moving with velocity $-v$ near spatial infinity, which translates into the boundary conditions $\psi, \Sigma \rightarrow 0$, $\delta \rightarrow -1$ and $\chi/r \rightarrow -1$ as $r \rightarrow \infty$ as shown in Sec. IV B.

Let us first attempt to impose regularity at the outermost of these positions, the matter horizon. If the potentials are regular there³, they can be Taylor-expanded

³One can show that analyticity of the potentials δ , χ , ψ and Σ is required to ensure finiteness of the invariants constructed with the metric, the æther vector, and the Killing vectors ∂_r and ∂_ϕ (e.g. R , $R_{\mu\nu}R^{\mu\nu}$, $R_{\mu\nu\alpha\beta}R^{\mu\nu\alpha\beta}$, and scalars obtained by contracting among themselves curvature tensors, Killing vectors and the æther).

as

$$\begin{aligned}
\delta(r) &= \sum_{k=0}^{\infty} \delta_{k,h} (r - r_h)^k, \\
\chi(r) &= \sum_{k=0}^{\infty} \chi_{k,h} (r - r_h)^k, \\
\psi(r) &= \sum_{k=0}^{\infty} \psi_{k,h} (r - r_h)^k, \\
\Sigma(r) &= \sum_{k=0}^{\infty} \Sigma_{k,h} (r - r_h)^k,
\end{aligned} \tag{58}$$

where r_h is the matter horizon's position, and the coefficients $\delta_{k,h}$, $\chi_{k,h}$, $\psi_{k,h}$ and $\Sigma_{k,h}$ must be determined by solving the field equations. Indeed, solving the evolution *and* constraint equations perturbatively near $r = r_h$ allows one to express those coefficients as a function of $\delta_{0,h}$ and $\Sigma_{0,h}$ alone, i.e. the solution only has two independent degrees of freedom near the matter horizon. Those can then be reduced to just one by rescaling the solution by a constant factor as described in the previous section, whereby one can set e.g. $\Sigma_{0,h} = 1$ and maintain $\delta_{0,h}$ free.⁴

This parameter then needs to be determined by imposing asymptotic flatness. We therefore use the perturbative solution (58) to move slightly away from $r = r_h$, and then integrate numerically the system given by eqs. (56) up to large radii. The value of $\delta_{0,h}$ is then determined by imposing that δ and χ/r asymptote to the (same) constant (which does not need to be -1 because we have rescaled the solution by a global unknown factor) and that $\psi, \Sigma \rightarrow 0$ at large radii. In practice, we perform a bisection procedure on the value of $\delta_{0,h}$, according to whether $\delta(r)$ diverges to positive or negative values as $r \rightarrow \infty$, as was done in Ref. [19] for the static, spherically symmetric and asymptotically flat solutions that we employ as our background.

In more detail, solving the evolution equations perturbatively near spatial infinity and assuming that $\delta(r)$

asymptotes to a constant there, one finds

$$\delta(r) = \delta_0 + \frac{2(\beta + \lambda)(G_N \tilde{m} \delta_0 + 2\chi_0)}{(1 - 3\beta - 2\lambda)r} + \mathcal{O}\left(\frac{1}{r^2}\right), \tag{59a}$$

$$\chi(r) = \delta_0 r + \chi_0 + \mathcal{O}\left(\frac{1}{r}\right), \tag{59b}$$

$$\psi(r) = \frac{3\beta[3(G_N \tilde{m})^2 - 2a_2]\delta_0 - 2\Sigma_1}{3r^2} + \mathcal{O}\left(\frac{1}{r^3}\right), \tag{59c}$$

$$\Sigma(r) = \frac{\Sigma_1}{r} + \mathcal{O}\left(\frac{1}{r^2}\right), \tag{59d}$$

where δ_0 , χ_0 , χ_2 and Σ_1 are free parameters that can be determined from our numerical solutions once the bisection has converged. Note that we use the consistency relations between the coefficients of the higher-order terms and these free parameters to *test a posteriori* our numerical solutions.

Note also that if one inserts the solution (59) into the metric ansatz (50), the resulting metric can be put in the same gauge as eq. (34) by the infinitesimal change of coordinates $t' = t + vr \cos \theta + \mathcal{O}(v)^2$. By comparing the metric obtained in this way to eq. (34), one can relate the sensitivity of the solution to the two parameters δ_0 and χ_0 :

$$\begin{aligned}
\sigma &= \frac{\alpha - \beta - 3\alpha\beta + 5\beta^2 + \lambda - 2\alpha\lambda + 3\beta\lambda}{(2 - \alpha)(1 - 3\beta - 2\lambda)} \\
&\quad + \frac{(1 - \beta)(\beta + \lambda)}{1 - 3\beta - 2\lambda} \frac{\chi_0}{G_N \tilde{m} \delta_0}.
\end{aligned} \tag{60}$$

We have also checked this equation by solving directly the field equations near spatial infinity for a point particle described by the action (22), in the gauge of the metric ansatz eq. (50), and then by comparing to the asymptotic solution given by eq. (59).

Our numerical solutions confirm that if one imposes regularity at the matter horizon and asymptotic boundary conditions corresponding to a flat spacetime and a khronon moving with velocity $-v$ relative to the BH, the sensitivities are non-vanishing. We did not investigate the viable region of the parameter space described in Sec. II A, because of the difficulty of obtaining numerical background solutions for the potentials f , A and B for small but non-zero value of α and β . We will however study later, in Sec. VI, solutions for $\alpha = \beta = 0$ and $\lambda \neq 0$, and extract their sensitivities. For the moment, let us mention that for values of $\alpha \sim \beta \sim 10^{-2}$ and $\lambda \sim 0.1$, we obtain $\sigma \sim 10^{-3}$.

One important caveat, however, is that it is not at all clear these solutions (and the corresponding values of the sensitivities) are physically significant, as the numerical solutions that we obtain diverge when integrating inwards from the matter horizon to the spin-0 horizon. We have also checked that this divergence extends to the

⁴Rescaling $\Sigma_{0,h} = 1$ is only possible if $\Sigma_{0,h} \neq 0$. However, setting $\Sigma_{0,h} = 0$ does not allow for a solution that is asymptotically flat at large radii.

curvature invariants, i.e. these solutions seem to present a finite-area curvature singularity at the spin-0 horizon. Indeed, because all free parameters of the solution were determined by imposing regularity at the metric horizon and by the boundary conditions at spatial infinity, that singularity, which was already visible in the field equations (56) and (57), seems almost unavoidable, and reminiscent of similar finite-area curvature singularities appearing at the spin-1 horizon of slowly rotating BHs in Einstein-æther theory [25]. Nevertheless, we will further investigate this singularity, and in particular whether it can be avoided thanks to a field redefinition, in the next section.

C. Solutions regular at the matter and spin-0 horizon

Curvature singularities at the spin-0 horizon also appear when studying spherical BHs in Hořava gravity and Einstein-Æther theory. Indeed, Ref. [19] found a two-parameter family of asymptotically flat, static and spherically symmetric BH solutions in those theories. One of the two free parameters is the mass of the BH, while the second is a “hair” regulating whether the spin-0 horizon is singular or not. Indeed, after imposing regularity at the matter horizon, for generic values of this parameter the spin-0 horizon is singular, and regularity at that location is obtained only for one specific, “tuned” value of that parameter. (That value is a function of the mass and the coupling constants of the theory.)

As argued in the previous section, in our case we have no free parameter to tune to impose regularity at the spin-0 horizon, which we therefore expect to be singular. Indeed, when we integrate inwards the asymptotically flat and regular (at the matter horizon) solution, we find that the curvature invariant diverge at the spin-0 horizon, already in regions where our numerical scheme is not yet breaking down. This is shown in Fig. 1, which plots the fastest growing curvature invariant of the geometry, as well as the constraint violations occurring in the numerical integration.

To verify even further the existence of a curvature singularity at the spin-0 horizon, one can follow Ref. [19] and note that the action (5) is invariant under the field redefinition [53]

$$g'_{\mu\nu} = g_{\mu\nu} + (\zeta - 1)u_\mu u_\nu, \quad T' = T, \quad (61)$$

where ζ is a constant, provided that the original α , β and λ are replaced by α' , β' and λ' satisfying

$$\begin{aligned} \alpha' &= \alpha, \\ \beta' + \lambda' &= \zeta(\beta + \lambda), \\ \beta' - 1 &= \zeta(\beta - 1). \end{aligned} \quad (62)$$

Choosing in particular $\zeta = s_0^2$, the redefined metric g' coincides with the spin-0 metric [c.f. eq. (43)]. This

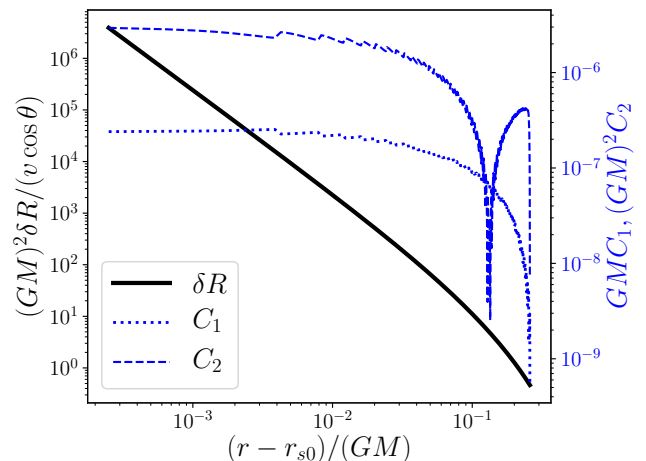


FIG. 1. $\mathcal{O}(v)$ contribution to the Ricci scalar near the spin-0 horizon, for the asymptotically flat solution regular at the matter horizon, and for $\alpha = 0.02$, $\beta = 0.01$ and $\lambda = 0.1$.

therefore allows one to cast the original problem, characterized by the metric g and the couplings α , β , λ , into one involving the spin-0 metric $g' = g^{(0)}$ and the new couplings α' , β' and λ' . The advantage of this second “spin-0 frame” is that the matter and spin-0 horizons now coincide (as they are both defined in terms of characteristics of the metric $g' = g^{(0)}$, i.e. by the condition $g'_{\nu\nu} = 0$ in spherical symmetry), so one can easily impose regularity at both. This is indeed the way Ref. [19] imposes regularity at both the matter and spin-0 horizon in the spherical static case.

Working therefore in the spin-0 frame, we impose regularity at the matter/spin-0 horizon location r_h by solving the evolution and constraint equations perturbatively with the ansatz given by Eq. (58). (Analyticity of the potentials δ , χ , ψ and Σ is again required to ensure finiteness of the invariants constructed with the metric, the æther vector, and the Killing vectors.) The number of free parameters of the resulting solution is however different than what we obtained in Sec. V B. This is because in the spin-0 frame one has $s_0 = 1$ (this can be verified explicitly by using the new coupling parameters given by Eq. (62), with $\zeta = s_0^2$, into Eq. (16a)), which changes the structure of the equations because of the presence of factors $s_0^2 - 1$ as denominators. (The explicit form of the equations is again too long to show and hardly enlightening.) As a result, the perturbative solution described by Eq. (58) has one, rather than two, free parameters.

Setting that parameter (say $\delta_{0,h}$) to zero yields the trivial solution $\delta(r) = \chi(r) = \psi(r) = \Sigma(r) = 0$. If instead $\delta_0 \neq 0$, homogeneity allows rescaling it to $\delta_{0,h} = 1$, i.e. the near-horizon solution has no free parameter which can be tuned to ensure that the solution reduces to a khronon moving with speed $-v$ on flat space at spatial infinity. Indeed, we have verified that the solution obtained by imposing regularity at the matter/spin-0 horizon and

integrating outwards is not asymptotically flat.

Moreover, as mentioned in Sec. VB, the field equations for the potentials δ , χ , ψ and Σ also present a singularity at the universal horizon. Therefore, even if one is willing to accept as physically relevant a BH with non-flat asymptotic boundary conditions, such a solution has no free parameters to tune to impose regularity at the universal horizon either. Indeed, we have verified that integrating the solution inwards from the (regular) spin-0/matter horizon, the curvature invariants blow up at the universal horizon (c.f. Fig. 2, where we also show the violations of the constraints).

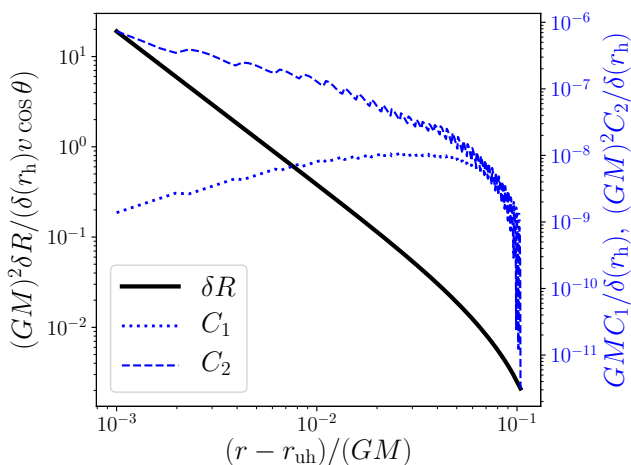


FIG. 2. $\mathcal{O}(v)$ contribution to the Ricci scalar near the universal horizon, in the spin-0 frame, for the solution regular at both the matter and spin-0 horizon. The theory's parameters are $\alpha = 0.02$, $\beta = 0.01$ and $\lambda = 0.1$, corresponding to $\alpha' = 0.02$, $\beta' = -4.161$ and $\lambda' = 4.735$. Note that this solution is not asymptotically flat, as discussed in the text, and that it is determined up to a global rescaling. Because of this, we normalize $\mathcal{O}(v)$ contribution to the Ricci scalar by the value of δ at the matter/spin-0 horizon.

To further validate this result, we have also tried to first impose regularity at the universal horizon, and then integrate outwards trying to match with the solution obtained by imposing regularity at the spin-0/matter horizon. In practice, we impose regularity at the universal horizon by solving the field equations perturbatively with the ansatz given by Eq. (58), where r_h is now meant to denote the universal horizon. (Barring cancellations, analyticity of the potentials is once again required to ensure that the æther, the two Killing vectors and the geometry are generically regular, i.e. that invariants constructed with the curvature tensors, the æther and the Killing vectors remain finite.)

Rescaling the solution by exploiting again the homogeneity of the problem, we are left with just two free

parameters⁵, which we try to tune by matching to the solution that is regular at the spin-0/matter horizon. That solution being completely determined, up to a global rescaling, necessary conditions for matching include the continuity conditions

$$\Delta\left(\frac{\delta'}{\delta}\right) = \Delta\left(\frac{\chi'}{\chi}\right) = \Delta\left(\frac{\psi'}{\psi}\right) = 0, \quad (63)$$

where $\Delta(X'/X)$ denotes the difference between X'/X (with $X = \delta, \chi, \psi$) given by the two solutions, at some reference point between the spin-0/matter horizon and the universal horizon. Note that it does not make sense to impose continuity of the two solutions ($\Delta X = 0$), since we have used the rescaling freedom of the problem to renormalize both. That rescaling clearly cancels out when considering the ratios X'/X . Note also that it does not make sense to impose continuity of Σ'/Σ , since Σ satisfies a first order equation (c.f. Eq. (56d)).

Quite unsurprisingly, we have verified numerically that for generic values of the coupling constants, the three conditions of eq. (63) cannot be all satisfied by tuning the two free parameters of the solutions regular at the universal horizon. The conclusion is therefore that even if one gives up asymptotic flatness, for generic values of the coupling the universal horizon is a finite-area curvature singularity. This is reminiscent of the occurrence of similar finite-area singularities at all but the outermost spin-1 horizon of slowly rotating BHs in Einstein-æther theory. Quite suggestively, Ref. [20] also finds that the universal horizon is unstable at second order in perturbation theory in khronometric theory and in the eikonal limit, and conjectures that it will become a finite-area curvature singularity. While our result is obtained in a completely different framework, it is interesting that it hints at the same conclusion.

VI. THE $\alpha = \beta = 0$ CASE

The results of Sec. V on the non-existence of slowly moving BH solutions regular everywhere outside $r = 0$ apply for generic values of the coupling constants, i.e. $\alpha, \beta, \lambda \neq 0$. As we have shown, it is possible to attain regularity of the spin-0 and matter horizons (even though at the cost of giving up asymptotic flatness), but regularity of the universal horizon remains impossible.

⁵More precisely, if we assume $\Sigma_{0,h} \neq 0$, we can use the rescaling freedom to set $\Sigma_{0,h} = 1$. This results in two free parameters, say $\delta_{0,h}$ and $\chi_{0,h}$. If instead $\Sigma_{0,h} = 0$, one is still left with two free parameters, say $\delta_{0,h}$ and $\chi_{0,h}$, and we can then use the rescaling freedom to set either to 1. Therefore, if $\Sigma_{0,h} = 0$ one has just one free parameter, which makes the matching to the solution regular at the spin-0/matter horizon even more difficult to achieve. We have indeed verified that the matching is not possible if one assumes $\Sigma_{0,h} = 0$.

However, if the coupling constants are such that the spin-0 speed s_0 diverges, the spin-0 horizon coincides with the universal horizon (since the latter is the horizon for modes of infinite speed). Therefore, imposing regularity of the universal horizon, spin-0 and matter horizons may become possible in that limit. From eq. (16a) it follows that $s_0 \rightarrow \infty$ when $\alpha \rightarrow 0$. This limit is particularly attractive as $|\alpha| \lesssim 10^{-7}$ experimentally (c.f. Sec. II A). Assuming $\alpha = 0$ alone, however, does not avoid the appearance of finite-area singularities at the universal/metric horizon, as can be seen from Fig. 3, where we show the divergence of the curvature invariants of the asymptotically flat solution regular at the matter horizon.

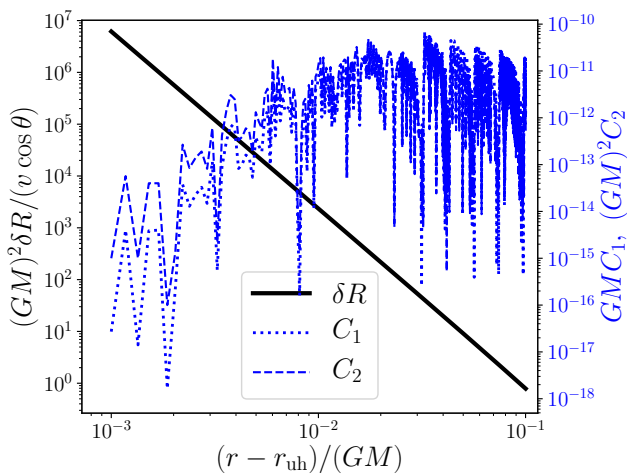


FIG. 3. $\mathcal{O}(v)$ contribution to the Ricci scalar near the universal/spin-0 horizon, for the asymptotically flat solution regular at the matter horizon, and for $\alpha = 0$, $\beta = 0.01$ and $\lambda = 0.1$.

However, from the experimental limits presented in Sec. II A, it follows that $|\beta| \lesssim 10^{-15}$, so it is attractive to also set $\beta = 0$ exactly. Indeed, spherical BH solutions for $\alpha = \beta = 0$ are very simple and known analytically in this limit, and are given by eqs. (45a)–(45c). Note in particular that the metric matches the Schwarzschild solution.

By solving the evolution and constraint equations near the metric horizon r_h by imposing regularity there, i.e. with the ansatz of eq. (58), one immediately finds that Σ and ψ must be exactly zero near r_h , i.e. $\Sigma = \mathcal{O}(r - r_h)^{n_{\max}}$ and $\psi = \mathcal{O}(r - r_h)^{n_{\max}}$, where n_{\max} is the order at which the series of eq. (58) is truncated. We have indeed verified this for n_{\max} as large as 10 or more. One reaches the same conclusions by considering series-expanded solutions to the field equations around any other radius (different from the metric horizon). Moreover, to further verify that Σ and ψ vanish, we have then replaced $\Sigma(r) = \psi(r) = 0$ in the field equations (56a)–(56d). The system is in principle overdetermined, but it turns out to

consist of just two independent equations:

$$\delta'(r) + \frac{4(8r^4 + 4G_N\tilde{m}r^3 - 27(G_N\tilde{m})^4)}{16r^5 - 21G_N\tilde{m}r^4 + 27(G_N\tilde{m})^4r} \delta(r) - \frac{32r^2}{16r^4 - 21G_N\tilde{m}r^3 + 27(G_N\tilde{m})^4} \chi(r) = 0, \quad (64)$$

$$\chi'(r) - \delta(r) = 0. \quad (65)$$

Note that these equations do not depend on λ , which we have anyway kept different from zero.

Eliminating χ from eqs. (64)–(65) then yields

$$\left(\frac{r^2}{2} - G_N\tilde{m}r + \frac{27(G_N\tilde{m})^4}{32r^2}\right) \delta''(r) + \left(2r - \frac{3G_N\tilde{m}}{2} - \frac{81(G_N\tilde{m})^4}{16r^3}\right) \delta'(r) + \frac{81(G_N\tilde{m})^4}{8r^4} \delta(r) = 0. \quad (66)$$

Solving this equation near spatial infinity gives

$$\delta(r) = \delta_0 + \frac{\delta_3}{r^3} + \mathcal{O}\left(\frac{1}{r^4}\right), \quad (67)$$

where δ_0 and δ_3 are integration constants. This in turn implies, through eq. (64), that $\chi(r)$ behaves asymptotically as

$$\chi(r) = \delta_0 r + \chi_0 - \frac{\delta_3}{2r^2} + \mathcal{O}\left(\frac{1}{r^4}\right), \quad (68)$$

where $\chi_0 = -\frac{G_N\tilde{m}}{2}\delta_0$. Replacing this relation in eq. (60) and evaluating for $\alpha = \beta = 0$ gives a vanishing sensitivity $\sigma = 0$. This result had to be expected from the fact that eqs. (64)–(66) do not depend on λ , and that σ must go to zero in the general-relativistic limit $\lambda \rightarrow 0$.

Moreover, one can push the argument even further, and note that since it is independent of λ and because it must reduce to the Schwarzschild solution in the general-relativistic limit $\lambda \rightarrow 0$, the solution to eqs. (64)–(65) must be the Schwarzschild metric in a weird gauge. Indeed, it is easy to check that the metric of eq. (50), with $\psi = \Sigma = 0$, becomes the Schwarzschild metric in Eddington-Finkelstein coordinates if one performs the gauge transformation $v' = v + v \chi(r) \cos \theta + \mathcal{O}(v)^2$ (note that we need to use eq. (65) to set $\chi'(r) = \delta(r)$).

In spite of this, the khronon field profile is non-trivial (even though its stress energy must vanish through order $\mathcal{O}(v)$ to allow for the metric to coincide with the Schwarzschild solution, i.e. the khronon is a “stealth” field). In more detail, even though it is clear that the universal horizon is more a regular surface (since the Schwarzschild metric has no curvature singularity at $r \neq 0$), it is interesting to look for an approximate solution to eq. (66) near the universal horizon position $r_{\text{uh}} = 3G_N\tilde{m}/2$, at which the equations are singular. For $r \approx r_{\text{uh}}$, eq. (66) becomes

$$x^2 \delta''(x) + 5x \delta'(x) + 2\delta(x) \simeq 0, \quad (69)$$

with $x = r - r_{\text{uh}}$, which yields the general solution

$$\delta(x) \simeq C_h x^{-\sqrt{2}(1+\sqrt{2})} + C_s x^{\sqrt{2}(1-\sqrt{2})}. \quad (70)$$

where C_h and C_s are integration constants (we refer to the mode with coefficient C_h as the “hard mode”, because it diverges faster than the “soft mode” with coefficient C_s).

While both the soft and hard modes diverge as $r \rightarrow r_{\text{uh}}$, it is easy to check that the curvature invariants R , $R_{\alpha\beta}R^{\alpha\beta}$ and $R_{\alpha\beta\gamma\delta}R^{\alpha\beta\gamma\delta}$ are regular (which must be the case since the metric is Schwarzschild in disguise). One can look however also at curvature invariants constructed with the æther vector and with the Killing vectors ∂_v and ∂_ϕ . The only non-trivial invariant (at order $\mathcal{O}(v)$) of these invariants is

$$R_{\mu\nu\alpha\beta} u^\mu u^\alpha (\partial_v)^\nu (\partial_v)^\beta \propto \cos\theta x^3 \delta(x). \quad (71)$$

Using eq. (70), this becomes

$$R_{\mu\nu\alpha\beta} u^\mu u^\alpha (\partial_v)^\nu (\partial_v)^\beta \propto \cos\theta (C_h x^{n_h} + C_s x^{n_s}), \quad (72)$$

with $n_h = 1 - \sqrt{2} < 0$ and $n_s = 1 + \sqrt{2} > 0$. Therefore, the hard mode produces a singularity at the universal horizon, while the soft mode is physically well-behaved.

One can therefore set $C_h = 0$ in eq. (70), set $C_s = 1$ by rescaling the solution (without loss of generality), and then use eq. (70) to provide initial conditions at $r = r_{\text{uh}}(1 + \epsilon)$ (with $\epsilon \ll 1$) for eq. (66). Integrating that equation outwards and matching to eq. (67), one can extract the integration constants δ_0 and δ_3 . Finally, one can rescale the obtained solution by a global factor to impose the boundary condition $\delta_0 = -1$ (c.f. Sec. IV B). Eq. (64) then allows one to obtain χ . The resulting solution for

$$\frac{\delta u_v}{v \cos\theta} = -\frac{(1 - A(r)^2 f(r)) (1 + A(r)^2 f(r))^2}{8A(r)^3} \delta(r), \quad (73)$$

$$\frac{\delta u_r}{v \cos\theta} = -\frac{(1 + A(r)^2 f(r))^2}{4A(r)} \delta(r), \quad (74)$$

is shown in Fig. 4.

Note that both quantities are regular at the universal horizon (as can also be verified analytically using the soft mode of the solution given by eq. (70)), which confirms that the khronon field is regular there.

VII. CONCLUSIONS

We have studied non-spinning BHs moving slowly compared to the preferred foliation of khronometric theory (the low energy limit of Hořava gravity). We have done so by reducing the field equations (through first order $\mathcal{O}(v)$ in the velocity relative to the preferred frame) to a system of ordinary differential equations in the radial coordinate, thanks to suitable ansätze for the metric and

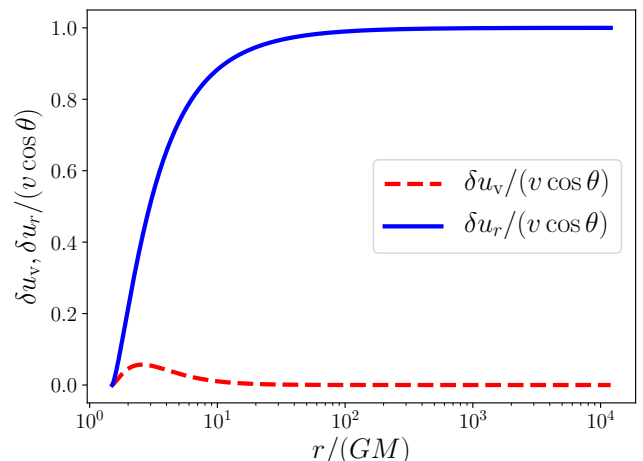


FIG. 4. $\mathcal{O}(v)$ æther perturbations δu_μ for the unique regular solution of the $\alpha = \beta = 0$ case, outside the universal/spin-0 horizon.

khronon fields, inspired by the cylindrical symmetry of the system. We have solved these equations numerically trying to impose both asymptotic flatness, and regularity at the multiple BH horizons that exist in Hořava gravity, i.e. the matter horizon; the horizons for spin-0 and spin-2 gravitons, and the universal horizon for modes whose speed diverges in the UV. While regularity at the spin-2 horizon does not pose any particular issue (as expected since spin-2 modes do not appear at order $\mathcal{O}(v)$), regularity at the other horizons is more problematic.

We have indeed found that if one imposes regularity at the matter horizon and asymptotic flatness, slowly moving BHs necessarily present (for generic values of the dimensionless coupling parameters α , β and λ) a curvature singularity at the spin-0 horizon (which lies inside the matter horizon for experimentally viable values of α , β and λ). By waiving the requirement of asymptotic flatness, solutions that are regular at the matter and spin-0 horizons can be obtained, but those are singular further inside, as they present a curvature singularity at the universal horizon. These pathological features cast doubts on the viability of the theory for generic values of the coupling parameters, although these curvature singularities strictly speaking signal simply that our slow-motion approximate scheme (which assumes implicitly that the “potentials” are small) breaks down. Also, these curvature singularities will probably be smoothed out by the higher energy UV corrections L_4 and L_6 in the Hořava gravity action (c.f. eq. (1)).

Nevertheless, adopting generic values of the coupling parameters α and β is not necessarily justified. The experimental constraints that we have reviewed in Sec. II A imply $|\alpha| \lesssim 10^{-7}$ and $|\beta| \lesssim 10^{-15}$, hence it would be quite natural to assume that α and β are *exactly* zero. In that case, slowly moving BH solutions exist and are regular everywhere outside the central $r = 0$ singularity.

More importantly, even though the gravitational theory is different than GR (because $\lambda \neq 0$), the khronon is a non-trivial “stealth” field in these BH solutions, whose metric therefore reduces exactly to the Schwarzschild one. This implies in particular that BH sensitivities are exactly zero for $\alpha = \beta = 0$, hence BH binaries do not emit dipolar radiation in this limit, nor they deviate from GR at Newtonian order in the conservative sector (c.f. eq. (26)).⁶ Indeed, these results confirm the conclusion of Refs. [39], namely that vacuum asymptotically flat solutions to khronometric theories with $\alpha = \beta = 0$ coincide with the general relativistic ones even though $\lambda \neq 0$.

We therefore expect GW generation to agree exactly with GR even at higher PN orders (quadrupolar emission and higher) if $\alpha = \beta = 0$. This is quite important from an observational point of view, because it implies that even if our results for the appearance of finite-area singularities in moving BHs were just an artifact of the breakdown of our approximation scheme, and moving BHs turned out to be regular (away from $r = 0$), deviations from GR in GW generation are bound to be small. Indeed, in such a situation, deviations away from the GR predictions for GW emission should be expected to be of (fractional) order $\mathcal{O}[\max(\alpha, \beta)] \sim 10^{-7}$ for viable values of $\alpha, \beta \neq 0$. Such small deviations are unlikely to be observable with present and future GW detectors, although the viable parameter space for α, β may further shrink by observations of GW and electromagnetic-wave propagation in multimessenger events.

However, if finite area singularities do indeed form in

moving BHs (though perhaps smoothed out by UV corrections), they could produce firewall-like surfaces that may in principle be tested with GW echos [54] or stochastic background measurements from LIGO/Virgo. As for λ , it is likely that improved constraints on it may come from cosmology. As mentioned, Ref. [39] showed that CMB measurements constrain $0 \neq \lambda \lesssim 10^{-2}$ when $\alpha = \beta = 0$, and one would expect this bound to be robust against small but finite values of α and β . Further improvements may come from future CMB experiments and/or from Euclid.

ACKNOWLEDGMENTS

We would like to warmly thank Daniele Steer, Niayesh Afshordi and Eugene Lim for providing insightful comments about this work. We also thank Ted Jacobson, Thomas Sotiriou, Diego Blas, Cliff Will and Anna Heffernan for useful discussions about Lorentz violating gravity and GW emission in theories of gravity extending GR. O.R. acknowledges support from a Lagrange Thesis Fellowship of the Institut Lagrange de Paris (ILP LABEX ANR-10-LABX-63), supported through the Investissements d’Avenir program under reference ANR-11-IDEX-0004-02. This project has received funding from the European Union’s Horizon 2020 research and innovation programme under the Marie Skłodowska-Curie grant agreement No 690904.

-
- [1] D. Colladay and V. A. Kostelecky, *Phys. Rev.* **D58**, 116002 (1998), arXiv:hep-ph/9809521 [hep-ph].
 - [2] V. A. Kostelecky, in *Physics of mass. Proceedings, 26th International Conference, Orbis Scientiae, Miami Beach, USA, December 12-15, 1997* (1998) pp. 89–94, arXiv:hep-ph/9810239 [hep-ph].
 - [3] V. A. Kostelecky, in *Beyond the desert: Accelerator, non-accelerator and space approaches into the next millennium. Proceedings, 2nd International Conference on particle physics beyond the standard model, Ringberg Castle, Tegernsee, Germany, June 6-12, 1999* (1999) pp. 151–163, arXiv:hep-ph/9912528 [hep-ph].
 - [4] A. O. Barvinsky, D. Blas, M. Herrero-Valea, S. M. Sibiryakov, and C. F. Steinwachs, *Phys. Rev. Lett.* **119**, 211301 (2017), arXiv:1706.06809 [hep-th].
 - [5] A. Coates, C. Melby-Thompson, and S. Mukohyama, (2018), arXiv:1805.10299 [hep-th].
 - [6] G. Bednik, O. Pujolas, and S. Sibiryakov, *JHEP* **11**, 064 (2013), arXiv:1305.0011 [hep-th].
 - [7] S. Groot Nibbelink and M. Pospelov, *Phys. Rev. Lett.* **94**, 081601 (2005), arXiv:hep-ph/0404271 [hep-ph].
 - [8] M. Pospelov and Y. Shang, *Phys. Rev.* **D85**, 105001 (2012), arXiv:1010.5249 [hep-th].
 - [9] V. A. Kostelecký and M. Mewes, *Phys. Lett.* **B757**, 510 (2016), arXiv:1602.04782 [gr-qc].
 - [10] T. Jacobson and D. Mattingly, *Phys. Rev.* **D64**, 024028 (2001), arXiv:gr-qc/0007031 [gr-qc].
 - [11] D. Blas, O. Pujolas, and S. Sibiryakov, *Phys. Rev. Lett.* **104**, 181302 (2010), arXiv:0909.3525 [hep-th].
 - [12] P. Hořava, *JHEP* **03**, 020 (2009), arXiv:0812.4287 [hep-th].
 - [13] P. Hořava, *Phys. Rev.* **D79**, 084008 (2009), arXiv:0901.3775 [hep-th].
 - [14] A. O. Barvinsky, D. Blas, M. Herrero-Valea, S. M. Sibiryakov, and C. F. Steinwachs, *Phys. Rev.* **D93**, 064022 (2016), arXiv:1512.02250 [hep-th].
 - [15] T. Jacobson and D. Mattingly, *Phys. Rev.* **D70**, 024003 (2004), arXiv:gr-qc/0402005 [gr-qc].
 - [16] D. Blas and H. Sanctuary, *Phys. Rev.* **D84**, 064004 (2011), arXiv:1105.5149 [gr-qc].
 - [17] A. Emir Gumrukcuoglu, M. Saravani, and T. P. Sotiriou, *Phys. Rev.* **D97**, 024032 (2018), arXiv:1711.08845 [gr-qc].
 - [18] T. P. Sotiriou, *Phys. Rev. Lett.* **120**, 041104 (2018), arXiv:1709.00940 [gr-qc].
 - [19] E. Barausse, T. Jacobson, and T. P. Sotiriou, *Phys. Rev.*

⁶Note that from eq. (28), it follows immediately that dipolar radiation – regulated by the coefficient C – vanishes automatically in the case when $\alpha = \beta = 0$ (even if the sensitivities were non-zero), because the spin-0 speed diverges. That means that the spin-0 mode becomes non-dynamical, and in particular that it does not produce a GW flux.

- D83**, 124043 (2011), arXiv:1104.2889 [gr-qc].
- [20] D. Blas and S. Sibiryakov, Phys. Rev. **D84**, 124043 (2011), arXiv:1110.2195 [hep-th].
- [21] C. Eling and T. Jacobson, Class. Quant. Grav. **23**, 5643 (2006), [Erratum: Class. Quant. Grav.27,049802(2010)], arXiv:gr-qc/0604088 [gr-qc].
- [22] D. Garfinkle, C. Eling, and T. Jacobson, Phys. Rev. **D76**, 024003 (2007), arXiv:gr-qc/0703093 [GR-QC].
- [23] E. Barausse and T. P. Sotiriou, Phys. Rev. **D87**, 087504 (2013), arXiv:1212.1334 [gr-qc].
- [24] E. Barausse and T. P. Sotiriou, Phys. Rev. Lett. **109**, 181101 (2012), [Erratum: Phys. Rev. Lett.110,no.3,039902(2013)], arXiv:1207.6370 [gr-qc].
- [25] E. Barausse, T. P. Sotiriou, and I. Vega, Phys. Rev. **D93**, 044044 (2016), arXiv:1512.05894 [gr-qc].
- [26] J. Bhattacharyya, A. Coates, M. Colombo, and T. P. Sotiriou, Phys. Rev. **D93**, 064056 (2016), arXiv:1512.04899 [gr-qc].
- [27] K. Yagi, D. Blas, E. Barausse, and N. Yunes, Phys. Rev. **D89**, 084067 (2014), [Erratum: Phys. Rev.D90,no.6,069901(2014)], arXiv:1311.7144 [gr-qc].
- [28] T. Damour and G. Esposito-Farese, Classical and Quantum Gravity **9**, 2093 (1992).
- [29] T. Damour and G. Esposito-Farèse, Phys. Rev. Lett. **70**, 2220 (1993).
- [30] P. C. C. Freire, N. Wex, G. Esposito-Farese, J. P. W. Verbiest, M. Bailes, B. A. Jacoby, M. Kramer, I. H. Stairs, J. Antoniadis, and G. H. Janssen, Mon. Not. Roy. Astron. Soc. **423**, 3328 (2012), arXiv:1205.1450 [astro-ph.GA].
- [31] N. Wex, (2014), arXiv:1402.5594 [gr-qc].
- [32] D. M. Eardley, **196**, L59 (1975).
- [33] C. M. Will and H. W. Zaglauer, Astrophys. J. **346**, 366 (1989).
- [34] E. Barausse, N. Yunes, and K. Chamberlain, Phys. Rev. Lett. **116**, 241104 (2016), arXiv:1603.04075 [gr-qc].
- [35] L. Blanchet, Living Rev. Rel. **17**, 2 (2014), arXiv:1310.1528 [gr-qc].
- [36] M. Fierz, Helv. Phys. Acta **29**, 128 (1956).
- [37] P. Jordan, Z. Phys. **157**, 112 (1959).
- [38] C. Brans and R. H. Dicke, Phys. Rev. **124**, 925 (1961), [142(1961)].
- [39] N. Afshordi, Phys. Rev. **D80**, 081502 (2009), arXiv:0907.5201 [hep-th].
- [40] S. M. Carroll and E. A. Lim, Phys. Rev. **D70**, 123525 (2004), arXiv:hep-th/0407149 [hep-th].
- [41] T. Jacobson, Phys. Rev. **D81**, 101502 (2010), [Erratum: Phys. Rev.D82,129901(2010)], arXiv:1001.4823 [hep-th].
- [42] C. D. Froggatt and H. B. Nielsen, *Origin of symmetries* (1991).
- [43] S. Chadha and H. B. Nielsen, Nucl. Phys. **B217**, 125 (1983).
- [44] D. Blas, O. Pujolas, and S. Sibiryakov, JHEP **04**, 018 (2011), arXiv:1007.3503 [hep-th].
- [45] C. M. Will, Living Rev. Rel. **17**, 4 (2014), arXiv:1403.7377 [gr-qc].
- [46] E. Barausse and T. P. Sotiriou, Class. Quant. Grav. **30**, 244010 (2013), arXiv:1307.3359 [gr-qc].
- [47] G. D. Moore and A. E. Nelson, JHEP **09**, 023 (2001), arXiv:hep-ph/0106220 [hep-ph].
- [48] J. W. Elliott, G. D. Moore, and H. Stoica, JHEP **08**, 066 (2005), arXiv:hep-ph/0505211 [hep-ph].
- [49] B. P. Abbott *et al.*, Astrophys. J. **848**, L12 (2017), arXiv:1710.05833 [astro-ph.HE].
- [50] B. Audren, D. Blas, J. Lesgourgues, and S. Sibiryakov, JCAP **1308**, 039 (2013), arXiv:1305.0009 [astro-ph.CO].
- [51] I. Carruthers and T. Jacobson, Phys. Rev. **D83**, 024034 (2011), arXiv:1011.6466 [gr-qc].
- [52] B. Z. Foster, Phys. Rev. **D76**, 084033 (2007), arXiv:0706.0704 [gr-qc].
- [53] B. Z. Foster, Phys. Rev. **D72**, 044017 (2005), arXiv:gr-qc/0502066 [gr-qc].
- [54] V. Cardoso, E. Franzin, and P. Pani, Phys. Rev. Lett. **116**, 171101 (2016), [Erratum: Phys. Rev. Lett.117,no.8,089902(2016)], arXiv:1602.07309 [gr-qc].

Bibliographie

- [1] C. W. MISNER, K. S. THORNE & J. A. WHEELER; *Gravitation* (W. H. Freeman, San Francisco) (1973); ISBN 9780716703440. :1974qy
- [2] M. MAGGIORE; *Gravitational Waves. Vol. 1 : Theory and Experiments*; Oxford Master Series in Physics (Oxford University Press) (2007); ISBN 9780198570745, 9780198520740. <http://www.oup.com/uk/catalogue/?ci=9780198570745>. :1900zz
- [3] E. E. FLANAGAN & S. A. HUGHES; «The Basics of gravitational wave theory»; <http://dx.doi.org/10.1088/1367-2630/7/1/204>New J. Phys. **7**, p. 204 (2005). gr-qc/0501041. :2005yc
- [4] M. BONETTI, E. BARAUSSE, G. FAYE, F. HAARDT & A. SESANA; «About gravitational-wave generation by a three-body system»; <http://dx.doi.org/10.1088/1361-6382/aa8da5>Class. Quant. Grav. **34**, p. 215 004 (2017). 1707.04902. :2017hnb
- [5] R. A. HULSE & J. H. TAYLOR; «Discovery of a pulsar in a binary system»; <http://dx.doi.org/10.1086/181708>Astrophys. J. **195**, p. L51–L53 (1975). :1974eb
- [6] J. M. WEISBERG & J. H. TAYLOR; «Relativistic binary pulsar B1913+16 : Thirty years of observations and analysis»; ASP Conf. Ser. **328**, p. 25 (2005)astro-ph/0407149. :2004hi
- [7] D. N. MATSAKIS, J. H. TAYLOR & T. M. EUBANKS; «A statistic for describing pulsar and clock stabilities.»; aap **326**, p. 924–928 (1997).
- [8] J. H. TAYLOR & J. M. WEISBERG; «A new test of general relativity : Gravitational radiation and the binary pulsar PS R 1913+16»; <http://dx.doi.org/10.1086/159690>Astrophys. J. **253**, p. 908–920 (1982). :1982zz
- [9] C. M. WILL; *Theory and Experiment in Gravitational Physics* (1993); ISBN 9780511564246. :1993hxx
- [10] C. M. WILL; «The Confrontation between General Relativity and Experiment»; <http://dx.doi.org/10.12942/lrr-2014-4>Living Rev. Rel. **17**, p. 4 (2014). 1403.7377. :2014kxa
- [11] G. HOBBS, R. MANCHESTER, A. TEOH & M. HOBBS; «The atnf pulsar catalogue»; IAU Symp. **218**, p. 139 (2004)astro-ph/0309219. :2003gk
- [12] I. H. STAIRS; «Testing General Relativity with Pulsar Timing»; <http://dx.doi.org/10.12942/lrr-2003-5>Living Rev. Rel. (2003). 1403.7377.
- [13] O. LOHMER, W. LEWANDOWSKI, A. WOLSZCZAN & R. WIELEBINSKI; «Shapiro delay in the PSR J1640+2224 binary system»; <http://dx.doi.org/10.1086/427404>Astrophys. J. **621**, p. 388–392 (2005). astro-ph/0411742. :2004zu

- [14] P. DEMOREST, T. PENNUCCI, S. RANSOM, M. ROBERTS & J. HESSELS; «Shapiro Delay Measurement of A Two Solar Mass Neutron Star»; <http://dx.doi.org/10.1038/nature09466> *Nature* **467**, p. 1081–1083 (2010). 1010.5788. :2010bx
- [15] J. ABADIE *et al.*; «Search for gravitational waves from low mass compact binary coalescence in LIGO’s sixth science run and Virgo’s science runs 2 and 3»; <http://dx.doi.org/10.1103/PhysRevD.85.082002> *Phys. Rev. D* **85**, p. 082002 (2012). <https://link.aps.org/doi/10.1103/PhysRevD.85.082002>.
- [16] J. AASI *et al.*; «Gravitational waves from known pulsars : results from the initial detector era»; <http://dx.doi.org/10.1088/0004-637X/785/2/119> *Astrophys. J.* **785**, p. 119 (2014). 1309.4027. :2013sia
- [17] N. ANDERSSON & G. L. COMER; «Probing Neutron-Star Superfluidity with Gravitational-Wave Data»; <http://dx.doi.org/10.1103/PhysRevLett.87.241101> *Phys. Rev. Lett.* **87**, p. 241101 (2001). <https://link.aps.org/doi/10.1103/PhysRevLett.87.241101>.
- [18] C. D. OTT; «The gravitational-wave signature of core-collapse supernovae»; *Classical and Quantum Gravity* **26**, p. 063001 (2009) <http://stacks.iop.org/0264-9381/26/i=6/a=063001>.
- [19] B. P. ABBOTT *et al.*; «An Upper Limit on the Stochastic Gravitational-Wave Background of Cosmological Origin»; <http://dx.doi.org/10.1038/nature08278> *Nature* **460**, p. 990 (2009). 0910.5772. :2009ws
- [20] J. ABADIE *et al.*; «Predictions for the Rates of Compact Binary Coalescences Observable by Ground-based Gravitational-wave Detectors»; <http://dx.doi.org/10.1088/0264-9381/27/17/173001> *Class. Quant. Grav.* **27**, p. 173001 (2010). 1003.2480. :2010cf
- [21] J. AASI *et al.*; «Advanced LIGO»; <http://dx.doi.org/10.1088/0264-9381/32/7/074001> *Class. Quant. Grav.* **32**, p. 074001 (2015). 1411.4547. :2014jea
- [22] B. P. ABBOTT *et al.*; «Observation of Gravitational Waves from a Binary Black Hole Merger»; <http://dx.doi.org/10.1103/PhysRevLett.116.061102> *Phys. Rev. Lett.* **116**, p. 061102 (2016). <https://link.aps.org/doi/10.1103/PhysRevLett.116.061102>.
- [23] B. P. ABBOTT *et al.*; «Observation of Gravitational Waves from a Binary Black Hole Merger»; <http://dx.doi.org/10.1103/PhysRevLett.116.061102> *Phys. Rev. Lett.* **116**, p. 061102 (2016). 1602.03837. :2016blz
- [24] B. P. ABBOTT *et al.*; «The Rate of Binary Black Hole Mergers Inferred from Advanced LIGO Observations Surrounding GW150914»; <http://dx.doi.org/10.3847/2041-8205/833/1/L1> *Astrophys. J.* **833**, p. L1 (2016). 1602.03842. :2016nhf
- [25] S. VITALE & W. M. FARR; «Measuring the star formation rate with gravitational waves from binary black holes»; (2018)1808.00901. :2018yhm
- [26] B. P. ABBOTT *et al.*; «GW170817 : Observation of Gravitational Waves from a Binary Neutron Star Inspiral»; <http://dx.doi.org/10.1103/PhysRevLett.119.161101> *Phys. Rev. Lett.* **119**, p. 161101 (2017). <https://link.aps.org/doi/10.1103/PhysRevLett.119.161101>.

- [27] D. KOCEVSKI, N. OMODEI & G. VIANELLO; «Fermi-LAT observations of the LIGO/Virgo event GW170817»; (2017)1710.05450. :2017uvi
- [28] B. P. ABBOTT *et al.*; «Multi-messenger Observations of a Binary Neutron Star Merger»; <http://dx.doi.org/10.3847/2041-8213/aa91c9>*Astrophys. J.* **848**, p. L12 (2017). 1710.05833. :2017lvd
- [29] B. J. OWEN & B. S. SATHYAPRAKASH; «Matched filtering of gravitational waves from inspiraling compact binaries : Computational cost and template placement»; <http://dx.doi.org/10.1103/PhysRevD.60.022002>*Phys. Rev. D* **60**, p. 022002 (1999). gr-qc/9808076. :1998dk
- [30] S. A. USMAN & OTHERS; «The PyCBC search for gravitational waves from compact binary coalescence»; *Classical and Quantum Gravity* **33**, p. 215004 (2016)<http://stacks.iop.org/0264-9381/33/i=21/a=215004>.
- [31] B. S. SATHYAPRAKASH & S. V. DHURANDHAR; «Choice of filters for the detection of gravitational waves from coalescing binaries»; <http://dx.doi.org/10.1103/PhysRevD.44.3819>*Phys. Rev. D* **44**, p. 3819–3834 (1991). <https://link.aps.org/doi/10.1103/PhysRevD.44.3819>.
- [32] I. W. HARRY, B. ALLEN & B. S. SATHYAPRAKASH; «Stochastic template placement algorithm for gravitational wave data analysis»; <http://dx.doi.org/10.1103/PhysRevD.80.104014>*Phys. Rev. D* **80**, p. 104014 (2009). <https://link.aps.org/doi/10.1103/PhysRevD.80.104014>.
- [33] K. CANNON, R. CARIOU, A. CHAPMAN, M. CRISPIN-ORTUZAR, N. FOTOPOULOS, M. FREI, C. HANNA, E. KARA, D. KEPPEL, L. LIAO, S. PRIVITERA, A. SEARLE, L. SINGER & A. WEINSTEIN; «Toward Early-warning Detection of Gravitational Waves from Compact Binary Coalescence»; *The Astrophysical Journal* **748**, p. 136 (2012)<http://stacks.iop.org/0004-637X/748/i=2/a=136>.
- [34] P. AJITH, N. FOTOPOULOS, S. PRIVITERA, A. NEUNZERT, N. MAZUMDER & A. J. WEINSTEIN; «Effectual template bank for the detection of gravitational waves from inspiralling compact binaries with generic spins»; <http://dx.doi.org/10.1103/PhysRevD.89.084041>*Phys. Rev. D* **89**, p. 084041 (2014). <https://link.aps.org/doi/10.1103/PhysRevD.89.084041>.
- [35] T. DAL CANTON & I. W. HARRY; «Designing a template bank to observe compact binary coalescences in Advanced LIGO’s second observing run»; (2017)1705.01845. :2017ala
- [36] L. T. BUCHMAN, H. P. PFEIFFER, M. A. SCHEEL & B. SZILAGYI; «Simulations of non-equal mass black hole binaries with spectral methods»; <http://dx.doi.org/10.1103/PhysRevD.86.084033>*Phys. Rev. D* **86**, p. 084033 (2012). 1206.3015. :2012dw
- [37] T. CHU, H. P. PFEIFFER & M. A. SCHEEL; «High accuracy simulations of black hole binaries : Spins anti-aligned with the orbital angular momentum»; <http://dx.doi.org/10.1103/PhysRevD.80.124051>*Phys. Rev. D* **80**, p. 124051 (2009). 0909.1313. :2009md
- [38] A. TARACCHINI, A. BUONANNO, Y. PAN, T. HINDERER, M. BOYLE, D. A. HEMBERGER, L. E. KIDDER, G. LOVELACE, A. H. MROUE, H. P. PFEIFFER,

- M. A. SCHEEL, B. SZILAGYI, N. W. TAYLOR & A. ZENGINOGLU; «Effective-one-body model for black-hole binaries with generic mass ratios and spins»; <http://dx.doi.org/10.1103/PhysRevD.89.061502> Phys. Rev. D **89**, p. 061 502 (2014). <https://link.aps.org/doi/10.1103/PhysRevD.89.061502>.
- [39] L. BARACK & A. POUND; «Self-force and radiation reaction in general relativity»; (2018)1805.10385. :2018yvvs
- [40] M. VAN DE MEENT; «Modelling EMRIs with gravitational self-force : a status report»; <http://dx.doi.org/10.1088/1742-6596/840/1/012022> J. Phys. Conf. Ser. **840**, p. 012 022 (2017). :2017zgy
- [41] H. AUDLEY *et al.*; «Laser Interferometer Space Antenna»; (2017)1702.00786. :2017drz
- [42] M. ARMANO *et al.*; «Sub-Femto- g Free Fall for Space-Based Gravitational Wave Observatories : LISA Pathfinder Results»; <http://dx.doi.org/10.1103/PhysRevLett.116.231101> Phys. Rev. Lett. **116**, p. 231 101 (2016).
- [43] A. KING; «Black holes, galaxy formation, and the $M_{BH} - \sigma$ relation »; <http://dx.doi.org/10.1086/379143> *Astrophys. J.* **596**, p.L27 – –L30(2003).astro-ph/0308342.
- [44] R. ANTONUCCI; «Unified models for active galactic nuclei and quasars»; <http://dx.doi.org/10.1146/annurev.aa.31.090193.002353> Ann. Rev. Astron. Astrophys. **31**, p. 473–521 (1993). :1993sg
- [45] C. M. URRY & P. PADOVANI; «Unified schemes for radio-loud active galactic nuclei»; <http://dx.doi.org/10.1086/133630> Publ. Astron. Soc. Pac. **107**, p. 803 (1995).astro-ph/9506063. :1995mg
- [46] A. CELOTTI, J. C. MILLER & D. W. SCIAMA; «Astrophysical evidence for the existence of black holes : Topical review»; <http://dx.doi.org/10.1088/0264-9381/16/12A/301> Class. Quant. Grav. **16**, p. A3 (1999).astro-ph/9912186. :1999tg
- [47] A. SESANA, F. HAARDT, P. MADAU & M. VOLONTERI; «Low - frequency gravitational radiation from coalescing massive black hole binaries in hierarchical cosmologies»; <http://dx.doi.org/10.1086/422185> *Astrophys. J.* **611**, p. 623–632 (2004).astro-ph/0401543. :2004sp
- [48] M. PRETO, I. BERENTZEN, P. BERCIK, D. MERRITT & R. SPURZEM; «Merger of Massive Black Holes using N-Body Simulations with Post-Newtonian Corrections»; <http://dx.doi.org/10.1088/1742-6596/154/1/012049> J. Phys. Conf. Ser. **154**, p. 012 049 (2009). 0811.3501. :2008ua
- [49] F. ANTONINI & D. MERRITT; «Dynamical Friction around Supermassive Black Holes»; <http://dx.doi.org/10.1088/0004-637X/745/1/83> *Astrophys. J.* **745**, p. 83 (2012). 1108.1163. :2011tu
- [50] M. VOLONTERI; «Formation of Supermassive Black Holes»; <http://dx.doi.org/10.1007/s00159-010-0029-x> *Astron. Astrophys. Rev.* **18**, p. 279–315 (2010). 1003.4404. :2010wz
- [51] A. KLEIN *et al.*; «Science with the space-based interferometer eLISA : Supermassive black hole binaries»; <http://dx.doi.org/10.1103/PhysRevD.93.024003> Phys. Rev. **D93**, p. 024 003 (2016). 1511.05581. :2015hvg

- [52] G. NELEMANS, L. R. YUNGELSON & S. F. PORTEGIES ZWART; «The gravitational wave signal from the galactic disk population of binaries containing two compact objects»; <http://dx.doi.org/10.1051/0004-6361/20010683> *Astron. Astrophys.* **375**, p. 890–898 (2001). astro-ph/0105221. :2001hp
- [53] V. KOROL, E. M. ROSSI, P. J. GROOT, G. NELEMANS, S. TOONEN & A. G. A. BROWN; «Prospects for detection of detached double white dwarf binaries with Gaia, LSST and LISA»; <http://dx.doi.org/10.1093/mnras/stx1285> *Mon. Not. Roy. Astron. Soc.* **470**, p. 1894–1910 (2017). 1703.02555. :2017qcx
- [54] J. H. DEBES, M. KILIC, P.-E. TREMBLAY, M. LÚPEZ-MORALES, G. ANGLADA-ESCUDÓ, R. NAPIWOTZKI, D. OSIP & A. WEINBERGER; «A New Merging Double Degenerate Binary in the Solar Neighborhood»; <http://dx.doi.org/10.1088/0004-6256/149/5/176> *Astron. J.* **149**, p. 176 (2015). 1503.00349. :2015qra
- [55] M. KILIC, W. R. BROWN, A. GIANNINAS, J. J. HERMES, C. ALLENDE PRIETO & S. J. KENYON; «A New Gravitational Wave Verification Source»; <http://dx.doi.org/10.1093/mnrasl/slu093> *Mon. Not. Roy. Astron. Soc.* **444**, p. 1 (2014). 1406.3346. :2014fea
- [56] M. KILIC, W. R. BROWN, J. J. HERMES & A. GIANNINAS; «Gravitational Wave Verification Sources»; http://dx.doi.org/10.1007/978-3-319-10488-1_4 *Astrophys.SpaceSci.Proc.* **40**, p.167 – 173(2015).
- [57] V. KOROL, E. M. ROSSI & E. BARAUSSE; «A multi-messenger study of the Milky Way’s stellar disc and bulge with LISA, Gaia and LSST»; (2018)1806.03306. :2018wep
- [58] S. TOONEN, G. NELEMANS & S. PORTEGIES ZWART; «Supernova Type Ia progenitors from merging double white dwarfs : Using a new population synthesis model»; <http://dx.doi.org/10.1051/0004-6361/201218966> *Astron. Astrophys.* **546**, p. A70 (2012). 1208.6446. :2012jj
- [59] P. AMARO-SEOANE, J. R. GAIR, M. FREITAG, M. COLEMAN MILLER, I. MANDEL, C. J. CUTLER & S. BABAK; «Astrophysics, detection and science applications of intermediate- and extreme mass-ratio inspirals»; <http://dx.doi.org/10.1088/0264-9381/24/17/R01> *Class. Quant. Grav.* **24**, p. R113–R169 (2007). astro-ph/0703495. :2007aw
- [60] L. BARACK & C. CUTLER; «LISA capture sources : Approximate waveforms, signal-to-noise ratios, and parameter estimation accuracy»; <http://dx.doi.org/10.1103/PhysRevD.69.082005> *Phys. Rev.* **D69**, p. 082005 (2004). gr-qc/0310125. :2003fp
- [61] L. BARACK & C. CUTLER; «Confusion noise from LISA capture sources»; <http://dx.doi.org/10.1103/PhysRevD.70.122002> *Phys. Rev.* **D70**, p. 122002 (2004). gr-qc/0409010. :2004wc
- [62] L. BARACK & C. CUTLER; «Using LISA EMRI sources to test off-Kerr deviations in the geometry of massive black holes»; <http://dx.doi.org/10.1103/PhysRevD.75.042003> *Phys. Rev.* **D75**, p. 042003 (2007). gr-qc/0612029. :2006pq
- [63] R. PENROSE; «Gravitational collapse and space-time singularities»; <http://dx.doi.org/10.1103/PhysRevLett.14.57> *Phys. Rev. Lett.* **14**, p. 57–59 (1965). :1964wq

- [64] W. ISRAEL; «Event Horizons in Static Vacuum Space-Times»; <http://dx.doi.org/10.1103/PhysRev.164.1776> *Physical Review* **164**, p. 1776–1779 (1967).
- [65] S. W. HAWKING; «Black holes in general relativity»; <http://dx.doi.org/10.1007/BF01877517> *Commun. Math. Phys.* **25**, p. 152–166 (1972). :1971vc
- [66] A. SESANA; «Multi-band gravitational wave astronomy : science with joint space- and ground-based observations of black hole binaries»; <http://dx.doi.org/10.1088/1742-6596/840/1/012018> *J. Phys. Conf. Ser.* **840**, p. 012018 (2017). [,59(2017)]; 1702.04356. :2017vsj
- [67] A. SESANA; «Prospects for Multiband Gravitational-Wave Astronomy after GW150914»; <http://dx.doi.org/10.1103/PhysRevLett.116.231102> *Phys. Rev. Lett.* **116**, p. 231102 (2016). 1602.06951. :2016ljz
- [68] E. BARAUSSE, N. YUNES & K. CHAMBERLAIN; «Theory-Agnostic Constraints on Black-Hole Dipole Radiation with Multiband Gravitational-Wave Astrophysics»; <http://dx.doi.org/10.1103/PhysRevLett.116.241104> *Phys. Rev. Lett.* **116**, p. 241104 (2016). 1603.04075. :2016eii
- [69] K. NORDTVEDT; «Equivalence Principle for Massive Bodies. I. Phenomenology»; <http://dx.doi.org/10.1103/PhysRev.169.1014> *Phys. Rev.* **169**, p. 1014–1016 (1968). <https://link.aps.org/doi/10.1103/PhysRev.169.1014>.
- [70] P. G. ROLL, R. KROTKOV & R. H. DICKE; «The Equivalence of inertial and passive gravitational mass»; [http://dx.doi.org/10.1016/0003-4916\(64\)90259-3](http://dx.doi.org/10.1016/0003-4916(64)90259-3) *Annals Phys.* **26**, p. 442–517 (1964). :1964rd
- [71] T. DAMOUR & G. ESPOSITO-FARESE; «Tensor-multi-scalar theories of gravitation»; *Classical and Quantum Gravity* **9**, p. 2093 (1992)<http://stacks.iop.org/0264-9381/9/i=9/a=015>.
- [72] C. M. WILL & H. W. ZAGLAUER; «Gravitational Radiation, Close Binary Systems, and the Brans-dicke Theory of Gravity»; <http://dx.doi.org/10.1086/168016> *Astrophys. J.* **346**, p. 366 (1989). :1989sk
- [73] K. YAGI; «New constraint on scalar Gauss-Bonnet gravity and a possible explanation for the excess of the orbital decay rate in a low-mass x-ray binary»; <http://dx.doi.org/10.1103/PhysRevD.86.081504> *Phys. Rev. D* **86**, p. 081504 (2012). <https://link.aps.org/doi/10.1103/PhysRevD.86.081504>.
- [74] E. BARAUSSE; «Testing the strong equivalence principle with gravitational-wave observations of binary black holes»; *PoS KMI2017*, p. 029 (2017)1703.05699. :2017gip
- [75] B. P. ABBOTT *et al.*; «Tests of general relativity with GW150914»; <http://dx.doi.org/10.1103/PhysRevLett.116.221101> *Phys. Rev. Lett.* **116**, p. 221101 (2016). 1602.03841. :2016src
- [76] N. WEX; «Testing Relativistic Gravity with Radio Pulsars»; (2014)1402.5594. :2014nva
- [77] P. HORAVA; «Membranes at Quantum Criticality»; <http://dx.doi.org/10.1088/1126-6708/2009/03/020> *JHEP* **03**, p. 020 (2009). 0812.4287. :2008ih

- [78] P. HORAVA; «Quantum Gravity at a Lifshitz Point»; <http://dx.doi.org/10.1103/PhysRevD.79.084008> Phys. Rev. **D79**, p. 084 008 (2009). 0901.3775. :2009uw
- [79] G. GALILEI; *Discorsi e dimostrazioni matematiche, intorno a Due Nuove Scienze* (Italy) (1638); ISBN 9781483285276, 9781483283111. <https://www.elsevier.com/books/discorsi-e-dimostrazioni-matematiche/galilei/978-1-4832-8527-6>
- [80] S. WEINBERG; *The Quantum theory of fields. Vol. 1 : Foundations* (Cambridge University Press) (2005); ISBN 9780521670531, 9780511252044. :1995mt
- [81] R. H. KRAICHNAN; «Special-Relativistic Derivation of Generally Covariant Gravitation Theory»; <http://dx.doi.org/10.1103/PhysRev.98.1118> Phys. Rev. **98**, p. 1118–1122 (1955). :1955zz
- [82] S. WEINBERG; «Photons and gravitons in perturbation theory : Derivation of Maxwell's and Einstein's equations»; <http://dx.doi.org/10.1103/PhysRev.138.B988> Phys. Rev. **138**, p. B988–B1002 (1965). :1965rz
- [83] S. DESER; «Selfinteraction and gauge invariance»; <http://dx.doi.org/10.1007/BF00759198> Gen. Rel. Grav. **1**, p. 9–18 (1970). gr-qc/0411023. :1969wk
- [84] R. H. DICKE; «Experimental relativity»; dans «Relativité, Groupes et Topologie : Proceedings, Ecole d'été de Physique Théorique, Session XIII, Les Houches, France, Jul 1 - Aug 24, 1963», p. 165–316 (1964). :1964pna
- [85] P. TOUBOUL *et al.*; «MICROSCOPE Mission : First Results of a Space Test of the Equivalence Principle»; <http://dx.doi.org/10.1103/PhysRevLett.119.231101> Phys. Rev. Lett. **119**, p. 231 101 (2017). 1712.01176. :2017grn
- [86] R. GEIGER & M. TRUPKE; «Proposal for a Quantum Test of the Weak Equivalence Principle with Entangled Atomic Species»; <http://dx.doi.org/10.1103/PhysRevLett.120.043602> Phys. Rev. Lett. **120**, p. 043 602 (2018). 1801.08604. :2018xwr
- [87] R. F. C. VESSOT *et al.*; «Test of Relativistic Gravitation with a Space-Borne Hydrogen Maser»; <http://dx.doi.org/10.1103/PhysRevLett.45.2081> Phys. Rev. Lett. **45**, p. 2081–2084 (1980). :1980zz
- [88] H. E. IVES & G. R. STILWELL; «An Experimental Study of the Rate of a Moving Atomic Clock»; <http://dx.doi.org/10.1364/JOSA.28.000215> J. Opt. Soc. Am. **28**, p. 215–226 (1938). <http://www.osapublishing.org/abstract.cfm?URI=josa-28-7-215>. :38
- [89] K. BRECHER; «Is the Speed of Light Independent of the Velocity of the Source?»; <http://dx.doi.org/10.1103/PhysRevLett.39.1051> Phys. Rev. Lett. **39**, p. 1051–1054 (1977). <https://link.aps.org/doi/10.1103/PhysRevLett.39.1051>.
- [90] E. RIIS, L.-U. A. ANDERSEN, N. BJERRE, O. POULSEN, S. A. LEE & J. L. HALL; «Test of the Isotropy of the Speed of Light Using Fast-Beam Laser Spectroscopy»; <http://dx.doi.org/10.1103/PhysRevLett.60.81> Phys. Rev. Lett. **60**, p. 81–84 (1988). <https://link.aps.org/doi/10.1103/PhysRevLett.60.81>.

- [91] A. A. MICHELSON & E. W. MORLEY; «On the Relative Motion of the Earth and the Luminiferous Ether»; <http://dx.doi.org/10.2475/ajs.s3-34.203.333> *Am. J. Sci.* **34**, p. 333–345 (1887). :1887zz
- [92] V. A. KOSTELECKY; «Gravity, Lorentz violation, and the standard model»; <http://dx.doi.org/10.1103/PhysRevD.69.105009> *Phys. Rev.* **D69**, p. 105 009 (2004). [hep-th/0312310](http://arxiv.org/abs/hep-th/0312310). :2003fs
- [93] V. A. KOSTELECKY & N. RUSSELL; «Data Tables for Lorentz and CPT Violation»; <http://dx.doi.org/10.1103/RevModPhys.83.11> *Rev. Mod. Phys.* **83**, p. 11–31 (2011). 0801.0287. :2008ts
- [94] D. MATTINGLY; «Modern tests of Lorentz invariance»; <http://dx.doi.org/10.12942/lrr-2005-5> *Living Rev. Rel.* **8**, p. 5 (2005). [gr-qc/0502097](http://arxiv.org/abs/gr-qc/0502097). :2005re
- [95] T. JACOBSON, S. LIBERATI & D. MATTINGLY; «Lorentz violation at high energy : Concepts, phenomena and astrophysical constraints»; <http://dx.doi.org/10.1016/j.aop.2005.06.004> *Annals Phys.* **321**, p. 150–196 (2006). [astro-ph/0505267](http://arxiv.org/abs/hep-ph/0505267). :2005bg
- [96] D. COLLADAY & V. A. KOSTELECKY; «Lorentz violating extension of the standard model»; <http://dx.doi.org/10.1103/PhysRevD.58.116002> *Phys. Rev.* **D58**, p. 116 002 (1998). [hep-ph/9809521](http://arxiv.org/abs/hep-ph/9809521). :1998fq
- [97] V. A. KOSTELECKY; «Testing a CPT violating and Lorentz violating extension of the standard model»; dans «Physics of mass. Proceedings, 26th International Conference, Orbis Scientiae, Miami Beach, USA, December 12-15, 1997», p. 89–94 (1998); [hep-ph/9810239](http://arxiv.org/abs/hep-ph/9810239). :1998id
- [98] V. A. KOSTELECKY; «Lorentz violating and CPT violating extension of the standard model»; dans «Beyond the desert : Accelerator, non-accelerator and space approaches into the next millennium. Proceedings, 2nd International Conference on particle physics beyond the standard model, Ringberg Castle, Tegernsee, Germany, June 6-12, 1999», p. 151–163 (1999); [hep-ph/9912528](http://arxiv.org/abs/hep-ph/9912528). :1999rh
- [99] A. V. KOSTELECKY & J. D. TASSON; «Matter-gravity couplings and Lorentz violation»; <http://dx.doi.org/10.1103/PhysRevD.83.016013> *Phys. Rev.* **D83**, p. 016 013 (2011). 1006.4106. :2010ze
- [100] V. A. KOSTELECKY & S. SAMUEL; «Spontaneous breaking of Lorentz symmetry in string theory»; <http://dx.doi.org/10.1103/PhysRevD.39.683> *Phys. Rev. D* **39**, p. 683–685 (1989). <https://link.aps.org/doi/10.1103/PhysRevD.39.683>.
- [101] S. M. CARROLL, J. A. HARVEY, V. A. KOSTELECKY, C. D. LANE & T. OKAMOTO; «Noncommutative field theory and Lorentz violation»; <http://dx.doi.org/10.1103/PhysRevLett.87.141601> *Phys. Rev. Lett.* **87**, p. 141 601 (2001). [hep-th/0105082](http://arxiv.org/abs/hep-th/0105082). :2001ws
- [102] A. COATES, C. MELBY-THOMPSON & S. MUKOHYAMA; «Revisiting Lorentz violation in Horava gravity»; (2018)1805.10299. :2018vub
- [103] C. D. FROGGATT & H. B. NIELSEN; *Origin of symmetries* (1991). :1991ft
- [104] S. CHADHA & H. B. NIELSEN; «LORENTZ INVARIANCE AS A LOW-ENERGY PHENOMENON»; [http://dx.doi.org/10.1016/0550-3213\(83\)90081-0](http://dx.doi.org/10.1016/0550-3213(83)90081-0) *Nucl. Phys.* **B217**, p. 125–144 (1983). :1982qq

- [105] G. BEDNIK, O. PUJOLLS & S. SIBIRYAKOV; «Emergent Lorentz invariance from Strong Dynamics : Holographic examples»; [http://dx.doi.org/10.1007/JHEP11\(2013\)064](http://dx.doi.org/10.1007/JHEP11(2013)064)JHEP **11**, p. 064 (2013). 1305.0011. :2013nxa
- [106] S. GROOT NIBBELINK & M. POSPELOV; «Lorentz violation in supersymmetric field theories»; <http://dx.doi.org/10.1103/PhysRevLett.94.081601>Phys. Rev. Lett. **94**, p. 081 601 (2005). hep-ph/0404271. :2004za
- [107] M. POSPELOV & Y. SHANG; «On Lorentz violation in Horava-Lifshitz type theories»; <http://dx.doi.org/10.1103/PhysRevD.85.105001>Phys. Rev. **D85**, p. 105 001 (2012). 1010.5249. :2010mp
- [108] D. LOVELOCK; «The Einstein tensor and its generalizations»; <http://dx.doi.org/10.1063/1.1665613>J. Math. Phys. **12**, p. 498–501 (1971). :1971yv
- [109] D. LOVELOCK; «The four-dimensionality of space and the einstein tensor»; <http://dx.doi.org/10.1063/1.1666069>J. Math. Phys. **13**, p. 874–876 (1972). :1972vz
- [110] T. JACOBSON & D. MATTINGLY; «Gravity with a dynamical preferred frame»; <http://dx.doi.org/10.1103/PhysRevD.64.024028>Phys. Rev. **D64**, p. 024 028 (2001). gr-qc/0007031. :2000xp
- [111] D. BLAS, O. PUJOLAS & S. SIBIRYAKOV; «Consistent Extension of Horava Gravity»; <http://dx.doi.org/10.1103/PhysRevLett.104.181302>Phys. Rev. Lett. **104**, p. 181 302 (2010). 0909.3525. :2009qj
- [112] A. O. BARVINSKY, D. BLAS, M. HERRERO-VALEA, S. M. SIBIRYAKOV & C. F. STEINWACHS; «Renormalization of Ho?ava gravity»; <http://dx.doi.org/10.1103/PhysRevD.93.064022>Phys. Rev. **D93**, p. 064 022 (2016). 1512.02250. :2015kil
- [113] H. B. LAWSON; «Foliations»; <http://dx.doi.org/10.1090/S0002-9904-1974-13432-4>Bulletin of American Mathematical Society p. 369–418 (1974).
- [114] I. MOERDIJK & J. MRCUN; *Introduction to foliations and Lie groupoids* (Cambridge University Press) (2003); ISBN 0 521 83197 0.
- [115] D. BLAS, O. PUJOLAS & S. SIBIRYAKOV; «Models of non-relativistic quantum gravity : The Good, the bad and the healthy»; [http://dx.doi.org/10.1007/JHEP04\(2011\)018](http://dx.doi.org/10.1007/JHEP04(2011)018)JHEP **04**, p. 018 (2011). 1007.3503. :2010hb
- [116] D. BLAS, O. PUJOLAS & S. SIBIRYAKOV; «Comment on ‘Strong coupling in extended Horava-Lifshitz gravity’»; <http://dx.doi.org/10.1016/j.physletb.2010.03.073>Phys. Lett. **B688**, p. 350–355 (2010). 0912.0550. :2009ck
- [117] A. PAPAZOGLU & T. P. SOTIRIOU; «Strong coupling in extended Horava-Lifshitz gravity»; <http://dx.doi.org/10.1016/j.physletb.2010.01.054>Phys. Lett. **B685**, p. 197–200 (2010). 0911.1299. :2009fj
- [118] I. KIMPTON & A. PADILLA; «Lessons from the decoupling limit of Horava gravity»; [http://dx.doi.org/10.1007/JHEP07\(2010\)014](http://dx.doi.org/10.1007/JHEP07(2010)014)JHEP **07**, p. 014 (2010). 1003.5666. :2010xi
- [119] S. M. CARROLL & E. A. LIM; «Lorentz-violating vector fields slow the universe down»; <http://dx.doi.org/10.1103/PhysRevD.70.123525>Phys. Rev. **D70**, p. 123 525 (2004). hep-th/0407149. :2004ai

- [120] T. JACOBSON; «Extended Horava gravity and Einstein-aether theory»; <http://dx.doi.org/10.1103/PhysRevD.82.129901>, 10.1103/PhysRevD.81.101502Phys. Rev. **D81**, p. 101502 (2010). [Erratum : Phys. Rev.D82,129901(2010)]; 1001.4823. :2010mx
- [121] B. Z. FOSTER & T. JACOBSON; «Post-Newtonian parameters and constraints on Einstein-aether theory»; <http://dx.doi.org/10.1103/PhysRevD.73.064015>Phys. Rev. **D73**, p. 064015 (2006). gr-qc/0509083. :2005dk
- [122] T. JACOBSON; «Einstein-aether gravity : A Status report»; PoS **QG-PH**, p. 020 (2007)0801.1547. :2008aj
- [123] T. JACOBSON & D. MATTINGLY; «Einstein-Aether waves»; <http://dx.doi.org/10.1103/PhysRevD.70.024003>Phys. Rev. **D70**, p. 024003 (2004). gr-qc/0402005. :2004ts
- [124] D. BLAS & H. SANCTUARY; «Gravitational Radiation in Horava Gravity»; <http://dx.doi.org/10.1103/PhysRevD.84.064004>Phys. Rev. **D84**, p. 064004 (2011). 1105.5149. :2011zd
- [125] G. D. MOORE & A. E. NELSON; «Lower bound on the propagation speed of gravity from gravitational Cherenkov radiation»; <http://dx.doi.org/10.1088/1126-6708/2001/09/023>JHEP **09**, p. 023 (2001). hep-ph/0106220. :2001bv
- [126] J. W. ELLIOTT, G. D. MOORE & H. STOICA; «Constraining the new Aether : Gravitational Cerenkov radiation»; <http://dx.doi.org/10.1088/1126-6708/2005/08/066>JHEP **08**, p. 066 (2005). hep-ph/0505211. :2005va
- [127] E. BARAUSSE, T. JACOBSON & T. P. SOTIRIOU; «Black holes in Einstein-aether and Horava-Lifshitz gravity»; <http://dx.doi.org/10.1103/PhysRevD.83.124043>Phys. Rev. **D83**, p. 124043 (2011). 1104.2889. :2011pu
- [128] B. AUDREN, D. BLAS, J. LESGOURGUES & S. SIBIRYAKOV; «Cosmological constraints on Lorentz violating dark energy»; <http://dx.doi.org/10.1088/1475-7516/2013/08/039>JCAP **1308**, p. 039 (2013). 1305.0009. :2013dwa
- [129] K. YAGI, D. BLAS, E. BARAUSSE & N. YUNES; «Constraints on Einstein-ether theory and Horava gravity from binary pulsar observations»; <http://dx.doi.org/10.1103/PhysRevD.90.069902>, 10.1103/PhysRevD.90.069901, 10.1103/PhysRevD.89.084067Phys. Rev. **D89**, p. 084067 (2014). [Erratum : Phys. Rev.D90,no.6,069901(2014)]; 1311.7144. :2013ava
- [130] J. A. ZUNTZ, P. G. FERREIRA & T. G. ZLOSNIK; «Constraining Lorentz violation with cosmology»; <http://dx.doi.org/10.1103/PhysRevLett.101.261102>Phys. Rev. Lett. **101**, p. 261102 (2008). 0808.1824. :2008zz
- [131] L. SHAO & N. WEX; «New tests of local Lorentz invariance of gravity with small-eccentricity binary pulsars»; <http://dx.doi.org/10.1088/0264-9381/29/21/215018>Class. Quant. Grav. **29**, p. 215018 (2012). 1209.4503. :2012eg
- [132] L. SHAO, R. N. CABALLERO, M. KRAMER, N. WEX, D. J. CHAMPION & A. JESSNER; «A new limit on local Lorentz invariance violation of gravity from solitary pulsars»; <http://dx.doi.org/10.1088/0264-9381/30/16/165019>Class. Quant. Grav. **30**, p. 165019 (2013). 1307.2552. :2013wga

- [133] E. BARAUSSE & T. P. SOTIRIOU; «Black holes in Lorentz-violating gravity theories»; <http://dx.doi.org/10.1088/0264-9381/30/24/244010> *Class. Quant. Grav.* **30**, p. 244 010 (2013). 1307.3359. :2013nwa
- [134] E. BARAUSSE & T. P. SOTIRIOU; «Slowly rotating black holes in Horava-Lifshitz gravity»; <http://dx.doi.org/10.1103/PhysRevD.87.087504> *Phys. Rev.* **D87**, p. 087 504 (2013). 1212.1334. :2012qh
- [135] E. BARAUSSE, T. P. SOTIRIOU & I. VEGA; «Slowly rotating black holes in Einstein-ther theory»; <http://dx.doi.org/10.1103/PhysRevD.93.044044> *Phys. Rev.* **D93**, p. 044 044 (2016). 1512.05894. :2015frm
- [136] C. ELING & T. JACOBSON; «Black Holes in Einstein-Aether Theory»; <http://dx.doi.org/10.1088/0264-9381/23/18/009>, 10.1088/0264-9381/27/4/049802 *Class. Quant. Grav.* **23**, p. 5643–5660 (2006). [Erratum : *Class. Quant. Grav.* 27,049802(2010)]; [gr-qc/0604088](http://arxiv.org/abs/gr-qc/0604088). :2006ec
- [137] T. TAMAKI & U. MIYAMOTO; «Generic features of Einstein-Aether black holes»; <http://dx.doi.org/10.1103/PhysRevD.77.024026> *Phys. Rev.* **D77**, p. 024 026 (2008). 0709.1011. :2007kz
- [138] D. GARFINKLE, C. ELING & T. JACOBSON; «Numerical simulations of gravitational collapse in Einstein-aether theory»; <http://dx.doi.org/10.1103/PhysRevD.76.024003> *Phys. Rev.* **D76**, p. 024 003 (2007). [gr-qc/0703093](http://arxiv.org/abs/gr-qc/0703093). :2007bk
- [139] N. I. SHAKURA & R. A. SUNYAEV; «Black holes in binary systems. Observational appearance»; *Astron. Astrophys.* **24**, p. 337–355 (1973). :1972te
- [140] J. M. MILLER, C. S. REYNOLDS, A. C. FABIAN, G. MINIUTTI & L. C. GALLO; «Stellar-Mass Black Hole Spin Constraints from Disk Reflection and Continuum Modeling»; <http://dx.doi.org/10.1088/0004-637X/697/1/900697>, p. 900–912 (2009). 0902.2840.
- [141] T. FUTAMASE; «The Strong Field Point Particle Limit and the Equations of Motion in the Binary Pulsar»; <http://dx.doi.org/10.1103/PhysRevD.36.321> *Phys. Rev.* **D36**, p. 321 (1987). :1987yy
- [142] Y. ITOH, T. FUTAMASE & H. ASADA; «Equation of motion for relativistic compact binaries with the strong field point particle limit : Formulation, the first post-Newtonian and multipole terms»; <http://dx.doi.org/10.1103/PhysRevD.62.064002> *Phys. Rev.* **D62**, p. 064 002 (2000). [gr-qc/9910052](http://arxiv.org/abs/gr-qc/9910052). :1999bf
- [143] Y. ITOH & T. FUTAMASE; «New derivation of a third postNewtonian equation of motion for relativistic compact binaries without ambiguity»; <http://dx.doi.org/10.1103/PhysRevD.68.121501> *Phys. Rev.* **D68**, p. 121 501 (2003). [gr-qc/0310028](http://arxiv.org/abs/gr-qc/0310028). :2003fy
- [144] L. BLANCHET; «Gravitational Radiation from Post-Newtonian Sources and Inspiral-ing Compact Binaries»; <http://dx.doi.org/10.12942/lrr-2014-2> *Living Rev. Rel.* **17**, p. 2 (2014). 1310.1528. :2013haa
- [145] C. BRANS & R. H. DICKE; «Mach's principle and a relativistic theory of gravitation»; <http://dx.doi.org/10.1103/PhysRev.124.925> *Phys. Rev.* **124**, p. 925–935 (1961). [142(1961)]. :1961sx

- [146] I. CARRUTHERS & T. JACOBSON; «Cosmic alignment of the aether»; <http://dx.doi.org/10.1103/PhysRevD.83.024034> Phys. Rev. **D83**, p. 024 034 (2011). 1011.6466. :2010ii
- [147] E. POISSON, A. POUND & I. VEGA; «The Motion of point particles in curved spacetime»; <http://dx.doi.org/10.12942/lrr-2011-7> Living Rev. Rel. **14**, p. 7 (2011). 1102.0529. :2011nh
- [148] D. M. EARDLEY; «Observable effects of a scalar gravitational field in a binary pulsar»; <http://dx.doi.org/10.1086/1817441> **196**, p. L59–L62 (1975).
- [149] B. Z. FOSTER; «Strong field effects on binary systems in Einstein-aether theory»; <http://dx.doi.org/10.1103/PhysRevD.76.084033> Phys. Rev. **D76**, p. 084 033 (2007). 0706.0704. :2007gr
- [150] C. ELING, T. JACOBSON & M. COLEMAN MILLER; «Neutron stars in Einstein-aether theory»; <http://dx.doi.org/10.1103/PhysRevD.76.042003>, [10.1103/PhysRevD.80.129906](http://dx.doi.org/10.1103/PhysRevD.80.129906) Phys. Rev. **D76**, p. 042 003 (2007). [Erratum : Phys. Rev. **D80**, 129906(2009)]; 0705.1565. :2007xh
- [151] B. Z. FOSTER; «Metric redefinitions in Einstein-Aether theory»; <http://dx.doi.org/10.1103/PhysRevD.72.044017> Phys. Rev. **D72**, p. 044 017 (2005). gr-qc/0502066. :2005ec
- [152] P. BERGLUND, J. BHATTACHARYYA & D. MATTINGLY; «Mechanics of universal horizons»; <http://dx.doi.org/10.1103/PhysRevD.85.124019> Phys. Rev. **D85**, p. 124 019 (2012). 1202.4497. :2012bu